Lipids as indicators of nitrogen cycling in present and past anoxic oceans

Martina Sollai

This research has been financially supported by the Darwin Center for Biogeosciences, the Netherlands Earth System Science Center (NESSC), and Soehngen Institute for Anaerobic Microbiology (SIAM) of the Netherlands Organization for Scientific Research (NWO), and the NIOZ – Royal Netherlands Institute For Sea Research.

ISBN: 978-90-6266-505-1

Cover design: Martina Sollai

Pictures by: Martina Sollai; Laura Tiano; Allison Myers Pigg

Printed by Ipskamp Printing, The Netherlands

Lipids as indicators of nitrogen cycling in present and past anoxic oceans

Lipiden als indicatoren voor de recirculatie van stikstof in de huidige en vroegere zuurstofloze oceanen

(met een samenvatting in het Nederlands)

Lipidi come indicatori del ciclo dell'azoto negli oceani anossici del presente e del passato

(con una sintesi in Italiano)

Proefschrift

ter verkrijging van de graad van doctor
aan de Universiteit Utrecht op
gezag van de rector magnificus, prof.dr. H.R.B.M. Kummeling,
ingevolg het besluit van het college voor promoties
in het openbaar te verdedigen
op maandag 25 juni 2018 des ochtends te 12.45 uur

door

Martina Sollai

geboren op 30 oktober 1980 te Cagliari, Italië

Promotor: Prof. dr. ir. J.S. Sinninghe Damsté

Copromotor: Dr. L. Villanueva

Now‘s the time to stop condemning things
and come up with some answers
Robert M. Pirsig,
Zen and the Art of Motorcycle Maintenance

La calma è la virtù dei Fonzie
Anonimo metropolitano cagliaritano

Table of contents

Summary

Samenvatting

Sintesi

Summary

Nitrogen (N) cycling influences primary production in the ocean and, hence, the global climate. It is performed by a variety of microorganisms, including eukaryotes, bacteria and archaea in oxic, suboxic, and anoxic waters. Our knowledge of the reactions involved in marine N cycling and its associated microorganisms has greatly increased in the last decade due to the development of multiple culture-independent methods. Among them are gene and lipid biomarkers, which hold taxonomic potential and can be successfully applied in modern day and paleoenvironmental studies. However, many aspects of N cycling and their long-term implications for the marine environment and the global climate still require more study, especially in suboxic and anoxic waters, including the oxygen-deficient zones (ODZs), which are expanding in the modern oceans. Oxygen-depleted waters are not an exclusive feature of the modern ocean as oceanic anoxic events (OAE) have been occurring in the geological past and severely affected N cycling. This thesis investigates aspects of the marine N cycle in the modern ocean by applying molecular biomarkers. Particular focus was put on the modern oxygen-depleted water systems and on how these systems can be helpful to understand the past OAEs and how in turn past anoxic events can be predictive of the future of the ocean.

The occurrence and distribution of thaumarchaeotal ammonia-oxidizing archaea (AOA) and anaerobic ammonia-oxidizing (anammox) bacteria in the water column of the eastern tropical North Pacific (ETNP) ODZ, one of the most prominent ODZs worldwide, is described in **Chapter 2**. Thaumarchaeota perform aerobic oxidation of NH_4^+ to NO_2^-, while anammox bacteria anaerobically oxidize NH_4^+ to N_2 using NO_2^- as electron acceptor. Hence, these two groups might either compete or cooperate. Both produce specific membrane intact polar lipids (IPLs) namely hexose-phosphohexose (HPH)-crenarchaeol and phosphatidylcholine (PC)-monoether ladderane, respectively, which were used as biomarkers to trace their presence in the environment. Suspended particulate matter (SPM) was collected at different depths of the water column in high resolution, at both a coastal and an open ocean station, and analyzed with high performance liquid chromatography coupled with an electrospray ionization mass spectrometry (HPLC/ESI-MS^2). This enabled to disentangle how Thaumarchaeota and anammox bacteria are distributed in the ETNP water column. These data revealed that both Thaumarchaeota and anammox bacteria were able to thrive at concentrations of oxygen as low as <1μM but they had a different distribution at the coastal station, where a clear segregation of Thaumarchaeotal and anammox bacterial niches existed. However, at the open ocean station the two distributions partially overlapped, suggesting that the two groups of microbes were potentially interacting.

Archaea other than the nitrifying Thaumarchaeota also occur ubiquitously in the ocean and are potentially involved in carbon and N cycling. Most Archaea, however, remain uncultured to date but their IPLs may be a powerful tool to study them. **Chapter 3** describes the diversity of archaea and their IPL biomarkers in waters of the eastern tropical South Pacific (ETSP) ODZ, one of the main permanent ODZs in the modern ocean. IPLs in SPM sampled in high depth resolution from a coastal and open ocean site were analyzed by Ultra High Pressure Liquid Chromatography coupled to High Resolution MS (UHPLC-HRMS). This was compared with the archaeal diversity and abundance as determined by 16S rRNA gene amplicon sequencing and quantitative PCR, respectively. In the oxic surface and upper ODZ, Marine Group I (MGI) Thaumarchaeota, i.e. *Ca*. Nitrosopelagicus and *Nitrosopumilus*, dominated together with Marine Group II (MGII) Euryarchaeota. This coincided with higher relative abundance of HPH-crenarchaeol, the specific biomarker for living Thaumarchaeota, and HPH-glycerol dibiphytanyl glycerol tetraether (GDGT)-0, dihexose- (DH) GDGT-3 and -4. In contrast, DPANN Woesearchaeota DHVE-6 and Marine Group III (MGIII) Euryarchaeota thrived within the ODZ and archaeol-based IPLs dominated, which were likely synthesized by MGIII archaea, as DPANN Woesearchaeota DHVE-6 are predicted to be unable to synthesize their own IPLs. In the deep oxic waters below the ODZ a different MGI population co-occurred with HPH-GDGT-1, -2 and DH-GDGT-0 and -crenarchaeol, indicating that these MGI archaea synthesize IPLs with a different composition, either due to environmental adaptation or to genetic differences. Archaea form a complex community in this setting and synthesize a diverse suite of IPL biomarkers which harbor taxonomic potential.

The Black Sea water column is characterized by a shallow redoxcline with euxinic bottom waters and is expected to host a wide variety of Archaea potentially involved in N cycling. In **Chapter 4** SPM of the Black Sea water column sampled at high resolution is studied using the same methods as described in Chapter 3. MGI Thaumarchaeota and MGII Euryarchaeota were dominant in the oxic/upper suboxic waters and this coincided with a high relative abundance of thaumarchaeotal HPH-crenarchaeol. In the suboxic waters, MGI *Nitrosopumilus* sp. was especially abundant, coinciding with a higher abundance of monohexose (MH)-GDGTs and hydroxy (OH)-GDGTs. In the deep sulfidic waters, the archaeal diversity increased and DPANN Woesearchaeota, Bathyarchaeota, and ANME-1b were the dominant groups, coinciding with the presence of archaeol lipids with a variety of polar headgroups. This study indicates that the Black Sea hosts an unexpectedly complex archaeal community corresponding with a high IPL diversity.

Summer phytoplankton blooms, dominated by a few species of heterocys-

tous N_2-fixing cyanobacteria, are a recurring feature of the modern, partially anoxic Baltic Sea. Since the last deglaciation the Baltic Sea has undergone geological changes which have affected its biogeochemistry. In **Chapter 5**, the abundance and distribution of heterocyst glycolipids (HGs), IPLs exclusively produced by heterocystous N_2-fixing cyanobacteria, were studied at high resolution in the sedimentary record of the Gotland Basin. The HG distribution of the sediments deposited during the Modern Warm Period was similar to that of cultivated heterocystous cyanobacteria, including isolates from Baltic Sea waters. The abundance of HGs dropped substantially with increasing sediment depth. This was a consequence of either a decrease in the occurrence of the cyanobacterial blooms or diagenesis, resulting in the partial destruction of the HGs. However, the overall HG distribution has remained stable since the Baltic turned into a brackish semi-enclosed basin ~7200 cal. yr BP, suggesting no substantial changes in the heterocystous cyanobacterial species composition. However, in the earlier freshwater phase of the Baltic, the distribution of the HGs was quite different and the abundance of HGs was much lower than during the brackish phase, indicating that the Baltic cyanobacterial community adjusted to the different environmental conditions. This indicates that HGs are valuable biomarkers for heterocystous cyanobacteria in paleoenvironmental studies.

The work described in this thesis provides new insights into N cycling in oxygen-depleted basins and ODZs. Additionally, it expands the current knowledge on the archaeal diversity in such settings. Finally, it has improved the understanding of past variations in N_2 fixation. Future investigations using biomarkers may help to further increase our understanding of present and past N cycling in the ocean.

De stikstofcyclus is van groot belang voor de primaire productie in de oceaan en daarmee voor het mondiale klimaat. Een verscheidenheid aan micro-organismen, waaronder eukaryoten, bacteriën en archaea in zowel oxische, suboxische als anoxische wateren zijn actief in deze cyclus. Onze kennis van de betrokken micro-organismen en de omzettingen die zij uitvoeren is sterk toegenomen in het afgelopen decennium als gevolg van de ontwikkeling van kweek-onafhankelijke methoden. Hiertoe behoren gen en lipide biomarkers, die beide taxonomisch potentieel hebben en met succes kunnen worden toegepast in zowel moderne als paleomilieu studies. Veel aspecten van de stikstofcyclus en hun lange-termijn implicaties voor het mariene milieu en het globale klimaat vereisen echter nog steeds meer studie, vooral in suboxische en anoxische wateren, waaronder de zuurstof-deficiënte zones (ODZs), die zich uitbreiden in de moderne oceanen. Zuurstofarme wateren zijn geen exclusief kenmerk van de moderne oceaan omdat oceanische anoxische gebeurtenissen (OAE) zich hebben voorgedaan in het geologische verleden en grote invloed gehad hebben op de stikstofcyclus. Dit proefschrift onderzoekt aspecten van de mariene stikstofcyclus in de moderne oceaan door het gebruik van moleculaire biomarkers. In het bijzonder is aandacht besteed aan zuurstofarme watersystemen en aan de manier waarop deze systemen kunnen helpen vroegere OAEs te begrijpen.

Het voorkomen en de verspreiding van ammoniak-oxiderende archaea (Thaumarchaeota) en anaerobe ammoniak-oxiderende (anammox) bacteriën in de waterkolom van de oostelijke tropische Noord-Pacific (ETNP) ODZ, een van de meest prominente ODZs wereldwijd, wordt beschreven in **Hoofdstuk 2**. Thaumarchaeota voeren de aerobe oxidatie van NH_4^+ tot NO_2^- uit, terwijl anammox-bacteriën anaeroob NH_4^+ oxideren tot N_2 met NO_2^- als elektronenacceptor. Daarom kunnen deze twee groepen micro-organismen concurreren of samenwerken. Beide produceren specifieke intacte polaire lipiden (IPLs), respectievelijk hexose-fosfohexose (HPH) -crenarchaeol en fosfatidylcholine (PC) -monoetherladderaan, die in deze studie werden gebruikt als biomarkers. Gesuspendeerde deeltjes (SPM) werden verzameld op verschillende diepten in de waterkolom in hoge resolutie, zowel op een kust- als een open oceaanstation, en geanalyseerd op IPLs met hoge-druk vloeistofchromatografie gekoppeld aan een elektrospray ionisatie massaspectrometrie. Hiermee werd de distributie van Thaumarchaeota en anammox-bacteriën in de ETNP-waterkolom vastgesteld. Hieruit bleek dat zowel Thaumarchaeota als anammox-bacteriën konden gedijen bij zuurstofconcentraties van $<1\mu M$, maar dat ze een andere distributie hadden in het kustwater, waar een duidelijke scheiding van de niches van Thaumarchaeota en anammox bacteriën bestond. In de open oceaan overlapten de twee distributies elkaar echter gedeeltelijk, hetgeen suggereert dat beide groepen microben mogelijk in wisselwerking staan.

Andere archaea dan de nitrificerende Thaumarchaeota komen ook wijdverspreid in de oceaan voor en zijn mogelijk actief in de koolstof- en stikstofcyclus. De meeste archaea zijn echter tot nu toe niet in cultuur gebracht maar hun IPLs kunnen mogelijk een krachtig hulpmiddel zijn om ze te bestuderen. **Hoofdstuk 3** beschrijft de diversiteit van archaea en hun IPL biomarkers in de wateren van de oostelijke tropische Zuid-Pacific (ETSP) ODZ, één van de belangrijkste permanente ODZs in de moderne oceaan. IPLs in SPM bemonsterd in grote diepte resolutie op zowel een kust- en open oceaanlocatie werden geanalyseerd met ultra hoge-druk vloeistofchromatografie gekoppeld met een massaspectrometer met hoge resolutie. Deze gegevens werden vergeleken met de archaeale diversiteit en abundantie zoals bepaald door respectievelijk 16S rRNA-gen amplicon-sequencing en kwantitatieve PCR. In het oxische oppervlaktewater en de bovenste ODZ domineerde Marine Group I (MGI) Thaumarchaeota, d.w.z. *Ca*. Nitrosopelagicus en *Nitrosopumilus*, samen met Marine Group II (MGII) Euryarchaeota. Dit viel samen met een hoge relatieve abundantie van HPH-crenarchaeol, de specifieke biomarker voor levende Thaumarchaeota en HPH-glycerol dibifytanyl glyceroltetraether (GDGT) -0, dihexose- (DH) GDGT-3 en -4. Daarentegen gedijen DPANN Woesearchaeota DHVE-6 en Marine Group III (MGIII) Euryarchaeota in de ODZ en domineerden op archaeol gebaseerde IPLs. Deze IPLs worden waarschijnlijk gesynthetiseerd door MGIII archaea, omdat DPANN Woesearchaeota DHVE-6 naar verwachting niet in staat zijn om via biosynthese IPLs te vormen. In de diepe zuurstofrijke wateren beneden de ODZ trad een andere MGI-populatie op met HPH-GDGT-1, -2 en DH-GDGT-0 en -crenarchaeol. Dit geeft aan dat deze MGI archaea IPLs synthetiseren met een andere samenstelling, hetzij vanwege aanpassing aan de omstandigheden of door genetische verschillen. Archaea vormen een complexe gemeenschap in deze omgeving en synthetiseren een diverse reeks IPL-biomarkers die een taxonomische potentieel herbergen.

De waterkolom van de Zwarte Zee wordt gekenmerkt door een ondiepe redoxcline met sulfidisch bodemwater en zou een grote verscheidenheid aan Archaea bevatten die mogelijk betrokken is in de stikstofcyclus kunnen bevatten. In **Hoofdstuk 4** wordt het SPM van de waterkolom in de Zwarte Zee, bemonsterd met hoge resolutie, bestudeerd volgens dezelfde methoden als beschreven in hoofdstuk 3. MGI Thaumarchaeota en MGII Euryarchaeota waren dominant in de oxische en het bovenste gedeelte van de suboxische zone en dit viel samen met een hoge relatieve abundantie van HPH-crenarchaeol afkomstig van Thaumarchaeota. In de suboxische zone domineerde MGI *Nitrosopumilus* sp., samenvallend met een grotere hoeveelheid monohexose- en hydroxy -GDGTs. In de diepe sulfidische wateren nam de archaeale diversiteit toe en DPANN Woesearchaeota, Bathyarchaeota en ANME-1b waren de

dominante groepen. Dit viel samen met de aanwezigheid van IPLs gebaseerd op archaeol met een verscheidenheid aan polaire groepen. Deze studie geeft aan dat de Zwarte Zee een onverwacht complexe archaeale levensgemeenschap heeft die overeenkomt met een hoge diversiteit aan IPLs.

Een terugkerend kenmerk van de moderne, gedeeltelijk anoxische Oostzee is de fytoplanktonbloei in de zomer die gedomineerd wordt door enkele soorten heterocyst-producerende N_2-fixerende cyanobacteriën. Sinds de laatste deglaciatie heeft de Oostzee geologische veranderingen ondergaan die haar biogeochemie hebben beïnvloed. In **Hoofdstuk 5** worden de concentratie en distributie van heterocystglycolipiden (HGs), IPLs die uitsluitend worden geproduceerd door heterocyst-producerende N_2-fixerende cyanobacteriën, bestudeerd in Holocene sedimentaire afzettingen van het Gotland bekken. De HG-distributie in de sedimenten afgezet tijdens de moderne warme periode was vergelijkbaar met die van gecultiveerde heterocyst-producerende cyanobacteriën, inclusief isolaten uit de Baltische wateren. De concentratie aan HGs daalde aanzienlijk met toenemende sedimentdiepte. Dit is een gevolg van ofwel een afname in het voorkomen van de cyanobacteriële zomerbloei of diagenese, resulterend in de gedeeltelijke afbraak van HGs. De HG-distributie bleef echter stabiel sinds het water in de Oostzee brak werd door de verbinding met de Noordzee ongeveer 7200 jaar geleden. Dit duidt op een stabiele cyanobacteriële samenstelling. In de vroegere zoetwaterfase van de Oostzee was de verdeling van de HGs echter behoorlijk verschillend en de concentratie van HGs was veel lager dan in de brakke fase, hetgeen aangeeft dat de Baltische cyanobacteriële gemeenschap zich aanpaste aan de veranderende milieuomstandigheden. HGs zijn dus waardevolle biomarkers voor heterocyst-producerende cyanobacteriën in paleomilieustudies.

Het werk beschreven in dit proefschrift biedt nieuwe inzichten in de stikstofcyclus in zuurstofarme bekkens en ODZs. Bovendien breidt het de huidige kennis over de archaeale diversiteit in dit soort milieus uit. Tenslotte leidt het tot een verbeterd inzicht in vroegere variaties in stikstoffixatie in de oceaan. Toekomstig biomarker onderzoek kan ons begrip van de huidige en vroegere stikstofcyclus in de oceaan helpen vergroten.

Il ciclo dell'azoto (N) influenza la produzione primaria nell'oceano e di conseguenza il clima mondiale. Ad esso prendono parte diversi microorganismi, inclusi eucarioti, batteri ed archaea; il ciclo si svolge in ambienti marini ossici, sub-ossici e anossici. La comprensione del ciclo marino dell'azoto e la conoscenza dei microorganismi coinvolti nelle reazioni che lo costituiscono è migliorata nell'ultimo decennio, grazie allo sviluppo di molteplici metodi di indagine indipendenti dalla coltivazione degli stessi microorganismi. Tra questi metodi vi è l'uso di biomarcatori genici e lipidici, i quali posseggono un potenziale tassonimico che consente di utilizzarli sia nello studio di ambienti attuali che di paleoambienti. Tuttavia molti aspetti del ciclo dell'azoto e le sue implicazioni a lungo termine per l'ambiente marino e per il clima necessitano ulteriori studi per essere pienamente compresi. In particolare gli ambienti marini in cui le condizioni di sub-ossia e anossia sono in aumento, come le aree oceaniche senza ossigeno (i.e. oxygen-deficient zones, ODZs). L'esistenza di ambienti marini sub-ossici e anossici non è esclusiva degli oceani moderni. Infatti i cosidetti eventi anossici oceanici (i.e. oceanic anoxic events, OAE) si sono verificati durante ere geologiche passate e hanno fortemente influenzato il ciclo dell'azoto. Questa tesi studia il ciclo marino dell'azoto negli oceani moderni grazie all'uso di biomarcatori molecolari. Particolare attenzione è stata posta sugli ambienti moderni caratterizzati dalla scarsità di ossigeno, e su come tali ambienti siano utili per comprendere gli OAE del passato e come questi eventi a loro volta possano servire a predire come saranno gli oceani futuri.

Il **Capitolo 2** di questa tesi descrive la presenza e la distribuzione degli archaea Thaumarchaeota ammonio-ossidanti (AOA) e dei batteri ammonio-ossidanti anaerobici (anammox) nella colonna d'acqua della ODZ del Nord Pacifico est tropicale (ETNP), una delle più importanti al mondo. I Thaumarchaeota svolgono l'ossidazione aerobica del NH_4^+ a NO_2^-, mentre i batteri anammox ossidano anaerobicamente NH_4^+ a N_2 utilizzando NO_2^- come accettore elettronico. Quindi potenzialmente i due gruppi potrebbero competere o cooperare. Entrambi producono specifici lipidi di membrana (i.e. intact polar lipids, IPLs), rispettivamente l'esoso fosfo-esoso crenarchaeol (i.e. hexose-phosphohexose (HPH)-crenarchaeol) e il ladderano fosfatidilcolina-monoetere (i.e. phosphatidylcholine (PC)-monoether ladderane) che in questa tesi sono stati utilizzati come biomarcatori per studiare i due gruppi microbici nel ETNP. Il particolato sospeso (i.e. suspended particulate matter, SPM) è stato raccolto a diverse profondità della colonna d'acqua, ad alta risoluzione, sia ad una stazione costiera che ad una in mare aperto, e analiz-

zato tramite cromatografia liquida ad alta prestazione/spettrometria di massa con ionizzazione a elettronebulizzazione (i.e. HPLC/ESI-MS^2). Ciò ha consentito di capire come Thaumarchaeota e batteri anammox sono distribuiti nella colonna d'acqua del ETNP. Si è visto che sia i Thaumarchaeota che i batteri anammox sono in grado di vivere a concentrazioni di ossigeno inferiori a 1μM. Tuttavia mentre alla stazione costiera le nicchie ecologiche dei due gruppi apparivano chiaramente separate, alla stazione in mare aperto le due si sovrapponevano parzialmente e quindi i due gruppi microbici stavano potenzialmente interagendo.

Anche altri gruppi di archaea oltre ai Thaumarchaeota sono diffusi negli oceani e possono contribuire ai cicli del carbonio e dell'azoto. La maggior parte non sono stati ancora isolati, tuttavia i loro IPL rappresentano dei potenti strumenti per poterli studiare. Il **Capitolo 3** riguarda la diversità degli archaea e dei loro biomarcatori IPL nelle acque della ODZ del Sud Pacifico est tropicale (ETSP), una delle maggiori ODZ. Gli IPL presenti nel SPM campionato ad alta risoluzione ad una stazione costiera e ad una in mare aperto sono stati analizzati tramite cromatografia liquida ad ultra alta prestazione/spettrometria di massa ad alta risoluzione (i.e. UHPLC/HRMS). Il risultato di tale analisi è stato poi confrontato con la diversità e l'abbondanza degli archaea presenti, determinate rispettivamente grazie al sequenziamento dell'amplicone del gene 16S rRNA e alla PCR quantitativa. Nelle acque superficiali ossiche e nella parte superiore della ODZ i Marine Group I (MGI) Thaumarchaeota, i.e. *Ca*. Nitrosopelagicus e *Nitrosopumilus*, erano dominanti insieme ai Marine Group II (MGII) Euryarchaeota. Ciò coincideva con una maggiore abbondanza del HPH-crenarchaeol, il biomarcatore specifico dei Thaumarchaeota viventi, e con quella degli IPL HPH-glicerol dibifitanil glicerol tetraetere (GDGT)-0, diesoso- (DH) GDGT-3 e -4. Al contrario, i DPANN Woesearchaeota DHVE-6 e i Marine Group III (MGIII) Euryarchaeota erano particolarmente abbondanti nella ODZ dove dominavano gli archaeol-IPL, presumibilmente sintetizzati dagli archaea MGIII. Infatti è altamente probabile che i DPANN Woesearchaeota DHVE-6 non siano in grado di sintetizzare i propri IPL. Nelle acque ossiche profonde al di sotto della ODZ è stata trovata una popolazione diversa di MGI, insieme agli IPL HPH-GDGT-1, -2, DH-GDGT-0 e -crenarchaeol. Ciò indica che questi archaea MGI sintetizzano IPLs con una diversa composizione, o per via di una adattamento ambientale o per differenze genetiche di questa popolazione MGI 'profonda' rispetto a quella presente in superficie. Gli archaea formano una comunità complessa nel ETSP e sintetizzano vari biomarcatori IPL con un potenziale tassonimico.

La colonna d'acqua del Mar Nero è caratterizzata da un chemoclino poco profondo e da acque profonde sulfidiche. Per questo motivo è adatta ad ospitare una grande varietà di Archaea potenzialemente coinvolti nel ciclo dell'azoto. Nel **Capitolo 4** il SPM del Mare Nero campionato ad alta risoluzione è stato studiato utilizzando lo stesso metodo descritto nel Capitolo 3. I MGI Thaumarchaeota e i MGII Euryarchaeota erano dominanti nelle acque ossiche e sub-ossiche superficiali; ciò coincideva con un'elevata abbondanza relativa del HPH-crenarchaeol, l'IPL specifico dei Thaumarchaeota. Nelle acque sub-ossiche i MGI *Nitrosopumilus* sp. erano particolarmente abbondanti, insieme ai monoesoso (MH)-GDGTs e agli idrossi (OH)-GDGTs. Nelle acque sulfidiche profonde la diversità degli Archaea era superiore rispetto alla superficie, DPANN Woesearchaeota, Bathyarchaeota, e ANME-1b erano i gruppi dominanti. Ciò coincideva con la presenza di IPL costituiti da archaeal legato a diversi gruppi polari. Questo studio indica che il Mar Nero ospita una comunità di Archaea inaspettatamente complessa a cui corrisponde una grande diversità di IPL.

Le fioriture estive di fitoplancton dominate da poche specie di cianobatteri eterocistici N_2-fissatori sono una caratteristica ricorrente del Mar Baltico moderno, un bacino parzialmente anossico. A partire dall'ultima deglaciazione il Mar Baltico ha subito vari cambiamenti geologici che hanno influenzato la sua biogeochimica. Nel **Capitolo 5** di questa tesi l'abbondanza e la distribuzione dei glicolipidi eterocistici (i.e. heterocyst glycolipids, HGs), gli IPL prodotti esclusivamente da cianobatteri eterocistici N_2-fissatori, sono state studiate ad alta risoluzione negli archivi sedimentari del bacino Gotland. La distribuzione degli HG nei sedimenti depositatisi durante il Periodo Caldo Moderno era simile a quella di colture di cianobatteri eterocistici, inclusi alcuni isolati provenienti dalle acque del Mar Baltico. L'abbondanza degli HGs calava sostanzialmente a profonidità crescenti dei sedimenti. Ciò poteva dipendere da una diminuzione delle fioriture algali o da un processo di diagenesi, risultante nella parziale degradazione degli HG. Tuttavia, complessivamente la distribuzione degli HG è rimasta stabile da quando il Baltico è diventato un bacino salmastro semi chiuso ~7200 cal. yr BP, e ciò suggerisce che da quel momento non siano avvenuti sostanziali cambiamenti nella composizione delle specie di cianobatteri eterocistici del Baltico. Al contrario, durante la precedente fase di acqua dolce, la distribuzione degli HG era molto diversa e la loro abbondanza molto inferiore, il che indica che la comunità di cianobatteri del Baltico si è adattata alle diverse condizioni ambientali. Gli HG sono dei validi biomarcatori dei cianobatteri eterocistici in studi paleo-

ambientali.

Lo studio descritto in questa tesi fornisce nuove conoscenze riguardo al ciclo dell'azoto in ambienti marini caratterizzati da scarsa presenza di ossigeno e nelle ODZ. Inoltre, estende la conoscenza della diversità di Archaea presenti in tali ambienti. Infine, questa tesi ha migliorato la comprensione delle variazioni riguardanti la fissazione dell'azoto nel passato. Ricerche future basate sull'uso di biomarcatori potranno ulteriormente accrescere la nostra comprensione del ciclo dell'azoto negli oceani del presente e del passato.

Chapter 1

Introduction

1.1 Nitrogen cycling in the ocean

Nitrogen is of great importance in the oceans, being one of the key nutrients in marine waters and consequently a limiting element for biological productivity (Falkowski, 1997). In this way, the nitrogen cycle is directly or indirectly connected to the carbon, oxygen and phosphorus cycles and to those of various micronutrients whose role is essential in many biological processes (see Canfield et al. 2010; Falkowski 1997; Morel and Price 2003 among others). Most notably, by limiting the primary production in the ocean, nitrogen has a regulatory effect on the amount of carbon dioxide (CO_2) present in the ocean and consequently in the atmosphere (Feely et al., 2009). This in turn affects the temperature of our planet through the greenhouse effect (Gruber and Galloway, 2008). The marine nitrogen cycle consists of thermodynamically favored reduction/oxidation (redox) reactions occurring throughout oxic and suboxic to anoxic conditions, mediated by chemical, physical and biological factors (Fig. 1). Indeed, most of the reactions involved in the cycling are performed by microorganisms of various lineages, eukaryotes, bacteria and archaea, as part of their assimilatory metabolisms to gain energy for their growth and/or to build their own organic matter (OM), or as part of their dissimilatory metabolisms when nitrogen is released in the environment during their decomposition (Gruber, 2008).

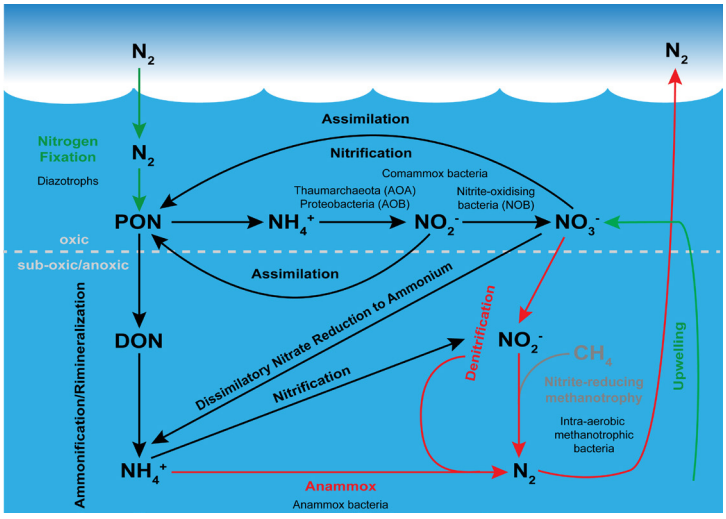

Figure 1. The marine nitrogen cycle. The diagram reports the main redox reactions involved and the microorganisms responsible for the nitrogen cycling in the oceans. Green and red arrows respectivelly represent the processes responsible for gains and losses of nitrogen to the ocean. Adapted from Arrigo, 2005.

In the N cycle, the processes that are responsible for the entry of new nitrogen within the marine environment and those which allow its exit back to the atmosphere (see later in the text atmospheric dinitrogen (N_2 fixation and denitrification/anammox are of particular interest, because they regulate the global budget of nitrogen within the ocean (Arrigo, 2005; Gruber, 2008. This budget is constantly in a dynamic equilibrium and difficult to quantify, as the residence time of reactive nitrogen in the ocean is fast – less than 3000 years – compared to that of other elements (Arrigo, 2005; Gruber, 2008. This dynamic condition makes the cycle more susceptible to external perturbations which may lead to unbalance the marine nitrogen budget itself (Galloway et al., 2004; Gruber and Galloway, 2008. The most relevant disturbances to the marine nitrogen cycle in the present-day ocean are human activities that tend to accelerate the cycling by introducing additional nitrogen in the form of fertilizers and fossil-fuel combustion products in the marine environment. On a global scale this extra supply doubles the total amount of fixed nitrogen within the ocean, as it is equivalent to the quantity fixed biologically through N_2-fixation (Galloway et al., 2004; Gruber and Galloway, 2008; Falkowski et al., 2000, which is a prominent process in the (subtropical oceans (Agawin et al., 2014; Benavides et al., 2011; Falcón et al., 2004; Montoya et al., 2004. Another factor increasingly affecting the nitrogen inventory of the ocean is the spreading of hypoxia/anoxia, in the form of oxygen-deficient zones (ODZs and anoxic basins or defined coastal areas, whose internal biogeochemical conditions favor and exacerbate the loss of nitrogen, including the greenhouse gas nitrous oxide (N_2O. The consequences for the biogeochemistry of the ocean and the global climate are potentially enormous although not entirely well established (Gruber and Galloway, 2008; Voss et al., 2013.

In the following sections, I introduce the reactions involved in the marine N cycle and the microorganisms known for performing them and give some perspective on the significance of nitrogen in the past oceans.

1.1.1 The nitrogen cycle in oxic waters

Atmospheric dinitrogen accounts for up to 94% (10^7 Tg N) of the nitrogen in the modern ocean (Gruber, 2008). N_2-fixation or diazotrophy is a reaction exclusively performed by prokaryotes, mostly bacteria, which converts the highly stable N_2 molecule into the bio-available ammonium (NH_4^+; Fig. 1). Only a few bacterial lineages are able to perform the reaction. Cyanobac-teria are a phylum of bacteria which perform oxygenic photosynthesis and

comprise the most important marine diazotrophs. They include the filamentous cyanobacterium *Trichodesmium* spp. and unicellular cyanobacteria (e.g. Group A–C, UCYN which are recognized as main contributor to N_2-fixation in the open tropical/subtropical oceans (Agawin et al., 2014; Benavides et al., 2011; Falcón et al., 2004; Montoya et al., 2004. It requires high activation energy to break the triple bond of the N_2 diatomic molecule, so that the reaction is favored in oligotrophic environments where organic forms of nitrogen are scarce. This condition makes cyanobacteria completely independent from organic sources for their energy, carbon and nitrogen requirements and gives them an extraordinary adaptive advantage in those environments that are depleted in nutrients or which experience fluctuations in their availability as is the case for the open ocean (Capone et al., 2005; Karl et al., 1997. As a result N_2-fixation has been estimated to provide between ca. 25–50% of the annual fixed nitrogen available in the Pacific and Atlantic gyres (Carpenter et al., 1999; Dore et al., 2002.

Most of the nitrogen fixed in the upper water column is efficiently recycled and remains in the euphotic zone, available for primary production (Fig. 1. The fraction which is not regenerated instead ends up sinking in the abyss where it is either remineralised into inorganic forms such as nitrate (NO_3^-, nitrite (NO_2^- and ammonium or it escapes the cycling been buried for a long term into the deep-sea sediments. Dissolved inorganic nitrogen (DIN however can be taken back to the upper waters if coastal upwelling occurs (Fig. 1. This process, initiated by physical forcing, has been proven to be sustained by the migration of diatom mats carrying DIN from nutrients-rich bottom waters (Moore and Villareal, 1996; Villareal et al., 1999. Close to the coasts NO_3^- is also provided by river discharge and together with NH_4^+ represent the most abundant form of nitrogen available for a wide diversity of either eukaryotic and prokaryotic phytoplankton which is not able of N_2-fixation and for heterotrophic bacteria (Zehr and Ward, 2002. All together this microbial diversity provides the source but also the sink for dissolved and particulate organic nitrogen (DON and PON; Fig. 1, a complex and highly variable pool of nitrogen in the ocean (Koper et al., 2004; McCarthy et al., 1998; Palenik and Morel, 1990a, 1990b; Zehr and Ward, 2002.

After the death of cells most organic nitrogen is remineralised back to NH_4^+ by heterotrophic bacteria. The NH_4^+ released in this process is the substrate for nitrification, a two-step process in which most of the oxidized nitrogen species in the ocean are generated. During nitrification NH_4^+ is firstly

oxidized to nitrite (NO_2^-) and then to nitrate (NO_3^-; Fig. 1). Different groups of microorganisms have been thought to be responsible for these two steps. The first step was thought to be performed exclusively by ammonia-oxidizing members of Proteobacteria (AOB), whereas the oxidation of nitrite to nitrate by nitrite-oxidizing bacteria (NOB; Fig. 1). This view has drastically changed when mesophilic ammonia-oxidizing archaea (AOA) of the Crenarchaeota phylum – now part of a phylum *per se* called Thaumarchaeota that includes three orders of autotrophic ammonia oxidizers (Brochier-Armanet et al., 2008; Spang et al., 2010) – have been recognized to dominate the marine mesopelagic zone (Karner et al., 2001; Venter et al., 2004). Subsequently the isolation of the first mesophilic Thaumarchaeota from a marine aquarium (Könneke et al., 2005) has confirmed the ability of these archaea to aerobically oxidize NH_4^+ to NO_2^- and Thaumarchaeota have been recognized as significant contributors to ammonia oxidation in the global ocean (Francis et al., 2005; Wuchter et al., 2006). Another groundbreaking discovery has been the high affinity of AOA for oxygen (O_2) and ammonium (Martens-Habbena et al., 2009; Park et al., 2010) which explain the dominance of AOA over AOB as ammonia oxidizers in the open oceans (Pester et al., 2011).

1.1.2. The nitrogen cycle in anoxic waters

Oxygen depletion may occur in different types of marine environments including defined coastal areas and semi-enclosed basins where the water is stratified due to reduced circulation, and often eutrophic, in some cases, due to human pressure. In these areas the amount of oxygen consumed by organic matter mineralization exceeds the oxygen supply, making the bottom of the water column anoxic, a condition increasingly documented worldwide. For instance, the Baltic Sea and the Black Sea are two of the largest permanently stratified anoxic basins in the world (Fig. 2a). The Black Sea water column, in particular, is 90% anoxic and hydrogen sulfide (HS^-) occurs naturally at the bottom of the basin, a condition known as euxinic (Fig. 2a). HS^- is known for be produced by sulfate-reducing bacteria re-mineralizing OM, making a total HS^- inventory of 4600×10^{12} g in the Black Sea (Volkov and Neretin, 2007).

Oxygen minimum zones (OMZs) represent a broad intrinsic phenomenon in the modern oceans. OMZs occur in poorly ventilated coastal and open regions of the ocean where the oxygen saturation of the water column is at its lowest (Wright et al., 2012). This typically occurs in the western boundary of continental margins, in the vicinity of highly productive waters fueled

by strong wind-driven upwelling systems, at depths of about 200 to 1000 meters (Fig. 2b). The upwelling has the effect of fertilizing the water surface and favors photosynthetic primary production to the point that respiratory O_2 demand during the degradation of OM exceeds O_2 availability (Wright et al., 2012). In many OMZ regions the oxygen concentration actually reaches zero, in which case the definition of oxygen-deficient zone (ODZ; Fig. 2b) appears more appropriate as these areas are considered functionally anoxic (Revsbech et al., 2009; Thamdrup et al., 2012; Ulloa et al., 2012). The Arabian Sea, the Eastern Tropical North and South Pacific (i.e. ETNP and ETSP) host the main permanent ODZs. ODZs are currently expanding in the tropical oceans worldwide (Helm et al., 2011; Karstensen et al., 2008; Stramma et al., 2008) as a consequence of ocean temperature increase linked to human-induced cli-mate change, which causes the decrease of O_2 solubility, and because of re-duced ventilation owing to thermal stratification (Keeling et al., 2010; Wright et al., 2012). Potential consequences of this ongoing trend include the decline of micro- and macro-fauna biodiversity, which has been estimated up to 50% of the total in the case of the main pelagic predators (Keeling et al., 2010; Stramma et al., 2011).

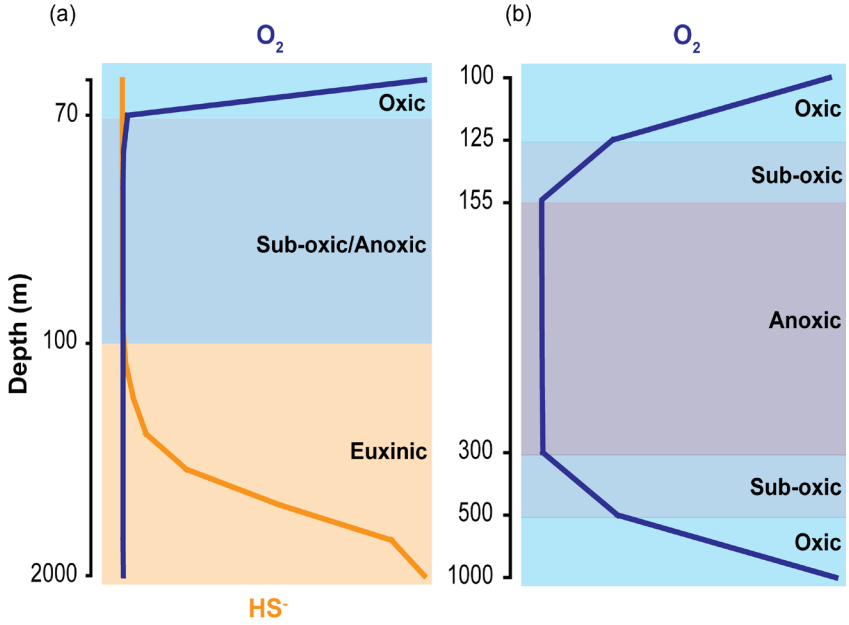

Figure 2. Schematical diagrams of the water column of (a) a generic anoxic/euxinic basin and of (b) a generic oxygen deficient zone (ODZ), revealing the concentration profiles of oxygen (O_2) and of hydrogen sulfide (HS^-).

Anoxic environments host a special part of the marine nitrogen cycle (Fig. 1), where up to 50% of marine bioavailable nitrogen loss occurs (Codispoti et al., 2001; Lam et al., 2009). When O_2 concentration declines below ca. 20 micromolar (μM), NO_3^- becomes energetically the best electron acceptor available for respiration, thus oxygen-depleted waters provide appropriate conditions to enable the substantial sink of nitrogen and eventually its loss from the ocean back to the atmosphere in the form of nitrogen-containing gases, including the greenhouse gas N_2O and N_2 (Mulder et al., 1995; Zumft, 1997). Until the mid-1990s denitrification was considered the only process responsible for the loss of N_2 in the atmosphere. The reaction consists in the stepwise reduction of NO_3^- to N_2 throughout NO_2^-, NO (i.e. nitric oxide) and N_2O as intermediates (Fig. 1). Each of these gases can also be an end product as every reaction is regulated differently at a genetic level depending on the surrounding environmental conditions, or depends on the presence or absence of specific genes in denitrifying microorganisms (Betlach and Tiedje, 1981; Härtig and Zumft, 1999; Hernandez and Rowe, 1987). Most denitrifiers are facultative anaerobes but the process is not exclusive of a specific taxonomic group, as either autotrophic and heterotrophic bacteria, archaea, but also eukaryotes as foraminifera and fungi are able to perform it (Cabello et al., 2004; Risgaard-Petersen et al., 2006; Shoun et al., 1992; Zumft, 1997).

The idea that denitrification is the only process responsible for the loss of nitrogen from the ocean was revolutionized after anammox bacteria were discovered in a wastewater treatment plant (Mulder et al., 1995). Until then NH_4^+ was considered as unreactive in anoxic conditions, although theoretically a good electron donor for NO_2^- or NO_3^- reduction to N_2 (Broda, 1977). Subsequently, these bacteria which anaerobically oxidize NH_4^+ using NO_2^- as electron acceptor (Fig. 1) have been found to occur in the Black Sea (Kuypers et al., 2003) and later to be ubiquitous in the modern ocean in oxygen-depleted waters and sediments, including some of the main ODZs (Hamersley et al., 2007; Kuypers et al., 2005b; Lam et al., 2009; Pitcher et al., 2011b). Anammox bacteria are a genetically homogeneous group of autotrophs belonging to the phylum of Planctomycetes (Strous et al., 1999, 2006). Their slow-growing lifestyle has been hypothesized as advantageous when sudden changes in substrate concentration occur, as they are not immediately reactive to them. This might also be the case when episodic oxygen intrusions occur in the ODZs (Ulloa et al., 2012). Accordingly, in the ETSP ODZ the anammox process was detected, though at low rates, even when denitrification was sporadic (Dalsgaard et al., 2012), suggesting that anammox has a constant

background role in the removal of nitrogen from anoxic systems.

Recently, the existence of specific species of the bacterial genus *Nitrospira* performing the complete ammonia oxidation (comammox) process have been identified (Daims et al., 2015; van Kessel et al., 2015; Pinto et al., 2016) but it remains uncertain how important they are in the oceanic N-cycle. Comammox bacteria were firstly isolated from a wastewater anoxic tank (Daims et al., 2015), but to date there is still scarce molecular support to the presence of these microorganisms in the marine environment and none in oxygen-depleted waters, although theoretically this process might be favored in oligotrophic environments (Bertagnolli and Ulloa, 2017; Kuypers, 2015).

Another metabolic pathway involving the transformation of NO_3^- mediated by microorganisms is the dissimilatory nitrate reduction to ammonium (i.e. DNRA; Fig. 1). This process is performed by a wide range of metabolically different bacteria and in different environments (Tiedje, 1988) and can occur as fermentative – which employs an organic substrate as electron donor – or as chemolithoautotrophic process – when the reduction of NO_3^- is coupled to the oxidation of reduced sulfur, including free sulfide (i.e. H_2S and S_2^-) and elemental sulfur (i.e. S) (Burgin and Hamilton, 2007). In both processes, the fate of the NH_4^+ generated is not clear and it has been hypothesized to be reconverted into NO_3^- by nitrification or to be assimilated into microbial biomass (Burgin and Hamilton, 2007). Two independent studies have detected the DNRA reaction, respectively, in the Benguela upwelling system and in the Peruvian ODZ where it was proposed as a significant source of NH_4^+ for the anammox bacteria (Kartal et al., 2007; Lam et al., 2009).

Recently, a new metabolic pathway was described in an enrichment culture of the anaerobic methanotrophic bacterium *Candidatus* Methylomirabilis oxyfera (Ettwig et al., 2010). It consists in a denitrification reaction in which no N_2O is produced because two NO molecules are converted into N_2 and O_2, which is then used to oxidize methane (CH_4; Fig. 1). A recent study has found genetic evidence of the presence of intra-aerobic methanotrophy in ODZ (Padilla et al., 2016).

Finally, in the last decade the occurrence of AOA in oxygen-depleted environments was confirmed by *in situ* studies (Beman et al., 2008; Coolen et al., 2007; Lam et al., 2007; Pitcher et al., 2011b), so that, in spite of being an aerobic process, nitrification performed by Thaumarchaeota is now considered a reaction that might occur also in suboxic waters (Fig. 1).

1.1.3. The nitrogen cycle of oceans in the geological past

Large scale water anoxia occurred already during the Paleozoic and the Permian-Triassic Transition (Strauss, 2006 and became more frequent in the Cretaceous and the Jurassic to which the term oceanic anoxic events (OAEs refers (Jenkyns, 1980; Schalnger and Jenkyns, 1976. During these events the ocean are believed to have been euxinic and resemble the present-day Black Sea (Sinninghe Damsté and Köster, 1998, the marine N cycling is likely to have been effected, like paleoclimate studies suggest (Kuypers et al., 2005a; Sachs and Repeta, 1999, and processes as the anammox reaction were likely forcing the sink of fixed nitrogen and consequently N_2-fixing cyanobacteria became dominant (Kuypers et al., 2005a. It is thus of great relevance to study the biogeochemistry of the modern anoxic oceans as this can give important clues on the biogeochemistry of past oceans when the OAEs occurred and in turn can provide valuable indications on the future global climate.

1.2. Methods used to investigate microbial communities in the ocean

The classical approach to study microorganisms and their physiological properties consists in obtaining pure cultures or enrichments from environmental samples. The main limitation to this approach is that in most cases pure cultures and enrichments are difficult to obtain. Moreover they provide only a partial view of the microbial diversity which might not be the most representative of the original environment (Rappé and Giovannoni, 2003. Accordingly, it has been estimated that only ~1% of all microorganisms in the environment can be cultivated *in vitro* (Amann et al., 1995; Stewart, 2012), severely limiting our knowledge of environmental microbial diversity (Rappé and Giovannoni, 2003).

Culture-independent approaches have proven successful to overcome these limitations and are used to investigate the abundance, diversity and metabolic activity of microbial communities directly in the environment. These techniques have been developed and improved especially in the last decades and employ a wide range of organic and inorganic molecules, which are used as biomarkers, and the incorporation of labelled substrates into biomarker molecules. In particular, the term biomarker refers to molecules which are specific to a certain microbial group, such as DNA, RNA and lipid molecules. Depending on its grade of specificity a biomarker can be diagnostic of a certain environment, or of a certain metabolic or biogeochemical process. Ideally,

biomarkers are also chemically stable enough to persist into the geological records. As any other approach, also culture-independent techniques are biased by intrinsic limitations (see Ranjard et al., 2000; Teske and Sørensen, 2008 among others. Therefore, the development of new techniques and the utilization of multi-approaches that complement each other for studying microbial communities in the environment are increasingly required.

In the following two sections the gene-based and lipid-based approaches employed in this thesis to investigate the microorganisms involved in the present and past marine nitrogen cycle are introduced.

1.2.1. Gene-based characterization of microbial communities involved in the marine nitrogen cycle

DNA has high taxonomic potential as biomarker and is diagnostic of living cells, which thing makes it especially suitable in environmental microbiology studies of the modern environments. Upon cell depth, DNA undergoes a rapid turnover thus its time of persistence in the records is highly debated making it less effective as biomarker in paleo-environmental studies (Hebsgaard et al., 2005; Willerslev et al., 2004). When microbial communities are studied directly in the field three types of basic information can be inferred thanks to DNA sequence analysis and their comparison to sequences that are already available in sequence databases. These are the quantification of the microbial components of a certain community, and the evaluation of the genetic and metabolic diversity of that community (see Junier et al., 2010 for a review). Quantitative PCR (qPCR) is instrumental to estimate the abundance of spe-cific groups of microorganisms through the real time quantification of select-ed DNA sequences (i.e. genes). Usually, the 16S rRNA gene and functional genes are targeted by this technique. The advantage of using the 16S rRNA gene sequence consists in the fact that the gene is ubiquitous in all domains of life and contains both variable regions, which are distinct in different groups of organisms, and highly conserved regions which can reveal the diversi-ty within microbial communities (Beman et al., 2008; Coolen et al., 2007; Hamersley et al., 2007; Mincer et al., 2007; Pitcher et al., 2011b). Moreover, 16S rRNA gene amplicon sequencing is the fundamental tool in the new gen-eration methods employed for high throughput sequencing which permit to study the diversity within microbial communities and the relative abundance of specific groups in a high resolution.

The use of functional genes provides information on the metabolism of the microorganisms which constitute a microbial community and can be applied if the DNA sequences of genes coding for the targeted enzymes are already known. The employment of functional genes has been essential in the study of the microorganisms involved in the marine N cycle. A membrane-bound putative ammonia monooxygenase (AMO) is the key-enzyme in the first step of nitrification (i.e. the aerobic oxidation of ammonium) in Bacteria (Rotthauwe and Witzel, 1997) and Archaea (Könneke et al., 2005; Venter et al., 2004; Yakimov et al., 2009), during which AMO catalyzes the oxidation of ammonium to the intermediate hydroxylamine. The gene *amo*A encoding for AMO, which exists with a bacterial and an archaeal variant, has been applied as biomarker of both Thaumarchaeota and nitrifying bacteria in numerous environmental studies to investigate the role of these groups in the N cycling of various oceanic regions (Francis et al., 2005; Mincer et al., 2007; Wuchter et al., 2006) including the principal ODZs and anoxic basins (Beman et al., 2008; Coolen et al., 2007; Lam et al., 2007, 2009; Pitcher et al., 2011b).

Other functional genes employed in the study of the microorganisms involved in the marine nitrogen cycle comprise the *hzs*A and *nir*S gene of anammox bacteria, which encode respectively for the hydrazine synthase (HZS) and the cytochrome *cd*1-containing nitrite reductase (NIR) (Kartal et al., 2011; Strous et al., 2006) and are successfully employed to detect anammox bacteria diversity and abundance in the marine environment (Harhangi et al., 2012; Lam et al., 2009, 2011). The cytochrome *cd*1-containing nitrite reductase, coded by the *nir*S gene, is also involved in the DNRA process, by catalyzing the reduction of NO_2^- to NO in the first steps of denitrification (Braker et al., 1998; Quaiser et al., 2011; Zumft, 1997). Finally, the *nir*S gene has been also used to study the diversity and to estimate the abundance of denitrifying microorganisms (Bulow et al., 2010; Castro-González et al., 2005; Jayakumar et al., 2009).

1.2.2. Intact polar lipids as biomarkers for the marine nitrogen cycle

Membrane lipids are also considered to be powerful biomarkers of the presence of specific organisms both in present and past ecosystems (Fig. 3a). In fact, these molecules hold a taxonomic potential which makes them suitable in microbial ecology studies in the modern environments, but they are also chemically stable, unlike DNA, to the point they can be preserved in the geological timescale in marine sediments and soils (Killops and Killops,

2005. Lipids are found in living cells as intact polar lipid molecules (IPLs; Fig. 3. IPLs are increasingly applied as biomarkers for tracing living bacteria and archaea in the marine environment and to study their role in the nitrogen cycle (Lipp et al., 2008; Lipp and Hinrichs, 2009; Pitcher et al., 2011b; Rossel et al., 2008; Schubotz et al., 2009. These molecules comprise a core lipid moiety (CL) bond to one or two polar headgroups (Fig. 3). Following the death of the cell the polar headgroup is readily hydrolyzed (Harvey et al., 1986 whereas the CL portion can persist in the environment thanks to its higher chemical stability and potentially preserve over geological time. These features on one hand make IPLs suitable biomarkers for specific living organisms, on the other make CL suitable as biomarkers of those organisms in the geological past. The time necessary for the head group to be released from the IPL depends on external environmental factors, including oxygen which is generally thought to accelerate the degradation process, and on the chemical structure of the head group moiety itself. Usually the polar headgroups of IPLs comprise phospho- or glyco-groups, of which the former type has been shown to degrade faster than the latter (Bauersachs et al., 2010; Harvey et al., 1986; Lengger et al., 2012; White et al., 1979.

In the membranes of bacteria and eukaryotes the CLs are fatty acid chains ester-linked to the polar headgroup containing glycerol unit in a *sn*-glycerol-1-phosphate (G1P configuration, and organized in a bilayer structure (Fig. 3b. The phospholipid-fatty acids (PLFAs can differ for carbon lengths, number of unsaturations, methylation and cyclization (Vestal and White, 1989. They can be analyzed by gas chromatography (GC)-flame ionization detection (FID and mass spectrometry (MS (Boschker et al., 1998 and their isotopic signature can be diagnostic of shifts in the bacterial and eukaryotic community composition (Boschker and Middelburg, 2002. These lipids have been extensively used as biomarkers to characterize bacteria and eukaryotic microorganisms in different environments (Kaur et al., 2005; Suzumura, 2005. Of particular mention are the highly specific CL synthesized by anammox bacteria, named ladderane lipids (Sinninghe Damsté et al., 2002d. These consist of three or five linearly concatenated cyclobutane rings bound through either an ester- or an ether-glycerol to polar headgroups (Fig. 4, forming the membrane of anammox intracellular compartment anammoxosome in which the anammox reaction occurs (Lindsay et al., 2001; van Niftrik et al., 2004; Sinninghe Damsté et al., 2002d.

In the membranes of archaea two possible basic structures can be recog-

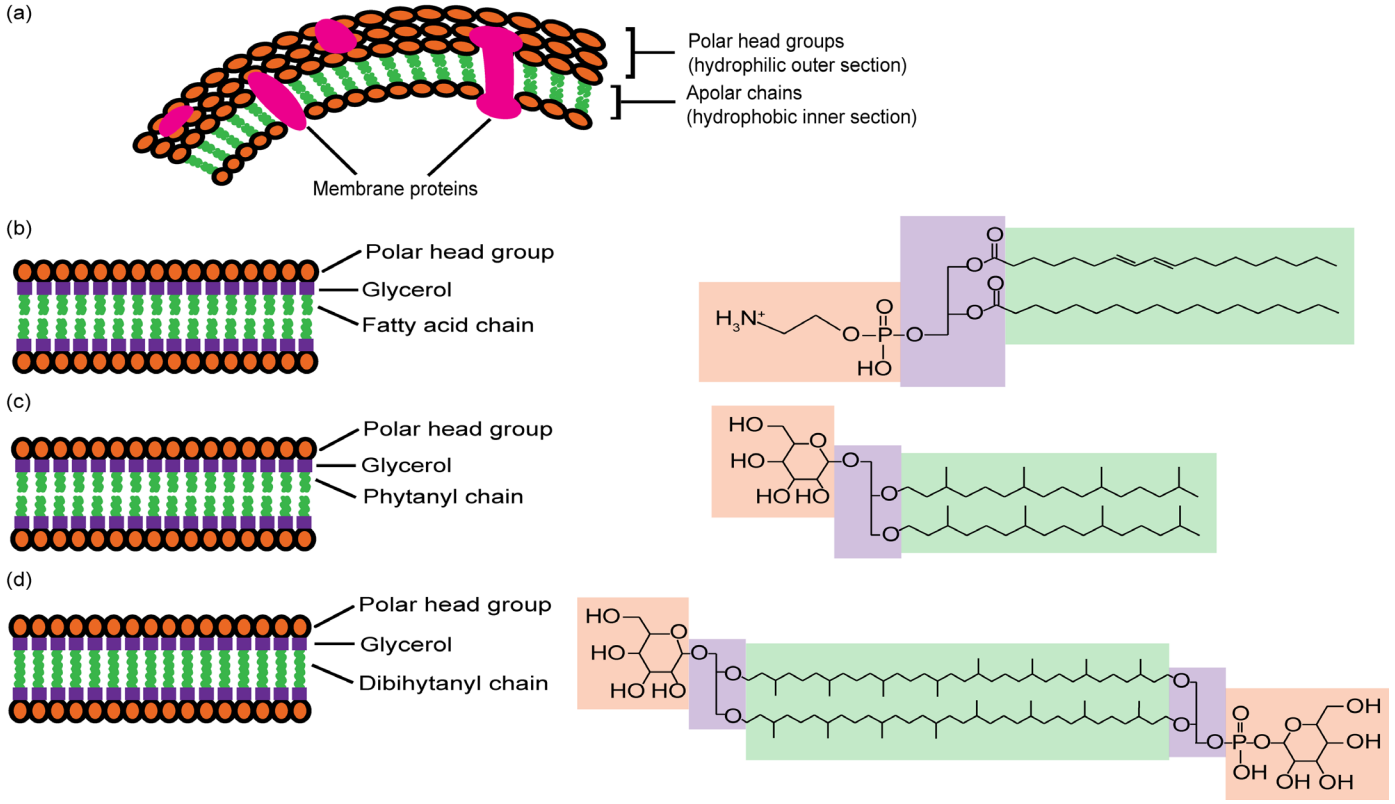

Figure 3. (a) A generic cell membrane including intact polar lipids (IPLs) and proteins. (b) A bacterial IPL structure consisting of a polar head group (phosphatidylcholine; orange) attached to the core lipid (CL) moiety (fatty acids; green) through an ester-glycerol bond (purple). (c) An archaeal IPL including an hexose sugar as polar head group (orange) attached through a ether-glycerol bond (purple) to the CL archaeol (green), and another (d) in which the polar head groups are respectively an hexose and a phospho-hexose sugar (orange) attached through two ether-glycerol moieties (purple) to the CL which is a GDGT-0 (green), forming a monolayer membrane.

nized: *sn*-2,3-diphytanylglycerol diether (i.e. archaeol; Fig. 3c) with phytanyl (C_{20}) chains in a bilayer structure, and *sn*-2,3-dibiphytanyl diglycerol tetra-ether (i.e. glycerol dibiphytanyl glycerol tetraether, GDGT; Fig. 3d), in which the two glycerol moieties are connected by two C_{40} isoprenoid chains and form monolayer membranes (Koga and Morii, 2007).

Although GDGTs are a common trait of the archaeal domain and are found ubiquitously in the oceans (Schouten et al., 2000, some differences exist among different groups of archaea which have important consequences for the use of GDGTs as biomarkers. In fact, isoprenoid GDGT containing 0–8 cyclopentane moieties (Fig. 4 are considered unspecific as they are commonly found in various archaeal groups, including extremophiles (Ellen et al., 2009; Lattuati et al., 1998; Schouten et al., 2007b, methanogens (Koga et al., 1993; Zhang et al., 2011, anaerobic methanotrophic (ANME archaea (Blumenberg et al., 2004; Pancost et al., 2001; Wakeham et al., 2004 and Thaumarchaeota (Schouten et al., 2008a; Sinninghe Damsté et al., 2002c. Crenarchaeol, the isoprenoid GDGT comprising four cyclopentane moieties and a cyclohexane moiety, instead, exclusively occurs in Thaumarchaeota (Schouten et al., 2008a; Sinninghe Damsté et al., 2002c.

The analysis of lipid biomarkers has greatly improved in the last decade and today it is possible to analyze both CL and IPLs using dedicated high performance liquid chromatography (HPLC-mass spectrometry (MS methods. For instance, IPL-derived core GDGTs can be analyzed, previous separation from the original IPL structure using silica gel chromatography and a mixture of hexane/EtOAc as eluent (Oba et al., 2006; Pitcher et al., 2009 followed by acid hydrolysis, by using a high pressure liquid chromatography coupled to a mass spectrometer equipped with an atmospheric pressure chemical ionization interface (HPLC/APCI-MS (Hopmans et al., 2000; Schouten et al., 2007a; Sturt et al., 2004. By adding an internal standard to the analyte it is also possible to quantify the IPL-derived GDGTs. Similarly, ladderane core lipids synthesized by anammox bacteria (Sinninghe Damsté et al., 2002d can be analyzed as fatty acid methyl esters (FAMEs by HPLC-APCI-MS^2 in selective reaction monitoring (SRM (Hopmans et al., 2006.

These methods, however, do not allow distinguishing which polar headgroups are attached to the CL analyzed. The development of methods in which HPLC is combined with electrospray chemical ionization mass spectrometry (HPLC/ESI-MS has been essential for analyzing IPLs with the polar head group still attached to the core (Boumann et al., 2006; Rütters et al., 2002;

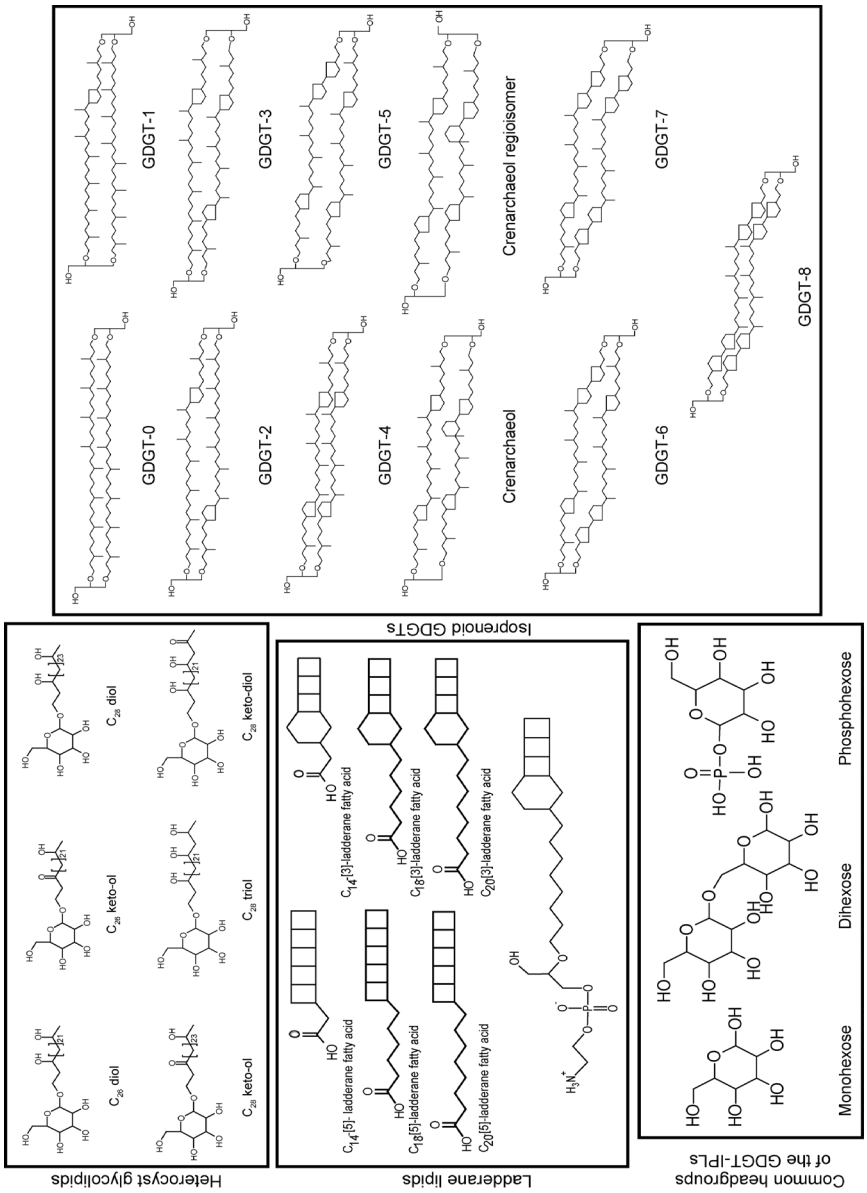

Figure 4. A selection of the most relevant lipid biomarkers of the microbial processes involved in the marine nitrogen cycle.

Sturt et al., 2004; Zink et al., 2003. For instance, the analysis of a culture of *Nitrosopumilus maritimus* – the first Thaumarchaeota representative to be isolated from a marine aquarium (Könneke et al., 2005 – with HPLC/ESI-MS^2 in selected reaction monitoring (SRM method has revealed the lipidome composition of AOA (Schouten et al., 2008a.

Specifically, the analysis has shown that monohexose (MH, dihexose (DH, phosphohexose (PH and hexose-phosphohexose (HPH sugars are the main polar headgroups of crenarchaeol (Fig. 4 and that, due to the labile nature of the phosphate bond and the specificity of crenarchaeol for Thaumarchaeota, HPH-crenarchaeol is the most suitable lipid biomarker to trace living Thaumarchaeota (Harvey et al., 1986; Schouten et al., 2010 in comparison with the more stable glycosidic-crenarchaeol and -GDGT-IPLs (Schouten et al., 2008a. Additionally, subsequent environmental studies have shown that HPH-crenarchaeol abundance corresponds well to DNA-based thaumarchaeotal abundance, confirming the efficiency of this IPL as biomarker of living Thaumarchaeota (Lengger et al., 2012; Pitcher et al., 2011b; Schouten et al., 2012.

In the case of the anammox bacteria the employment of HPLC/ESI-MS has been essential to be able to identify the most common polar headgroups which are found attached to the ladderane CLs, which comprise phosphatidylcholine (PC, phosphoethanolamine (PE and phosphoglycerol (PG (Boumann et al., 2006; Rattray et al., 2008. In particular, this approach has shown that the C_{20}-[3]-monoether ladderane lipid attached to a PC headgroup (Fig. 4 is a particularly suitable biomarker for living anammox bacteria in the marine environment (Pitcher et al., 2011b, additionally it can be analyzed by HPLC/ESI-MS^2 and quantified using an external PC-monoether ladderane standard (Jaeschke et al., 2009.

The analysis of the heterocyst glycolipids (HGs is another successful example of the application of the HPLC/ESI-MS^2 in the use of IPLs as biomarkers of the microbial processes involved in the marine nitrogen cycle (Bauersachs et al., 2009b. In fact, these lipids are excellent biomarkers of a selected group of diazotrophic cyanobacteria which form a cell structure called heterocyst where the fixation of N_2 takes place (Fig. 4). HGs consist in a sugar moiety – typically an hexose – glycosidically bound to a long *n*-alkyl chain with an even number of carbon atoms (26 to 32, which can include hydroxyl and keto functional groups attached at the C-3, ω-1 and ω-3 positions (Gambacorta et al., 1995, 1998. The resulting structure is particularly stable and

suitable for the use of HGs as paleo-biomarkers of the presence of N_2-fixing heterocystous cyanobacteria in the geological past. The recent development of a dedicated HPLC/ESI-MS^2 SRM method for the rapid analysis of these IPLs and its application to marine sediments from the Pleistocene and in lacustrine deposits from the Eocene has confirmed the potential for HGs preservation in sedimentary records (Bauersachs et al., 2009b, 2010).

1.3. Objectives and outline of the thesis

This thesis aims to develop and apply microbial biomarkers for the detection of environmentally significant microorganisms involved in the cycling of nitrogen in suboxic/anoxic environments of the present and past oceans, according to the principle that "the present is the key to the past". This approach allowed studying the interaction of microorganisms involved in the marine N cycle in suboxic settings and its consequences for the oceanic nitrogen budget. These results were used to go back in time and provide a detailed view on past marine nitrogen cycling and specifically on nitrogen-fixing cyanobacteria, providing further insight in the functioning of the past nitrogen and carbon cycles. Detailed understanding of these settings is important since the preservation of organic matter in these environments has often resulted in major perturbations of the carbon cycle with large climatic consequences.

Chapter 2 reports the occurrence and distribution of Thaumarchaeota and anammox bacteria in the water column of the ETNP ODZ. The two groups play important roles in the marine nitrogen cycling and the ETNP ODZ is a main nitrogen sink area worldwide. The investigation was performed by collecting suspended particulate matter (SPM) at different depths of the water column at a coastal and an open ocean station in high resolution, and analyzing the SPM for HPH-crenarchaeol and PC-monoether ladderane, the two specific IPLs of living Thaumarchaeota and anammox bacteria. Our study reveals that both the microbial groups were able to thrive at low (<1 μM) concentrations of oxygen. The comparison between coastal and open ocean stations indicates a clear niche segregation of Thaumarchaeota and anammox bacteria in the coastal waters of the ETNP, but a partial overlap of the two niches of these microbial species in the open water setting. The latter distribution suggests the potential for an interaction between the two microbial groups at the open ocean site, either as competition or cooperation.

Chapter 3 focuses on determining possible biological sources of archaeal

IPLs in the ETSP ODZ by comparing their composition – analyzed by Ultra high Pressure Liquid Chromatography coupled to high resolution mass spectrometry – with the local archaeal diversity and abundance as determined by 16S rRNA gene amplicon sequencing and quantitative PCR, at a coastal and an open ocean station sampled in high resolution for SPM. Our results reveal that in the stratified archaeal community of the ETSP Thaumarchaeota and euryarchaeotal MGII are abundant in the upper and deep oxic and suboxic waters, although with different subgroups, whereas euryarchaeotal MGIII and DPANN Woesearchaeota DHVE-6 are prominent within the core ODZ. The IPLs detected in the ETSP water column are also diverse and were tentatively assigned to the specific archaeal groups detected.

In **Chapter 4** the archaeal community of the Black Sea water column, sampled at high resolution, is investigated with the aim of expanding the knowledge on archaeal lipid biomarkers and determine the potential sources of those lipids. The Black Sea is the largest permanently stratified anoxic basin in the world and its water column is characterized by the presence of strong redox gradients, which makes it ideal to study microbial communities involved in alternative biogeochemical cycles. The archaeal community was evaluated by using combined gene-based and lipid-based approaches (i.e. 16S rRNA gene amplicon sequencing and qPCR; Ultra high Pressure Liquid Chromatography coupled to high resolution mass spectrometry) applied on the SPM collected by sampling the water column at high resolution. A complex archaeal community and unexpected lipid diversity were discovered to thrive in the Black Sea.

In **Chapter 5** the record of heterocyst glycolipids (HGs) in the Baltic Sea over the past 7000 years is examined for the first time and in high resolution. The Baltic Sea is a semi-enclosed anoxic basin characterized by recurring summer phytoplankton blooms, dominated by a few cyanobacterial species. These bacteria are able to use dinitrogen gas as the source for nitrogen and produce the very specific HGs as membrane lipids. By analyzing these lipids in a sediment core we wanted to evaluate the potential of HGs as biomarkers for cyanobacterial blooms in the past and its consequences for nitrogen fix-ation, and provide more detailed insight in the development of the Holocene Baltic Sea. Our investigation revealed that cyanobacterial blooms are not only occurring in the last decades but were common at times when the Baltic was connected to the North Sea.

Chapter 2

Intact polar lipids of Thaumarchaeota and anammox bacteria as indicators of N cycling in the eastern tropical North Pacific oxygen-deficient zone

Martina Sollai, Ellen C. Hopmans, Stefan Schouten, Richard G. Keil, Jaap S. Sinninghe Damsté

Published in *Biogeosciences*, 12, 4725–4737, 2015

doi:10.5194/bg-12-4725-2015

Abstract. In the last decade our understanding of the marine nitrogen cycle has improved considerably thanks to the discovery of two novel groups of microorganisms: ammonia-oxidizing archaea (AOA and anaerobic ammonia-oxidizing (anammox bacteria. Both groups are important in oxygen-deficient zones (ODZs, where they substantially affect the marine N budget. These two groups of microbes are also well known for producing specific membrane lipids, which can be used as biomarkers to trace their presence in the environment. We investigated the occurrence and distribution of AOA and anammox bacteria in the water column of the eastern tropical North Pacific (ETNP ODZ, one of the most prominent ODZs worldwide. Suspended particulate matter (SPM was collected at different depths of the water column in high resolution, at both a coastal and an open ocean setting. The SPM was analyzed for AOA- and anammox bacteria-specific intact polar lipids (IPLs, i.e., hexose-phosphohexose (HPH-crenarchaeol and phosphatidylcholine (PC-monoether ladderane. Comparison with oxygen profiles reveals that both the microbial groups are able to thrive at low (<1 μM concentrations of oxygen. Our results indicate a clear niche segregation of AOA and anammox bacteria in the coastal waters of the ETNP but a partial overlap of the two niches of these microbial species in the open water setting. The latter distribution suggests the potential for an interaction between the two microbial groups at the open ocean site, although the nature of this hypothetical interaction (i.e., either competition or cooperation remains unclear.

2.1. Introduction

The marine nitrogen cycle has been widely investigated, as nitrogen is one of the main limiting factors of primary production in the upper sunlit layers of the oceans (Arrigo, 2005; Codispoti, 1997 and the ocean accounts for about half of the global net primary production (Field et al., 1998; Gruber and Galloway, 2008). In the traditional view, the marine nitrogen cycle includes nitrogen fixation as the main input of nitrogen in the ocean and dinitrogen gas formed by denitrification as the main output, so that these two pathways are mainly responsible for the marine nitrogen budget status (Karl et al., 1997. Codispoti et al. (2001 suggested that, in the present day ocean, the nitrogen budget is not in a steady state but rather out of balance, with denitrification fluxes being underestimated. Nitrogen fixation is mediated by few microorganisms, including cyanobacteria, while denitrification is performed by a wide range of microorganisms with different metabolic features, able to

switch from aerobic to anaerobic nitrate (NO_3^--dependent respiration modes (Lam and Kuypers, 2011. In this classical view, nitrification, representing the major oxidative part of the cycle, connecting organic nitrogen to NO_3^- (Codispoti et al., 2001; Lam and Kuypers, 2011, was seen exclusively as an aerobic process carried out by ammonia-oxidizing bacteria (AOB and nitrite-oxidizing bacteria, members of the β- and γ-proteobacteria. The nitrification reaction is divided into two steps, performed by distinct bacterial groups. In the first part, ammonium (NH_4^+ is oxidized to nitrite (NO_2^-, whereas in the second NO_2^- is oxidized to nitrate (NO_3^-. In both cases, oxygen serves as the electron acceptor, although AOB have been reported to perform nitrification in suboxic conditions (Lam et al., 2007; Schmidt and Bock, 1997.

The overall understanding of the marine nitrogen cycle has substantially changed in the last decade (Fig. 1. Specific archaea were discovered to be important players in the marine nitrogen cycle (Venter et al., 2004) as some of them perform nitrification in the marine water column and sediment (Francis et al., 2005; Könneke et al., 2005; Wuchter et al., 2006). The group of archaea capable of nitrification has recently been relocated in a separate phylum named Thaumarchaeota (Brochier-Armanet et al., 2008; Spang et al., 2010). Compared to their bacterial counterpart, ammonia-oxidizing archaea (AOA) are often more abundant in the ocean (Karner et al., 2001; Lam et al., 2007;Wuchter et al., 2006), accounting for 20% of picoplankton and 40% of the estimated total number of cells (Karner et al., 2001). These microorgan-isms are able to cope with low-oxygen conditions (Coolen et al., 2007; Lam et al., 2007; Park et al., 2010; Pitcher et al., 2011b; Sinninghe Damsté et al., 2002a), have low substrate requirements (Martens-Habbena et al., 2009) and are able to utilize a highly energy-efficient CO_2-fixation pathway (Könneke et al., 2014); new coastal marine AOA isolates show obligate mixotrophy and vary in their adaptive ability to different environmental parameters (Qin et al., 2014). All these features have been suggested to provide a reason for the observed dominance of AOA over AOB as ammonia oxidizers in the open oceans (Könneke et al., 2014; Pester et al., 2011).

Moreover, a "novel" process in the nitrogen cycle, named anammox, was discovered. Anaerobic ammonia oxidizing (anammox) bacteria are a unique group of microorganisms member of the order Planctomycetales (Strous et al., 1999). They are able to oxidize ammonium (NH_4^+) to molecular nitrogen (N_2) under anoxic conditions, using nitrite (NO_2^-) as the electron acceptor (van de Graaf et al., 1995). Anammox bacterial activity has been detected in

marine anoxic sediments and waters (Dalsgaard et al., 2003; Kuypers et al., 2003; Thamdrup and Dalsgaard, 2002 and has been recognized to contribute, along with denitrifying bacteria, to the loss of N_2 from the ocean (Galán et al., 2009; Hamersley et al., 2007; Kuypers et al., 2005b; Lam et al., 2009; Thamdrup et al., 2006. Despite different oxygen tolerances, anammox bacteria and Thaumarchaeota have been observed to coexist in different settings, particularly in oxygen-deficient zones (ODZs and anoxic waters (Coolen et al., 2007; Francis et al., 2005; Lam et al., 2007; Pitcher et al., 2011b;Woebken et al., 2007. These two microbial groups can potentially benefit from each other, because the thaumarchaeotal nitrification might be coupled with the anammox process by providing the NO_2^- anammox bacteria need and, at the same time, consume oxygen, to which anammox bacteria are sensitive. Alternatively, when nitrite is provided to anammox by other sources, the two groups might compete for NH_4^+ (Yan et al., 2012.

In this study we investigated the occurrence and depth distribution of Thaumarchaeota and anammox bacteria in the eastern tropical North Pacific (ETNP ODZ, one of the most extended ODZs in the contemporary ocean. The presence of AOA and anammox bacteria has been reported in the ETNP ODZ by a few studies (Beman et al., 2008, 2012, 2013; Francis et al., 2005; Podlaska et al., 2012; Rush et al., 2012 and the significance of the two microbial groups to local marine nitrogen cycling is starting to be elucidated for other ODZs (Dalsgaard et al., 2003; Galán et al., 2009; Kalvelage et al., 2013; Kuypers et al., 2003, 2005b; Lam et al., 2007, 2009; Pitcher et al., 2011b; Ward et al., 2009. However, the spatial distribution and the possible co-occurrence of the two groups in the ETNP have not been investigated in detail, nor has the relative contribution of AOA and anammox to the local N cycle and their possible interactions. To the best of our knowledge only one study so far has concurrently examined the presence of the two microbial groups in the southern part of the ETNP (Podlaska et al., 2012). Other studies on the ETNP ODZ have investigated the presence of AOA along a north–south tran-sects following the coastal line of southern California (Beman et al., 2008, 2012, 2013) and the occurrence of anammox bacteria in the southern ETNP ODZ (Rush et al., 2012). These studies did not investigate the occurrence of AOA and anammox bacteria at true open ocean sites, and a comparison of AOA and anammox bacteria dynamics between coastal and open-ocean wa-ters is still missing.

To fill this gap in the current knowledge we performed high-resolution

water sampling, at both coastal and open-ocean settings in the ETNP ODZ. To trace the two microbial groups we applied intact polar lipids (IPLs specific for these groups, which have proven to be good biomarkers in various settings (Bale et al., 2013; Buckles et al., 2013; Lengger et al., 2012; Pitcher et al., 2011b, c. Anammox bacteria produce unique ladderane fatty acids which contain 3–5 concatenated cyclobutane moieties (Sinninghe Damsté et al., 2002d. They are attached to the glycerol backbone with polar headgroups comprising phosphocholine (PC and phosphoethanolamine (PE (Boumann et al., 2006; Rattray et al., 2008. Thaumarchaeota produce also specific biomarker lipids, i.e., crenarchaeol, a glycerol dibiphytanyl glycerol tetraether (GDGT lipid containing a cyclohexane moiety in addition to four cyclopentane moieties (de la Torre et al., 2008; Pitcher et al., 2010; Schouten et al., 2008; Sinninghe Damsté et al., 2002d, c. Attached to crenarchaeol are various polar headgroups such as monohexose (MH, dihexose (DH and hexose-phosphohexose (HPH) (Schouten et al., 2008a), with the latter being the most suitable for tracing living active cells (Pitcher et al., 2011a). By applying these specific IPLs, i.e., HPH-crenarchaeol and PC-monoether ladderane, we investigated the depth habitat of Thaumarchaeota and anammox bacteria, respectively, in the ETNP ODZ and the factors controlling their ecological niche.

2.2. Material and Methods

2.2.1. Environmental setting of the ETNP

The ETNP ODZ is one of the thickest in the contemporary ocean and extends to depths as deep as ~1000 m. Geographically it ranges from ~25° N (i.e., Baja California to ~10° N (i.e., Costa Rica and from ~160° W in the North Pacific Ocean to the coast of Mexico and Costa Rica. It is a permanent feature of the eastern tropical Pacific region (Paulmier and Ruiz-Pino, 2009. The region is important for its role in the global carbon cycle, for its involvement in El Nio–Southern Oscillation, and it is economically relevant for fishery (Fiedler and Lavn, 2006. A shallow and strong thermocline causes water stratification and weak exchanges of nutrients and oxygen between surface waters and sub-thermocline layers, which are poorly ventilated (Lavn et al., 2006. This feature is further exacerbated by Ekman pumping, which causes coastal and open-ocean upwelling (Lavn et al., 2006.

The hydrology of the eastern tropical Pacific is influenced by water circulation features and by strong winds in the part close to the American continent (Kessler, 2006. The ETNP ODZ comprises part of the North Pacific subtropical gyre; specifically, it is delimited south-eastern by the California Current (CC, the North Equatorial Current (NEC and the North Equatorial Countercurrent (NECC (Karstensen et al., 2008. The boundary area where the CC, flowing along the coast of the Baja California and northern Mexico, encounters the NEC is characterized by Ekman transport westward and upwelling mainly off the Californian coast and in a weakened magnitude off the northern Mexico coast (Kessler, 2006; Lavn et al., 2006. Our sampling area lies in this transition region; however the upper water circulation in this region is not yet fully understood (Kessler, 2006. Although ODZs have now been studied for almost a century, it has only recently become possible to determine *in situ* concentration in these areas to the accuracy of nanomolar O_2 (Revsbech et al., 2009. This has allowed for it to be proven that ODZs, including the ETNP, are functionally devoid of oxygen, although respiratory rates indicate that aerobic metabolisms successfully occur, even in such extreme conditions (Canfield et al., 2010; Jensen et al., 2011; Revsbech et al., 2009; Thamdrup et al., 2012; Tiano et al., 2014.

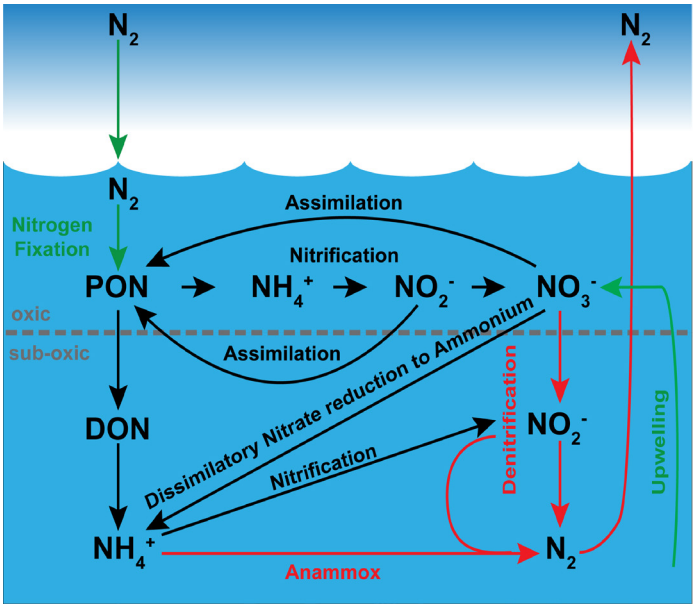

Figure 1. The marine biogeochemical nitrogen cycle. The main redox reactions involved are included: in green are the processes responsible for gains of nitrogen to the ocean, and in red are the losses. Modified from Arrigo (2005).

2.2.2. Sampling

Sampling was performed at twelve stations during the eastern tropical North Pacific (TN278 cruise (*R/V Thomas G. Thompson*, March–April 2012 (Fig. 2a. The cruise route was split into two legs, with the former one comprising six sampling stations (Fig. 2b, in very close proximity to each other, in coastal waters, northwest of the departure port of Manzanillo (Colima, Mexico, and the latter including six sampling stations, clustered closely together, in open- ocean waters southwest of the departure port, around the area known as the Moctezuma Trough (Fig. 2c. SPM samples were collected on pre-ashed 0.7µm pore size glass fiber (GF) filters, mounted in McLane WTS-LV *in situ* filtration systems. At each sampling site four McLane pumps were deployed simultaneously at different depths (Table 1). The volume of water filtered varied according to the depth and the material collected (Table 1). Upon the recovery of the pumps the GF filters were removed, split into two halves and frozen at −40 °C.

Physical parameters of the water column were recorded using conductivity–temperature–density (CTD equipment (SBE-911, Sea-Bird Electronics; dissolved-oxygen depth concentrations were measured by a SBE 43 electrochemical sensor mounted on the CTD rosette. Sensor oxygen concentrations were calibrated against on-deck Winkler titrations. The data reported here do not take into account recent evidence that these techniques (i.e., Clark electrodes, Winkler titrations overestimate oxygen at the very lowest concentrations (Tiano et al., 2014. Water samples for inorganic nutrient profiles were collected using 24 × 10 L Niskin bottles mounted on a rosette to the CTD. The CTD was cast shortly before or after the deployment of the McLane pumps. In case this was not possible, data from another station, the closest in time and space to that of the deployed *in situ* pumps, were used. This means that at some sites the depths sampled for nutrients data do not always directly corre-spond to the depths at which SPM was sampled with the *in situ* pumps (Table 1). The detection limits for NO_3^-, NO_2^-, and NH_4^+ were respectively 0.08, 0.01 and 0.07 µM. The electrochemical oxygen sensor SBE 43 has a detection limit of 1–2 µM (Tiano et al., 2014).

2.2.3. Intact polar lipids analysis

The intact polar lipids were extracted from freeze-dried SPM filter halves using a modified Bligh–Dyer technique as described in Sturt et al. (2004 with

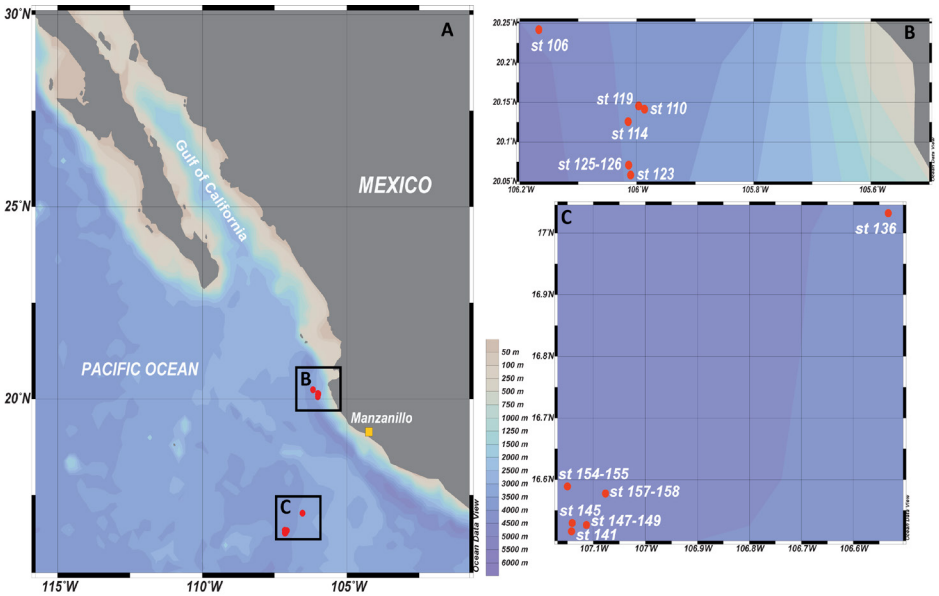

Figure 2. (a) Map of the sampling area of the eastern tropical North Pacific cruise (March–April 2012) and sampling stations (red dots); panel (b) shows the coastal site and panel (c) the open-ocean site. The coastal sampling site (i.e., st 106, st 110, st 114, st 119, st 123, and st 125–126) is placed in the area between 20°25.00' N and 105°60.00' W; the open-ocean sampling site (i.e., st 136, st 141, st 145, st 147–149, st 154–155, st 157–158) is placed in the area between 17°00.00' N and 106°60.00' W.

some adjustments as described in Schouten et al. (2008a). Briefly, a known volume of methanol (MeOH:dichloromethane (DCM:phosphate buffer (P buffer) (2 : 1 : 0.8, *v*/*v*/*v* was added to the filter in a glass centrifuge tube and the total lipid contents were extracted in a sonication bath for 10 min. After centrifugation for 3 min at 2000 rpm the supernatant was removed. The extraction was repeated two more times and the supernatants combined. To induce separation of the combined supernatant into two phases, additional DCM and P buffer were added to a new volume ratio of 1 : 1 : 0.9 DCM:MeOH: P buffer. The mixture was centrifuged for 2 min at 3000 rpm, after which the DCM layer was removed. The procedure was repeated two more times and the combined DCM phases were collected in a round bottom flask, reduced under rotary vacuum and completely dried under N_2 (Schouten et al., 2008a; Sturt et al., 2004).

The IPLs were analyzed directly in the extract using a high-performance liquid chromatography (HPLC–electrospray ionization (ESI/triple-quadrupole mass spectrometry (MS in selected reaction monitoring (SRM mode

as described by Pitcher et al. (2010). In order to minimize possible variations in the IPLs response factors, the extract was analyzed in the same batch. Briefly, an Agilent (Palo Alto, CA, US) 1100 series LC equipped with a thermostat-controlled auto-injector was used coupled to a Thermo TSQ Quantum EM triple-quadrupole MS equipped with an Ion Max source with ESI probe. The SRM method for the crenarchaeol IPLs was specifically targeting HPH-crenarchaeol (Schouten et al., 2008a; Pitcher et al., 2010). Due to the lack of a standard, HPH-crenarchaeol was quantified as the integrated IPL area peak response units per Liter (i.e., r.u. L^{-1}), revealed the relative depth distribution of the lipid biomarker in the water column but not providing information on its absolute abundance. The anammox-specific membrane lipid C_{20}-[3]-ladderane with a PC-monoether was analyzed according to Jaeschke et al. (2009). The intact ladderane monoether lipid was quantified referring to an external calibration curve of an isolated C_{20}-[3]-ladderane PC-monoether standard (Jaeschke et al., 2009).

2.3. Results

2.3.1. Physicochemical parameters of the sampling sites

During the ETNP (TN278) cruise in March–April 2012 the water column of the ETNP ODZ was sampled at high resolution for SPM, at depths from 20 to 2000 m in coastal waters and from 50 to 2500 m in open ocean waters at a number of geographically nearby stations (Fig. 2; Table 1). To compile all our data in two (coastal and open ocean) composite profiles, we report our nutrient (Fig. 3a–c, g–i), oxygen (Fig. 3d and l), and lipid SPM (Fig. 3e, f and m, n) data relative to the potential density anomaly, σθ (kg m^{3-}), of the water masses sampled at each of the coastal or open ocean stations. In the upper water column, values for σθ differ at the two sampling sites as a consequence of differences in salinity (data not shown).

For both locations, the oxygen profiles (Fig. 3d and l) obtained by an oxygen electrochemical sensor mounted on the CTD of the nearby stations were virtually identical. Station 106, which is slightly further away from the other coastal stations (Fig. 2), is an exception since the upper oxycline is located at a σθ of 25.5, ca. 30 m deeper than at the other stations. For the other coastal stations the oxycline occurs in shallow waters at a σθ of 25.0, i.e., ~30 m depth, while for the in open-ocean waters it is located at σθ 25.5, which core-

Table 1. Sampling locations for SPM during the eastern tropical North Pacific cruise aboard the *R/V Thomas G. Thompson* (March–April 2012). For each sampling location the table reports the depth of SPM sampling, the volume of water filtered by each pump deployed, and physical parameters of the water at these depths, i.e., temperature and oxygen concentration (O_2). Nutrients concentrations, i.e., nitrate (NO_3^-), nitrite (NO_2^-) and ammonium (NH_4^+) and corresponding station and depth of sampling, when available, are also reported. n.d.: not detected. [a] Sample not analyzed for lipids.

Station	Location	Temperature CTD (°C)	Depth of SPM sampling (m)	Water filtered (L)	O_2 (μM)	Depth of nutrients sampling (m)	NO_3^- (μM)	NO_2^- (μM)	NH_4^+ (μM)
106	20°14.49' N 106°10.00' W	15	70	1627.72	0.75	n.d.	n.d.	n.d.	n.d.
		13	105	200.00	0.81	n.d.	n.d.	n.d.	n.d.
		10	365	699.50	0.97	n.d.	n.d.	n.d.	n.d.
110	20° 08.48' N 105° 59.18' W	14	70	128.50	0.67	50	20.14	2.32	0.02
		13	125	336.14	0.77	100	15.27	7.06	0.01
		12	150	511.79	0.86	150	20.13	5.12	0.00
		6	710	999.50	1.05	n.d.	n.d.	n.d.	n.d.
114	20° 07.54' N 106° 00.84' W	18	25	104.10	26.20	n.d.	n.d.	n.d.	n.d.
		17	35	97.40	0.78	n.d.	n.d.	n.d.	n.d.
		15	45	255.51	0.71	n.d.	n.d.	n.d.	n.d.
		15	55	230.50	0.71	n.d.	n.d.	n.d.	n.d.
119	20° 08.72' N 105° 59.77' W	14	80	211.60	0.72	100	16.55	5.74	0.00
		8	500	932.50	0.95	501	31.27	1.50	0.00
		5	800	595.50	1.61	800	43.66	0.00	0.00
		5	1000	1069.38	8.78	1001	45.42	0.00	0.00
123	20° 03.50' N 106° 00.59' W	19	20	41.50	51.16	n.d.	n.d.	n.d.	n.d.
		14	60	181.70	0.71	n.d.	n.d.	n.d.	n.d.
		13	90	179.81	0.76	n.d.	n.d.	n.d.	n.d.
		12	200	210.50	0.87	n.d.	n.d.	n.d.	n.d.
125-126	20° 04.26' N 106° 00.81' W	20	15a	¬	72.05	15	12.55	0.96	0.36
		n.d.	1300	1003.00	n.d.	n.d.	n.d.	n.d.	n.d.
		n.d.	1600a	¬	n.d.	n.d.	n.d.	n.d.	n.d.
		n.d.	2000	859.66	n.d.	n.d.	n.d.	n.d.	n.d.
136	17° 01.95' N 106° 31.96' W	14	110	755.19	0.74	110	21.54	1.07	0.00
		13	150	747.50	0.74	160	19.24	4.74	0.00
		11	250	987.99	0.87	200	21.30	3.37	0.00
		10	350	714.90	0.88	300	23.39	1.97	0.00

141	16° 30.98' N 107° 08.52 W	23	60	482.64	108.13	60	7.00	1.14	0.16
		16	90	997.00	0.88	80	22.91	0.45	0.00
		15	105	496.00	0.77	100	24.20	0.09	0.00
		12	200	864.96	0.89	181	23.62	5.21	0.00
145	16° 31.78' N 107° 08.45'W	26	50	368.00	189.01	n.d.	n.d.	n.d.	n.d.
		21	65a	¬	69.83	n.d.	n.d.	n.d.	n.d.
		13	155	768.44	0.99	n.d.	n.d.	n.d.	n.d.
		n.d.	710	1417.63	n.d.	n.d.	n.d.	n.d.	n.d.
147-149	16° 31.60' N 107° 06.80' W	13	170	668.00	0.84	175	27.54	4.04	0.00
		5	990	1249.18	7.30	n.d.	n.d.	n.d.	n.d.
		4	1100	689.50	13.11	1100	46.27	0.01	0.00
		n.d.	2500	567.81	n.d.	n.d.	n.d.	n.d.	n.d.
154-155	16° 35.34' N 107° 08.98' W	25	55	382.80	176.12	n.d.	n.d.	n.d.	n.d.
		15	100	686.29	1.09	104	23.40	0.65	0.00
		13	145	334.50	1.06	n.d.	n.d.	n.d.	n.d.
		n.d.	160	612.86	n.d.	n.d.	n.d.	n.d.	n.d.
157-158	16° 34.66'N 107° 04.61' W	19	80	3287.62	3.49	n.d.	n.d.	n.d.	n.d.
		13	140	1178.02	0.75	141	25.70	3.89	0.02
		9	450	3484.84	0.96	n.d.	n.d.	n.d.	n.d.
		8	550a	¬	1.02	n.d.	n.d.	n.d.	n.d.

sponds to ~100 m depth. Because of the virtual identical oxygen–σθ profiles, it was decided that all the data for the coastal (except for station 106) and open-ocean stations could be combined in presenting the nutrient concentrations and IPL data from SPM. In this way we provide an expanded view of the vertical distribution of the two microbial species along the water column.

In the upper coastal waters the oxygen concentration varies between 250 and 50 μM until σθ 23.5 (i.e., ~15–20 m), then drops to values below 20 μM at the upper oxycline (Fig. 3d). In this setting, the ODZ spans from σθ 25.0 to 27.0 (i.e., between ~35 and ~800 m), with a minimal oxygen concentration below 1μM in the core (Fig. 3d) (see also Tiano et al., 2014). Below 850 m, σθ is between 27.0 and 27.5 and the oxygen concentration increases gradually again until ~75 μM, at 2000 m depth (Fig. 3d). In the open-ocean waters, oxygen concentration is stable at ~200 μM until σθ 22.5, at ~55 m depth, and rapidly decreases to values close to 1 μM at σθ 25.5, at 100 m depth. The ODZ extends until σθ 27.0, at 850 m depth. Below the lower oxycline the oxygen concentration increases again to ~120 μM at 3000 m depth, where σθ ranged between 27.5 and 28.0 (Fig. 3l).

Nutrient concentration data (i.e., NO_3^-, NO_2^-, NH_4^+ from different stations were combined in one coastal and one open ocean setting, as described above for the oxygen depth profiles. The resulting profiles show distinct patterns (Fig. 3a–c, g–i. In both coastal and open waters, nitrate is the most abundant nitrogen species and shows two maxima at different σθ (Fig. 3a and g). In coastal waters the first maximum of ~25 μM occurs at the upper oxycline at σθ 25, then the concentrations decrease to 15–20 μM until σθ 26.5. The second maximum of ~45 μM occurs at σθ 27.4, just below the lower oxycline (i.e., at 1000 m depth (Fig. 3a. In open ocean waters the trend in nitrate appears similar to the one in the coastal waters, although some differences can be noticed (Fig. 3g. The first maximum (i.e., ~25 μM in this case is broader and deeper, spanning from σθ 24.5 to 26, where the upper oxycline is located. The second deeper maximum (i.e., ~50 μM also occurs where the waters start to be re-oxygenated (i.e., σθ 27.4, depth 1100 m)Like for nitrate, the profiles of nitrite are slightly different for the coast and open-ocean waters (Fig. 3b and h). In the former setting the shallow maximum occurs at σθ 24.6, at declining oxygen concentrations. The peak is only ~1 μM and rather narrow. The lower peak of ~8 μM is located at σθ 26 (i.e., 88 m depth) in the core ODZ (Fig. 3b). The first nitrite maximum in the open ocean reaches 1 to 2 μM and spans from fully oxygenated waters to the oxycline (i.e., σθ from ~23 to ~25). The deeper maximum on the other hand (i.e., ~6 μM) occurs in the upper ODZ (i.e., σθ 26.2) (Fig. 3h). Finally, at both sampling sites NH_4^+ concentrations are mostly below the detection limit of 0.07 μM (Fig. 3c and i), with the exception of a few data points at the costal oxycline (i.e., σθ 24.6) and in the open water where the oxygen decreases, and the NH_4^+ concentra-tions are respectively 0.6 and ~0.1 μM.

2.3.2. Biomarker lipid profile

The SPM for biomarker analysis was collected on 0.7 μm pore size GF filters. Limitations related to the use of 0.7 μm filters to collect archaeal living cells have been reported (Ingalls et al., 2012; Schouten et al., 2012, as the typical size of thaumarchaeotal cells is <0.6 μm (Könneke et al., 2005 and they are suggested to be predominantly free-living during their lifetime (Ingalls et al., 2012. Although the pore size tends to diminish as the particulate material accumulates, the employment of 0.7 μm filters likely causes an underestimation of the archaeal population and thus archaeal IPL abundance (Schouten et al., 2012. However, Pitcher et al. (2011b showed that depth

profiles of HPH-crenarchaeol, analyzed on SPM collected using 0.7 μm GFF filters, in the Arabian Sea ODZ were similar to the profile of thaumarchaeotal genes, analyzed on SPM collected using 0.2 μm filters (Pitcher et al., 2011b). Therefore, our results are likely still suitable to probe the depth habitat of Thaumarchaeota. Figure 3e and m show HPH-crenarchaeol vertical profile for the coastal and the open-ocean sites, respectively. In the coastal setting, HPH-crenarchaeol has a maximum in abundance at the interface between the oxycline and the upper ODZ, where σθ is ~25 (i.e., ~30 m depth) (Fig. 3e). In the open ocean setting, HPH-crenarchaeol starts to increase at declining oxygen concentrations and peaks at the base of the oxycline (i.e., at σθ 25.8 and 100 m depth). Deeper in the water column (i.e., at σθ 27.4 corresponding to ~1000 m water depth) a secondary minor maximum in HPH-crenarchaeol was detected (Fig. 3m).

In the coastal waters, the ladderane PC-monoether concentration stays low, except for one data point (i.e., ~17 pg L^{-1} at 55 m depth), until the upper ODZ, where it starts to increase to its maximum (i.e., ~251 pg L^{-1}) at σθ 26.4 in the core ODZ (i.e., 150 m depth) (Fig. 3f). In the open ocean, the PC-monoether maximum in concentration (i.e., ~122 pg L^{-1}) is located at the oxycline (i.e., at σθ 25.9 and 105 m depth).

2.4. Discussion

2.4.1. Depth distributions and abundance of AOA and anammox bacteria in the ETNP

In this study we have been able to investigate concurrently, for the first time, the vertical distribution of AOA and anammox bacteria in both coastal and open waters of the ETNP ODZ. The IPL-biomarker profiles show that AOA and anammox bacteria are present in the region and partially coexist along the water column (Fig. 3e, f and m, n). Such a distribution has already been observed in other dysoxic or anoxic marine systems worldwide such as the Black Sea and the ODZs of the eastern tropical South Pacific (ETSP) and the Benguela upwelling system (Lam et al., 2007, 2009; Woebken et al., 2007), whereas in the southern part of the ETNP ODZ (Podlaska et al., 2012) and in the Arabian Sea (Pitcher et al., 2011b) the two microbial groups are reported to thrive at different water depths. In the northern ETNP our IPL depth

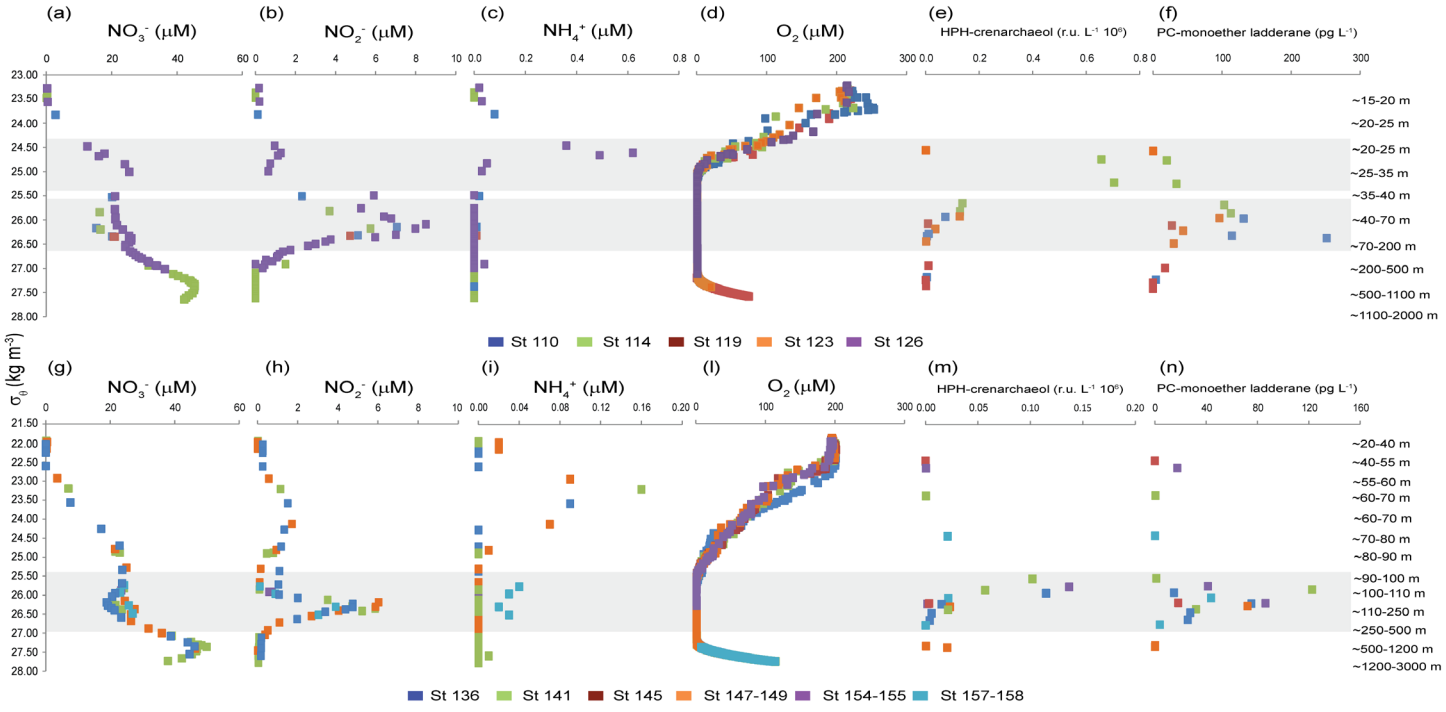

Figure 3. Concentration profiles of (a, g) nitrate (NO_3^-), (b, h) nitrite (NO_2^-), (c, i) ammonium (NH_4^+), (d, l) oxygen, (e, m) hexose- phosphohexose (HPH)-crenarchaeol, and (f, n) phosphocholine (PC)-monoether ladderane according to the potential density anomalies (σθ) of the water column of the ETNP. The corresponding depths intervals are reported on the right side of the figure as a reference. The upper panels (a–f) provide an overview of the complete water column (2000 m) of the coastal sampling site; the lower panels (g–n) show the complete water column (3000 m) relative to the open-ocean sampling site. All profiles are obtained by combining the coastal and the open-ocean stations sampled. The gray bars highlight the main differences observed between the two sampling sites with respect to the distribution of the two microbial species: i.e., on the one hand a clear niche segregation of AOA and anammox bacteria in the coastal waters of the ETNP and on the other hand a partial overlap of the two niches of these microbial species in the open-water setting.

profiles highlight some substantial differences in the distribution and abudance of the two groups between the different settings.

In the coastal setting, the two microbial groups show clear niche segregation in the upper part of the water column. Here, AOA thrive at the bottom of the oxycline, at a σθ of ~25, whereas anammox bacteria are just starting to increase in abundance at that point and exhibit a clear maximum only in the core ODZ (Fig. 3e and 3f), where σθ has shifted to ~26. The trend of our coastal HPH-crenarchaeol depth profile agrees with previously reported data for thaumarchaeotal 16S rRNA, archaeal *amo*A gene concentration and rate measurements from the same area (station 3 in Beman et al., 2012), which also revealed an AOA maximum at the base of the oxycline. Consequently, Beman et al. (2012) suggested a prominent role of AOA in performing nitrification in shallow O_2-depleted waters. The observed maximum abundance of anammox bacteria in the core ODZ as based on the ladderane lipid profile is in agreement with previous investigations in the ETSP ODZ, where it has been proposed as a preferential niche for anammox activity (De Brabandere et al., 2014; Hamersley et al., 2007; Ward et al., 2009). Moreover, similar to De Brabandere et al. (2014), who also reported low anammox rates at the oxycline in one of their sampling stations in the ETSP, we also observed low ladderane concentrations in the ETNP coastal setting.

At the open ocean site, we also find the maximum abundance of anammox bacteria between the base of the oxycline and the upper part of the ODZ. However, here the anammox bacterial abundance displays a concurrent maximum with that of AOA (Fig. 3m and n). The segregation of AOA and anammox bacteria niches in the coastal waters of the ETNP ODZ and their contrasting co-occurrence in the open waters clearly indicates a different behavior of the two microbial species at different locations of the ETNP. To the best of our knowledge this is the first study that highlights such different vertical distribution of the two groups on a local scale.

We also note that both IPL biomarkers exhibit higher concentration maxima in coastal waters (Fig. 3e and f) than in the open ocean (Fig. 3m and n), i.e., the concentration of HPH-crenarchaeol is 5 times higher and that of the PC-monoether ladderane is more than twice that found in the open ocean. This suggests that both AOA and anammox bacteria are more abundant in the coastal waters of the ETNP. The reasons for such divergence may be various. For instance, the complex and so far not fully resolved upper water circulation in this region may play a role (Fiedler and Talley, 2006; Kessler, 2006).

The proximity of the American continent is likely to have a greater influence on the hydrography of the coastal site (i.e., in a straight line the closest point on the Mexican coastline to our coastal settings is roughly 40 km away than on the open ocean site. At these latitudes the continental wind forcing is a dominant factor and, together with the variations in the coastline, influences the local upper circulation (Fiedler and Talley, 2006; Kessler, 2006 and might have an effect on the different vertical distribution and abundance observed in the two microbial species as well. In the same way, the nitrogen species profiles are likely to be influenced by variable hydrographical features (Fig. 3).

2.4.2. Influence o nitrogen species on the abundance and the distribution of Thaumarchaeota and anammox bacteria in the ETNP

Ammonium and nitrite concentrations have been proposed as critical factors in determining the vertical distribution and the abundance of Thaumarchaeota and anammox bacteria (Hamersley et al., 2007; Jaeschke et al., 2007; Jensen et al., 2009; Kuypers et al., 2005b; Martens-Habbena et al., 2009; Stahl and de la Torre, 2012; Thamdrup et al., 2006;Ward et al., 2009.

NH_4^+ serves as a substrate for both Thaumarchaeota and anammox bacteria and has been observed to not accumulate in ODZs as a result of efficient turnover between sources and sinks (Kalvelage et al., 2013). In the ETNP ODZ, we found both Thaumarchaeota and anammox bacteria in sub-oxic and anoxic waters. Ammonium concentrations are low and mostly under the detection limit, likely due to the consumption of the nutrient by both (or other microorganisms (Fig. 3c and i. Even at concentrations <1 μM, NH_4^+ may support anammox reaction, which is considered the main sink for this nitrogen species in the core ODZs (Bianchi et al., 2014. Nitrite is the electron acceptor in the anammox process, and it has been already described as a limiting factor to anammox bacteria activity in the southern ETNP ODZ (Rush et al., 2012.

In the coastal waters, thaumarchaeotal nitrification is probably taking place at the bottom of the oxycline, as indicated by the HPH-crenarchaeol maximum (Fig. 3e and the concurrent ammonium concentration peak (Fig. 3c, most likely resulting from the mineralization of organic matter. Moreover, thaumarchaeotal nitrification, which converts ammonium into nitrite (Arrigo, 2005, may cause the observed minor primary peak in the nitrite concentration profile (the so-called primary nitrite maximum, or PNM occurring at

the bottom of the oxycline in these waters (Fig. 3b), which coincides with the maximum of AOA abundance (Fig. 3b and e). In the core ODZ a clear secondary nitrite maximum (SNM) co-occurs with the maximum in anammox bacteria concentration (Fig. 3b and f). Although heterotrophic denitrification represents the obvious candidate as main provider of nitrite to anammox bacteria in oceanic settings (Ward et al., 2009), the two processes are usually not found coupled together (Dalsgaard et al., 2012). Alternatively, a combination of several pathways including dissimilatory NO_3^- reduction to NO_2^- (DNRN) or NH_4^+ (DNRA) plays a role, as has been observed in other ODZs (Canfield et al., 2010; Kartal et al., 2007; Lam et al., 2009, 2011; Lipschultz et al., 1990; Ward et al., 2009). The extent of the contribution of these processes as nutrients providers to anammox bacteria is still unclear (Lam and Kuypers, 2011). Finally, a recent study has also brought to attention zooplankton migrators as an alternative source of substrates to the anammox metabolism, previously overlooked in ODZs (Bianchi et al., 2014). In total, these things suggest that those mechanisms are all feasible to feed the anammox process in the coastal waters of the core ETNP ODZ with the nutrients required.

In the open ocean ETNP, AOA and anammox bacteria maxima may be coupled in the upper ODZ because of the (partial) overlap of the ecological niches of the two groups in this setting (Fig. 3m and n). In this case, AOA and anammox bacteria could either compete or cooperate for the substrates they require, as already proved in laboratory-scale models (Yan et al., 2010, 2012). The nutrient profiles are also consistent with the co-occurrence of the two metabolic processes (Fig. 3h and i): the secondary nitrite maximum is concurrent with the two biomarker maxima (Fig. 3h, m and n), whereas NH_4^+ is either possibly consumed by anammox as the water column turns suboxic or by nitrification by AOA successfully adapted to conditions of low nutrients and oxygen (Coolen et al., 2007; Francis et al., 2005; Lam et al., 2007, 2009; Martens-Habbena et al., 2009; Park et al., 2010; Pitcher et al., 2011b; Schouten et al., 2004; Sinninghe Damsté et al., 2002a; Stahl and de la Torre, 2012; Stolper et al., 2010; Tiano et al., 2014; Woebken et al., 2007) and potentially to a broad variety of different environmental conditions (Qin et al., 2014).

The role of NO_2^- and NH_4^+ in differentiating the distribution of Thaumarchaeota and anammox bacteria observed at the coastal and at the open-water sites of the ETNP ODZ is not clear; when the NO_2^- and NH_4^+ concentrations were compared with those of the specific biomarkers studied at both sites, no

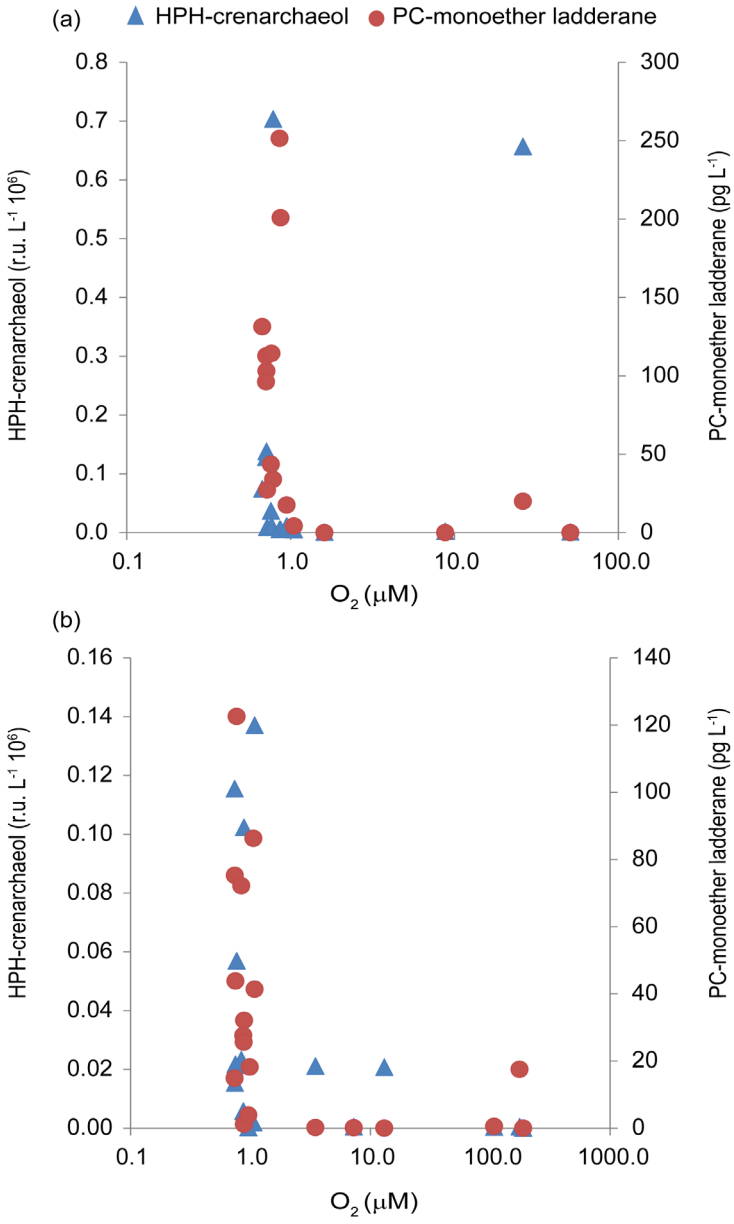

Figure 4. Abundance of HPH-crenarchaeol (r.u.L^{-1}, i.e., response units per liter) and PC-monoether ladderane lipids (pg L^{-1}) according to the concentration of oxygen (µM). The upper panel (a) shows the response of the two biomarkers at the coastal site, while the lower panel shows (b) the response at the open-ocean site.

evident relationship was apparent (data not shown). In conclusion, further investigation is required to establish the contribution of the single processes to the N cycle occurring in the settings investigated in this study and to explain the divergence between the two. Other studies have called attention to the relevance of organic matter fluxes as a control over these metabolic pathways and ultimately over the balance between the two mainly responsible for the N_2 removal from the oceans, i.e., anammox and denitrification (Babbin et al., 2014; Chang et al., 2014; Kalvelage et al., 2013; Koevef and Kähler, 2010; Ward, 2013; Ward et al., 2008, 2009). Specifically, variations in the C/N ratio content of the particulate organic matter (POM) entering the ODZ may play a prominent role in determining anammox and heterotrophic denitrification rates, with anammox being favored by nitrogen-rich OM (Babbin et al., 2014).

2.4.3. The role of the oxygen

As the features of ODZs suggest, oxygen might play a pivotal role in controlling the abundance and the special distribution of Thaumarchaeota and anammox bacteria in the ETNP ODZ. Previous studies have already pointed to this in other ODZs (Jaeschke et al., 2007; Kuypers et al., 2005b; Stahl and de la Torre, 2012; Thamdrup et al., 2006) and in the southern ETNP ODZ itself (Rush et al., 2012). To investigate whether oxygen concentration is influencing the abundance of Thaumarchaeota and anammox bacteria in our study sites in the ETNP ODZ, we compared our biomarker concentrations with oxygen concentrations in both the coastal and open ocean sites (Fig. 4a and b).

Figure 4a and b show how PC-monoether ladderane and HPH-crenarchaeol are distributed according to O_2 concentration at the two sites. The two distributions appear rather similar, with both biomarkers being more abundant at an oxygen concentration below the detection limit, i.e., ca. 1 μM, which is even overestimated by the CTD sensor employed for the measurements, as suggested by O_2 measurements taken with the STOX microsensor during the same cruise (Tiano et al., 2014). The only evident difference between the two plots is found in one HPH-crenarchaeol data point from the coastal site, corresponding to an oxygen concentration of ~26 μM, which reflects the much broader range of tolerance of AOA to O_2 compared to the strictly anaerobic anammox bacteria (Tiano et al., 2014).

However, the relation revealed by our plots suggests that both microbial

species are potentially able to cope with low oxygen concentrations and O_2 plays a primary role in controlling the distribution of the two microbial species, as shown previously (Martens-Habbena et al., 2009; Park et al., 2010; Pitcher et al., 2011b; Rush et al., 2012; Stahl and de la Torre, 2012; Tiano et al., 2014). The high relative abundance of HPH-crenarchaeol in the poorly oxygenated waters of the ETNP is consistent with the ability of AOA to thrive and perform nitrification under low-oxygen conditions (Coolen et al., 2007; Francis et al., 2005; Lam et al., 2007, 2009; Park et al., 2010; Pitcher et al., 2011b; Schouten et al., 2004; Sinninghe Damsté et al., 2002a; Stolper et al., 2010; Woebken et al., 2007). In the open ocean site a secondary minor peak of HPH-crenarchaeol at the lower oxycline, i.e., 1100 m depth (Fig. 3m), supports the hypothesis. Pitcher et al. (2011b) also observed a secondary maximum of AOA at the bottom of the Arabian Sea ODZ. Our findings thus confirm oxygen concentration as an important environmental control in determining the distribution of Thaumarchaeota and anammox bacteria in the water column of the ETNP ODZ.

2.5. Conclusion

In this study, high-resolution profiles of the two specific IPL biomarkers of AOA and anammox bacteria, i.e., HPH-crenarchaeol and PC-monoether ladderane, allowed us to gain a detailed insight into the vertical distribution of these microbial groups in the ETNP ODZ. It shows that AOA and anammox bacteria are abundant at both shallow coastal and open-ocean waters of the ETNP ODZ. Our findings also indicate that the ecological niches of the two species diverge on a local scale in the ETNP. Different O_2 concentration and water stratification features between the two study sites play an important role in determining such differences, whereas the role of NO_2^- and NH_4^+ is not clear. Further studies are needed to elucidate potential interactions between AOA and anammox in this ODZ. However future investigations on the N cycle in the ETNP and other ODZs might take into a greater account the importance of regional differences in the ecological niches of these microbial species.

Acknowledgment

We thank the captain and the crew of the *R/V Thomas G. Thompson* for their help and hospitality. The chief scientists, Allan Devol and Bess Ward,

are thanked for organizing and supervising the ETNP (TN278) cruise. We thank Stuart G. Wakeham for the invitation to take part in this cruise. Allison Myers-Pigg, Jaqui Neibauer and Rodolfo Alatorre- Gutierrez are thanked for assistance in the sampling. We also thank Rachel Horack for providing potential density data and for helpful discussions. Additional thanks are due to Laura Villanueva, Anna Rabitti, Laura Tiano, Yvonne Lipsewers and Borja Aguiar-González for helpful discussions and comments. This research was funded by a grant to J. S. Sinninghe Damsté from the Darwin Center for Biogeosciences (project no. 3012). In situ pump sampling and nutrient analyses were funded by grants to R. G. Keil (USA NSF #1153935) and Allan Devol (USA NSF #1029951).

Chapter 3

Archaeal sources of intact membrane lipid biomarkers in the oxygen-deficient zone of the eastern tropical South Pacific

Martina Sollai, Laura Villanueva, Ellen C. Hopmans, Richard G. Keil, Jaap S. Sinninghe Damsté

To be submitted to *Frontiers in Microbiology*

Abstract. Archaea are ubiquitous in the modern ocean where they are involved in the carbon and nitrogen biogeochemical cycles. However, the majority of Archaea remain uncultured. Archaeal specific membrane intact polar lipids (IPLs) are biomarkers of the presence and abundance of living cells. They comprise archaeol and glycerol dibiphytanyl glycerol tetraethers (GDGTs) attached to various polar headgroups. However, little is known of the IPLs of uncultured marine Archaea, complicating their use as biomarkers. Here, we analyzed suspended particulate matter (SPM) obtained in high depth resolution from a coastal and open ocean site in the eastern tropical South Pacific (ETSP) oxygen deficient zone (ODZ) with the aim of determining possible biological sources of archaeal IPL by comparing their composition by Ultra high Pressure Liquid Chromatography coupled to high resolution mass spectrometry with the archaeal diversity by 16S rRNA gene amplicon sequencing and their abundance by quantitative PCR. Thaumarchaeotal Marine Group I (MGI) closely related to *Ca.* Nitrosopelagicus and *Nitrosopumilus* dominated in the oxic surface and upper ODZ water together with Marine euryarchaeota Group II (MGII). High relative abundance of hexose phosphohexose- (HPH) crenarchaeol, the specific biomarker for living Thaumarchaeota, and HPH-GDGT-0, dihexose- (DH) GDGT-3 and -4 were detected in these water masses. Within the ODZ, DPANN Woesearchaeota DHVE-6 and Marine euryarchaeota Group III (MGIII) were present together with a higher proportion of archaeol-based IPLs, which were likely made by MGIII, since DPANN archaea are supposedly unable to synthesize their own IPLs and possibly have a symbiotic or parasitic partnership with MGIII. Finally, in deep suboxic/oxic waters a different MGI population occurred with HPH-GDGT-1, -2 and DH-GDGT-0 and -crenarchaeol, indicating that here MGI synthesize membranes with IPLs in a different relative abundance which could be attributed to the different detected population or to an environmental adaptation. Our study sheds light on the complex archaeal community of one of the most prominent ODZs and on the IPL biomarkers they potentially synthesize.

3.1. Introduction

Archaea are numerous in the modern ocean (e.g. DeLong 1992; Karner et al. 2001) where they constitute highly diverse communities (see Eme and Ford Doolittle 2015 for a general review on the archaeal diversity) and participate in the biogeochemical cycles of elements (Offre et al., 2013). However, only a few members of Archaea have been isolated and their physiology re-

mains therefore largely elusive.

Members of the phylum Thaumarchaeota (Brochier-Armanet et al., 2008), formerly known as Marine Group I (MGI) (Delong, 1992; Fuhrman et al., 1992) have been successfully enriched and isolated (Könneke et al., 2005; Santoro et al., 2015). Marine euryarchaeota Group II (MGII) and III (MGIII), whilst already detected by the pioneering studies of marine archaeal diversity (Delong, 1992; Fuhrman et al., 1992), are yet to be isolated. The former group mostly includes motile photoheterotrophs living in the marine photic zone; other ecotypes, however, have been detected in deeper waters (Baker et al., 2013; Deschamps et al., 2014; Frigaard et al., 2006). MGIII have been mostly associated to oxic meso- and bathypelagic environments and are considered a rare component of deep-sea archaeal communities (Bano et al., 2004; Haro-Moreno et al., 2017; López-García et al., 2001; Martin-Cuadrado et al., 2008; Massana et al., 2000), albeit they were one of the most relevant lineages detected in the deep Arctic Ocean (Galand et al., 2009). A recent metagenomic analysis has found MGIII in epipelagic waters, containing genes of photolyases and rhodopsin that suggest a photoheterotrophic lifestyle (Haro-Moreno et al., 2017). Other uncultured planktonic archaeal lineages include members of the archaeal superphylum DPANN (Castelle et al., 2015; Rinke et al., 2013), which have recently also been described as important components of the euxinic waters of the Black Sea (Sollai et al., 2018).

In the last decade the abundance, environmental niche and involvement into marine biogeochemistry of yet uncultured Archaea have started to be successfully investigated thanks to culture-independent techniques mostly based on DNA/RNA analysis (see Adam et al., 2017 for an updated review on the Archaea domain). These approaches, however, are subject to biases such as those regarding the primers used for amplification with PCR (see Eloe-Fadrosh et al., 2016; Marine et al., 2014; Pinto and Raskin, 2012; Teske and Sørensen, 2008 among others) which may be compensated by combining these techniques with other biogeochemical approaches (e.g. Biddle et al. 2006; Hinrichs et al. 2000; Orphan et al. 2001b; Pitcher et al. 2011b). One successful example of this kind consists in coupling genomic and lipidomic techniques (Besseling et al., 2018; Coolen et al., 2007; Lipsewers et al., 2014; Pitcher et al., 2011b; Wakeham et al., 2007, 2012). Indeed, archaeal membrane lipids have proven to hold taxonomic potential (Sinninghe Damsté et al., 2002c) and to be highly versatile as biomarkers in both present and past environments, as they preserve better than DNA and RNA in soil

and sedimentary records (Castañeda and Schouten, 2011; Eglinton and Eglinton, 2008; Kuypers et al., 2001). Archaeal membrane lipids are comprised of diphytanyl glycerol diether (archaeol) and/or glycerol dibiphytanyl glycerol tetraethers (GDGTs), which may contain 0–8 cyclopentane moieties. In general, GDGTs are widespread among the archaeal domain (Schouten et al., 2013a). The only documented exception is crenarchaeol, the GDGT containing a cyclohexane moiety and four cyclopentanes (Sinninghe Damsté et al., 2002c) which is considered exclusive to Thaumarchaeota (Sinninghe Damsté et al., 2012). In the lipid membranes of living archaea the core lipids (CLs) are attached by a glycerol-ether bond to one or two polar headgroups, which mainly include glyco- and phospholipids, forming structures known as intact polar lipids (IPLs) (Sturt et al., 2004). Compared to CL, which have high preservation potential that makes them suitable for providing information of both present and past archaeal communities (Schouten et al., 2013a), IPLs have been suggested to be especially useful as biomarkers of the living archaea. Indeed, the death of cells leads to the hydrolysis of IPLs, which results in the prompt release of the polar headgroups. In particular, the phosphate-ester bond of the IPL phospho headgroup has been demonstrated to be more liable than the glycosidic ones that is found in the monohexose (MH) and dihexose (DH) IPL types, for instance (Harvey et al., 1986; Schouten et al., 2010; White et al., 1979). This feature makes the IPL hexose-phosphohexose (HPH)-crenarchaeol an excellent marker of living Thaumarchaeota (Lengger et al. 2012; Pitcher et al. 2011a,b). Studies of thaumarchaeotal cultures have demonstrated that HPH-crenarchaeol is indeed an important IPL (Pitcher et al., 2011a; Schouten et al., 2008a; Sinninghe Damsté et al., 2012) although its abundance seems to vary according to the growth phase (Elling et al., 2014).

The lack of cultures of marine archaea complicates the identification of specific biomarkers, similar to the HPH-crenarchaeol for the Thaumarchaeota group, for the various archaeal lineages. The use of DNA and biogeochemical tools that allow the identification of archaeal groups as sources of specific IPLs, directly in the environment, represents a valid alternative to the availability of isolates (Meador et al., 2015; Pitcher et al., 2011b; Rossel et al., 2008). Consequently, environments which are likely to sustain diverse archaeal communities are ideal for this type of investigation. Among these are those regions of the modern oceans hosting oxygen deficient zones (ODZs), areas where the concentration of oxygen may drop far below 20 μM across the water column, as a result of high O_2 demand combined with weak ventilation (Paulmier and Ruiz-Pino, 2009). ODZs are characterized by multiple

biogeochemical gradients that support complex archaeal communities taking part in alternative biogeochemical cycles such as the nitrogen, the carbon and in some settings the sulfur cycle (Canfield et al., 2010; Ulloa et al., 2012). Thaumarchaeota have been found to thrive and perform nitrification at the upper oxic–suboxic boundary of the main ODZs and other archaeal lineages are starting to be linked to the biogeochemistry of these regions (Lam and Kuypers, 2011). However, the presence and distribution of other archaeal groups in the ODZs are much less characterized, and so are the potential IPL biomarkers they synthesize *in situ*. Therefore, ODZs are interesting sites to study the presence of archaeal lineages and the IPLs they may produce.

Here, in order to expand the current knowledge on the distribution of marine archaea and their IPL biomarkers, we sampled a coastal and open ocean station of the eastern tropical South Pacific (ETSP) at high depth resolution for suspended particulate matter (SPM). We characterized the archaeal diversity of the ETSP by 16S rRNA gene amplicon sequencing, and quantified the archaeal presence in the region by quantitative PCR. Archaeal IPL biomarkers were also investigated by using Ultra High Pressure Liquid Chromatography coupled to high resolution mass spectrometry (UHPLC-HRMS). In this way we were able to identify new archaeal IPL biomarkers and link them to specific archaeal groups.

3.2. Material and Methods

3.2.1. Sampling and physicochemical determinations

The ETSP water column was sampled during the NBP13-05 cruise aboard *R/V Nathaniel B. Palmer*, between 24th June and 27th July 2013 at coastal and open ocean sites (Fig. 1). At each site a number of geographically nearby locations showing similar physicochemical features (based on the estimated potential density, oxygen and nutrient profiles) were surveyed. A conductivity-temperature-density (CTD) equipment (SBE-911, Sea-Bird Electronics) recorded the physicochemical parameters of the water column. A SBE 43 electrochemical sensor mounted on the CTD rosette measured the dissolved-oxygen concentrations, which were calibrated against on-deck Winkler titrations. The electrochemical oxygen sensor SBE 43 has a detection limit of 1–2 µmol kg^{-1} (Tiano et al., 2014). Although recent evidence suggests that techniques such as Clark electrodes or Winkler titrations overestimate oxygen at the very

lowest concentrations (Tiano et al., 2014), the O_2 data here reported do not account for this discrepancy. Water samples for inorganic nutrient profiles were collected using a 24-bottle General Oceanics rosette sampler. Preferably, the CTD was cast shortly before or after the deployment of the McLane pumps (see below), otherwise data from another station, the closest in time and space to that of the deployed *in situ* pumps were used for the profiles. This means that the depths sampled for obtaining nutrient data do not always directly correspond to the depths at which the SPM was sampled with the *in situ* pumps.

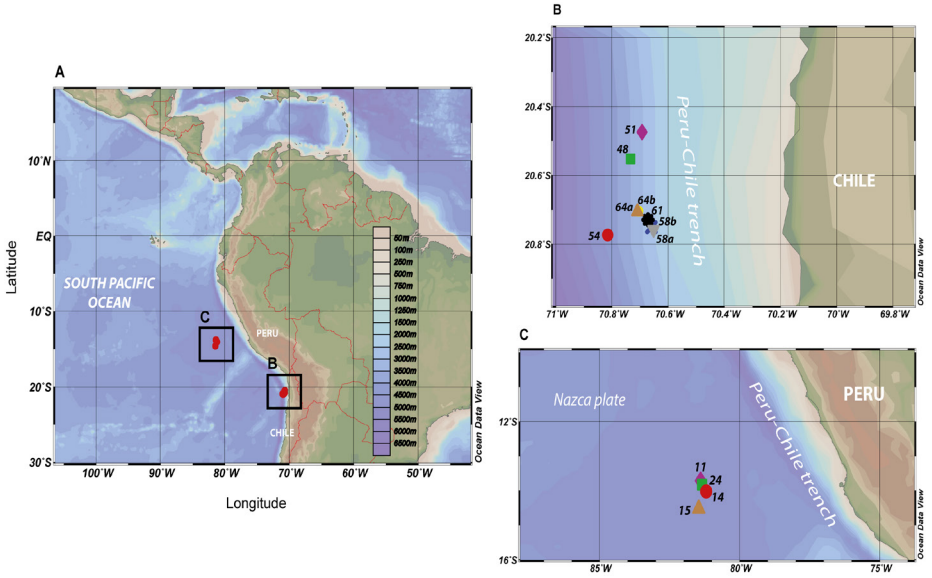

Figure 1. (a) Map of the eastern tropical South Pacific (ETSP) surveyed during the NBP13-0 cruise (June–July 2013) aboard of the *R/V Nathaniel B. Palmer*, including the location of the stations sampled for SPM by using multiple in situ pumps systems. Sampling locations (b) at the coastal station (i.e. 48; 51; 54; 58a; 58b; 61; 64a; 64b) and (c) at the open ocean station (i.e. 11; 14; 15; 24).

Suspended particulate matter (SPM) was collected on 142 mm diameter pre-ashed 0.7 µm pore size glass fiber (GF) filters (Whatman®), mounted in McLane WTS-LV *in situ* filtration systems. Two McLane pumps were deployed simultaneously at different depths, at each site. At the coastal site fifteen depths from 22 to 1000 m were sampled for IPL and gene analysis; at the open ocean site the samples were collected at nine discrete depths, comprised between 100 and 1000 m. The volume of water filtered varied according to the depth and the material collected. Upon the recovery of the pumps the GF filters were removed, split in two halves, one of which was used for IPL and gene analysis, and frozen at –80 °C.

3.2.2. DNA-based analysis

SPM filter halves were further subdivided into two quarter filters, which were used for genomic and for lipidomic analysis. DNA/RNA were extracted with the RNA PowerSoil® Total Isolation Kit plus the DNA elution accessory (Mo Bio Laboratories, Carlsbad, CA). The concentration of DNA was quantified by NanoDrop™ spectrophotometer (ThermoFisher Scientific, Waltham, MA) and fluorometrically with Quant-iT™ PicoGreen® dsDNA Assay Kit (Life technologies, Netherlands).

Amplification (primers: S-D-Arch-0159-a-S-15 and S-D-Bact-785-a-A-21; Klindworth et al., 2013) and sequencing of the 16S rRNA gene amplicon was performed as described in Moore et al. (2015). The QIIME v1.9 software was employed to analyze the archaeal 16S rRNA gene amplicon sequences (Caporaso et al., 2010). The raw sequences were demultiplexed and subsequently quality-filtered with a minimum quality score of 25 length between 250–350, a maximum two errors in the barcode sequence were allowed. OTU picking step was performed with Usearch with a threshold of 0.97 (roughly corresponding to species-level OTUs). Taxonomy was assigned based on blast and the SILVA database version 123 (Altschul et al., 1990; Quast et al., 2013). The phylogenetic affiliation of selected 16S rRNA gene sequences was compared to release 123 of the Silva NR SSU Ref database (http://www.arb-silva.de/; Quast et al., 2013) using the ARB software package (Ludwig et al., 2004). Sequences were added to the reference tree supplied by the Silva database using the ARB Parsimony tool.

Quantitative PCR (qPCR) was used to estimate archaeal 16S rRNA gene copies quantification, by using the primers Parch519F and Arc915R as previously described (Pitcher et al., 2011b). The qPCR reaction mixture (25 µl) contained 1 U of Pico Maxx high fidelity DNA polymerase (Stratagene, Agilent Technologies, Santa Clara, CA) 2.5 µl of 10x Pico Maxx PCR buffer, 2.5 µl 2.5 mM of each dNTP, 0.5 µl BSA (20 mg/ml), 0.02 pmol/µl of primers, 10 000 times diluted SYBR Green® (Invitrogen) (optimized concentration), 0.5 µl 50 mM of $MgCl_2$ and ultrapure sterile water. All reactions were performed in iCycler iQ™ 96-well plates (Bio-Rad, Hercules CA). A gradient melting temperature assay was utilized to test the specificity of the reaction. The cycling conditions for the qPCR reaction consisted of 95 °C, 4 min; 40–45× [95 °C, 30 s; 62 °C, 40 s; 72 °C, 30 s]; final extension 80 °C, 25 s. The qPCR reactions were performed in triplicate with standard curves from 10^0 to 10^7

molecules per microliter. Efficiency of the qPCR assay was reported to be 98–100% and R^2= 0.996.

3.2.3. Intact polar lipids analysis

One fourth of the GF/F filters were used for lipidomic analysis purpose. A modified Bligh-Dyer technique (Sturt et al., 2004 was used to extract intact polar lipids (IPLs, with some adjustments as reported by Sollai et al. (2018. Briefly, 1-O-hexadecyl-2-acetyl-sn-glycero-3-phosphocholine (PAF) internal standard was added to the extracts and dried under a stream of nitrogen. The IPL injection solvent (hexane:isopropanol:H_2O 718:271:10 *vol*/*vol*/*vol*) was added to re-dissolved the dried extract and the resulting solution was fil-tered through a 0.45 µm, 4 mm-diameter True Regenerated Cellulose syringe filter (Grace Davison, Columbia, MD, USA). The analysis was performed as described by Sollai et al. (2018), by using an Ultimate 3000 RS UHPLC, equipped with thermostated auto-injector and column oven, coupled to a Q Exactive Orbitrap MS with Ion Max source with heated electrospray ion-ization (HESI) probe (Thermo Fisher Scientific, Waltham, MA). Separation was achieved using an YMC-Triart Diol-HILIC column (250 × 2.0 mm, 1.9 µm particles, pore size 12 nm; YMC Co., Ltd, Kyoto, Japan) held at 30 °C. The mass range for the analysis of the lipids was *m/z* 375 to 2000 at a reso-lution 140,000. The chromatographic conditions and source settings were as described by Sollai et al. (2018), similarly the data dependent MS^2 settings. The list of the IPLs targeted during the analysis, using a mass tolerance of 3 ppm, is also available in Sollai et al. (2018). Integration of the combined mass chromatogram (within a mass tolerance of 3 ppm) of the monoisotopic and first isotope peak of all relevant adducts formed was performed to determine the peak areas for each individual IPL. Depending on the type of IPL, proton-ated, ammoniated and/or sodiated adducts may form in different proportions. Possible matrix effects and variations in mass spectrometer performance were corrected when necessary by monitoring the response of the internal standard PAF. Reported peak areas were also corrected for these effects. The abun-dances of individual IPLs are here reported as response units per Liter of wa-ter (r.u. L^{-1}), due to the lack of authentic standards for absolute quantitation.

3.2.4. Data analysis

Pearson correlation analysis performed by using the R software package for statistical computing (http://cran.r-project.org/) was applied to the data collected at both stations in order to test the existence of a linear correlation between the abundances of specific archaeal groups and the IPLs detected in the ETSP. Spurious correlations were also tested by applying the same statistical analysis among the archaeal lineages detected. A third matrix was made by correlating the IPLs detected. The absolute abundance of specific archaeal groups, as calculated from the total archaeal 16S rRNA gene (copies L^{-1}) estimated by qPCR (assuming one 16S rRNA gene copy number per genome) detected in the ETSP SPM at different depths and the abundance of the IPL classes as obtained with the UHPLC-HRMS analysis of the ETSP SPM at different depths (expressed as response units per Liter of water, r.u. L^{-1}; Table S5) were the data employed to build the correlation matrices. Data from 60 m depth at the coastal station were excluded from the analysis (see discussion). The correlation was expressed as coefficients (r values) ranging from –1 to +1, where negative r values indicate a negative linear correlation between the two variables, positive values indicate a positive linear correlation and 0 indicates no existing correlation.

3.3. Results

The data obtained from casting geographically contiguous sites at both the study locations were compiled into two composite (i.e. coastal and offshore) stations (Fig. 1). This was possible due to the large similarities of the physical and chemical profiles the various sites from one location shared. The results are reported as tables or plots in which the potential density anomaly, σ_θ (kg
m^{-3}) corresponding to the depths sampled at the two stations are used (Table S1; Fig. 1).

3.3.1. Physicochemical parameters of the sampling sites

The water column of the coastal station was oxic for the first ~70 m, with O_2 concentrations of 212 μmol kg^{-1} at 22 m depth (σ_θ ~25.6) and 21.5 μmol kg^{-1} at 60 m depth (σ_θ ~26.0), respectively. The oxycline was steep and at 75 m depth (σ_θ ~26.2) suboxic waters (2.1 μmol kg^{-1} of O_2) were detected. In the core ODZ (up to σ_θ ~26.7–26.8, corresponding to ~350–400 m) the concentration of O_2 remained close to 2 μmol kg^{-1}. At σ_θ ~27.0 (~500 m) the oxygen concentration increased to 14.6 μmol kg^{-1} (Table S1; Fig. 2a). For the purpose of this study four distinct zones are defined in the coastal station, based on the

O_2 profile, and are used later in the text. These include the shallow oxic zone (22–75 m), the upper ODZ (75–135 m), the core ODZ (135–350 m), the deep oxic zone (350–1000 m; Fig. 2). The concentrations of nitrate (NO_3^-), nitrite (NO_2^-) and ammonium (NH_4^+) were also determined. The NO_3^- peaked (~15–22 μmol L^{-1}) in the upper oxycline (σ_θ ~25.8–26.0, which correspond to ~40 to 60 m) and again (~41–43 μmol L^{-1}) in the deep one (σ_θ ~27.0–27.4, ~500–1000 m). The NO_3^- concentration reached its lowest point (~9 μmol L^{-1}) in the core ODZ, (at σ_θ ~26.3, ~115 m) (Table S2; Fig. S1a). The NO_2^- concentration was ~0.7 μmol L^{-1} at ~40–50 m depth (σ_θ ~25.8 to 26.0) and showed a peak (up to 7.5 μmol L^{-1}) in the core ODZ, at σ_θ ~26.3 to 26.6, which correspond to a depth range of ~115–325 m (Table S2; Fig. S1b). The NH_4^+ concentration reached its maximum (~1.5 μmol L^{-1}) at σ_θ ~25.8 (~30 m), it decreased to 0.1 μmol L^{-1} at σ_θ ~26.0 (~40 m) and remained close to this value in the deeper water (Table S2; Fig. S1c).

At the open ocean station the water column was fully oxic (~215 μmol kg^{-1}) for the first 100 m (σ_θ ~26.0) and became suboxic in the following 25 m, with the O_2 concentration already ~2.1–5.5 μmol kg^{-1} at 125 m (σ_θ ~26.2). Within the ODZ (σ_θ ~26.2–26.8, ~125–300 m) O_2 reached as low as ~2–3 μmol kg^{-1}, but it increased to ~11–16 μmol kg^{-1} at ~500 m (σ_θ ~27.0) and to ~56 μmol kg^{-1} at 1000 m (σ_θ ~27.4) (Table S1; Fig. 2a). Similarly to the coastal station also in the open ocean one, four distinct zones are defined based on the O_2 profile: the shallow oxic zone (100–125 m), the upper ODZ (125–175 m), the core ODZ (175–300 m), the deep oxic zone (300–1000 m; Fig. 3). The NO_3^- concentration displayed a first maximum of ~23.6 μmol L^{-1} at σ_θ ~26.1 (~100 m). The NO_3^- concentration decreased to ~20 μmol L^{-1} in the upper ODZ (~150–160 m, σ_θ ~26.4), a second peak of ~45.7 μmol L^{-1} occurred in the lower oxycline, at σ_θ ~27.2–27.3 (~700–800 m) (Table S2; Fig. S1d). The NO_2^- was barely detectable in the upper oxic water column and at the oxycline (0.2 μmol L^{-1} at σ_θ ~25.3–25.4, which corresponds to ~50–60 m), but peaked (8.9 μmol L^{-1}) within the core ODZ, at σ_θ ~26.2–26.6, ~120–270 m (Table S2; Fig. S1e). The NH_4^+ concentration was at its maximum (0.5 μmol L^{-1}) in the upper oxic waters (σ_θ ~25.4, ~50 m), then decreased to <0.1 μmol L^{-1} at ~75–80 m, (σ_θ ~25.5) and did not increase in the deeper water (Table S2; Fig. S1f).

3.3.2. Diversity and abundance of archaeal groups

We investigated the archaeal community composition and abundance at both coastal and open ocean stations in the ETSP region. Partial 16S rRNA

gene sequences were amplified and their sequence determined by amplicon sequencing of the DNA extracted from the SPM across the two water column vertical profiles (Table 1; Figs. 2 and 3). For both stations we quantified the total archaeal 16S rRNA gene with qPCR by using specific primers (Figs. 2b and 3b; Table S3). At the coastal station the total archaeal 16S rRNA gene copy number was 2×10^5 copies L^{-1} in shallow oxic water (22 m) and was under the detection limit in the oxycline (60 m depth), but increased maximizing within the ODZ (175–350 m) with up to 2×10^7 copies L^{-1}. In deeper waters, it was ca. 3 to 5×10^6 copies L^{-1} (Fig. 2b; Table S3a). At the open ocean station the total archaeal 16S rRNA gene copy number varied between 2×10^5 to 7×10^7 copies L^{-1}. The maximum was located within the core ODZ (200 m) and a second maximum (3×10^7 copies L^{-1}) was detected at the lower oxycline at 500 m depth (Fig. 3b; Table S3b). Archaeal diversity was studied by 16S rRNA gene amplicon sequencing. At the coastal station, four major archaeal groups were detected, which could be related to various subgroups, i.e. the marine Thaumarchaeota (subdivided in operational taxonomic units (OTUs) closely related to *Candidatus* Nitrosopelagicus brevis and *Nitrosopumilus maritimus*, and two other uncultured MGI OTUs: OTU-1 and -2, Euryarchaeota MGII (as OTU-1 and -2) and MGIII (as OTU-1, -2 and -3) (Fig. 4), and uncultured DPANN Woesearchaeota Deep Hydrothermal Vent Group (DHVE)-6 (Fig. 2c). At the open ocean station, the same archaeal taxa of the coastal station were detected with one more euryarchaeotal MGII subgroup (OTU-3; Fig. 4B). Other archaeal groups (less than 3% each) represented <10 % of total archaeal reads (Fig. 3c).

The archaeal groups showed a distinct distribution with depth. At the coastal station, Thaumarchaeota affiliated to *Ca.* Nitrosopelagicus and *Nitrosopumilus* dominated in oxic surface waters (at 22 m) with 55 and 25% of the total archaeal 16S rRNA gene reads, respectively. At the oxycline (60 m), MGII OTU-2 and -1 (75 and 25%, respectively) were the only archaeal groups detected. MGIII-affiliated OTUs were low (<2.5%) or undetected in the surface and subsurface water (Table 1; Fig. 2c). In the upper ODZ (75–83 m) MGII OTU-1 comprised 41 and 17% of reads, together with MGI archaea related to *Ca.* Nitrosopelagicus (11–28%) and *Nitrosopumilus* (19–36%). The distribution of these two groups of MGI archaea extended somewhat deeper in the water column; at 100 m MGI archaea (including OTU-1 and -2) still comprised 44% of all archaeal reads. Within the core ODZ (~135–350 m) the archaeal taxa that were prominent in the upper 100 m declined to <10% of archaeal reads in favor of other taxa. Specifically, euryarchaeotal MGIII

OTU-3 increased gradually, reaching 42–63% at depths >150 m in the ODZ. In addition, archaea affiliated to the DPANN Woesearchaeota DHVE-6 group became increasingly abundant in the 135–350 m depth range, comprising 15–26% of total archaeal reads with the lowest relative abundance in the deeper part of the ODZ (Table 1; Fig. 2c). With the increased oxygen concentration at the lower oxycline (500–1000 m) the relative abundance of MGIII and DPANN DHVE-6-affiliated reads declined sharply, whereas MGI OTU-1 and -2 increased sharply to a summed relative abundance of >50%. In contrast to the surface waters, MGI archaea related to *Ca.* Nitrosopelagicus and *Nitrosopumilus* were much lower in relative abundance in the oxygenated bottom water below the ODZ. Comparably, the relative abundance of MGII OTU-2, but not OTU-1, reads also increased substantially to 29–32% (Table 1; Fig. 2c).

The depth distribution of the archaeal taxa of the open ocean site was in general similar to that of the coastal site (cf. Table 1; Fig. 3c. The relative abundance of thaumarchaeotal *Ca.* Nitrosopelagicus and *Nitrosopumilus* reads in the oxic surface waters (100 m was also high at 33 and 16%, respectively. In contrast to the coastal site, however, MGI OTU-1 was also relatively abundant (14%. MGI archaea remained the most prominent group of archaea (i.e. 40–62% of total archaeal reads in the upper ODZ (125–155 m, but clear differences in the relative abundance of the various OTUs are observed. Specifically, *Ca.* Nitrosopelagicus-related archaea comprised 33% of reads at 100 m and decreased to <5% reads at 155 m, whereas MGI OTU-1 increased from 14 to 21%. The archaea related to *Nitrosopumilus* increased firstly to 18% and still represented 13% at 155 m. Another relevant group of archaea in the surface waters was euryarchaeotal MGII, comprising 22–27% of total archaeal reads at 100–155 m. In contrast to the coastal station, OTU-2 (14–18% of 16S rRNA gene reads and not OTU-1 was most prominent (Table 1; Fig. 3c. Like in the coastal station, the relative abundance of MGI (<6% and MGII (<8% archaea strongly decreased within the core ODZ (175–300 m, with the only exception being MGI OTU-1, whose reads reached 16% at 200 m. In contrast, the MGIII-affiliated OTUs and the DPANN group became prominent in the core ODZ, with relative abundances of individual OTUs reaching 30%. In the deep oxygenated waters (500–1000 m MGI OTU-1 was prominent again with 52% and 43% of reads. In these deep waters other relevant archaeal taxa include MGII OTU-1 (14 and 21% and -2 (13% at 500 m and, to a minor extent, MGIII OTU-3 and MGI OTU-2 (8–9% at 1000 m; Table 1; Fig. 3c.

Table 1. Distribution of the archaeal 16S rRNA gene reads per depth, detected in the ETSP at the (a) coastal and (b) open ocean station. Colour coding: from dark red to white corresponds to 75–60%; 60–40%; 40–20%; 20–10%; 10–0% of archaeal 16S rRNA gene reads.

Station	Potential density (kg m^{-3})	Depth (m)	Thaumarchaeota Marine Group I				Euryarchaeota Marine Group II			Euryarchaeota Marine Group III			DPANN Woesearchaeota DHVE-6	*% of reads
			Ca. Nitrosopelagicus	*Nitrosopumilus*	OTU-1	OTU-2	OTU-1	OTU-2	OTU-3	OTU-1	OTU-2	OTU-3		
Coastal	25.63	22	55.3	24.6	1.9	1.7	6.6	6.6			2.5	0.6	0.2	17.7
	26.05	60					25.0	75.0						0.1
	26.19	75	16.8	19.0	2.4	1.0	41.1	6.2		0.2	7.2	2.6	2.2	13.3
	26.18	83	27.9	36.4	3.9	1.1	17.0	4.6		0.7	1.8	3.2	1.8	12.7
	26.30	100	10.9	16.9	10.7	5.4	6.7	5.9		3.0	5.9	16.3	11.9	9.4
	26.30	135	4.1	6.0	8.1	3.8	0.7	4.0		7.8	7.6	23.2	23.8	15.0
	26.40	150	1.2	3.0	4.8	1.8		10.2		7.8	9.6	28.7	22.2	6.5
	26.45	175	1.9	2.5	7.2	5.5	4.2	5.5		10.2	10.0	22.2	23.3	2.7
	26.42	200	1.3	1.3	9.7	3.5		5.3		15.0	11.5	25.2	17.7	2.9
	26.50	235	1.7	1.7	1.7	1.7		1.7		16.7	15.0	36.7	21.7	2.6
	26.48	250		3.2	10.1	3.2	5.3	3.7		14.3	5.8	21.7	25.9	5.0
	26.61	300		0.5	5.7	4.8	0.5	2.9		14.4	12.9	31.1	16.3	2.7
	26.71	350	0.3	2.3	4.9	2.6		4.9		21.4	13.8	27.0	14.8	7.0
	26.95	500	0.2	4.7	23.2	30.1	0.3	31.7		1.3	1.8	4.8	0.2	17.7
	27.39	1000		5.5	27.0	25.9	0.5	29.2		1.7	1.7	7.1	0.5	27.3
Open ocean	26.00	100	33.0	15.7	13.6	2.1	3.7	17.8	5.4		4.9	1.6		15.8
	26.18	125	22.7	18.4	19.4	1.6	3.7	16.6	5.5	0.1	7.7	2.2	0.4	14.5
	26.35	155	4.8	13.5	21.0	0.3	4.1	14.3	3.2	6.7	8.9	11.6	9.6	10.2
	26.35	175	0.5	1.4	5.2	0.5	0.5	4.1		15.8	12.4	26.4	24.6	7.9
	26.45	200	1.3	4.5	16.0	0.2	1.6	7.4	1.0	14.6	7.4	22.1	16.0	7.9
	26.50	235	0.6	1.2	4.7		0.6	1.2		27.2	16.6	23.7	16.6	9.2
	26.69	300		0.3	5.0	0.3		3.3		30.8	14.2	22.2	16.6	6.2
	26.99	500	0.5		52.3	2.7	13.7	12.7	1.3	2.3	2.9	5.5	1.1	14.1
	27.37	1000	0.2		43.1	8.4	21.1	5.8	0.5	4.5	1.0	8.6	1.5	17.0

*percentage of archaeal 16S rRNA gene reads of the total bacterial plus archaeal 16S rRNA gene reads detected in the analysis. Only archaeal groups with more than 3% of total archaeal reads are listed.

3.3.3. Archaeal intact polar lipid biomarkers

An UHPLC-HRMS method was set-up to detect 193 structurally different archaeal IPLs (see methods and Sollai et al. 2018). The distribution of individual IPLs versus depth (and corresponding estimated potential density, σ_θ) was presented as the percentage of the relative abundance of each IPL normalized for its total amount detected across the full depth profile (Tables 2 and 3). Because no authentic standards were available for absolute quantitation of the individual IPLs (MS response factors of different IPLs might vary substantially), it was not possible to compare the relative abundances of the IPLs at one specific depth. 14 GDGT -IPLs and 4 archaeol-IPLs were detected in the ETSP in this study (Tables 2 and 3). The IPLs detected included various head group types attached in different combinations to crenarchaeol, GDGT-0 to -4 and archaeol CLs. Specifically, they included monohexose (MH); dihexose (DH), which in this study stands for one DH moiety when attached to archaeol CL or for two MH moieties when attached to crenarchaeol or GDGT CLs; hexose phosphohexose (HPH), which stands for two headgroups, namely one MH and one phosphatidyl MH; phosphatidyl glycerol (PG), and phosphatidyl ethanolamine (PE).

At the coastal station all IPLs with crenarchaeol and GDGT-0 to -4 as CLs showed similar depth profiles (Table 2). Specifically, these IPLs displayed their highest relative abundance in the upper ODZ (i.e. at 75–83 m) and gradually decreased within the core ODZ and deeper in the water column (see MH-crenarchaeol, DH-GDGT-3 and -4 for instance). The relative abundance of most HPH- and DH-GDGTs (except for DH-GDGT-3) sharply increased again at 500–1000 m. At 1000 m the relative abundance of the MH-GDGTs also increased. DH-crenarchaeol was an exception as it reached its highest relative abundance (18%) at 500 m depth. All archaeol-IPLs displayed a substantially different distribution being mostly detected in the core ODZ (Table 2). These IPLs were present with MH, DH, PG and PE attached as polar head groups. MH- and DH-archaeol were for the first time detected at 100 m depth, in the upper ODZ, while PG- and PE-archaeol were already detected in the upper oxycline, although at very low relative abundance (Table 2). Every archaeol-IPL type reached its own highest relative abundance at a different depth in the core ODZ: MH-archaeol generally increased in the deep ODZ, DH/PG/PE-archaeol respectively at 135, 200 and again at 300–350 m (Table 2).

Table 2. Depth distribution of the archaeal IPLs detected in the ETSP at the coastal station.

Potential density (kg m^{-3})	Depth (m)	GDGT-0			GDGT-1			GDGT-2			GDGT-3	GDGT-4	Crenarchaeol			Archaeol			
		MH	DH	HPH	MH	DH	HPH	MH	DH	HPH	DH	DH	MH	DH	HPH	MH	DH	PG	PE
25.63	22	0.1							0.1				0.2						
26.05	60	15.3	20.4	8.9	11.2	17.5	4.8	11.5	16.9	4.9	27.1	17.9	13.2	17.1	7.4			0.8	1.6
26.19	75	32.5	22.4	26.3	25.3	22.6	21.6	34.7	18.9	27.2	33.1	42.2	19.2	11.5	27.8			4.5	2.6
26.18	83	27.2	24.5	30.5	28.2	27.0	29.7	26.8	22.0	28.9	32.9	26.3	27.8	17.5	31.2			3.7	2.8
26.30	100	4.6	6.9	7.9	3.9	7.2	6.4	4.8	6.3	4.7	4.5	5.3	5.8	5.7	7.1	1.2	6.6	5.5	5.7
26.30	135	3.5	5.4	7.2	4.6	3.9	10.0	2.2	5.3	11.6	1.6	2.0	6.3	6.2	8.5	7.6	17.8	14.2	11.8
26.40	150	1.6	0.7	0.7	2.8	0.8		3.3	1.4				3.5		0.9	7.9	5.2	5.7	7.3
26.45	175	3.1		1.2	4.4	2.4	1.1	3.0	2.4				5.2	3.0	1.2	13.0	9.3	7.8	10.9
26.42	200	1.1	1.7	0.7	2.3	1.7		2.0	2.9				3.8	3.0	0.9	17.0	19.0	12.9	17.3
26.50	235	1.3		1.2	2.1	1.0	1.0	2.8	1.7				2.2	2.1	1.1	11.5	7.9	9.0	8.1
26.48	250	1.1		0.5	1.3	0.5	0.2	1.0	1.2				2.0	1.4	0.6	11.2	11.9	7.6	10.0
26.61	300	0.7	0.2	2.1	1.2	0.6	2.2	0.7	1.5			0.3	1.9	0.9	2.3	14.7	10.1	12.5	10.9
26.71	350	1.0		0.9	1.9	0.8	0.8	1.6	1.5				2.5	1.3	1.0	15.7	12.2	14.1	8.7
26.95	500	1.4	7.6	8.2	2.2	6.1	17.4	2.4	7.8	22.8	0.5	1.9	2.2	18.3	8.0	0.1		0.7	1.7
27.39	1000	5.5	10.3	3.6	8.7	7.7	4.7	3.2	10.4		0.3	4.1	4.2	11.8	2.0	0.1		1.1	0.7

These distributions are normalized on the summed abundance (response units per Liter, r.u. L^{-1}) over all depths of each IPL detected. IPLs are listed according to the core lipid and the polar head groups attached to them. Abbreviation include: glycerol dialkyl glycerol tetraether (GDGT), monohexose (MH), dihexose (DH), hexose phospho-hexose (HPH), PG (phosphatidyl glycerol), PE (phosphatidyl ethanolamine). Colour coding: from dark red to white corresponds to 42–32%; 32–22%; 22–12%; 12–0% of archaeal 16S rRNA gene reads. The table should be read in a vertical direction since the differences in MS response factors for different IPLs do not allow a direct comparison of the abundance of IPLs at one depth.

At the open ocean station the general distribution of the IPLs detected was rather similar to that of the coastal station (Table 3). Most of the crenarchaeol- and GDGT-IPLs had their highest relative abundance at the oxycline and the upper ODZ, which in this station corresponded to 100–125 m depth and then their abundance decreased within the core ODZ. As observed at the coastal station, for all HPH- and DH-GDGT-IPLs, but not for MH-GDGT-IPLs, the relative abundances increased sharply again at 500 m (Table 3), whilst the concentration of MH-GDGTs showed an increase in the deepest water layer studied (i.e. 1000 m). In contrast with the coastal station, for the open ocean station the maximum relative abundance often occurred in the deep oxycline. This was the case for DH-crenarchaeol, DH-GDGT-0 and -2, HPH-GDGT-1 and, especially, -2. As for the coastal station also for the open ocean station, the archaeol-based IPLs were prominent only in the core ODZ (Table 3). In particular, MH- and DH-archaeol were only detected at 155–300 m and showed their highest relative abundance (28% and 34%, respectively) at 300 m. PG- and PE-archaeol, although present at all depths, also had their highest relative abundance within the core ODZ (175–300 m), specifically at 300 m for PG-archaeol (26%) and at 235 m for PE-archaeol (24%; Table 3).

3.3.4. Statistical analysis

The first type of correlation matrix (Fig. 5; Table S5) was made using the abundance of specific archaeal groups (Table S3) and the concentration of the IPLs detected (Table S4) as variables and was aimed to help corroborating or dismissing the tentative assignment of specific IPLs to specific archaeal groups. Both matrices – obtained from the data collected at the coastal (Fig. 5a; Table S5a) and open ocean stations (Fig. 5b; Table S5b) – revealed clear patterns of positive and negative correlations between various archaeal groups and archaeal IPLs in the water column of the ETSP, suggesting potential relationships between the variables that will be discuss later in detail. The second type of matrix used the abundance of the archaeal groups detected as variables (Table S3) with the aim of identify possible biases in the correlations between archaeal groups and IPLs (Fig. S2; Table S6). The third type of correlation matrix (Fig. S3; Table S7) was obtained by using the concentrations of archaeal IPLs detected as variables (Table S4) and revealed similarities and hence potential similar sources of IPLs.

Table 3. Depth distribution of the archaeal IPLs detected in the ETSP at the open ocean station

Potential density (kg m^{-3})	Depth (m)	GDGT-0			GDGT-1			GDGT-2			GDGT-3	GDGT-4	Crenarchaeol			Archaeol			
		MH	DH	HPH	MH	DH	HPH	MH	DH	HPH	DH	DH	MH	DH	HPH	MH	DH	PG	PE
26.00	100	28.2	12.0	12.9	22.8	23.3	7.0	21.3	19.8		39.8	29.6	29.5	22.1	11.5			1.8	7.1
26.18	125	22.1	19.1	38.8	22.8	18.5	32.0	21.5	15.5	24.7	38.3	31.6	17.4	17.0	42.2			2.0	3.8
26.31	155	9.9	6.7	5.7	9.7	7.7	4.1	9.9	6.6	1.5	8.1	11.8	9.9	5.2	6.0	4.6	2.8	4.0	5.5
26.35	175	9.7	5.2	0.5	6.2	2.5		6.6	4.4				9.1	4.9	0.3	22.3	26.1	19.4	18.0
26.45	200	6.2	6.3	6.6	6.0	4.1	7.7	8.9	6.7	3.8	5.6	9.4	10.0	5.6	9.8	24.4	19.1	24.4	15.4
26.50	235	2.0	0.9	1.8	1.8	2.5		2.3	2.5		0.9		4.1	1.5	2.1	20.7	17.6	16.4	24.1
26.62	300	6.3	6.3	2.3	8.2	4.7	1.9	9.3	5.7	0.8			8.9	4.9	3.5	28.1	34.4	25.6	17.3
26.99	500	4.0	22.7	24.6	4.7	18.1	38.7	1.5	21.3	64.2	4.2	17.7	3.5	27.4	21.2			1.5	3.9
27.39	1000	11.6	20.9	6.9	17.7	18.6	8.6	18.8	17.5	5.0	3.1		7.7	11.4	3.5			4.9	5.0

These distributions are normalized on the summed abundance (response units per Liter, r.u. L^{-1}) over all depths of each IPL detected. IPLs are listed according to the core lipid and the polar head groups attached to them. Abbreviation include: glycerol dialkyl glycerol tetraether (GDGT), monohexose (MH), dihexose (DH), hexose phospho-hexose (HPH), PG (phosphatidyl glycerol), PE (phosphatidyl ethanolamine). Colour coding: from dark red to white corresponds to 64–42%; 42–32%; 32–22%; 22–12%; 12–0% of archaeal 16S rRNA gene reads. The table should be read in a vertical direction since the differences in MS response factors for different IPLs do not allow a direct comparison of the abundance of IPLs at one depth.

3.4. Discussion

The biogeochemistry of the ETSP ODZ has been extensively studied with an emphasis on the nitrogen cycle (see Canfield et al., 2010; Lam et al., 2009; Ulloa et al., 2012 among others. Thaumarchaeota have attracted most of the attention among archaea, because they perform the oxidation of ammonium to nitrite in a broad range of O_2 regimes (Beman et al., 2008; Bristow et al., 2016; Coolen et al., 2007; Lam et al., 2007, 2009; Molina et al., 2010; Pitcher et al., 2011b. In our study, we observed a higher archaeal diversity in the ESTP water column than previously reported (Belmar et al., 2011; Quiones et al., 2009; Stewart et al., 2011, and a clear niche occupancy of archaeal groups (Figs. 2 and 3. Archaea were less numerous in the surface waters, upper ODZ and in the deep oxycline in comparison with the core of the ODZ (Figs. 2b and 3b, and this difference was more evident for the coastal station where the archaeal 16S rRNA gene abundance was at least one order of magnitude higher in the core of the ODZ (cf. Fig. 2b and 3b. This suggests that archaea within the ODZ have a relevant role in the biogeochemistry of oxygen-deficient waters. In our study, we applied a combined IPL and gene-based approach which has already proven successful in other locations with similar features to the ETSP, including the Arabian Sea (Besseling et al., 2018; Pitcher et al., 2011b; Schouten et al., 2012 and the Black Sea (Sollai et al., 2018. However, the use of UHPLC-HRMS greatly improves the IPL approach as it makes possible to reveal a broader IPL diversity (Liu et al., 2016; Wörmer et al., 2013; Xie et al., 2014; Zhu et al., 2013) and its taxonomic potential, normally a substantial limitation of the approach, thus improving the association of these lipids with their biological sources (Besseling et al., 2018; Lipsewers et al., 2018). Here, we also apply a statistical analysis to tentatively assign the detected IPLs to specific archaeal lineages.

3.4.1. A diverse Thaumarchaeotal population resides in the shallow oxic waters, the upper ODZ, and in the deep oxic waters of the ETSP

Thaumarchaeota formed a prominent component of the archaeal population in the shallow oxic waters down to the upper ODZ at both stations. At the coastal station these Thaumarchaeota were mostly related to MGI *Nitrosopumilus* and the recently isolated MGI *Ca*. Nitrosopelagicus (Santoro et al., 2015) (Table 1; Figs. 2c, and 4a). At the open ocean station an uncultured MGI OTU (MGI OTU-1; Fig. 4a) also comprised a substantial part of the

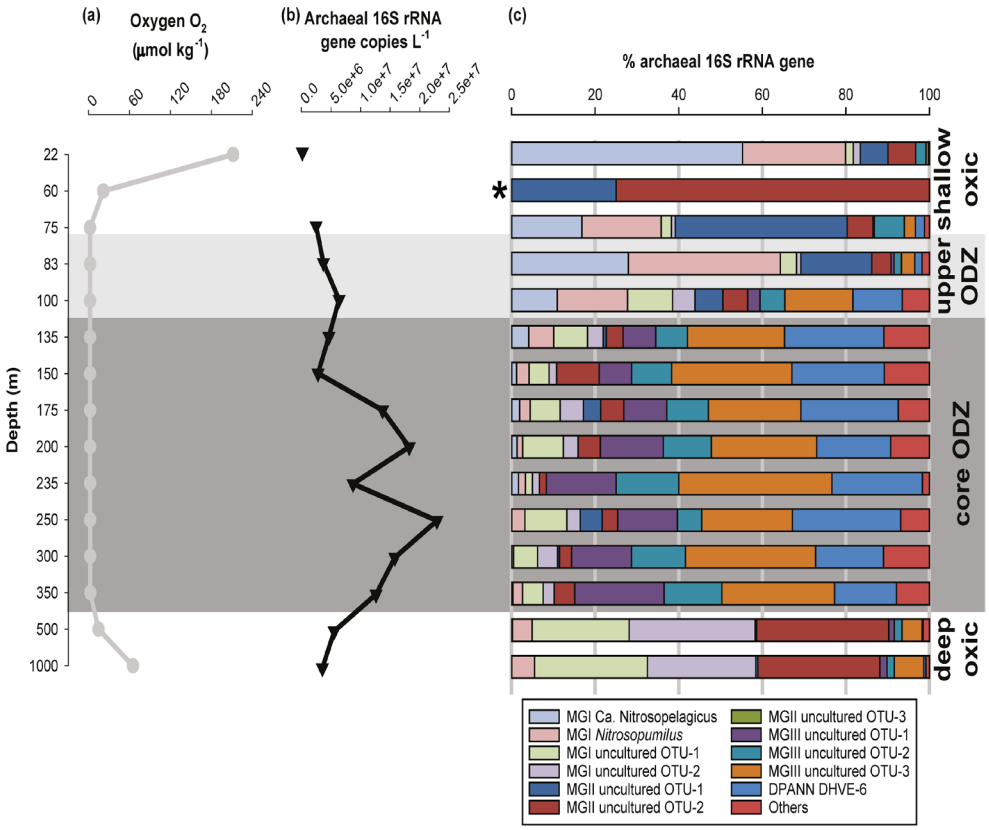

Figure 2. (a) Concentration profile of oxygen (O_2, µmol kg^{-1}), (b) absolute number of total archaeal 16S rRNA gene (copies L^{-1}), and (c) percentage of the archaeal 16S rRNA gene reads of the archaeal groups detected across the ETSP water column at the coastal station. *At this depth only 4 of the 8127 recovered sequences were derived from archaea. Therefore, the distribution of archaeal sequences is not statistically significant but it gives some feel for the distribution of the MGII archaeal group.

total thaumarchaeotal 16S rRNA gene reads, together with sequences affiliated to *Nitrosopumilus* and *Ca*. Nitrosopelagicus (Table 1; Fig. 3c). At both stations *Ca*. Nitrosopelagicus was dominant over *Nitrosopumilus* and MGI OTU-1 at the uppermost depth (55% of 16S rRNA gene reads compared to 25% at 22 m at the costal station; 33% compared to 16% and 15% at 100 m at the open ocean station) and MGI OTU-2 (Fig. 4a) was only detected in low relative abundance (Table 1; Figs. 2c and 3c). At the open ocean station, where sampling only started at 100 m, we suspect the same distribution also at shallower depths. MGI *Ca.* Nitrosopelagicus, although genetically close-

ly related to *Nitrosopumilus*, is expected to be better adapted to the pelagic environment (Santoro et al., 2015). Its higher relative abundance at the shallower depths might be due to a better response to photo-inhibition stress or to a more efficient uptake of ammonium (Merbt et al., 2012; Santoro et al., 2015; Smith et al., 2014). At the coastal station no thaumarchaeotal 16S rRNA gene sequences were detected at the oxycline (60 m; Table 1; Fig. 2c). This coincided with no amplification of the archaeal 16S rRNA gene (Fig. 2b), meaning that at this depth the number of archaeal 16S rRNA gene copies was below the level of detection using our qPCR approach. At both stations *Ca*. Nitrosopelagicus tended to decrease in relative abundance towards the upper ODZ, confirming the preference of this group for a shallow oxic water niche (Table 1; Figs. 2c and 3c). On the contrary, at the coastal station *Nitrosopumilus* maximized in the upper ODZ at 83 m (36% of total archaeal reads; Table 1; Fig. 2c).

At the open ocean station *Nitrosopumilus* relative abundance remained stable down to the oxycline (18% at 125 m) and in the upper ODZ (13% at 155 m; Fig. 3c). The high affinity of *Nitrosopumilus* for NH_4^+ (Martens-Habbena et al., 2009) and its proven adaptability to micro to nanomolar O_2 concentrations (Bristow et al., 2016) are probably among the reasons why members of this group occupy that specific niche at the two stations. At the open ocean station, the relative abundance of sequences affiliated to the MGI OTU-1 increased from the shallow oxic waters (14% at 100 m) to the oxycline and then remained stable at the upper ODZ (ca. 20% at 125–155 m; Table 1; Fig. 3c). A higher relative abundance of Thaumarchaeota in the oxycline/upper ETSP ODZ has been previously reported by archaeal *amo*A gene copy numbers, CARD-FISH and protein-coding transcript counts attributed to Thaumarchaeota (Belmar et al., 2011; Lam et al., 2009; Molina et al., 2010; Stewart et al., 2011). Additionally, the tendency of Thaumarchaeota to occupy the niche at the oxycline/upper ODZ has been described as a recurring feature of the other main ODZs such as the eastern tropical North Pacific (ETNP) and the Arabian Sea ODZs (Beman et al., 2008, 2012; Pitcher et al., 2011b), and anoxic basins such as the Black Sea, the Cariaco Basin, and the Gotland Basin of the Baltic Sea (Berg et al., 2014; Coolen et al., 2007; Wakeham et al., 2012).

Within the core ODZ, Thaumarchaeota became a minor component of the archaeal community at both stations, only making up <20% of the 16S rRNA gene reads (Table 1; Figs. 2c and 3c). Moreover, within the core ODZ the composition of the thaumarchaeotal population changed and, whereas MGI

OTU-1 maintained some relevance at both stations, *Ca*. Nitrosopelagicus and *Nitrosopumilus* were all minor components of the archaeal population (Table 1; Figs. 2c and 3c). This decrease in the core ODZ is consistent with previous studies (Belmar et al., 2011; Stewart et al., 2011) and suggests that the Thaumarchaeota are not well adapted to the core ODZ environment, likely because of the lack of oxygen. However, the thaumarchaeotal groups remained detectable throughout the ODZ, but this may simply be due to preservation of DNA produced in the upper water masses favored by anoxic conditions, as suggested in a recent study which found fossil 16S rRNA and *amo*A gene copies in anoxic sediments from the Arabian Sea (Besseling et al., 2018).

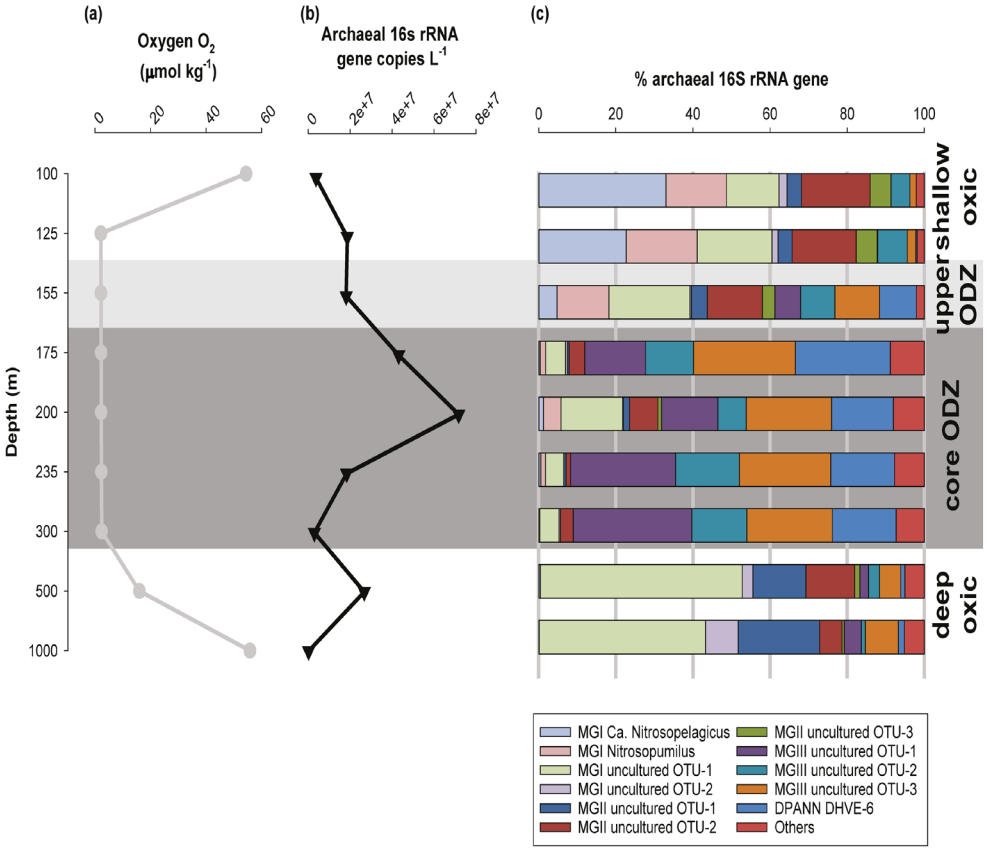

Figure 3. (a) Concentration profile of oxygen (O_2, µmol kg^{-1}), (b) absolute number of total archaeal 16S rRNA gene (copies L^{-1}), and (c) percentage of the archaeal 16S rRNA gene reads of the archaeal groups detected across the ETSP water column at the open ocean station.

Peng et al. (2013) actually reported a higher number of *amo*A gene copies in the core ETSP ODZ off the Peruvian coastline (i.e. at 260 m) compared to the oxic surface (i.e. at 20 m) and suggested that the thaumarchaeotal cells were dormant or somehow able of an alternative energetic metabolism to aerobic ammonia oxidation to nitrite. However, the occurrence of periodic aerobic metabolisms including ammonia oxidation, likely fueled by episodic intrusions of O_2 within the ODZ (Bristow et al., 2016; Ulloa et al., 2012), cannot be ruled out.

At both stations, Thaumarchaeota regained relevance below the ODZ (below 350 m at the coastal station and below 300 m at the open ocean station) dominating the archaeal community at those depths, accounting for up to 58% of the archaeal 16S rRNA gene reads at the coastal station and 50–55% at the open ocean station (Table 1; Figs. 2c and 3c). *Nitrosopumilus* was part of the population at the coastal station in low abundances but the two MGI OTUs, not related to any cultured archaeon (Fig. 4a), were particularly abundant (Table 1; Figs. 2c and 3c). Sequences affiliated to the MGI OTU-1 and OTU-2 are closely related to sequences previously detected both in the upper oxycline, within the ODZ and in the deep oxycline in the water column of the Northeast Subarctic Pacific Ocean oxygen minimum zone (NESAP OMZ, also referred to as the Eastern Subtropical North Pacific OMZ; Fig. 4a). The core of the NESAP was characterized, at the time of sampling, by O_2 concentrations of 8.6–15 $\mu mol\,kg^{-1}$ and in some cases even reached 60 $\mu mol\,kg^{-1}$ (Freeland et al., 1997; Whitney et al., 2007). We found similar oxygen concentrations in the upper oxycline and deep oxic waters of the ETSP (Figs. 2a and 3a), which supports the idea that these sequences represent Thaumarchaeota adapted to waters with oxygen levels in the range of approximately 9-60 $\mu mol\,kg^{-1}$. Of the two uncultured MGI OTUs, MGI OTU-1 was more abundant than MGI OTU-2 in the open ocean station, while they have similar abundance in the oxygenated waters below the ODZ of the coastal station. However, in general these two OTUs had a much higher relative abundance in the deeper oxygenic water in comparison with the archaea closely related to *Nitrosopumilus* and *Ca.* Nitrosopelagicus. This specific 'deep water' niche occupancy of MGI has been previously observed for many locations including the ETSP, the ETNP and the Arabian Sea ODZs among others, with the presence of a shallow cluster (i.e. cluster A) genetically different from the deep water one (i.e. cluster B) (Belmar et al., 2011; Beman et al., 2008; Francis et al., 2005; Hallam et al., 2006; Hu et al., 2011; Mincer et al., 2007; Santoro et al., 2010; Villanueva et al., 2015). Previous studies have suggested ammonia availability as a driver

of the diversification of Thaumarchaeota in the water column (Sintes et al., 2016 among others. However, the concentrations of ammonia reported here throughout the water column (Fig. S1c and S1f; Table S2 are low and similar, which suggests that alternative factors other than ammonia and oxygen levels may play a role in this differentiation.

Based on its large contribution to the archaeal population of the upper ETSP (Table 1; Figs. 2c and 3c, the shallow thaumarchaeotal population is likely to be the predominant source of IPLs present in the uppermost oxic waters down to the upper ODZ at both stations (22–83 m at the coastal station, and 100, and probably even shallower depths, to 125 m at the open ocean station; Tables 2 and 3. This is in good agreement with culture studies of the lipidome of *Nitrosopumilus* revealing that MH/DH/HPH-GDGT-0–4 and -crenarchaeol IPLs comprise its major membrane lipids (Elling et al., 2014, 2017; Schouten et al., 2008a. The IPLs detected at 60 m depth of the coastal station though were likely of fossil origin as the archaeal 16S rRNA genes quantification was under detection limit at that specific depth (cf. Table 1, 2 and Fig. 2b. This is confirmed by the relatively low abundance of HPH IPLs at this depth. HPH IPLs are believed to be most prone to degradation and are therefore believed to be the best 'life markers' for Thaumarchaeota (Pitcher et al., 2011a; Schouten et al., 2012. Indeed, Elling et al. (2014 showed that HPH-crenarchaeol is mostly synthesized when cells are actively growing (Elling et al., 2014. HPH-crenarchaeol was especially abundant in the ETSP at the boundary between the oxycline and the upper ODZ (75–83 m at the coastal station, and at 125 m at the open ocean station; Tables 2 and 3), which was also where MGI *Nitrosopumilus* was most abundant together with MGI OTU-1 (Table 1; Figs. 2c and 3c). This suggests that these are living populations, which would confirm a preferred niche of *Nitrosopumilus* and, possibly, MGI OTU-1 for suboxic conditions. A predominant origin of the archaeal IPLs in the surface waters from Thaumarchaeota is also evident from our analysis of the correlation between archaeal copy numbers and the concentration of individual IPLs (Fig. 5). This analysis for the coastal station revealed that both *Ca*. Nitrosopelagicus (r value > 0.60; Fig. 5a; Table S5a) and *Nitrosopumilus* (r value > 0.50) had the highest correlation with the MH/DH/HPH-GDGT-0–4 and -crenarchaeol IPLs. At the open ocean site, these correlations were still evident for *Ca*. Nitrosopelagicus but somewhat less ev-ident for *Nitrosopumilus* (Fig. 5b; Table S5b). Together, our findings indicate that both *Nitrosopumilus* and *Ca.* Nitrosopelagicus were actively growing and were the main contributors to the IPL inventory in the upper ETSP.

The IPLs detected in the upper ETSP (i.e. GDGT-0–4 and crenarchaeol with MH/DH/HPH-headgroups have previously been reported in other similar locations, including the Arabian Sea, where MH/DH/HPH-GDGT-0–3 and -crenarchaeol peaked in the upper ODZ (Schouten et al., 2012, and the ETNP, where MH/DH-GDGT-0, -2 and -crenarchaeol were also especially abundant in the upper ODZ (Xie et al., 2014. In contrast, in the Cariaco Basin MH-GDGT-0–3 and -crenarchaeol were detected already in the oxycline, followed by DH-GDGT-0–3 and -crenarchaeol in the deeper suboxic waters (Wakeham et al., 2012. In the Black Sea, albeit with different individual distributions, MH/DH/HPH-GDGT-0–4 and -crenarchaeol were already present in the oxic surface and remained prominent down to the upper suboxic zone (Schubotz et al., 2009; Sollai et al., 2018. However, IPLs with hydroxy GDGT cores were also prominent in the sub-oxic zone of the Black Sea (Sollai et al., 2018 and were not detected in the waters of the ETSP.

PE/PG-archaeol IPLs were also detected in the shallow ETSP, although their concentrations were low compared to deeper waters where they became much more abundant (below 135 m at the coastal station and below 175 m at the open ocean station; Tables 2 and 3). All archaeal lineages thriving in the upper ETSP show a negative correlation with those IPLs, with the exception of MGI OTU-1 at the coastal station (r values ca. 0.20–0.46; Fig. 5; Table S5) suggesting that the thaumarchaeotal population was not strongly contributing to the synthesis of the PE/PG-archaeol IPLs in the shallow ETSP waters.

After a strong decline in the core of the ODZ, GDGT-0–4 and crenar-chaeol IPLs became prominent again in the deep oxygenated waters (Tables 2 and 3). However, the distribution of the archaeal IPLs did not revert com-pletely to the one observed in the upper ETPS. Here, HPH-GDGT-1, -2 and DH-GDGT-0 and -crenarchaeol became especially abundant resulting in a distinct distribution of archaeal IPLs (Tables 2 and 3). The concentration of these four IPLs showed a strong positive correlation with each other at both stations, suggesting a common thaumarchaeotal origin (Fig. S3; Table S7). The specific distribution is most evident from the depth-concentration profile of HPH-GDGT-2 at the open ocean site, which shows a distinct maximum at 500 m (Table 3), where the concentration is almost three times higher as in the surface waters. Earlier studies from other oceanic regions have shown that the fractional abundance of GDGT-2 relative to other core GDGTs increases with increasing water depth and that this increase is more pronounced for IPL-GDGTs as for CL-GDGTs (Hernández-Sánchez et al., 2014; Kim et al.,

2015, 2016; Taylor et al., 2013; Villanueva et al., 2015. Our data reveal that GDGT-2 is likely actively produced in the deeper waters since it is predominantly present as a CL of the most labile form of archaeal IPLs, i.e. with the HPH head group. For the open ocean site the concentration of HPH-GDGT-2 had a highly positive correlation with the copy number of MGI OTU-2, and to a slightly lesser degree, MGI OTU-1 (Fig. 5b; Table S5, the two Thaumarchaeota thriving in the deep oxygenated waters. Positive correlations were also observed for DH- and HPH-GDGT-0, -GDGT-1, and crenarchaeol. For the coastal sites, these correlations are not evident, although most of these IPLs show a clear sub-maximum in their concentration profile at 500 m (Table 2. The correlations between thaumarchaeotal cell abundance (as expressed by copy numbers and IPL concentrations may be obscured by the fact that all the four different groups of Thaumarchaeota detected in the ETSP waters produce the same type of IPLs but in a different distribution. Overall these results suggest that the IPLs found in the deep ETSP originated from the thaumarchaeotal groups present (Fig. S3; Table S7.

3.4.2. Marine euryarchaeota group II (MGII) co-exists with the shallow and deep thaumarchaeotal populations

At the coastal station the MGII population was formed by two uncultured OTUs, and accounted for 13% of the total archaeal 16S rRNA gene reads at the uppermost depth (22 m but became the second archaeal group after the Thaumarchaeota at 75 m accounting for 47% of the total archaeal reads, and MGII OTU-1 was clearly dominant over OTU-2 (41% compared to 6%). The lack of archaeal 16S rRNA gene detection by qPCR at 60 m (Fig. 2b) and the few archaeal sequences recovered with 16S rRNA gene amplicon analysis indicate that the dominance of MGII (Fig. 2c) at this depth is unreliable. At the open ocean site, the MGII shallow population included a third OTU (i.e. MGII OTU-3 that was not found at the coastal station (cf. Fig. 2c and 3c. At this station the MGII population accounted for 20–25% of the archaeal reads in the 100–155 m interval and OTU-2 was clearly the most abundant MGII OTU (14–18% compared to ca. 4% of OTU-1 and ca. 5% of OTU-3; Table 1; Fig. 3c. The distribution displayed by MGII in the shallow oxic waters and upper ODZ of the ETSP at both stations agrees with precedent reports in which the group was found as particularly prominent in

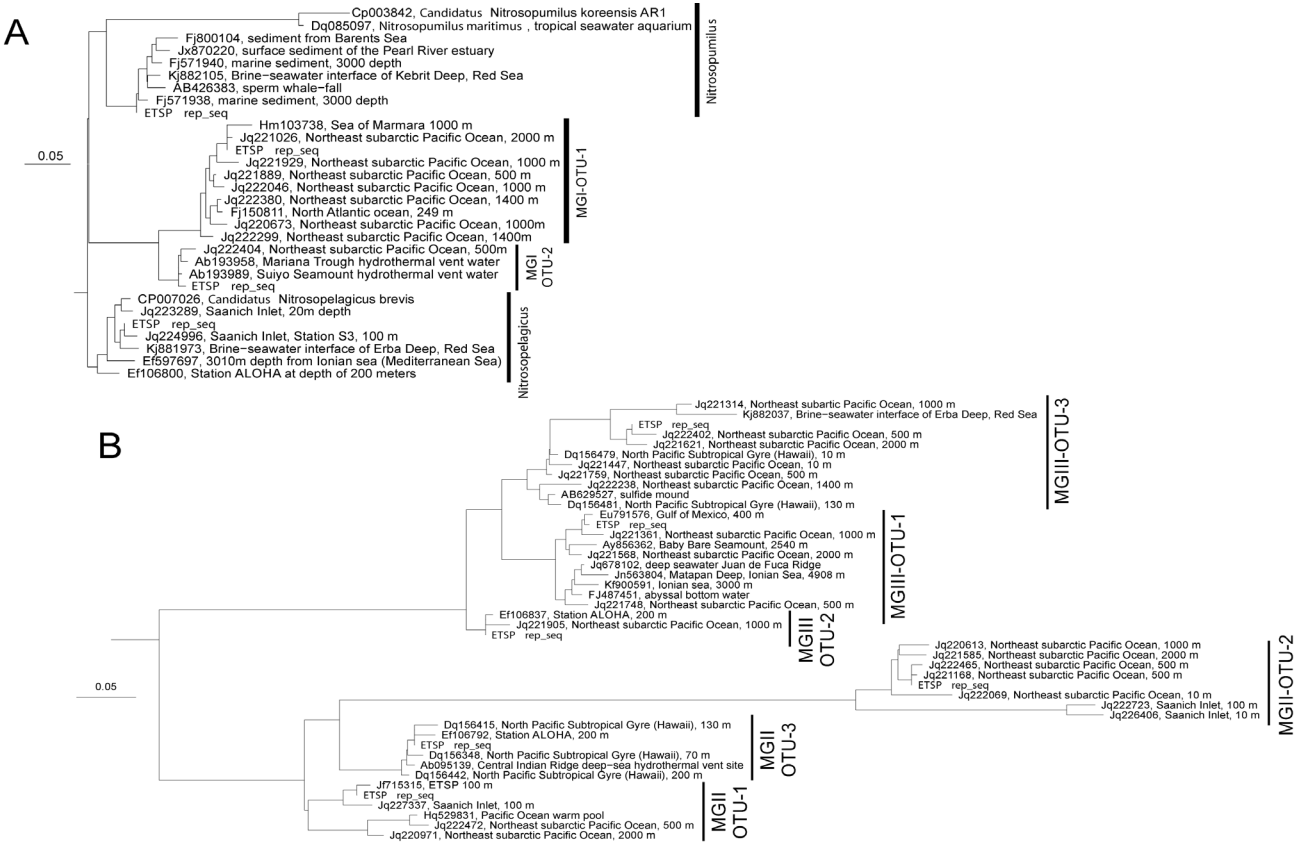

Figure 4. Phylogenetic trees showing the representative sequences (rep_seq, obtained by pick_rep_set.py in qiime of the OTUs picked by Usearch as specified in the material and methods) present in the ETSP of the four OTUs of Thaumarchaeota (A), and the three OTUs of MGII and MGIII archaea (B) in relation to closely related sequences. Scale bar indicates estimated sequence divergence (i.e. 5%).

shallow oxic waters (ca. 0–50 m) and in the suboxic waters (ca. 60–200 m), although to a lower extent (Belmar et al., 2011; Quiñones et al., 2009). This suggests that, especially at the open ocean station where the sampling started from 100 m depth, the group might be present also in shallower waters (Hugoni et al., 2013). In fact, MGII are believed to have a heterotrophic lifestyle and a putative proteorhodopsin gene, whose expressed protein, powered by light, would allow the cells to move towards preferential food sources, has been found in the genomes of MGII detected in the photic zones in the North Pacific Ocean (Frigaard et al., 2006; Iverson et al., 2012). Their abundance in the shallow ETSP is also in line with the distribution from other locations worldwide (Galand et al., 2009; Iverson et al., 2012; Massana et al., 2000; Podlaska et al., 2012). Sequences affiliated to MGII OTU-1 and OTU-2 detected by this study were closely related to sequences previous detected in the ETSP and in the Saanich inlet at 100 m depth, and to sequences detected in the NESAP OMZ at various depths (Fig. 4b). Sequences affiliated to the MGII OTU-3 were closely related to sequences previous amplified in the north Pacific subtropical gyre (NPSG; Fig. 4b).

In the core ODZ, the MGII archaea decreased drastically and accounted for <12% of the total archaeal 16S rRNA reads at the coastal station and <10% at the open ocean station and only at specific depths (Table 1; Figs. 2c and 3c), meaning that as for Thaumarchaeota also MGII was not well adapted to the core ODZ environment and the group was only barely detected throughout the ODZ (Table 1; Figs. 2c and 3c).

In the deep oxic waters below the ODZ MGII archaea regained importance especially as OTU-2 at the coastal station (29–32% of the total archaeal reads) and as OTU-1 (14–21%) and OTU-2 (6–13%) at the open ocean site (Table 1; Figs. 2c and 3c). The relative change in the composition of the MGII population from the shallow oxic waters and upper ODZ to the deep oxic waters was not as obvious as for the MGI population. Indeed, only the relative abundance of the uncultured OTUs comprising the MGII population was affected (Table 1; Figs. 2c and 3c), indicating the ability of the ETSP MGII population to adapt either to the surface and to the deep sea conditions rather than the differentiation of a specific deep MGII population in contrast to the shallow one. MGII sequences have been detected also from deep waters in multiple locations, although they are typically less abundant compared to the shallow waters (Baker et al., 2013; Deschamps et al., 2014; Frigaard et al., 2006). Interestingly, the genomes of these MGII archaea thriving in deep

waters did not harbour any homolog of the proteorhodopsin gene found in the shallow MGII ecotypes, but were found to hold multiple genes typical of heterotrophic prokaryotes involved in amino acid, carbohydrate and lipid transport and metabolism (Deschamps et al., 2014.

The appointment of specific IPLs to the MGII is problematic because of the lack of pure cultures of this lineage and, in fact, previous attempts to do so remain not conclusive to date (Lincoln et al., 2014a; Schouten et al., 2008b, 2014; Turich et al., 2007. At both stations MGII archaea co-existed with Thaumarchaeota in the ETSP water column (Table 1; Figs. 2c and 3c. At the coastal station, copy numbers of MGII OTU-1 were positively correlated with those of *Ca.* Nitrosopelagicus, MGI OTU-1 and, especially *Nitrosopumilus*, whereas MGII OTU-2 correlated with the two "uncultured" MGI OTUs (Fig. S2a; Table S6a). At the open ocean station, copy numbers of MGII OTU-1 correlate highly positively with those of the two "uncultured" MGI OTUs. MGII OTU-2 scored highly positive with *Nitrosopumilus* and MGI OTU-1, and MGII OTU-3 with *Ca*. Nitrosopelagicus and *Nitrosopumilus* (Fig. S2b; Table S6b). These results indicate that MGII and MGI archaea occupy the same niche and, consequently, the positive correlation of the copy numbers of MGII OTU-1 and -3 with the concentrations of some of the GDGT IPLs (Fig. 5; Table S5) cannot be used to safely appoint these IPLs detected to the MGII affiliates. Confirmation from pure culture experiments is needed as in the case of Thaumarchaeota.

3.4.3. Marine euryarchaeota group III (MGIII) and DPANN Woesearchaeota thrive in the ODZ of the ETSP water column

At both stations MGIII accounted for 40–70% of the total archaeal diversi-ty in the core ODZ, depending on the depth (Table 1; Figs. 2c and 3c). MGIII OTU-3 was the most abundant at the coastal station (16–38%). At the open ocean station OTU-1 and OTU-3 accounted respectively for 7–30% and for 12–26% of the total archaeal 16S rRNA gene reads; OTU-2 instead accounted for less than 17% (Table 1; Figs. 2c and 3c). MGIII archaea have previous-ly been detected within the ETSP ODZ (Belmar et al., 2011; Stewart et al., 2011) and in suboxic and euxinic waters of the Black Sea (Sollai et al., 2018), although in these studies this group did not represent such a large part (i.e. up to 70%) of the archaeal community as reported in our study (Table 1; Figs. 2c and 3c). Metagenomic studies have found evidence of fermentation-related genes, including those potentially involved in the metabolism of peptide and

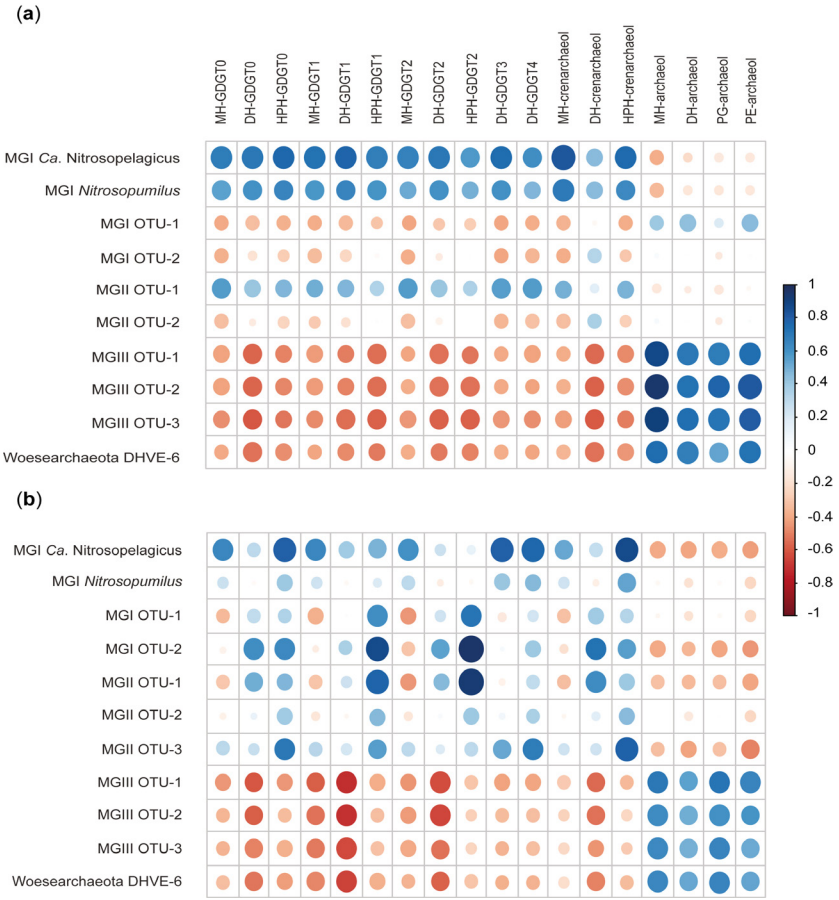

Figure 5. Dot plot of the correlation matrix obtained by applying a Pearson analysis to the total archaeal 16S rRNA gene reads (copies L^{-1}) of the archaeal groups and to the abundances of the archaeal IPLs (response units per Liter; r.u. L^{-1}) detected at the (a) coastal and (b) open ocean stations of the ETSP. Dark blue corresponds to +1 r values, indicating a strong positive linear correlation between archaeal groups and IPLs; white corresponds to 0 r values, indicating that no correlation exists; dark red corresponds to -1 r values, indicating a strong negative linear correlation.

lipids, in genomes of many MGIII archaea, suggesting they could be facultative anaerobes (Martin-Cuadrado et al., 2008). Previous studies have also detected MGIII archaea in the marine photic zone; their genomes containing numerous photolyase and rhodopsin genes suggesting a photoheterotrophic lifestyle (Galand et al., 2009; Haro-Moreno et al., 2017; Martin-Cuadrado et al., 2008). In the ETSP, MGIII archaea were also present in the shallow oxic waters, with three OTUs at both stations but they represented only a minor

group (3–10% of total archaeal reads at 22–75 m at the coastal station and 6–10% at 100–125 m at the open ocean station). Sequences affiliated to the three MGIII OTUs were closely related to sequences previously detected in deep-sea waters as well as at the various depths of the NESAP OMZ (Fig. 4b), therefore it seems that the factor depth does not play a role in the dif-ferentiation of these three group, whereas the presence of oxygen might be key in the distribution of the different MGIII groups. In the deep oxic waters, MGIII archaea, mostly represented as OTU-3, became a minor group, ac-counting for not more than 15% of the total archaeal reads at both stations (Table 1; Figs. 2c and 3c). The presence of OTU-3 throughout the ETSP water column suggests high flexibility of this OTU to different water conditions compared with the other MGIII OTUs detected.

Members of the DPANN superphylum are increasingly reported in anoxic water columns including the ETSP ODZ, and the Black Sea (Belmar et al., 2011; Sollai et al., 2018). In the ETSP, Belmar et al. (2011) detected a se-quence related to the DHVE-5 group within the ODZ (Belmar et al., 2011). Here, we report the presence of the DPANN Woesearchaeota DHVE-6 group as a major component of the archaeal ETSP ODZ community (accounting for 10–26% of the total archaeal reads in the core ODZ; Table 1; Figs. 2c and 3c). Recently, this same group was also found to be prominent in the euxinic waters of the Black Sea (Sollai et al., 2018), in euxinic surface marine sediments of Lake Grevelingen in The Netherlands (Lipsewers et al., 2018), in the anoxic surface sediments below the Arabian Sea ODZ (Besseling et al., 2018), as well as in lacustrine and estuarine systems (Lazar et al., 2017; Ortiz-Alvarez and Casamayor, 2016). Although their metabolic traits are still largely unknown, DPANN archaea are likely to depend greatly on others for their metabolic needs due to the reported small size of their cells and genomes (Castelle et al., 2015; Rinke et al., 2013).

At both stations archaeol-IPLs were hardly detected in the shallow oxic waters and in the upper ODZ, but became the most prominent archaeal IPL group within the ODZ (Tables 2 and 3). This is the first study to report archae-ol-IPLs within the core of one of the main ODZs worldwide. Archaeol-IPLs have been previously detected in suboxic and euxinic waters and in microbial mats in the Black Sea (Rossel et al., 2008; Sollai et al., 2018), but not in the ETNP (Xie et al., 2014), nor in the Arabian Sea ODZs (Schouten et al., 2012). In the ETSP, all archaeol-IPLs maximized within the ODZ, while the GDGT-0–4 and crenarchaeol-IPLs instead drastically decreased (Tables 2 and

3. The concentrations of archaeol-IPLs correlated positively with each other but negatively with GDGT-0–4 and crenarchaeol IPLs. This strongly suggests a common origin for the archaeol-IPLs distinct from that of the other IPLs (Fig. S3; Table S7. The copy numbers of both MGIII and DPANN archaea correlated positively with the concentrations of all archaeol-IPLs and negatively with those of the GDGT-0–4 and crenarchaeol-IPLs (Fig. 5; Table S5. Since neither MGIII nor Woesearchaeota cultures are yet available, we suggest, by combining the result of the correlation analysis and the known metabolic features of the two archaeal groups, that MGIII archaea were primarily responsible for synthesizing the archaeol-IPLs detected the ETSP ODZ. Most of the currently available genomes of DPANN archaea lack most, if not all, the genes coding for the enzymes of the archaeal lipid biosynthetic pathway with the exception of the genomes of the phylum *Ca.* Micrarchaeota and the genome of *Ca.* Iainarchaeum andersonii (Jahn et al., 2004; Villanueva et al., 2017. Therefore, it is likely that the DPANN Woesearchaeota (i.e. DHVE-6 detected here within the core of the ODZ do not have the ability to synthesize their own archaeal membrane lipids and are dependent on others to acquire a membrane. This would imply that MGIII would be the likely candidate for the synthesis of archaeol-IPLs. If so, these MGIII lipids could also be the source of the membrane of the DPANN Woesearchaeota present in the ETSP ODZ. A recent study has described a relationship of dependency between of an acidophilic archaeon of the ARMAN group belonging to the DPANN superphylum and a representative of Thermoplasmatales, the order to which the MGIII group belongs (Golyshina et al., 2017. According with this study many fundamental metabolic pathways, including phospholipid biosynthesis, were absent in the ARMAN archaeon and the authors assumed a mutualistic interaction between the two archaea that included gene transfer, an evidence that might corroborate our speculation of some sort of symbiosis/parasitic lifestyle between the MGIII and the DPANN Woesearchaeota detected in this study.

3.5. Conclusion

Our study expands the knowledge on the archaeal community thriving in the ETSP region, including its ODZ. We have found that this region harbors a highly diverse assemblage of archaeal lineages that are distributed across the water column according to a clear depth partitioning. This seems to be mostly depending on the oxygen changing concentration across the water col-

umn. We also shade light for the first time on the IPLs synthesized by these archaeal communities; the IPL distribution follows similar depth segregation as that of the archaeal lineages detected, and we tentatively assigned specific IPLs to specific archaeal groups based on statistical evidence. Specifically, HPH-crenarchaeol, the specific biomarker for living Thaumarchaeota, HPH-GDGT-0, DH-GDGT-3 and -4 were likely synthesized by Thaumarchaeota related to *Ca.* Nitrosopelagicus and *Nitrosopumilus* from the shallow oxic waters and the upper ODZ. MGII affiliated sequences were also abundant in the shallow ETSP, but we could not assign specific IPLs to this group. MGIII dominated the archaeal community within the ODZ together with DPANN ar-chaea, but the former group was the one likely synthesizing the archaeol-IPLs detected. It may have also provided the membrane lipids to the DPANN Wo-esearchaeota group, which is predicted to lack lipid biosynthetic pathways. In the deep, oxic waters below the ODZ, the composition of the deep MGI and MGII archaeal populations was different from the shallow one, being mostly represented by uncultured MGI and MGII OTUs. The MGI OTU-1 and -2 archaea synthesized a different suite of IPLs, which was characterized by higher proportions of HPH-GDGT-1, -2 and DH-GDGT-0 and crenarchaeol.

Acknowledgements

We thank the captain and the crew of the *R/V Nathaniel B. Palmer* for assistance and technical support and the chief scientists, Allan H. Devol and Bess B. Ward, for organizing and supervising the NBP13-05 cruise. Addi-tional thanks are due to Anna Rabitti and Borja Aguiar-González for helpful discussion and comments on the physical features of the ETSP water column. This research was funded by a grant to JSSD from the Darwin Center for Biogeosciences (project nr. 3012). This research was further supported by the NESSC and SIAM Gravitation Grants (024.002.001 and 024.002.002) from the Dutch Ministry of Education, Culture and Science (OCW) to JSSD.

Table S1. The table lists the coastal (48, 51, 54, 58a, 58b, 61, 64a, 64b) and open ocean (11, 14, 15, 24) stations sampled for SPM using multiple *in situ* pump devices, during the NBP13-0 cruise (June–July 2013) aboard of the *R/V Nathaniel B. Palmer*. For each cast the depth (meters) of the sampling and the corresponding potential density (σθ, kg m^{-3}, the oxygen concentration measured (μmol kg^{-1}, the location (DMS, longitude and latitude, the date (dd/mm/yyyy and the volume of water filtered by the pump deployed (Liters are reported.

Station*	Depth of SPM sampling (m)	Potential density (kg m^{-3})	O_2 (μmol kg^{-1})	Location DMS (lon/lat) S	W	Date dd/mm/yyyy	Amount of water filtered** (L)
58b	22	25.63	211.8	20°44'59.7"	70°39'30.6"	19/07/2013	264
64a	60	26.05	21.5	20°42'23.2"	70°42'31.1"	21/07/2013	382
54	75	26.19	2.1	20°46'22.6"	70°48'51.6"	18/07/2013	452
64b	83	26.18	2.2	20°42'23.5"	70°42'29.0"	21/07/2013	1567
58a	100	26.30	2.2	20°45'23.3"	70°39'06.4"	19/07/2013	1834
51	135	26.30	2.2	20°28'27.6"	70°41'32.4"	17/07/2013	977
58a	150	26.40	2.2	20°45'23.3"	70°39'06.4"	19/07/2013	740
58b	175	26.45	2.2	20°44'59.7"	70°39'30.6"	19/07/2013	2286
64a	200	26.42	2.2	20°42'23.2"	70°42'31.1"	21/07/2013	1477
51	235	26.50	2.2	20°28'27.6"	70°41'32.4"	17/07/2013	3014
61	250	26.48	2.3	20°43'46.5	70°40'15.0"	20/07/2013	2668
61	300	26.61	2.4	20°43'46.5	70°40'15.0"	20/07/2013	745
64b	350	26.71	2.5	20°42'23.5"	70°42'29.0"	21/07/2013	549
48	500	26.95	14.6	20°33'07.1"	70°44'00.0"	16/07/2013	1031
48	1000	27.39	65.0	20°33'07.1"	70°44'00.0"	16/07/2013	4028
15	100	26.00	54.4	13°55'19.7"	81°16'38.8"	03/07/2013	2306
14	125	26.18	2.1	13°29'36.0"	81°12'06.2"	04/07/2013	3400
11	155	26.35	2.1	14°00'44.8"	81°07'10.1"	05/07/2013	851
14	175	26.35	2.1	13°29'36.0"	81°12'06.2"	06/07/2013	783
24	200	26.45	2.2	13°25'30.6"	81°13'50.5"	07/07/2013	3391
11	235	26.50	2.2	14°00'44.8"	81°07'10.1"	08/07/2013	3209
24	300	26.69	2.4	13°25'30.6"	81°13'50.5"	09/07/2013	875
24	500	26.99	15.9	13°25'30.6"	81°13'50.5"	10/07/2013	1036
24	1000	27.37	55.8	13°25'30.6"	81°13'50.5"	11/07/2013	4051

*Station 58 and 64 were sampled twice
**Reading of the flow meter

Table S2. Physicochemical conditions in the ETSP water column at the coastal (st. 48, 54, 58, 61, 64) and open ocean (st. 14, 24, 26) stations, indicated as water depth (meters) and corresponding potential density (σθ, kg m^{-3}), oxygen concentration (O_2, μmol kg^{-1}), nitrate, (NO_3^-, μM), nitrite, (NO_2^-, μM) and ammonium, (NH_4^+, μM).

Station	Depth (m)	Potential density (kg m^{-3})	O_2 (μmol kg^{-1})	NO_3^- (μM)	NO_2^- (μM)	NH_4^+ (μM)
48	20	25.63	211.8	4.2	0.2	0.54
	94	26.27	2.1	11.9	3.8	0.06
	198	26.47	2.2	15.7	6.7	0.05
	230	26.50	2.3	17.1	6.5	0.03
	300	26.61	2.4	21.2	6.7	0.04
	500	26.95	14.7	41.2	0.0	0.06
54	30	25.85	123.1	11.4	0.5	1.48
	70	26.19	2.1	13.6	2.8	0.08
	115	26.31	2.1	9.7	5.6	0.03
	125	26.33	2.2	9.9	5.6	0.03
	281	26.50	2.3	16.4	6.6	0.05
	301	26.54	2.3	17.9	6.5	0.02
	323	26.60	2.4	21.0	5.6	0.02
	370	26.71	2.5	30.7	1.0	0.04
58	11	25.62	212	3.5	0.1	0.32
	19	25.61	214	4.3	0.2	0.35
	41	25.83	107	15.1	0.5	1.04
	51	25.96	44	19.5	0.6	0.70
	90	26.27	2	11.8	3.5	0.02
	100	26.30	2	10.2	5.3	0.03
	115	26.34	2	8.8	7.5	0.05
61	200	26.42	2	13.5	7.2	0.12
	998	27.38	65	43.5	0.0	0.12
	15	25.63	216	3.7	0.1	0.45
	29	25.69	192	6.9	0.2	0.83
64	60	26.05	21	22.2	0.1	0.01
	79	26.19	2	15.2	1.6	0.02
	100	26.30	2	10.8	5.0	0.01
	2	25.58	220	3.2	0.1	0.18
	15	25.61	217	3.6	0.1	0.36
	20	25.64	211	4.0	0.1	0.47
	25	25.66	201	5.5	0.2	0.61
	29	25.72	181	8.5	0.2	0.70

	40	25.97	43	21.8	0.3	0.09
	50	26.10	4	20.5	0.2	0.01
	60	26.17	2	15.9	1.6	0.02
64	150	26.40	2	12.8	7.4	0.03
	239	26.46	2	15.6	7.2	0.02
	250	26.48	2	16.2	7.1	0.06
	325	26.59	2	20.8	6.6	0.01
	375	26.73	3	32.3	0.3	0.03
	2	25.37	214.1	2.6	0.2	0.20
	29	25.37	214.0	2.6	0.2	0.20
	35	25.37	213.3	2.6	0.2	0.20
	40	25.37	213.4	2.6	0.2	0.20
	64	25.46	191.7	5.5	0.2	0.26
	74	25.69	142.0	15.2	0.1	0.02
	159	26.37	2.3	19.6	0.6	0.00
14	250	26.55	2.3	20.0	6.7	0.01
	500	26.99	15.9	42.3	0.02	0.02
	699	27.19	23.4	45.7	0.02	0.04
	900	27.33	46.4	44.9	0.01	0.03
	900	27.33	46.4	44.8	0.02	0.04
	1000	27.39	55.7	44.1	0.01	0.02
	1300	27.53	76.2	42.3	0.02	0.02
	1401	27.56	81.1	41.9	0.02	0.06
	3	25.39	213.4	2.5	0.2	0.49
	20	25.38	212.8	2.5	0.2	0.50
	49	25.39	211.3	2.5	0.2	0.54
	79	25.92	93.2	20.7	0.06	0.06
	98	26.10	36.4	23.6	0.03	0.01
	124	26.25	5.5	19.9	0.03	0.06
	151	26.35	2.1	19.8	0.3	0.01
	201	26.49		23.0	1.7	0.03
24	249	26.58		25.2	3.0	0.01
	300	26.69		28.2	4.0	0.02
	350	26.77		35.7	0.04	0.02
	399	26.85		38.8	0.01	0.02
	500	27.01		43.0	0.01	0.03
	599	27.12		45.0	0.01	0.04
	800	27.28		45.7	0.01	0.04
	879	27.34		45.0	0.0	0.03
	1248	27.51		42.8	0.0	0.01

	1498	27.58		41.9	0.0	0.04
	1748	27.64		40.8	0.0	0.02
	2000	27.68		40.0	0.0	0.03
24	2251	27.71		39.1	0.0	0.04
	2501	27.73		38.4	0.0	0.03
	2999	27.75		38.3	0.0	0.02
	3501	27.75		37.6	0.0	0.02
	2	25.22	216.2	4.6	0.4	0.40
	51	25.26	212.4	2.5	0.2	0.38
	101	26.06	2.8	20.9	8.8	0.03
	124	26.18	2.1	9.4	8.0	0.01
	147	26.27	2.1	10.0	4.3	0.01
	175	26.35	2.1	14.7	4.7	0.02
	199	26.41	2.2	16.8	5.4	0.02
	226	26.47	2.2	20.1	5.8	0.01
	239	26.50	2.2	20.2	5.9	0.01
	252	26.53	2.2	21.6	8.6	0.02
	258	26.54	2.3	18.7	8.8	0.09
	270	26.56	2.3	18.8	8.9	0.02
26	273	26.57	2.3	18.9	8.0	0.02
	280	26.59	2.3	20.6	6.5	0.02
	289	26.61	2.3	23.2	6.0	0.02
	301	26.62	2.4	24.4	1.0	0.02
	350	26.72	2.5	32.9	0.02	0.00
	398	26.82	3.8	37.9	0.01	0.05
	500	26.98	11.4	41.8	0.01	0.02
	600	27.09	19.9	44.1	0.0	0.04
	799	27.26	32.1	45.7	0.0	0.02
	1001	27.37	52.9	44.4	0.0	0.05
	1252	27.49	69.7	42.9	0.0	0.34
	1500	27.59	81.1	41.9	0.0	0.03

Table S3. Estimations of the archaeal 16S rRNA gene reads (copies L^{-1}) of specific archaeal groups detected in the ETSP SPM at (a) the coastal station and at the (b) open ocean station, obtained as described in the experimental procedures.

(a)

Depth (m)	MGI *Ca.* Nitrosope-lagicus	MGI *Nitro-sopumilus*	MGI uncultured OTU-1	MGI uncultured OTU-2	MGII un-cultured OTU-1	MGII uncultured OTU-2	MGIII uncultured OTU-1	MGIII uncultured OTU-2	MGIII uncultured OTU-3	DPANN Wo-esearchaeota DHVE-6
22	8.4E+04	3.7E+04	2.8E+03	2.5E+03	1.0E+04	1.0E+04	0.0E+00	3.8E+03	9.4E+02	3.1E+02
*60	0.0E+00	0.0E+00	0.0E+00	0.0E+00	0.0E+00	0.0E+00	0.0E+00	0.0E+00	0.0E+00	0.0E+00
75	4.2E+05	4.7E+05	6.0E+04	2.4E+04	1.0E+06	1.5E+05	6.0E+03	1.8E+05	6.6E+04	5.4E+04
83	1.0E+06	1.4E+06	1.4E+05	3.9E+04	6.3E+05	1.7E+05	2.6E+04	6.6E+04	1.2E+05	6.6E+04
100	7.0E+05	1.1E+06	6.8E+05	3.4E+05	4.2E+05	3.8E+05	1.9E+05	3.8E+05	1.0E+06	7.5E+05
135	1.9E+05	2.8E+05	3.8E+05	1.7E+05	3.4E+04	1.9E+05	3.6E+05	3.5E+05	1.1E+06	1.1E+06
150	3.4E+04	8.4E+04	1.3E+05	5.0E+04	0.0E+00	2.9E+05	2.2E+05	2.7E+05	8.0E+05	6.2E+05
175	2.7E+05	3.4E+05	9.9E+05	7.6E+05	5.7E+05	7.6E+05	1.4E+06	1.4E+06	3.0E+06	3.2E+06
200	2.4E+05	2.4E+05	1.8E+06	6.4E+05	0.0E+00	9.7E+05	2.7E+06	2.1E+06	4.6E+06	3.2E+06
235	1.5E+05	1.5E+05	1.5E+05	1.5E+05	0.0E+00	1.5E+05	1.5E+06	1.3E+06	3.2E+06	1.9E+06
250	0.0E+00	7.3E+05	2.3E+06	7.3E+05	1.2E+06	8.5E+05	3.3E+06	1.3E+06	5.0E+06	5.9E+06
300	0.0E+00	7.6E+04	9.1E+05	7.6E+05	7.6E+04	4.5E+05	2.3E+06	2.0E+06	4.9E+06	2.6E+06
350	4.1E+04	2.9E+05	6.2E+05	3.3E+05	0.0E+00	6.2E+05	2.7E+06	1.7E+06	3.4E+06	1.9E+06
500	1.4E+04	2.6E+05	1.3E+06	1.7E+06	1.9E+04	1.8E+06	7.2E+04	1.0E+05	2.6E+05	1.4E+04
1000	0.0E+00	2.0E+05	9.6E+05	9.2E+05	1.8E+04	1.0E+06	6.1E+04	6.1E+04	2.5E+05	1.8E+04

*Samples from 60 m depth were not included into the Pearson correlation analysis

(b)

Depth (m)	MGI *Ca.* Nitrosopelagicus	MGI *Nitrosopumilus*	MGI uncultured OTU-1	MGI uncultured OTU-2	MGII uncultured OTU-1	MGII uncultured OTU-2	MGII uncultured OTU-3	MGIII uncultured OTU-1	MGIII uncultured OTU-2	MGIII uncultured OTU-3	DPANN Woesearchaeota DHVE-6
100	1.2E+06	5.8E+05	5.0E+05	7.8E+04	1.4E+05	6.6E+05	2.0E+05	0.0E+00	1.8E+05	6.1E+04	0.0E+00
125	4.2E+06	3.4E+06	3.6E+06	3.0E+05	6.8E+05	3.1E+06	1.0E+06	2.3E+04	1.4E+06	4.1E+05	6.8E+04
155	8.6E+05	2.4E+06	3.8E+06	6.2E+04	7.4E+05	2.6E+06	5.9E+05	1.2E+06	1.6E+06	2.1E+06	1.7E+06
175	1.9E+05	5.8E+05	2.2E+06	1.9E+05	1.9E+05	1.8E+06	0.0E+00	6.8E+06	5.4E+06	1.1E+07	1.1E+07
200	9.2E+05	3.2E+06	1.1E+07	1.1E+05	1.1E+06	5.3E+06	6.9E+05	1.0E+07	5.3E+06	1.6E+07	1.1E+07
235	1.1E+05	2.2E+05	8.7E+05	0.0E+00	1.1E+05	2.2E+05	0.0E+00	5.0E+06	3.0E+06	4.3E+06	3.0E+06
300	0.0E+00	9.7E+03	1.5E+05	9.7E+03	0.0E+00	9.7E+04	0.0E+00	9.0E+05	4.2E+05	6.5E+05	4.9E+05
500	1.3E+05	0.0E+00	1.4E+07	7.3E+05	3.7E+06	3.4E+06	3.5E+05	6.1E+05	7.7E+05	1.5E+06	2.9E+05
1000	2.9E+02	0.0E+00	7.2E+04	1.4E+04	3.5E+04	9.8E+03	8.6E+02	7.5E+03	1.7E+03	1.4E+04	2.6E+03

Table S4. Abundances of the archaeal IPLs (response units per Liter; r.u. L^{-1}) detected in the ETSP SPM at (a) the coastal station and at the (b) open ocean station.

(a)

Depth (m)	GDGT-0			GDGT-1			GDGT-2		
	MH	DH	HPH	MH	DH	HPH	MH	DH	HPH
22	1.6E+04	0.0E+00	0.0E+00	0.0E+00	0.0E+00	0.0E+00	0.0E+00	1.3E+05	0.0E+00
*60	1.7E+06	8.3E+06	1.0E+08	2.0E+05	2.3E+07	5.9E+06	6.1E+04	4.4E+07	1.2E+06
75	3.7E+06	9.1E+06	3.1E+08	4.4E+05	3.0E+07	2.7E+07	1.8E+05	4.9E+07	6.5E+06
83	3.1E+06	1.0E+07	3.6E+08	4.9E+05	3.5E+07	3.7E+07	1.4E+05	5.7E+07	6.9E+06
100	5.2E+05	2.8E+06	9.2E+07	6.8E+04	9.4E+06	7.9E+06	2.5E+04	1.6E+07	1.1E+06
135	4.0E+05	2.2E+06	8.5E+07	8.0E+04	5.1E+06	1.2E+07	1.2E+04	1.4E+07	2.8E+06
150	1.8E+05	2.7E+05	8.0E+06	4.9E+04	1.1E+06	0.0E+00	1.8E+04	3.6E+06	0.0E+00
175	3.5E+05	0.0E+00	1.5E+07	7.7E+04	3.1E+06	1.4E+06	1.6E+04	6.2E+06	0.0E+00
200	1.3E+05	7.0E+05	7.6E+06	4.1E+04	2.3E+06	0.0E+00	1.1E+04	7.5E+06	0.0E+00
235	1.4E+05	0.0E+00	1.4E+07	3.6E+04	1.3E+06	1.3E+06	1.5E+04	4.4E+06	0.0E+00
250	1.3E+05	0.0E+00	5.9E+06	2.3E+04	6.7E+05	2.2E+05	5.1E+03	3.0E+06	0.0E+00
300	7.7E+04	6.9E+04	2.5E+07	2.0E+04	8.2E+05	2.8E+06	3.9E+03	3.9E+06	0.0E+00
350	1.1E+05	0.0E+00	1.1E+07	3.3E+04	1.1E+06	1.0E+06	8.2E+03	3.8E+06	0.0E+00
500	1.6E+05	3.1E+06	9.6E+07	3.8E+04	8.0E+06	2.1E+07	1.3E+04	2.0E+07	5.4E+06
1000	6.3E+05	4.2E+06	4.3E+07	1.5E+05	1.0E+07	5.7E+06	1.7E+04	2.7E+07	0.0E+00

Depth (m)	GDGT-3	GDGT-4	Crenarchaeol			Archaeol			
	DH	DH	MH	DH	HPH	MH	DH	PG	PE
22	0.0E+00	0.0E+00	4.4E+04	0.0E+00	0.0E+00	0.0E+00	0.0E+00	0.0E+00	0.0E+00
*60	9.8E+06	2.4E+06	2.4E+06	1.0E+07	6.7E+07	0.0E+00	0.0E+00	4.3E+06	1.6E+06
75	1.2E+07	5.6E+06	3.5E+06	6.7E+06	2.5E+08	0.0E+00	0.0E+00	2.4E+07	2.6E+06
83	1.2E+07	3.5E+06	5.0E+06	1.0E+07	2.9E+08	0.0E+00	0.0E+00	1.9E+07	2.8E+06
100	1.6E+06	7.1E+05	1.1E+06	3.3E+06	6.5E+07	2.4E+04	8.4E+05	2.9E+07	5.7E+06
135	5.7E+05	2.6E+05	1.1E+06	3.6E+06	7.7E+07	1.5E+05	2.2E+06	7.5E+07	1.2E+07
150	0.0E+00	0.0E+00	6.3E+05	0.0E+00	8.0E+06	1.6E+05	6.5E+05	3.0E+07	7.3E+06
175	0.0E+00	0.0E+00	9.3E+05	1.8E+06	1.1E+07	2.6E+05	1.2E+06	4.1E+07	1.1E+07
200	0.0E+00	0.0E+00	6.9E+05	1.7E+06	8.4E+06	3.4E+05	2.4E+06	6.8E+07	1.7E+07
235	0.0E+00	0.0E+00	3.9E+05	1.2E+06	9.9E+06	2.3E+05	1.0E+06	4.7E+07	8.0E+06
250	0.0E+00	0.0E+00	3.7E+05	8.3E+05	5.8E+06	2.2E+05	1.5E+06	4.0E+07	1.0E+07
300	0.0E+00	4.4E+04	3.5E+05	5.4E+05	2.1E+07	2.9E+05	1.3E+06	6.6E+07	1.1E+07
350	0.0E+00	0.0E+00	4.5E+05	7.3E+05	9.2E+06	3.1E+05	1.5E+06	7.4E+07	8.6E+06
500	1.7E+05	2.5E+05	3.9E+05	1.1E+07	7.3E+07	2.3E+03	0.0E+00	3.4E+06	1.7E+06
1000	1.2E+05	5.5E+05	7.6E+05	6.9E+06	1.8E+07	1.9E+03	0.0E+00	5.7E+06	6.7E+05

*Samples from 60 m depth were not included into the Pearson correlation analysis

(b)

Depth (m)	GDGT-0			GDGT-1			GDGT-2		
	MH	DH	HPH	MH	DH	HPH	MH	DH	HPH
100	8.3E+05	1.6E+06	4.5E+07	1.2E+05	1.0E+07	3.2E+06	5.4E+04	2.5E+07	0.0E+00
125	6.5E+05	2.5E+06	1.3E+08	1.2E+05	8.2E+06	1.5E+07	5.5E+04	2.0E+07	2.0E+06
155	2.9E+05	8.7E+05	2.0E+07	5.2E+04	3.4E+06	1.9E+06	2.5E+04	8.3E+06	1.2E+05
175	2.9E+05	6.7E+05	1.7E+06	3.3E+04	1.1E+06	0.0E+00	1.7E+04	5.5E+06	0.0E+00
200	1.8E+05	8.3E+05	2.3E+07	3.3E+04	1.8E+06	3.5E+06	2.3E+04	8.5E+06	3.1E+05
235	5.9E+04	1.2E+05	6.2E+06	9.9E+03	1.1E+06	0.0E+00	6.0E+03	3.1E+06	0.0E+00
300	1.9E+05	8.2E+05	8.0E+06	4.4E+04	2.0E+06	8.7E+05	2.4E+04	7.1E+06	6.6E+04
500	1.2E+05	3.0E+06	8.5E+07	2.5E+04	8.0E+06	1.8E+07	3.7E+03	2.7E+07	5.1E+06
1000	3.4E+05	2.7E+06	2.4E+07	9.6E+04	8.2E+06	4.0E+06	4.8E+04	2.2E+07	4.0E+05

Depth (m)	GDGT-3	GDGT-4	Crenarchaeol			Archaeol			
	DH	DH	MH	DH	HPH	MH	DH	PG	PE
100	2.6E+06	5.0E+05	1.7E+06	9.8E+06	3.1E+07	0.0E+00	0.0E+00	3.1E+06	1.7E+06
125	2.5E+06	5.4E+05	1.0E+06	7.5E+06	1.1E+08	0.0E+00	0.0E+00	3.6E+06	8.7E+05
155	5.3E+05	2.0E+05	5.8E+05	2.3E+06	1.6E+07	3.4E+04	6.8E+04	7.0E+06	1.3E+06
175	0.0E+00	0.0E+00	5.3E+05	2.2E+06	9.0E+05	1.6E+05	6.4E+05	3.4E+07	4.2E+06
200	3.7E+05	1.6E+05	5.9E+05	2.5E+06	2.6E+07	1.8E+05	4.7E+05	4.3E+07	3.6E+06
235	5.8E+04	0.0E+00	2.4E+05	6.6E+05	5.6E+06	1.5E+05	4.3E+05	2.9E+07	5.6E+06
300	0.0E+00	0.0E+00	5.2E+05	2.2E+06	9.3E+06	2.1E+05	8.4E+05	4.5E+07	4.0E+06
500	2.7E+05	3.0E+05	2.1E+05	1.2E+07	5.7E+07	0.0E+00	0.0E+00	2.7E+06	9.2E+05
1000	2.0E+05	0.0E+00	4.5E+05	5.1E+06	9.4E+06	0.0E+00	0.0E+00	8.7E+06	1.2E+06

Table S5. Values of the Pearson correlation coefficients (r values) obtained from the correlation matrix created using as variables the total archaeal 16S rRNA gene reads of the archaeal groups (copies L^{-1}) and the absolute abundance of the archaeal IPLs (response units per Liter; r.u. L^{-1}) detected in the ETSP at the (a) coastal and (b) open ocean stations.

(a)

	GDGT-0			GDGT-1			GDGT-2			GDGT-3	GDGT-4	Crenarchaeol			Archaeol			
	MH	DH	HPH	MH	DH	HPH	MH	DH	HPH	DH	DH	MH	DH	HPH	MH	DH	PG	PE
MGI *Ca.* Nitrosopelagicus	0.68	0.70	0.77	0.72	0.77	0.67	0.67	0.70	0.58	0.74	0.61	0.83	0.46	0.76	-0.38	-0.22	-0.15	-0.16
MGI *Nitrosopumilus*	0.55	0.60	0.65	0.59	0.66	0.59	0.52	0.61	0.50	0.61	0.48	0.69	0.45	0.63	-0.34	-0.16	-0.16	-0.15
MGI uncultured OTU-1	-0.39	-0.33	-0.38	-0.38	-0.35	-0.30	-0.40	-0.30	-0.28	-0.40	-0.39	-0.37	-0.06	-0.39	0.41	0.43	0.19	0.46
MGI uncultured OTU-2	-0.37	-0.18	-0.27	-0.34	-0.24	-0.05	-0.38	-0.14	-0.02	-0.40	-0.35	-0.38	0.34	-0.29	0.06	-0.01	-0.15	0.02
MGII uncultured OTU-1	0.56	0.42	0.48	0.50	0.48	0.35	0.56	0.41	0.36	0.55	0.57	0.49	0.17	0.48	-0.16	-0.13	-0.15	-0.06
MGII uncultured OTU-2	-0.33	-0.14	-0.25	-0.29	-0.20	-0.04	-0.33	-0.09	0.00	-0.36	-0.31	-0.33	0.36	-0.27	0.07	0.02	-0.15	0.04
MGIII uncultured OTU-1	-0.42	-0.56	-0.49	-0.43	-0.50	-0.54	-0.40	-0.53	-0.53	-0.40	-0.42	-0.39	-0.56	-0.47	0.87	0.71	0.68	0.74
MGIII uncultured OTU-2	-0.42	-0.57	-0.48	-0.43	-0.50	-0.55	-0.39	-0.53	-0.54	-0.40	-0.41	-0.38	-0.57	-0.46	0.94	0.73	0.77	0.81
MGIII uncultured OTU-3	-0.46	-0.61	-0.52	-0.48	-0.54	-0.58	-0.44	-0.57	-0.57	-0.44	-0.46	-0.42	-0.59	-0.50	0.91	0.73	0.71	0.80
DPANN Woesearchaeota	-0.39	-0.54	-0.46	-0.41	-0.48	-0.52	-0.38	-0.51	-0.50	-0.38	-0.40	-0.35	-0.53	-0.44	0.75	0.67	0.54	0.72

(b)

MGI *Ca.* Nitrosopelagicus	0.64	0.30	0.80	0.64	0.39	0.49	0.61	0.26	0.14	0.80	0.77	0.52	0.29	0.87	-0.39	-0.40	-0.39	-0.43
MGI *Nitrosopumilus*	0.26	-0.04	0.41	0.24	-0.05	0.20	0.30	-0.13	-0.06	0.41	0.46	0.25	-0.11	0.53	-0.06	-0.19	-0.04	-0.24
MGI uncultured OTU-1	-0.35	0.30	0.35	-0.38	0.03	0.61	-0.44	0.24	0.71	-0.14	0.23	-0.31	0.39	0.34	-0.08	-0.18	-0.05	-0.24
MGI uncultured OTU-2	-0.10	0.61	0.64	-0.13	0.36	0.87	-0.30	0.54	0.96	0.07	0.41	-0.20	0.73	0.56	-0.39	-0.36	-0.40	-0.44
MGII uncultured OTU-1	-0.30	0.51	0.47	-0.30	0.25	0.77	-0.45	0.46	0.92	-0.10	0.30	-0.33	0.62	0.40	-0.32	-0.35	-0.32	-0.40
MGII uncultured OTU-2	-0.10	0.13	0.39	-0.16	-0.07	0.46	-0.17	0.05	0.41	0.08	0.36	-0.07	0.17	0.45	-0.02	-0.15	0.01	-0.24
MGII uncultured OTU-3	0.31	0.28	0.71	0.32	0.23	0.56	0.31	0.19	0.31	0.53	0.68	0.25	0.24	0.79	-0.33	-0.42	-0.31	-0.49
MGIII uncultured OTU-1	-0.45	-0.60	-0.45	-0.59	-0.71	-0.39	-0.46	-0.63	-0.30	-0.42	-0.40	-0.29	-0.55	-0.35	0.71	0.55	0.71	0.65
MGIII uncultured OTU-2	-0.36	-0.58	-0.34	-0.53	-0.71	-0.32	-0.44	-0.65	-0.26	-0.34	-0.32	-0.26	-0.53	-0.23	0.63	0.50	0.60	0.59
MGIII uncultured OTU-3	-0.37	-0.50	-0.38	-0.51	-0.64	-0.31	-0.39	-0.54	-0.24	-0.37	-0.32	-0.23	-0.46	-0.28	0.63	0.49	0.65	0.52
DPANN Woesearchaeota	-0.33	-0.53	-0.43	-0.49	-0.66	-0.38	-0.37	-0.57	-0.30	-0.37	-0.36	-0.21	-0.50	-0.33	0.64	0.53	0.66	0.54

Table S6. Values of the Pearson correlation coefficients (r values) obtained from the correlation matrix created using as variables the total archaeal 16S rRNA gene reads of the archaeal groups (copies L^{-1}) detected in the ETSP at the (a) coastal and (b) open ocean stations.

(a)

	Thaumarchaeota Marine Group I				Euryarchaeota Marine Group II		Euryarchaeota Marine Group III			DPANN
	Ca. Nitrosopelagicus	*Nitrosopumilus*	MGI uncultured OTU-1	MGI uncultured OTU-2	MGII uncultured OTU-1	MGII uncultured OTU-2	MGIII uncultured OTU-1	MGIII uncultured OTU-2	MGIII uncultured OTU-3	Woesearchaeota DHVE-6
MGI *Ca.* Nitrosopelagicus	1.00									
MGI *Nitrosopumilus*	0.86	1.00								
MGI uncultured OTU-1	-0.32	0.05	1.00							
MGI uncultured OTU-2	-0.40	-0.17	0.69	1.00						
MGII uncultured OTU-1	0.38	0.61	0.25	-0.10	1.00					
MGII uncultured OTU-2	-0.37	-0.12	0.73	0.95	-0.09	1.00				
MGIII uncultured OTU-1	-0.36	-0.13	0.66	0.19	0.12	0.21	1.00			
MGIII uncultured OTU-2	-0.30	-0.24	0.49	0.16	-0.07	0.14	0.92	1.00		
MGIII uncultured OTU-3	-0.34	-0.17	0.63	0.20	0.08	0.16	0.96	0.96	1.00	
DPANN Woesearchaeota	-0.29	0.00	0.74	0.20	0.38	0.19	0.89	0.76	0.90	1.00

(b)

	Thaumarchaeota Marine Group I				Euryarchaeota Marine Group II			Euryarchaeota Marine Group III			DPANN
	Ca. Nitrosopelagicus	*Nitrosopumilus*	MGI uncultured OTU-1	MGI uncultured OTU-2	MGII uncultured OTU-1	MGII uncultured OTU-2	MGII uncultured OTU-3	MGIII uncultured OTU-1	MGIII uncultured OTU-2	MGIII uncultured OTU-3	Woesearchaeota DHVE-6
MGI *Ca.* Nitrosopelagicus	1.00										
MGI *Nitrosopumilus*	0.74	1.00									
MGI uncultured OTU-1	0.01	0.30	1.00								
MGI uncultured OTU-2	0.14	-0.02	0.75	1.00							
MGII uncultured OTU-1	-0.04	0.02	0.90	0.92	1.00						
MGII uncultured OTU-2	0.37	0.73	0.85	0.50	0.60	1.00					
MGII uncultured OTU-3	0.82	0.91	0.47	0.31	0.32	0.77	1.00				
MGIII uncultured OTU-1	-0.21	0.29	0.33	-0.16	-0.05	0.47	0.02	1.00			
MGIII uncultured OTU-2	-0.06	0.36	0.28	-0.07	-0.05	0.49	0.10	0.94	1.00		
MGIII uncultured OTU-3	-0.16	0.35	0.40	-0.06	0.02	0.57	0.09	0.98	0.95	1.00	
DPANN Woesearchaeota	-0.18	0.30	0.30	-0.10	-0.06	0.49	0.02	0.95	0.96	0.99	1.00

Table S7. Pearson correlation coefficients (r values) obtained from the correlation matrix created using as variables the absolute abundance of the archaeal IPLs (response units per Liter; r.u. L^{-1}) detected in the ETSP at the (a) coastal and (b) open ocean stations.

(a)

		GDGT-0			GDGT-1			GDGT-2			GDGT-3	GDGT-4	Crenarchaeol			Archaeol			
		MH	DH	HPH	MH	DH	HPH	MH	DH	HPH	DH	DH	MH	DH	HPH	MH	DH	PG	PE
GDGT-0	MH	1.00																	
	DH	0.93	1.00																
	HPH	0.95	0.96	1.00															
GDGT-1	MH	0.98	0.95	0.95	1.00														
	DH	0.96	0.99	0.98	0.98	1.00													
	HPH	0.83	0.93	0.95	0.85	0.92	1.00												
GDGT-2	MH	0.99	0.91	0.94	0.96	0.94	0.82	1.00											
	DH	0.93	1.00	0.96	0.96	0.99	0.93	0.90	1.00										
	HPH	0.80	0.87	0.91	0.79	0.86	0.98	0.80	0.86	1.00									
GDGT-3	DH	0.99	0.92	0.97	0.97	0.96	0.86	0.98	0.91	0.82	1.00								
GDGT-4	DH	0.99	0.91	0.92	0.94	0.92	0.80	0.99	0.89	0.80	0.97	1.00							
Crenarchaeol	MH	0.94	0.92	0.96	0.97	0.96	0.86	0.92	0.92	0.80	0.96	0.88	1.00						
	DH	0.60	0.81	0.74	0.66	0.76	0.88	0.57	0.83	0.84	0.59	0.57	0.62	1.00					
	HPH	0.95	0.95	1.00	0.95	0.97	0.95	0.94	0.94	0.92	0.97	0.93	0.96	0.71	1.00				
Archaeol	MH	-0.50	-0.67	-0.57	-0.50	-0.60	-0.63	-0.47	-0.63	-0.60	-0.49	-0.51	-0.43	-0.67	-0.54	1.00			
	DH	-0.46	-0.54	-0.47	-0.47	-0.52	-0.49	-0.46	-0.53	-0.46	-0.45	-0.47	-0.36	-0.55	-0.43	0.82	1.00		
	PG	-0.27	-0.40	-0.29	-0.29	-0.36	-0.35	-0.26	-0.39	-0.34	-0.26	-0.28	-0.19	-0.50	-0.25	0.85	0.91	1.00	
	PE	-0.38	-0.51	-0.41	-0.39	-0.46	-0.46	-0.36	-0.48	-0.43	-0.37	-0.40	-0.28	-0.53	-0.38	0.88	0.95	0.87	1.00

(b)

		GDGT-0			GDGT-1			GDGT-2			GDGT-3	GDGT-4	Crenarchaeol			Archaeol			
		MH	DH	HPH	MH	DH	HPH	MH	DH	HPH	DH	DH	MH	DH	HPH	MH	DH	PG	PE
GDGT-0	MH	1.00																	
	DH	0.33	1.00																
	HPH	0.47	0.73	1.00															
GDGT-1	MH	0.93	0.52	0.53	1.00														
	DH	0.70	0.84	0.67	0.78	1.00													
	HPH	0.15	0.81	0.91	0.24	0.61	1.00												
GDGT-2	MH	0.88	0.40	0.39	0.97	0.66	0.08	1.00											
	DH	0.53	0.91	0.66	0.62	0.96	0.71	0.48	1.00										
	HPH	-0.14	0.71	0.69	-0.08	0.44	0.92	-0.26	0.61	1.00									
GDGT-3	DH	0.93	0.34	0.67	0.84	0.69	0.36	0.77	0.54	0.05	1.00								
GDGT-4	DH	0.76	0.48	0.82	0.66	0.72	0.63	0.54	0.65	0.39	0.91	1.00							
Crenarchaeol	MH	0.94	0.10	0.29	0.80	0.56	-0.01	0.77	0.40	-0.26	0.89	0.72	1.00						
	DH	0.47	0.81	0.72	0.47	0.87	0.80	0.29	0.94	0.75	0.55	0.73	0.38	1.00					
	HPH	0.46	0.61	0.98	0.51	0.56	0.85	0.40	0.54	0.60	0.68	0.81	0.31	0.61	1.00				
Archaeol	MH	-0.56	-0.79	-0.65	-0.66	-0.89	-0.61	-0.52	-0.84	-0.47	-0.58	-0.66	-0.37	-0.75	-0.53	1.00			
	DH	-0.50	-0.71	-0.62	-0.58	-0.83	-0.58	-0.46	-0.78	-0.44	-0.56	-0.66	-0.33	-0.69	-0.52	0.97	1.00		
	PG	-0.54	-0.71	-0.63	-0.59	-0.84	-0.59	-0.44	-0.78	-0.47	-0.58	-0.67	-0.35	-0.73	-0.52	0.98	0.95	1.00	
	PE	-0.52	-0.84	-0.67	-0.65	-0.83	-0.66	-0.54	-0.82	-0.51	-0.51	-0.65	-0.33	-0.73	-0.58	0.90	0.84	0.8	1.00

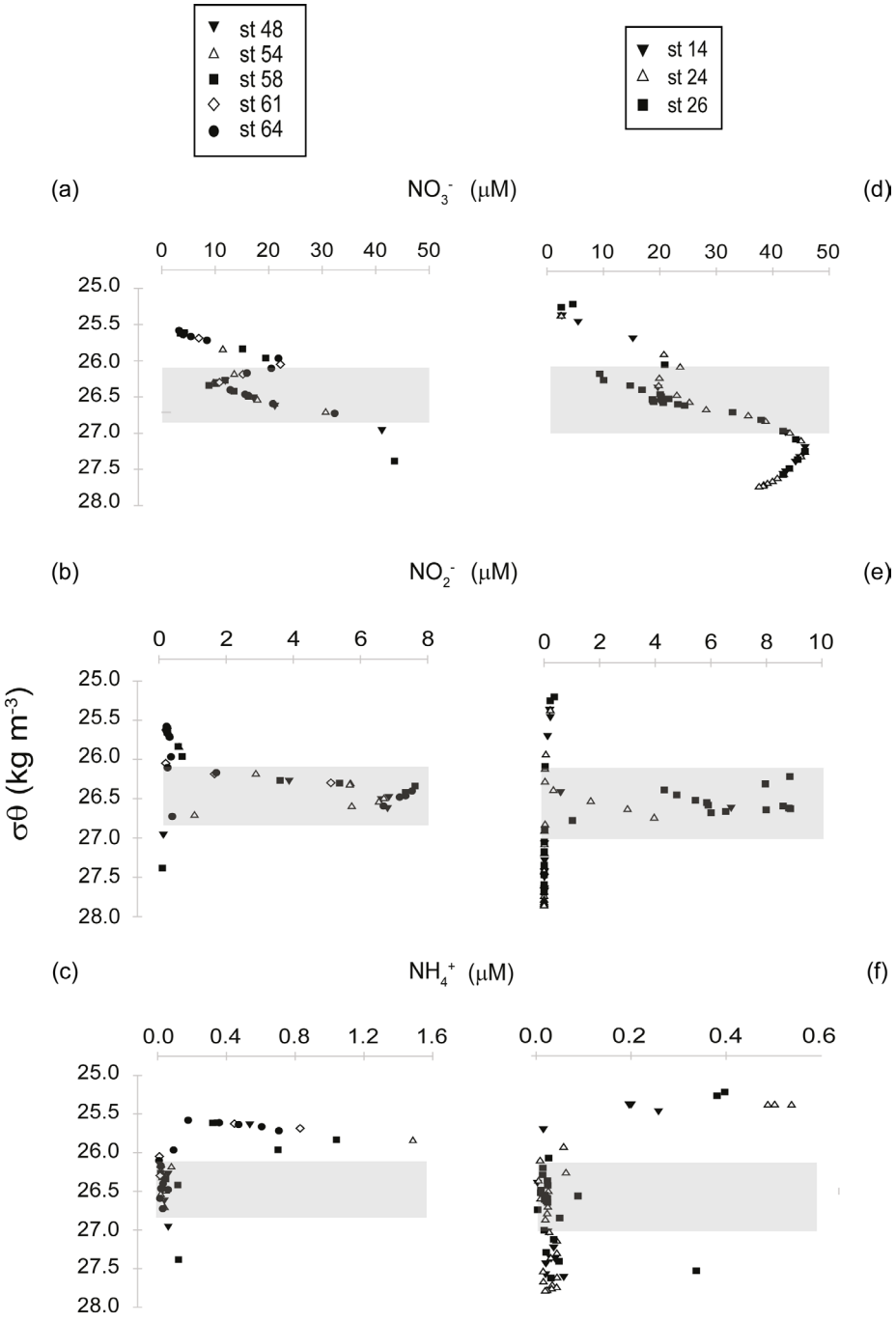

Figure S1. Profiles of nitrogen species detected (nitrate, NO_3^-; nitrite, NO_2^-; ammonium, NH_4^+) in the in the ETSP at the (a, b, c) coastal and (d, e, f) open ocean station.

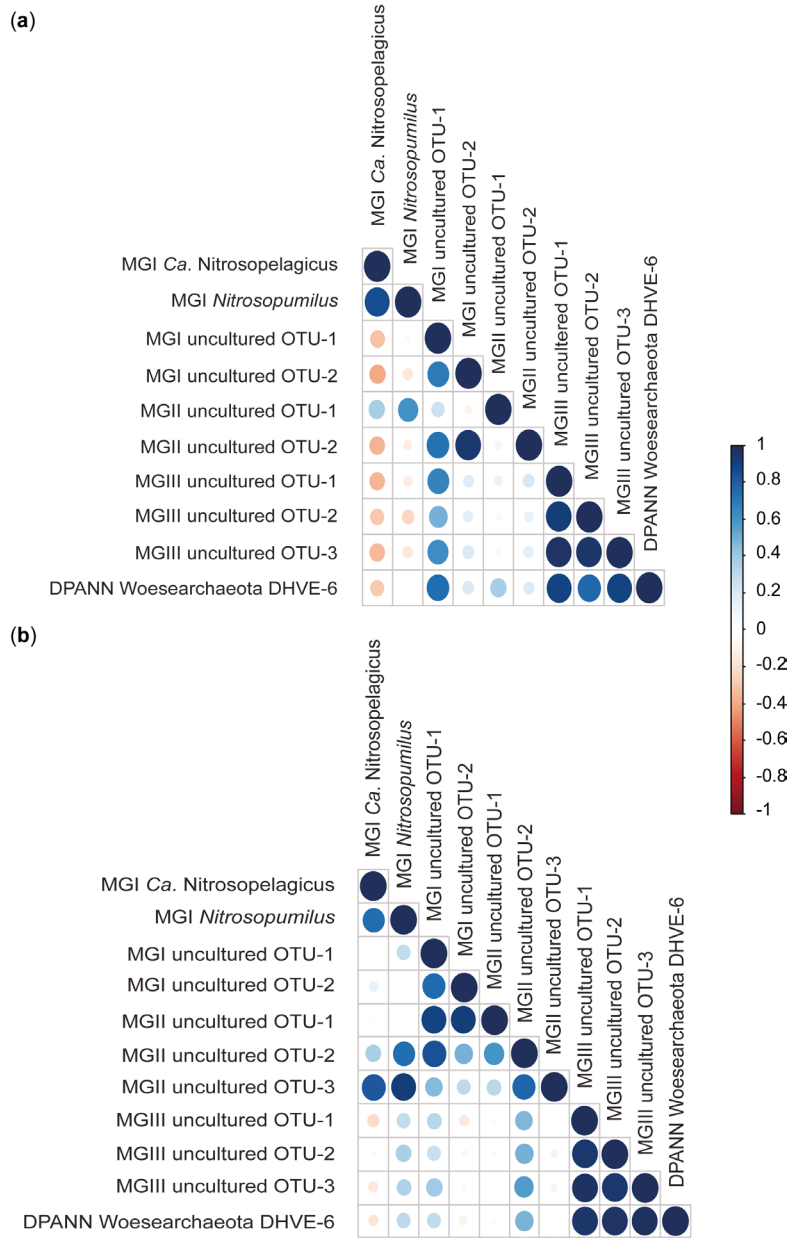

Figure S2. Dot plot of the correlation matrix obtained by applying a Pearson analysis to the total archaeal 16S rRNA gene reads (copies L^{-1}) of the archaeal groups detected in the ETSP at the (a) coastal and (b) open ocean stations. Dark blue corresponds to +1 r values, indicating a strong positive linear correlation between archaeal groups; white corresponds to 0 r values, indicating that no correlation exists; dark red corresponds to -1 r values, indicating a strong negative linear correlation.

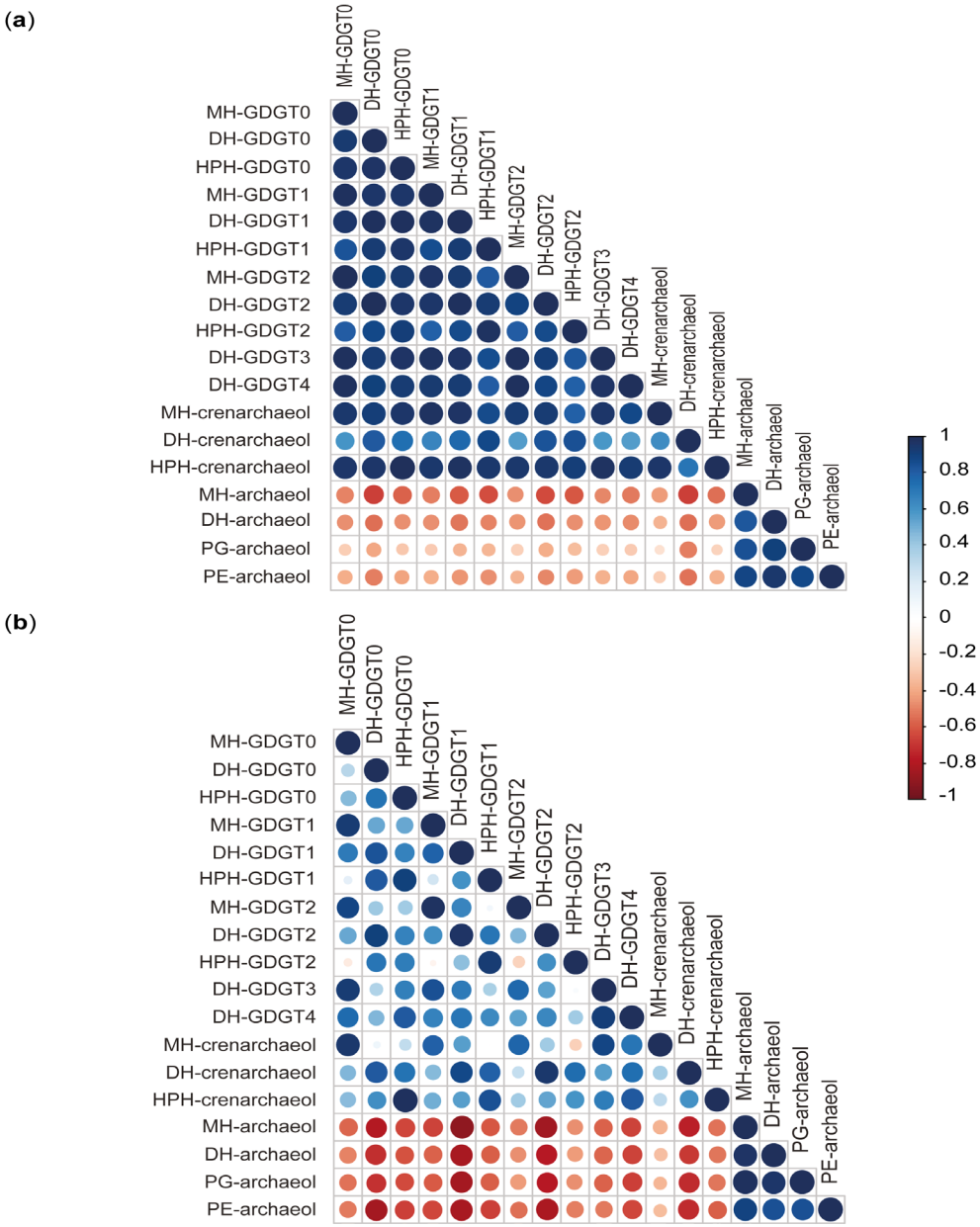

Figure S3. Dot plot of the correlation matrix obtained by applying a Pearson analysis to the archaeal IPLs (response units per Liter; r.u. L^{-1}) detected in the ETSP, at the (a) coastal and (b) open ocean stations. Dark blue corresponds to +1 r values, indicating a strong positive linear correlation between archaeal groups; white corresponds to 0 r values, indicating that no correlation exists; dark red corresponds to -1 r values, indicating a strong negative linear correlation.

Chapter 4

A combined lipidomic and 16S rRNA gene amplicon sequencing approach reveals archaeal sources of intact polar lipids in the stratified Black Sea water column

Martina Sollai, Laura Villanueva, Ellen C. Hopmans, Gert-Jan Reichart, Jaap S. Sinninghe Damsté

Submitted to *Geobiology*

Abstract. Archaea are important players in the marine biogeochemical cycles and their membrane lipids are powerful biomarkers in environmental studies. However, many archaeal groups remain uncultured and their lipid composition unknown. Here, we aim to expand the knowledge on archaeal lipid biomarkers and determine the potential sources of those lipids in the water column of the Black Sea sampled at high resolution. The archaeal community was evaluated by 16S rRNA gene amplicon sequencing and by quantitative PCR. The archaeal intact polar lipids were investigated by Ultra high Pressure Liquid Chromatography coupled to high resolution mass spectrometry. In the oxic/upper suboxic waters of the Black Sea water column, the archaeal community was dominated by MGI Thaumarchaeota and MGII euryarchaeota, coinciding with a higher relative abundance of hexose phospho-hexose-crenarchaeol. In the suboxic waters, MGI *Nitrosopumilus* sp. dominated and monohexose glycerol dialkyl glycerol tetraethers (GDGTs) and hydroxy (OH)-GDGTs lipids increased. In the deep sulfidic waters, DPANN Woesearchaeota, Bathyarchaeota, and ANME-1b dominated coinciding with the presence of archaeol lipids with diverse polar headgroups, which we tentatively assign to these groups. Our study revealed both a complex archaeal community and a large lipid diversity in the Black Sea.

4.1. Introduction

Archaea form a broad and diverse domain with a complex phylogeny that has started to be elucidated only recently by the application of culture-independent approaches (e.g. Castelle et al., 2015; Iverson et al., 2012; Spang et al., 2015). The marine water column and sediments have been shown to be a niche for complex archaeal communities. Some of the archaea comprising these communities have been successfully cultivated providing clues on their physiology. For example, marine Thaumarchaeota (previously known as Marine Group I (MGI); Brochier-Armanet et al., 2008; Spang et al., 2010) are aerobic ammonia oxidizers commonly found in epipelagic and mesopelagic water column and in sediments (Francis et al., 2005; Könneke et al., 2005; Venter et al., 2004; Wuchter et al., 2006). Other archaeal planktonic lineages include euryarchaeotal Marine Group II (MGII) (Delong, 1992; Fuhrman et al., 1992) and the closely related Marine Group III (MGIII) (Fuhrman et al., 1992).

MGII are predicted to be motile photoheterotrophs based on genome analysis (Iverson et al., 2012) but remain uncultured. Members of the MGII reside

mainly in the marine photic zone although other ecotypes have been detected in deeper water columns (see Zhang et al., 2015 for a review). MGIII archaea have been mainly detected in deep mesopelagic and bathypelagic, and most recently also in epipelagic waters, but their physiology is essentially unknown (Bano et al., 2004; Haro-Moreno et al., 2017; López-García et al., 2001; Massana et al., 2000), also because they remain uncultured. In addition, the presence of members of the archaeal superphylum DPANN in marine settings, mainly in microbial mats, sediments, plankton and hydrothermal vents is increasingly reported (Pachiadaki et al., 2011; Robertson et al., 2009). Studies based on genome analysis have concluded that members of this superphylum lack important metabolic pathways, suggesting that they have a symbiotic or parasitic lifestyle (Castelle et al., 2015; Rinke et al., 2013).

Other yet-uncultured archaeal groups have been detected in marine sediments. For example, members of the anaerobic methanotrophic archaea (ANME), performing the anaerobic oxidation of methane (AOM), have been identified in shallow marine anoxic sediments rich in methane hydrates (Boetius et al., 2000; Hinrichs et al., 1999; Orphan et al., 2001a; Pancost et al., 2000). ANME have also been detected in the anoxic water column based on specific membrane lipids (Schouten et al., 2001; Wakeham et al., 2003), and, subsequently, based on genomic data (Vetriani et al., 2003). Archaeal benthic groups include the Marine Benthic Group B (MBG-B), the Marine Benthic Group D (MBG-D) and the phylum Bathyarchaeota (formerly known as the Miscellaneous Crenarchaeotal Group, MCG) (Inagaki et al., 2003; Spang et al., 2015; Vetriani & Jannasch, 1999), which often co-occur, supposedly living as heterotrophs consuming buried recalcitrant organic matter, degrading proteins and lipids (Biddle et al., 2006; Kubo et al., 2012; Lloyd et al., 2013; Meng et al., 2014). More recently, lineages of the Bathyarchaeota phylum have been suggested to be homoacetogens, as well as involved in methane metabolism, based on genomic and enzymatic evidences (Evans et al., 2015; He et al., 2016).

Despite the huge effort of molecular ecologists to untangle archaeal diversity in the marine environment, many aspects of archaeal physiology, abundance and preferred niche still need to be addressed. The employment of combined approaches may be more effective in overcoming limitation deriving from the lack of cultivated representatives and the intrinsic biases of many DNA-based techniques (Marine et al., 2014; Pinto and Raskin, 2012; Teske and Sørensen, 2008). A powerful complementary method of investi-

gation is supplied by lipidomics. Targeting microbial lipids (Schouten et al., 2008a; Sturt et al., 2004) may offer a technical advantage compared to PCR-based approaches avoiding potential biases. Additionally, lipid molecules can be preserved longer than nucleic acids in the sedimentary record thus providing information of both present and past microbial communities (Castañeda and Schouten, 2011; Eglinton and Eglinton, 2008; Kuypers et al., 2001). Lastly, some lipids have been shown to be specific of certain microbial groups and used as taxonomic biomarkers of their presence in the environment (e.g. Hamersley et al., 2007; Rush et al., 2012; Sinninghe Damsté et al., 2002c).

Archaeal membranes are formed by unique core lipids (CL), specifically phytanyl glycerol diether (archaeol) and glycerol dibiphytanyl glycerol tetraethers (GDGTs). GDGTs may contain up to 8 cyclopentane moieties; many studies have shown they are generally non-specific and occur in a wide range of archaea such as extremophiles (Bauersachs et al., 2015b; Ellen et al., 2009; Schouten et al., 2007b), methanogens (Bauersachs et al., 2015b; Koga et al., 1993), ANMEs (Blumenberg et al., 2004; Pancost et al., 2001; Wakeham et al., 2004; Wegener et al., 2016), and Thaumarchaeota (Elling et al., 2017; Pitcher et al., 2011b; Schouten et al., 2008a; Sinninghe Damsté et al., 2002c). To date crenarchaeol, the GDGT containing four cyclopentane moieties and a cyclohexane moiety (Sinninghe Damsté et al., 2002c), represents an unique case being considered characteristic of Thaumarchaeota (Schouten et al., 2008a; Sinninghe Damsté et al., 2012). Knowledge on the membrane lipid composition of archaeal groups is based on the availability of cultures, but some recent studies have inferred the lipid membrane composition of certain archaea based on correlations between a specific lipid and 16S rRNA gene reads of a specific group. For example, butane-triol dibiphytanyl glycerol tetraether (BDGTs) has also been attributed to the MCG (Meador et al., 2015) using this approach. However, Becker et al. (2016) questioned this attribution as they identified BDGTs also in the methanogen *Methanomassilicoccus luminyensis* (Becker et al., 2016). MGII has been suggested to synthesize GDGTs including crenarchaeol (Lincoln et al., 2014a), and unsaturated archaeol with 0 to 4 double bonds (Zhu et al., 2016). However, lack of detailed characterization of the taxonomic composition of the analyzed samples, differences in the resilience times between CL-GDGTs (attributed to dead biomass) and DNA can jeopardize the association of lipid biomarkers with their potential biological sources (e.g. Lincoln et al., 2014b; Schouten et al., 2014).

An important breakthrough for lipid-based studies has been the devel-

opment of methods that allow to detect archaeal intact polar lipids (IPLs), which are composed of the core lipid attached to one or two polar headgroups (Sturt et al., 2004). Such bonds are relatively easily hydrolyzed once the cell dies. Therefore, IPLs are considered as biomarkers of living biomass. The phosphate-ester bond has been experimentally proven to be especially liable (White et al., 1979; Harvey et al., 1986). Consequently, the IPL hexose-phosphohexose (HPH)-crenarchaeol is considered as an excellent biomarker of living Thaumarchaeota (Lengger et al., 2012; Schouten et al., 2010, 2012). However, such instances are rare and due to the difficulties still associated to the isolation and cultivation of archaea, the need for new reliable archaeal biomarkers is critical to study these microorganisms in the environment.

This study is aimed at expanding the array of known archaeal IPLs in the marine environment and to provide clues on the archaeal groups as potential sources of IPLs. To this end, we analyzed the archaeal diversity based on 16S rRNA gene amplicon sequencing, as well as the archaeal IPL composition by Ultra high Pressure Liquid Chromatography coupled to high resolution mass spectrometry in the Black Sea water column. The Black Sea is the largest permanently stratified anoxic basin in the world and its water column is characterized by the presence of strong redox gradients, and, therefore, represents an excellent setting to target diverse archaeal groups with this approach.

4.2. Material and Methods

4.2.1. Sampling and physicochemical measurements

Sampling was performed during the Phoxy cruise (June–July 2013) aboard of the *R/V Pelagia*. The sampling station (PHOX2) was located at 42°53.8'N and 30°40.7'E in the western gyre of the Black Sea. SPM (water volume 148–796 L) was collected on pre-ashed 142 mm diameter 0.7 μm pore size glass fiber GF/F filters (Pall Corporation, Washington) mounted on McLane WTS-LV *in situ* pumps (McLane Laboratories Inc., Falmouth). We did take into account the reported limitations associated to the use of this pore size in terms of underestimation of free-living archaea and their IPL abundance (Ingalls et al., 2012; Schouten et al., 2012). However, this is not considered to affect the variations in the distribution in this study. Besides, both lipid and DNA-based characterization was performed in the same filters thus avoiding the lack of correspondence between the two pools. In each cast three

pumps were deployed simultaneously at different depths. During a total of five pumping sessions, SPM from 15 different water depths was obtained. Upon the recovery of the *in situ* pumps on the deck of the ship the filters were immediately stored at -80 °C. Physical parameters of the water column were recorded by a conductivity-temperature-density (CTD) unit (SBE 911 plus, Sea-Bird Electronics). Samples for inorganic nitrogen nutrients (i.e. NO_3^-, NO_2^- and NH_4^+) and for hydrogen sulfide (HS^-) were obtained with a GoFlow rosette sampler (General Oceanics, Miami) from the same water depths sampled for SPM. Dissolved-oxygen (O_2) depth concentrations were measured by a SBE 43 electrochemical sensor mounted on the CTD rosette. The sensor has a detection limit of 1–2 μM, which has been recently proven to overestimate the oxygen level at the lowest concentrations (Tiano et al., 2014). For nutrient analysis the water collected in the CTD bottles at various depths was immediately processed on-board and the concentrations were determined within 18 h on a QuAAtro autoanalyzer. Specifically, ca. 5 ml samples were filtered over Acrodisc PF (pre-filter) Syringe Filter with 0.8/0.2 μm Supor membrane (Pall Corporation, Washington) into separate pre-rinsed pony vials. One vial already containing 40 μl 1N NaOH was used for HS^- analysis and one without any addition of NaOH for DIC. Another glass vial was used for NO_3^-, NO_2^- and NH_4^+ analysis. The detection limits for NO_3^-, NO_2^-, and NH_4^+ were in average 0.008 μM, 0.006 μM and 0.044 μM, respectively. The detection limit for HS^- was 0.263 μmol L^{-1}.

4.2.2. DNA-based analyses

DNA/RNA was extracted from 1/8 (SPM samples from 50–110 m depth) or 1/4 (SPM samples from 130–2000 m depth) sections of the GF/F filter with the RNA PowerSoil® Total Isolation Kit plus the DNA elution accessory (Mo Bio Laboratories, Carlsbad, CA). Concentration of DNA was quantified by Nanodrop (Thermo Scientific, Waltham, MA) and fluorometrically with Quant-iT™ PicoGreen® dsDNA Assay Kit (Life technologies, Netherlands).

The 16S rRNA gene amplicon sequencing and analysis was performed with the primers S-D-Arch-0159-a-S-15 and S-D-Bact-785-a-A-21 (Klindworth et al., 2013) as described in Moore et al. (2015). The archaeal 16S rRNA gene amplicon sequences were analyzed by QIIME v1.9 (Caporaso et al., 2010). Raw sequences were demultiplexed and then quality-filtered with a minimum quality score of 25, length between 250-350, and allowing maximum two errors in the barcode sequence. OTU picking step was performed

with Usearch with a threshold of 0.97 (roughly corresponding to species-level OTUs. Taxonomy was assigned based on blast and the SILVA database version 123 (Altschul et al., 1990; Quast et al., 2013. The 16S rRNA gene amplicon reads (raw data have been deposited in the NCBI Sequence Read Archive (SRA under BioProject number PRJNA423140.

Amplification of the archaeal *amo*A gene was performed as described by Yakimov et al. (2011 with DNA extracts of the SPM samples at 50, 85, 100, 500 and 2000 m depth. PCR reaction mixture was the following (final concentration: Q-solution 1× (PCR additive, Qiagen; PCR buffer 1×; BSA (200 μg ml^{-1}; dNTPs (20 μM; primers (0.2 pmol μl^{-1}; $MgCl_2$ (1.5 mM; 1.25 U Taq polymerase (Qiagen, Valencia, CA, USA. PCR conditions were the following: 95 °C, 5 min; 35 × [95 °C, 1 min; 55 °C, 1 min; 72 °C, 1 min]; final extension 72 °C, 5 min. PCR products were gel purified (QIAquick gel purification kit, Qiagen and cloned in the TOPO-TA cloning® kit from Invitrogen (Carlsbad, CA, USA and transformed in *E. coli* TOP10 cells following the manufacturer's recommendations. Recombinant clones plasmid DNAs were purified by Qiagen Miniprep kit and screened by sequencing (total n = 115 using M13R primer by Macrogen Europe Inc. (Amsterdam, The Netherlands. Archaeal *amo*A gene sequences are deposited in the NCBI database with accession numbers MG760455–MG760569. Obtained archaeal *amo*A gene sequences were translated into protein sequences that were aligned with already annotated *amo*A sequences by using the Muscle application (Edgar, 2004. Phylogenetic trees were constructed with the Neighbor-Joining method (Saitou and Nei, 1987 and evolutionary distances computed using the Poisson correction method with a bootstrap test of 1,000 replicates. The *amo*A-based phylogenetic trees were used to relate the thaumarchaeotal sequences detected in this study with others of the same phylum detected in other settings.

Quantification of archaeal 16S rRNA gene copies were estimated by quantitative PCR (qPCR by using the primers Parch519F and Arc915R as previously described (Pitcher et al., 2011b. The standard curve was generated by PCR amplifying an insert of an archaeal 16S rRNA gene (as in Pitcher et al., 2011a).The qPCR reaction mixture (25 μl) contained 1 U of Pico Maxx high fidelity DNA p olymerase (Stratagene, A gilent Technologies, S anta Clara, CA)2.5 μl of 10x Pico Maxx PCR buffer, 2.5 μl 2.5 mM of each dNTP, 0.5 μl BSA (20 mg/ml), 0.02 pmol/μl of primers, 10 000 times diluted SYBR Green® (Invitrogen) (optimized concentration), 0.5 μl 50 mM of $MgCl_2$ and

ultrapure sterile water. All reactions were performed in iCycler iQ™ 96-well plates (Bio-Rad, Hercules CA). Specificity of the reaction was tested with a gradient melting temperature assay. The cycling conditions for the qPCR reaction were the following: 95 °C, 4 min; 40–45× [95 °C, 30 s; 62 °C , 40 s; 72 °C, 30 s]; final extension 80 °C, 25 s. The qPCR reactions were performed in triplicate with standard curves from 10^0 to 10^7 molecules per microliter. qPCR efficiency was 98.6% and R_2=0.995.

4.2.3. Lipid extraction and analysis

Intact polar lipids (IPLs) were extracted from the GF/F filter using a modified Bligh-Dyer method and analyzed as described in Sturt et al. (2004) with some modifications. 1-O-hexadecyl-2-acetyl-sn-glycero-3-phosphocholine (PAF) was added as internal standard to the extracts and dried under a stream of nitrogen. The extracts with the added standard were then dissolved in the injection solvent (hexane:isopropanol:H_2O 718:271:10 *v*ol/*v*ol/*v*ol) and filtered through a 0.45 µm, 4 mm-diameter True Regenerated Cellulose syringe filter (Grace Davison, Columbia, MD, USA). For IPL analysis an Ultimate 3000 RS UHPLC, equipped with thermostated auto-injector and column oven, coupled to a Q Exactive Orbitrap MS with Ion Max source with heated electrospray ionization (HESI) probe (Thermo Fisher Scientific, Waltham, MA) was used. Separation was achieved at 30 °C, on a YMC-Triart Diol-HILIC column (250 x 2.0 mm, 1.9 µm particles, pore size 12 nm; YMC Co., Ltd, Kyoto, Japan). The elution program employed comprised a flow rate of 0.2 mL min^{-1}: 100% A for 5 min, followed by a linear gradient to 66% A: 34% B in 20 min, maintained for 15 min, followed by a linear gradient to 40% A: 60% B in 15 min, followed by a linear gradient to 30% A: 70% B in 10 min, where A = hexane/2-propanol/formic acid/14.8 M NH_{3aq} (79:20:0.12:0.04 [volume in volume in volume in volume, v/v/v/v]) and B = 2-propanol/water/formic acid/ 14.8 M NH_{3aq} (88:10:0.12:0.04 [v/v/v/v]). Total run time was 70 min with a re-equilibration period of 20 min in between runs. HESI settings comprised: sheath gas (N_2) pressure 35 (arbitrary units), auxiliary gas (N_2) pressure 10 (arbitrary units), auxiliary gas (N_2) T 50 ˚C, sweep gas (N_2) pressure 10 (arbitrary units), spray voltage 4.0 kV (positive ion ESI), capillary temperature 275 °C, S-Lens 70 V. Lipids were analyzed with a mass range of *m/z* 375 to 2000 with a resolving power of 70,000 and 140,000 followed by data dependent MS^2 (resolution 17,500), in which the ten most abundant masses in the mass spectrum (with the exclusion of isotope

peaks) were fragmented successively (stepped normalized collision energy 15, 22.5, 30; isolation window 1.0 *m/z*). A dynamic exclusion window of 6 sec, with a mass tolerance of 3 ppm, was applied. In order to target specific IPLs, we used an inclusion list with a mass tolerance of 3 ppm (Table S2). The Q Exactive was calibrated within a mass accuracy range of 1 ppm using the Thermo Scientific Pierce LTQ Velos ESI Positive Ion Calibration Solution (containing a mixture of caffeine, MRFA, Ultramark 1621, and *N*-butylamine in an acetonitrile/methanol/acetic acid solution).

Peak areas for each individual IPL were determined by integrating the combined mass chromatogram (within 3 ppm) of the monoisotopic and first isotope peak of all relevant adducts formed (protonated, ammoniated and/or sodiated adducts may be formed in different proportions depending on the type of IPL). The response of the internal standard PAF was monitored to correct for possible matrix effects and variations in mass spectrometer performance. Reported peak areas have been corrected for these effects. As no authentic standards were available for absolute quantitation of the individual IPLs, the abundances are reported as response units per liter of water (r.u. L^{-1}).

4.2.4. Statistical analyses

The existence of a linear correlation between the abundances of specific archaeal groups and the IPLs detected in the Black Sea was tested by applying a Pearson correlation analysis, performed with the R software package for statistical computing (http://cran.r-project.org/). Possible spurious correlations were also tested by applying the same statistical analysis among the archaeal lineages detected. The data employed to build the correlation matrices included the total archaeal 16S rRNA gene reads of the different archaeal classes (as determined by amplicon sequencing) detected in the Black Sea SPM at different depths (copies L^{-1}) and the abundance of the IPL classes as obtained with the Ultra high Pressure Liquid Chromatography coupled to high resolution mass spectrometry analysis of the Black Sea SPM at different depths (expressed as response units per Liter, r.u. L^{-1}). Quantification of IPLs, however, remains semi-quantitative due to the lack of authentic standards for structurally different IPLs that may cause variations in the MS signal response factors (Sturt et al., 2004). The correlation was expressed as coefficients (r values) ranging from –1 to +1, where negative r values indicate a negative linear correlation between the two variables, positive values indicate a positive linear correlation and 0 indicates no correlation.

4.3. Results

We collected suspended particulate matter (SPM in higher resolution than previous studies (15 depths from 50 to 2000 m depth across the water column of the Black Sea at station PHOX2, which is located in the western basin of the Black Sea at 2179 m water depth in Bulgarian waters (Fig. S1. Temperature and salinity measurements were obtained by CTD measurements and allowed calculation of the potential density ($\sigma\theta$) of the water masses. Physicochemical parameters were measured in water collected from the Niskin bottles connected to the CTD rosette (Table S1; Reichart et al., 2013.

4.3.1. Physicochemical conditions in the water column

The oxygen concentration was 121 μmol kg^{-1} at 50 m depth ($\sigma\theta$ ~14.9), decreased to 2.2 μmol kg^{-1} at 70 m depth ($\sigma\theta$ ~15.7), and to 0.5 μmol kg^{-1} at 80 m ($\sigma\theta$ ~15.9) (Fig. 1a). From 80 to 2000 m depth, O_2 was below the limit of detection (0.3 μmol kg^{-1}. The sulfide concentration was below the limit of detection from 50 to 100 m depth, increased up to 0.9 μmol L^{-1} at 105 m and to 4.6 μmol L^{-1} at 110 m depth (Fig. 1a. From this depth on, the sulfide concentration increased steadily reaching approximately 400 μmol L^{-1} at 2000 m ($\sigma\theta$ ~17.2. On the basis of these profiles, we define for this study the 'oxic zone' as the 0–70 m depth range, the 'suboxic zone' as the 80–110 m range, and the 'euxinic zone' as the 130–2000 m range. The nitrate concentration was ~1.3 μmol L^{-1} at 50 m depth ($\sigma\theta$ ~14.9) and reached its maximum (i.e. ~2.5 μmol L^{-1}) between 70–80 m depth ($\sigma\theta$ ~15.7 – 15.9) (Fig. 1b). Subsequently, it gradually decreased to the limit of detection, which was reached at the transition from the suboxic to the euxinic zone (at 105 m, $\sigma\theta$ ~16.2). In the oxic zone (i.e. at 50 m, corresponding to $\sigma\theta$ ~14.9) the nitrite concentration displayed the highest values at 0.08 μmol L^{-1} (Fig. 1b). It subsequently decreased but showed two more peaks: one (i.e. 0.04 μmol L^{-1}) in the middle of the suboxic zone (at 85 m depth, corresponding to $\sigma\theta$ ~16.0), and a second one (i.e. 0.02 μmol L^{-1}) at the boundary of the suboxic and euxinic zones. In the deeper euxinic zone the NO_2^- concentration was below the limit of detection. Up to 90 m depth ($\sigma\theta$ ~16.0) ammonium concentrations were <0.1 μmol L^{-1} (Fig. 1b). From this point on they gradually increased following the trend of HS^-, and reached~100 μmol L^{-1} at 2000 m depth (Fig. 1b).

4.3.2. Abundance and diversity of archaeal groups in the water column

Total archaeal 16S rRNA gene copies were quantified in the water column by qPCR by using specific primers. The abundance of total archaeal 16S rRNA gene copies L^{-1} ranged by two orders of magnitude, i.e. from 0.045–2.4 × 10^8 copies L^{-1}. It was high at the oxic-suboxic interface (70–80 m; ca. 1 × 10^8 copies L^{-1} and revealed a maximum within the suboxic zone (105 m; 2.4 × 10^8 copies L^{-1} and in the deepest euxinic waters (2000 m; 1.2 × 10^8 copies L^{-1} (Fig. 1c.

In order to determine the archaeal diversity, partial 16S rRNA gene sequences were retrieved by amplicon sequencing of the DNA extracted from the SPM samples across the Black Sea water column vertical profile (Table 1; Fig. 1d. The percentage of archaeal 16S rRNA gene reads of the total (i.e. bacterial plus archaeal 16S rRNA gene reads ranged from 1.2 to 18.5%. The percentage of archaeal 16S rRNA gene reads was higher between 70 to 100 m depth (8–18% of the total, and then decreased down to 1.2% of the total at 170 m. At greater depths, it slightly increased at 2000 m to approximately 5% of the total. The distribution of the archaeal 16S rRNA gene reads (between 50 to 2000 in different archaeal groups is specified in Table 1 and Figure 1d (only those archaeal groups with % 16S rRNA gene reads higher than 3% were plotted and discussed below.

In the oxic and suboxic zones (up to 110 m depth, Thaumarchaeota comprised most of the archaeal reads (72–95%. The reads attributed to the Thaumarchaeota were classified in three OTUs; one including reads closely related to the 16S rRNA gene sequence of *Candidatus* Nitrosopelagicus brevis (Santoro et al., 2015, a second one to sequences closely related to the thaumarchaeon *Nitrosopumilus maritimus* (Könneke et al., 2005, and a third group including sequence reads affiliated to an uncultured MGI cluster (see Fig. 2a. The relative abundance of the sequences related to *Ca.* Nitrosopelagicus was highest at 50–70 m (64–70% of total archaeal 16S rRNA gene reads) and then decreased (30–42%), while the relative abundance of the sequences affiliated to the MGI uncultured OTU (named here as MGI-unc) increased at 80–85 m (up to 30%). The 16S rRNA gene sequences affiliated to *Nitrosopumilus* were dominant in suboxic waters (72–83% of total archaeal reads between 90–110 m; Table 1; Fig. 1d). Sequences closely related to the euryarchaeotal MGII (Fig. 2b) were also present above and within the suboxic zone, with 10% of the reads attributed to MGII OTU-1 at 50 m depth, while MGII OTU-

2 comprised 5–9% of the archaeal 16S rRNA gene reads at 70–95 m depth (Fig. 1d). Both MGII OTUs were not related to any cultured relatives. Other archaeal groups such as MGIII, Thermoplasmatales, Bathyarchaeota (named here MCG for simplicity) and group C3 (a subgroup within the Bathyarchaeota) were also present in the suboxic waters but at low relative abundance (average 1.5% of the archaeal 16S rRNA gene reads; Fig. 1d).

In the euxinic water column, different archaeal groups of those present in the oxic and suboxic zones comprised the majority of the archaea 16S rRNA gene reads (Table 1; Fig. 1d). Archaea closely related to uncultured Thermoplasmatales, i.e. the VC2.1Arc6 and CCA47 groups, made up to 5–6% reads between 130–250 m, and 250–2000 m depth, respectively. The percentage of reads attributed to the MCG+C3 increased in the euxinic water column reaching maximum values between 500–2000 m depth (average 47%). In addition, 13% of the reads at 2000 m depth were attributed to the Euryarchaeota ANME-1b group. Moreover, the MGIII was represented by approximately 5% of the reads at 170 m depth and 3% at 500 m depth. DPANN Woesearchaeota Deep Hydrothermal Vent Group (DHVE)-6, whose relative abundance increased already in the suboxic zone (up to 18%), continued increasing in the euxinic zone with values increasing from 34 to 59% (Table 1; Fig. 1d).

In order to investigate the diversity of Thaumarchaeota in the Black Sea water column, the archaeal *amo*A gene was amplified and sequenced from DNA extracts obtained from SPM samples at 50, 85, 100, 500 and 2000 m depth. All the archaeal *amo*A gene coding sequences were closely related to *amo*A gene sequences previously reported in 'shallow water' environments (0–200 m depth; 'Water column A' clade of Francis et al., 2005), as well as in sediments (Fig. S2). Within the cluster including the 'shallow water/sediment' *amo*A gene coding sequences, most of the sequences recovered at 50 m (90%) were grouped in cluster 1 (Fig. S2) closely related to the *amo*A gene coding sequence of *Ca.* Nitrosopelagicus brevis, while the majority of the *amo*A gene coding sequences obtained from 85, 100, 500, 2000 m depth grouped in cluster 2, which is more closely related to *amo*A gene sequences previously amplified from marine sediments and also closely related to the *amo*A protein sequence of *N. maritimus* (Fig. S2).

Table 1. Physical properties (potential density and oxygen concentration), absolute abundance of the archaeal 16S rRNA gene copies, and the distribution of the reads over the various detected archaeal phylogenetic groups per depth in the Black Sea water column at station PHOX2. Only archaeal groups that represent >3% of total archaeal reads at any sampled depth have been taken into consideration. Color coding: from dark red to white corresponds to 83–70%; 70–50%; 50–30%; 30–15%; 15–10%, 10–0% of archaeal 16S rRNA gene reads at a specific depth. bdl = below detection limit.

	Depth (m)	Potential density (kg m^{-3})	O_2 (nmol kg^{-1})	Archaeal 16S rRNA (gene copies L^{-1})	Thaumarchaeota Marine Group I			Marine Euryarchaeota Group II		Marine Euryarchaeota Group III	Euryarchaeota Thermoplasmatales		Euryarchaeota Methanomicrobia ANME1b	Crenarchaeota Thermoprotеales Thermofilum	Bathyarchaeota MCG+C3	DPANN Woesearchaeota DHVE-6	Others
					Ca. Nitrosopelagicus	*Nitrosopumilus*	uncultured OTU	uncultured OTU-1	uncultured OTU-2		VC2.1Arc6	CCA47					
Oxic	50	14.91	121	7.4×10^7	70.4	19.6		9.6	0.4								
	70	15.73	2.2	1.2×10^8	64.0	21.8	9.1	0.6	3.8							0.1	0.5
Suboxic	80	15.94	bdl	1.1×10^8	41.9	23.3	28.7	0.2	3.7							1.2	1.0
	85	15.98	bdl	5.9×10^7	28.8	36.8	16.9	0.1	7.9					1.0		7.1	1.3
	90	16.01	bdl	9.3×10^7	5.5	77.4	2.0	0.2	8.4					0.3	0.1	5.6	0.5
	95	16.07	bdl	1.8×10^8	1.9	72.1	0.2		4.9	1.5		0.4			1.1	17.9	
	100	16.13	bdl	1.5×10^8	1.3	81.8	0.2		0.3	1.2	0.3	0.2			1.1	13.7	
	105	16.18	bdl	2.4×10^8	2.1	82.6	0.4			0.9	1.3				1.7	11.1	
	110	16.24	bdl	7.6×10^7	0.5	71.9					2.0				4.6	20.4	0.5
Euxinic	130	16.38	bdl	5.4×10^7		33.3					5.6	2.8		6.9	16.7	34.7	
	170	16.57	bdl	4.5×10^6		14.3				4.8	2.4	2.4			14.3	59.5	2.4
	250	16.79	bdl	4.9×10^7	0.5	4.5	1.4			0.5	5.4	8.1			30.3	42.5	6.8
	500	17.04	bdl	6.0×10^6		8.7				2.9	1.4	8.7			50.7	23.2	4.3
	1000	17.20	bdl	2.2×10^7		2.5						1.6	2.5		54.9	35.2	3.3
	2000	17.23	bdl	1.2×10^8							2.2	7.7	13.2	0.9	34.8	34.5	6.8

4.3.3. Diversity and distribution of archaeal intact polar lipids

To examine the diversity and distribution of archaeal IPLs across the Black Sea water column 193 individual IPLs were analyzed using Ultra high Pressure Liquid Chromatography coupled to high resolution mass spectrometry. Table 2 shows the distribution of the 38 individual archaeal IPLs that were actually detected. These are reported as a heat map of the relative abundance (% of the total amounts of each individual IPL over the full depth range. The lack of authentic standards for these IPLs makes it difficult to compare the relative abundances of all IPLs at one specific water depth.

The detected IPL types included a number of different headgroups attached in various combinations to GDGT-0 to -4, crenarchaeol, OH-GDGT-0 to -4, and archaeol as core apolar lipids. Detected headgroups are: monohexose (MH; dihexose (DH, here indicating two MH moieties when attached to crenarchaeol or the other GDGT CLs, or one DH moiety when attached to archaeol CL; hexose phosphohexose (HPH, corresponding to two headgroups, namely one MH and one phosphatidyl MH; methyl-hexose phosphohexose (MeHPH); 2-phosphatidylglycerol (2PG); monohexose 2-phosphatydylglycerol (MH-2PG); hexose-glucuronic acid (MHgluA); phospho-dihexose (PDH); phosphatidylglycerol (PG); phosphatidylethanolamine (PE); phosphatidylser-ine (PS). Most of the targeted archaeal IPLs have been detected previously in environmental IPL surveys (Besseling et al., 2018; Liu et al., 2012; Meador et al., 2015; Rossel et al., 2008, 2011; Schubotz et al., 2009). Two new IPLs, MeHPH-GDGT-0 and MHgluA-archaeol, however, are reported here for the first time (see Figures S3 and S4 for details).

GDGT-0 to -2 and crenarchaeol were detected with MH, DH and HPH as headgroups; GDGT-3 and -4 only occurred with MH and DH headgroups. In addition, GDGT-0 to -2 also occurred as 2PG IPL, and GDGT-1 and -2 as MH-2PG IPLs (Table 2). The depth profiles of these IPL-GDGTs were similar for the various core GDGTs with the same headgroup. For example, all MH-GDGTs had a low relative abundance in the shallow oxic and upper suboxic waters (50–85 m; σ_θ ~14.9–15.9) but tended to increase towards the core suboxic and the upper euxinic waters (90–130 m; σ_θ ~16.0–16.4). In addition, MH-GDGT-4 showed high relative abundance also at 70 m. All DH-GDGTs had higher relative abundance in the upper suboxic waters (70–80 m, σ_θ ~15.7–15.9), then rapidly decreased with depth except for DH-GDGT-3 and -4, whose relative abundance remained stable down to 105 m (σ_θ ~16.2).

The HPH-GDGTs displayed a maximum in relative abundance in the oxic zone (50 m, σ_θ ~14.9) and again at 90 m (σ_θ ~16.0) in the core suboxic waters. HPH-GDGT-2 was an exception as it only had a maximum at 90 m depth (Table 2). The 2PG-GDGT-0 to -2 and the MH-2PG-GDGT-1 and -2 were only detected in the deep euxinic waters (1000–2000 m, σ_θ ~17.2) and had their highest relative abundance at 2000 m. In addition, MeHPH-GDGT-0, one of the two IPLs newly described in this study (Fig. S3), had a profile that differs from all others IPL-GDGTs as it was only detected at a discrete depth interval within the deep euxinic water column (250–1000 m, σ_θ ~16.8–17.2; Table 2).

Another group of archaeal IPLs detected was that with OH-GDGT-0 to -4 as CLs (Table 2). These IPLs were primarily detected with MH and DH as polar headgroups for OH-GDGT-1 and -2, and only with DH for OH-GDGT-3 and -4. The OH-GDGT-0 was also present with HPH as polar headgroup. In general, these IPLs were occurring between 90–130 m (σ_θ ~16.0–16.4), i.e. in the core suboxic and upper euxinic waters. The DH-OH-GDGT-1 and -2 were also present, albeit at lower relative abundance, at shallower depths up to the oxic surface. In contrast, the relative abundance of DH- and HPH-OH-GDGT-0 also peaked in the oxic surface waters at 50 m, in addition to a peak in the core suboxic waters (i.e. at ca. 100–105 m; Table 2).

The archaeol-based IPLs showed an entirely different distribution than the GDGT-based IPLs. They were undetectable or present only in traces down to ~100 m, where they started to increase and displayed their maxima below the HS^- redoxcline and in the deep euxinic waters (130–2000 m, σ_θ ~16.4–17.2). The archaeol-IPLs showed specific depth distributions according to the various polar headgroups. The relative abundance of MH/DH/PDH-archaeol increased gradually from ca. 95–100 m towards 130 m, where they reached a maximum. DH/PDH-archaeol showed a second maximum at 2000 m (Table 2). The newly described MHgluA-archaeol (see Figure S4 for details) was present only in traces down to 130 m where its relative abundance started to increase and had a maximum at 250–1000 m (Table 2). The PG/PE/PS-archaeol IPLs were manly detected between 1000–2000 m and displayed a prominent maximum at 2000 m (Table 2).

Table 2. Depth distributions of the archaeal IPLs detected in the Black Sea water column

Depth (m)	Potential density (kg m^{-3})	O_2 (mmol kg^{-1})	GDGT-0					GDGT-1					GDGT-2					GDGT-3		GDGT-4	
			MH	DH	HPH	MeHPH	2PG	MH	DH	HPH	2PG	MH-2PG	MH	DH	HPH	2PG	MH-2PG	MH	DH	MH	DH
50	14.91	121	5.6	16.5	30.1		2.8	2.4	17.3	15.0				13.1	3.1				11.8		8.4
70	15.73	2.2	11.4	37.6	15.6		4.4	9.4	30.7	13.6			8.3	28.1	8.6				16.5	23.9	14.4
80	15.94	bdl	2.8	19.6	6.8		2.0	3.4	17.6	7.6			2.9	22.2	3.2				9.2		12.5
85	15.98	bdl	3.0	8.3	3.9		0.2	3.8	8.2	4.8			4.6	10.0	4.8				7.4		6.8
90	16.01	bdl	9.0	6.7	12.5		0.2	13.5	7.6	22.0			13.9	8.8	37.4				16.1		11.6
95	16.07	bdl	6.1	3.3	8.6		0.4	8.8	5.5	12.9			11.7	4.8	17.3			22.6	11.4		10.7
100	16.13	bdl	13.1	2.1	12.0		0.8	16.4	3.9	15.5	0.1		18.2	4.2	19.3			26.4	12.0	23.3	13.0
105	16.18	bdl	17.6	2.8	5.0		0.4	18.0	3.6	4.9			19.9	3.5	4.3			27.8	8.0	19.4	11.1
110	16.24	bdl	11.6	1.5	3.5		1.0	10.9	1.9	2.7	0.2		10.2	1.8	1.8			16.7	3.5	14.5	4.9
130	16.38	bdl	15.4	1.0	1.7		1.5	11.3	2.6	0.8	0.7		9.2	2.5	0.2	0.2		6.5	3.6	16.8	5.5
170	16.57	bdl	3.0	0.5	0.3		0.3	1.6	0.6		0.1		0.8	0.8					0.4		1.1
250	16.79	bdl	0.8	0.1	0.1	29.4	0.4	0.4	0.3		0.2		0.3	0.3		0.1			0.1		
500	17.04	bdl	0.4			41.9	0.9	0.2	0.1		1.0			0.1		0.8					
1000	17.20	bdl	0.1			28.7	13.9	0.1			16.3	39.7				16.7	51.9			2.1	
2000	17.23	bdl	0.1				70.9				81.3	60.3				82.2	48.1				

These distributions are normalized on the summed abundance (r.u. L^{-1}) over all depths of each individual IPL detected. IPLs are listed according to the core lipid and the polar headgroups attached to them. Abbreviations used are: glycerol dialkyl glycerol tetraether (GDGT, hydroxyl GDGT (OH-GDGT, monohexose (MH, dihexose (DH, hexose phospho-hexose (HPH, phospho-dihexose (PDH, methyl-hexose phospho-hexose (MeHPH, 2-phosphatidyl glycerol (2PG, monohexose 2-phosphatidyl glycerol (MH-2PG, monohexose-glucuronic acid (MHgluA, phosphatidyl ethanolamine (PE, phosphatidyl serine (PS. Color code: from dark red to white corresponds to 84–70%, 70–50%, 50–30%, 30–20%, 20–10%, 10–0%. Note that this should be read in a vertical direction since the differences in MS response factors for different IPLs do not allow a direct comparison of the abundances of IPLs at one depth.

Depth (m)	Potential density (kg m^{-3})	O_2 (mmol kg^{-1})	Crenarchaeol			OH-GDGT-0			OH-GDGT-1		OH-GDGT-2		OH-GDGT-3	OH-GDGT-4	Archaeol						
			MH	DH	HPH	MH	DH	HPH	MH	DH	MH	DH	DH	DH	MH	DH	PDH	MHgluA	PG	PE	PS
50	14.91	121	2.8	13.1	36.1	3.1	22.3	15.6		5.9		3.1									
70	15.73	2.2	12.1	33.5	16.6	2.3	7.5		0.3	3.7		3.3							0.4		
80	15.94	bdl	3.5	32.1	5.6	0.2	1.4			1.0		1.6							0.1		
85	15.98	bdl	3.3	11.8	4.0	0.6	1.4	0.0	0.4	4.3	2.0	6.4	2.1								
90	16.01	bdl	8.2	4.3	16.6	4.0	4.5	8.7	15.1	15.7	19.7	20.3	23.6						0.1		
95	16.07	bdl	5.7	1.6	6.2	3.9	7.9	10.2	13.0	13.9	24.7	15.1	26.7	33.7	0.7	1.9			0.3	0.1	
100	16.13	bdl	11.0	1.6	7.7	12.2	13.8	30.1	18.7	19.7	22.6	19.4	29.0	42.6	3.7	4.5	2.5	0.3	0.7		
105	16.18	bdl	17.0	1.2	3.6	24.3	16.5	12.2	21.1	16.4	16.5	14.1	11.6	17.4	14.4	8.7	5.3	1.0	0.9	0.1	
110	16.24	bdl	11.4	0.4	2.1	17.6	8.9	15.9	13.2	7.7	8.1	6.9	5.9	6.3	9.2	5.6	3.4	1.3	0.6	0.0	
130	16.38	bdl	18.4	0.4	1.3	25.5	11.9	6.6	15.1	8.6	6.4	7.7	1.2		27.0	23.0	20.6	8.6	1.8	0.2	
170	16.57	bdl	4.2		0.1	5.4	3.1	0.7	2.7	2.4		1.6			16.0	14.3	10.0	10.9	1.0	0.2	
250	16.79	bdl	1.4	0.0	0.0	0.7	0.7		0.3	0.6		0.5			7.9	9.2	6.2	19.8	0.6	0.1	
500	17.04	bdl	0.6			0.2	0.1			0.1					7.5	9.0	11.4	24.0	1.1	0.8	
1000	17.20	bdl	0.2												6.2	7.6	10.1	19.9	11.7	14.2	17.0
2000	17.23	bdl	0.4												7.4	16.1	30.7	14.3	80.5	84.2	83.0

These distributions are normalized on the summed abundance (r.u. L^{-1}) over all depths of each individual IPL detected. IPLs are listed according to the core lipid and the polar headgroups attached to them. Abbreviations used are: glycerol dialkyl glycerol tetraether (GDGT, hydroxyl GDGT (OH-GDGT, monohexose (MH, dihexose (DH, hexose phospho-hexose (HPH, phospho-dihexose (PDH, methyl-hexose phospho-hexose (MeHPH, 2-phosphatidyl glycerol (2PG, monohexose 2-phosphatidyl glycerol (MH-2PG, monohexose-glucuronic acid (MHgluA, phosphatidyl ethanolamine (PE, phosphatidyl serine (PS. Color code: from dark red to white corresponds to 84–70%, 70–50%, 50–30%, 30–20%, 20–10%, 10–0%. Note that this should be read in a vertical direction since the differences in MS response factors for different IPLs do not allow a direct comparison of the abundances of IPLs at one depth.

4.3.4. Statistical analyses

Three correlation matrices were obtained with the available dataset. The first was developed to corroborate or dismiss the tentative assignment of specific IPLs to specific archaeal groups. To this end, the absolute abundance of specific archaeal groups, as calculated from the total archaeal 16S rRNA gene (copies L^{-1}; Table S3 estimated by qPCR (assuming one 16S rRNA gene copy number per genome and the relative abundance of the archaea (Table 1, was correlated with the absolute abundances of the archaeal IPLs expressed as response units per Liter (r.u. L^{-1}; Table S4 detected by mean of the Ultra high Pressure Liquid Chromatography coupled to high resolution mass spectrometry for each depth (Fig. 3; Table S5. It reveals clear positive correlations between various archaeal IPLs and archaeal groups in the water column of the Black Sea, suggesting potential relationships. In a second analysis the absolute abundance of the various archaeal groups detected at each depth were correlated to each other (Fig. S5; Table S6. This was meant to identify spurious correlations between specific archaeal IPLs and archaeal groups provided by the first correlation analysis, which are simply due to different archaeal groups occupying the same niche. This was apparent for MGI *Ca*. Nitrosopelagicus, MGI-unc OTU, and MGII OTU-1, for MGI *Nitrosopumilus*, MGIII and DPANN Woesearchaeota, and for Thermoplasmatales CCA47, euryarchaeotal ANME-1b, Bathyarchaeota (MCG+C3. The abundance of the DPANN Woesearchaeota showed weaker positive correlations with quite some groups of archaea residing in the deeper euxinic waters. The fact that some of these archaea occupy the same niches complicates the assignment of sources of archaeal IPLs as will be discussed.

A third correlation analysis (Fig. S6; Table S7 was performed on the depth profiles of archaeal IPLs quantified in response units per Liter (r.u. L^{-1}; Table S4 to reveal potential similarities and hence potential similar sources and will be discussed where appropriate.

4.4. Discussion

We have investigated the archaeal diversity and distribution in the Black Sea water column by means of a 16S rRNA amplicon sequencing approach and revealed the archaeal diversity to be substantially higher in comparison to previous studies of the Black Sea water column (Coolen et al., 2007; Lin et al., 2006; Vetriani et al., 2003; Wakeham et al., 2007. Our data allow associ-

ating certain archaeal groups with specific niches within the water column. In addition, we have encountered a high diversity of archaeal IPLs and, by using an unprecedented comparison with the gene-based data we discuss potential specific sources associated to specific IPL archaeal lipids.

The total archaeal abundance (based on archaeal 16S rRNA gene quantification in the Black Sea water column at the time of sampling reached highest numbers in both the suboxic and in the bottom euxinic waters (Fig. 1c. A peak abundance of archaea at 90–110 m depth has previously been reported in the central Black Sea by fluorescence *in situ* hybridization (Wakeham et al., 2007), but the second maximum has remained unnoticed, perhaps because of the under sampling of deep waters of the Black Sea in previous studies. The higher archaeal diversity we found throughout the water column, compared to earlier studies is due to the improved resolution of the more advanced 16S rRNA gene amplicon sequencing technique used here. The archaeal groups detected include various Thaumarchaeota, Euryarchaeota of the MGII and MGIII, Thermoplasmatales, ANME-1b, Woesearchaeota and MCG (Table 1; Figs. 1d and 2). The high archaeal diversity based on the 16S rRNA gene also coincided with a high variety of archaeal IPLs (Table 2), as discussed below.

4.4.1. Ammonia-oxidizing Thaumarchaeota reside predominantly in oxic and suboxic waters

In the oxic and suboxic waters, members of the Thaumarchaeota phylum were dominant representing 86–99.5% of all archaea (Table 1). Thaumarchaeota closely related to *Ca.* Nitrosopelagicus were the dominant archaeal group in the fully oxygenated surface waters, where they represented 67 –78% of all Thaumarchaeota, and became minor (<7%) at >85 m. This is supported by the *amo*A protein diversity analysis since in the shallow waters most of the *amo*A sequences were closely related to that of *Ca.* Nitrosopelagicus (Fig. S2). The genome of the thaumarchaeon *Ca.* Nitrosopelagicus, which was en-riched from open ocean water, codes for proteins involved in stress responses upon UV radiation and reactive oxygen species, suggesting adaptations to the oligotrophic surface ocean (Santoro et al., 2015). The preference for the upper water column of *Ca.* Nitrosopelagicus agrees with its dominant presence in the Black Sea uppermost water column. The reasons for this niche preference, e.g. metabolic advantage, competition with other microbial groups, remain unresolved. However, the low ammonia concentrations in waters from 50 to 85 m depth (i.e. on average 0.06 μM; Fig. 1b) are compatible with the oligo-

trophic lifestyle predicted for the nitrifier *Ca.* Nitrosopelagicus. In addition, sequences closely affiliated to the MGI-unc OTU (with no closely related cultured relatives) were also detected in the oxic/upper suboxic waters but peaked in absolute abundance at 80 m, where it contributed 31% of all Thaumarchaeotal 16S rRNA gene reads.

In the deeper part of the suboxic zone (90–110 m depth), the summed relative abundance of these two archaeal OTUs decreased to <10% of the total Thaumarchaeotal 16S rRNA gene reads and they were dominated by *Nitrosopumilus*-related sequences, which represented up to 83% of the total archaeal 16S rRNA gene reads (Table 1). Again, this is supported by the nucleotide-derived amino acid analysis of *amo*A as most of the *amo*A sequences in the suboxic waters were closely related to that of *Nitrosopumilus* (Fig. S2). *Nitrosopumilus* has previously been reported to thrive at the redoxclines of the Black Sea (Coolen et al., 2007; Lam et al., 2007) and of the Gotland Deep in the Baltic Sea (Labrenz et al., 2010). In the study of Coolen *et al*. (2007), the MGI 16S rRNA gene diversity was evaluated by denaturing gradient gel electrophoresis, and also three different MGI OTUs where detected throughout the water column of three stations in the Black Sea, specifically sequences closely related to *Nitrosopumilus maritimus* were detected in oxic/suboxic waters. The dominance of *Nitrosopumilus* 16S rRNA gene sequences in the suboxic zone in our study coincided with the maximum of total archaeal 16S rRNA gene copies (i.e. at 105 m; Figs. 1c and d). This has been attributed to the preference of Thaumarchaeota for niches with relatively low concentrations of oxygen and ammonia, enabling this group to outcompete bacterial nitrifiers (see Erguder et al., 2009 for a review).

From 90 to 110 m, sulfide concentrations are apparently still low enough (maximum of 0.85 μM at 105 m) to allow the proliferation of Thaumarchaeota. These archaea are believed to be inhibited by high sulfide concentrations, but also have an advantage over bacteria in sulfide-containing waters because the sulfide inhibition is more severe for bacterial than for archaeal nitrifiers (Erguder et al., 2009). It is also possible that the interaction of *Nitrosopumilus* with sulfur-oxidizing bacteria (SOB) in the upper redoxcline of the Black Sea allows the proliferation of this archaeal group. In fact, previous studies have reported the successful establishment of co-cultures between sedimentary ammonia oxidizing archaea (AOA) and SOB (Park et al., 2014) that would explain the co-existence of these groups in sediment redox gradients. Indeed, previous studies have reported the presence of SOB at the Black Sea redox-

cline, like the uncultured group SUP05 and members of the Epsilonproteobacteria (Glaubitz et al., 2013; Grote et al., 2008), which would support the niche preference of *Nitrosopumilus*-related Thaumarchaeota at the redoxcline of the Black Sea. In the euxinic zone, thaumarchaeotal 16S rRNA gene reads related to *Nitrosopumilus* were also detected although their contribution to the total archaeal reads readily declined with increasing depth (Fig. 1d). The conditions in the shallow euxinic zone (absence of oxygen and increasing sulfide concentrations) are believed to be incompatible with the physiology of the cultivated members of the Thaumarchaeota. This together with the fact that the 16S rRNA gene sequences recovered from these euxinic waters were closely related to the 16S rRNA gene sequences of the *Nitrosopumilus* group of the suboxic waters supports the hypothesis that this DNA signal is preserved and exported from the chemocline rather than derived from living thaumarchaeotal cells.

Considering the gene-based results, Thaumarchaeota are likely the predominant source for the archaeal IPLs present in the waters of the oxic and suboxic zones and the changes in the thaumarchaeotal composition are probably an important factor for the observed changes in IPL distribution (Tables 1 and 2; Fig. 1d). Indeed, the cross-correlation analysis among archaeal groups confirms that genetic variability existed among the Thaumarchaeota detected in the oxic and suboxic zones (Fig. S5; Table S6) and that those that shared similar IPL correlation patterns (see *Ca*. Nitrosopelagicus and MGI-unc OTU in Fig. 3) scored positively with each other, while where the IPL correlation patterns were dissimilar (see *Ca*. Nitrosopelagicus and *Nitrosopumilus* in Fig. 3) the scores were negative (Fig. S5; Table S6).

Culture studies have shown that Thaumarchaeota synthesize mainly GDGT-0 and crenarchaeol and, in lower abundance, GDGT-1 to -4 as their core lipids (Elling et al., 2014, 2017; Pitcher et al., 2011b; Schouten et al., 2008a; Sinninghe Damsté et al., 2002c, 2012). More recently, mono- (OH-) and dihydroxy- (2OH-) GDGTs have also been reported in thaumarchaeotal cultures (Liu et al., 2012). This is in good agreement with our data since we detected predominantly crenarchaeol and GDGT-0 to -4 as well as OH-GDGTs, mostly with MH, DH and HPH head groups, in the oxic/suboxic zones (Table 2). The IPL-crenarchaeol absolute abundances (Table S4) were highest in the oxic zone confirming Thaumarchaeota as its main biological source since 90–95% of 16S rRNA gene reads belongs to this group (Table 1; Fig. 1c). Assuming similar response factors, HPH-crenarchaeol was the pre-

vailing IPL at 50 m depth, but at 70–80 m DH-crenarchaeol was predominant (Table 2). The Pearson correlation analysis also showed that both DH and HPH-crenarchaeol were positively correlated to the presence of the MGI *Ca.* Nitrosopelagicus and the MGI-unc OTU (Fig. 3). MGII OTU-1 also correlated with DH and HPH-crenarchaeol but this is likely due to the fact that they occupy the same niche as is evident from the correlation matrix (Fig. S5).

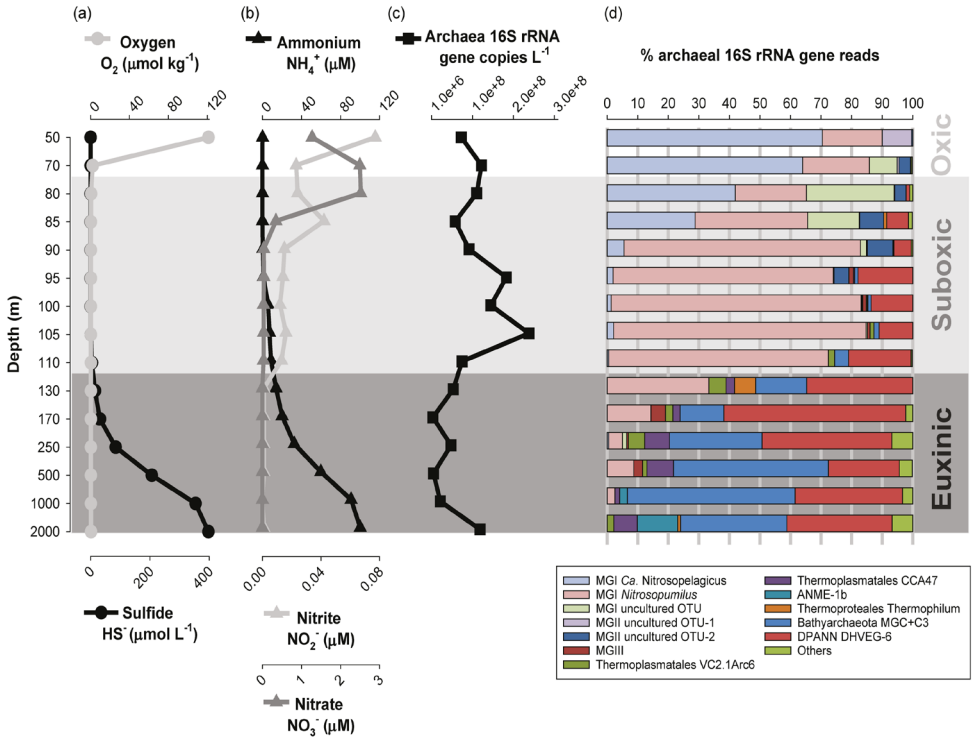

Figure 1. Concentration profiles of (a) oxygen (O_2, µmol kg^{-1}) and sulfide (HS^-, µmol L^{-1}), (b) ammonia (NH_4^+, µM), nitrite (NO_2^-, µM) and nitrate (NO_3^-, µM). (c) The absolute number of total archaeal 16S rRNA gene (copies L^{-1}), and (d) percentage of the archaeal 16S rRNA gene reads of the archaeal groups detected across the water column of the Black Sea at station PHOX2.

The high percentage of 16S rRNA gene reads attributed to the thaumarchaeotal *Nitrosopumilus* OTU and the maximum archaeal 16S rRNA gene abundance detected in the suboxic water (Table 1; Figs. 1c and d) coincided with high relative abundances of OH-GDGT IPLs, with MH, DH and HPH as polar headgroups (up to the order of 10^7 r.u. L^{-1}; Table 2). This suggests that

Nitrosopumilus-like Thaumarchaeota might be the source of the OH-GDGT IPLs. This assumption is further corroborated by the positive scores obtained in the correlation matrix (Fig. 3 and Table S5). Indeed, the relative abundance of OH-GDGT-1 and -2 with MH and DH as polar headgroups and, to a certain degree, of DH-OH-GDGT-3 and -4 was higher in the suboxic waters compared to the shallower oxic and the deeper euxinic water (Table 2). Previous studies that detected glycosidic OH-GDGTs in marine sediments (Lipp and Hinrichs, 2009) and in cultures (Liu et al., 2012) tentatively proposed them as originating from both crenarchaeota and euryarchaeota.

At a sampling station located at the center of the basin with comparable conditions to the one reported in this study, Schubotz et al. (2009) reported MH-GDGT-0 and -crenarchaeol as the main archaeal IPLs in the suboxic waters, accounting together for up to 80% in relative abundance, but they did not detect HPH-crenarchaeol. These lipids, whose glycosidic polar headgroup is generally considered as deriving from preservation rather than living biomass, could be attributed to a Thaumarchaeota fossil signal sinking down from the chemocline. Schubotz et al. (2009) also reported GDGT-2 and -3 attached to DH and to an unidentified headgroup MH341 – tentatively identified as a DH-OH-GDGT in a subsequent study (Liu et al., 2012) – as secondary IPLs and suggested methanotrophic euryarchaeota as a possible source (Schubotz et al., 2009). However, in our study the dominant presence of *Nitrosopumilus* over the other archaeal groups in the suboxic waters and the highly positive scores in the correlation analysis strongly suggests this group as the most likely source of the DH-OH-GDGT IPLs (Figs. 1c and 3).

4.4.2. MGII Euryarchaeota in the suboxic zone

Sequences of the MGII OTU-1 (Fig. 2) were almost exclusively detected in the oxic waters at 50 m depth, representing ca. 10% of the archaeal 16S rRNA gene reads (Table 1; Fig. 1d). Below 50 m, calculated cell numbers (Table S3) declined by 1–2 orders of magnitude and at depths >90 m, this group was no longer detected. This indicates a preference of this MGII group for the photic zone and it may be possible that they were even more abundant in the shallower waters not examined in this study. The presence of genes encoding proteorhodopsin homologs in metagenomes of MGII suggested a photoheterotrophic lifestyle (Iverson et al., 2012) and this would be in agreement with the niche of this group in the Black Sea waters.

MGII OTU-2 occupied a different niche than MGII OTU-1 with calculated copy numbers maximizing at 90–95 m in the suboxic zone (Table S3), suggesting an adaptation to very low oxygen concentrations. The negative correlation of the abundances of these two MGII uncultured OTUs is a confirmation of the genetic diversity occurring between the two OTUs (Fig. S5; Table S6. Because of the high abundance of the Thaumarchaeota, MGII OTU-2 reads never exceed 9% (Table 1; Fig. 1d. Early studies on the distribution of MGII concluded that they are predominant in surface waters of the ocean (Massana et al., 1997, 2000 but subsequent studies revealed that other ecotypes exist in deeper waters (see Zhang et al., 2015 for a review. Genomic analyses of these deep water MGII suggested the capacity of anaerobic respiration using organic matter as electron donor (Orsi et al., 2015, which would be in good agreement with the niche observed in Black Sea waters. The restriction of MGII OTU-2 to the suboxic zone of the Black Sea (i.e. they are absent in the sulfidic waters below 105 m suggests that these archaea are sensitive to sulfide. Hence, the intense activity of SOB, alleviating the presence of sulfide in the suboxic zones, probably allows the proliferation of the MGII OTU-2 in the suboxic zone.

As mentioned above, the lipid composition of the upper suboxic waters (80–90 m depth)was dominated by GDGT-0, -1, and -2 as well as crenarchaeol mostly with DH polar headgroup (Table 2, which are attributed to the MGI Thaumarchaeota. Recently, Lincoln et al. (2014a and Wang et al. (2015 provided evidence that MGII may be synthesizing GDGTs in the marine water column. However, this is still a highly debated topic (Lincoln et al., 2014b; Schouten et al., 2014). The question if MGII archaea are able to synthesize GDGTs, and specifically crenarchaeol, can only be ultimately answered by cultivation of this group of archaea. In our study, in the correlation matrix of the IPLs *vs* the archaeal groups the two MGII OTUs scored positively with several IPL GDGTs and especially MGII OTU-1 was positively correlated with HPH-GDGT-0 and -crenarchaeol (Fig. 3; Table S5). However, the correlation matrix of the archaeal groups (Fig. S5; Table S6) in-dicates that this correlation was probably the result of MGII OTU-1 sharing the same ecological niche of *Ca*. Nitrosopelagicus and MGI-unc OTU (Fig. 1d). This together with the low relative abundance of MGII archaea (up to 10 % of the total archaeal population) in the suboxic waters does not allow correlating their presence with the specific lipids detected here and, hence, cannot contribute in determining the IPLs synthesized by MGII archaea.

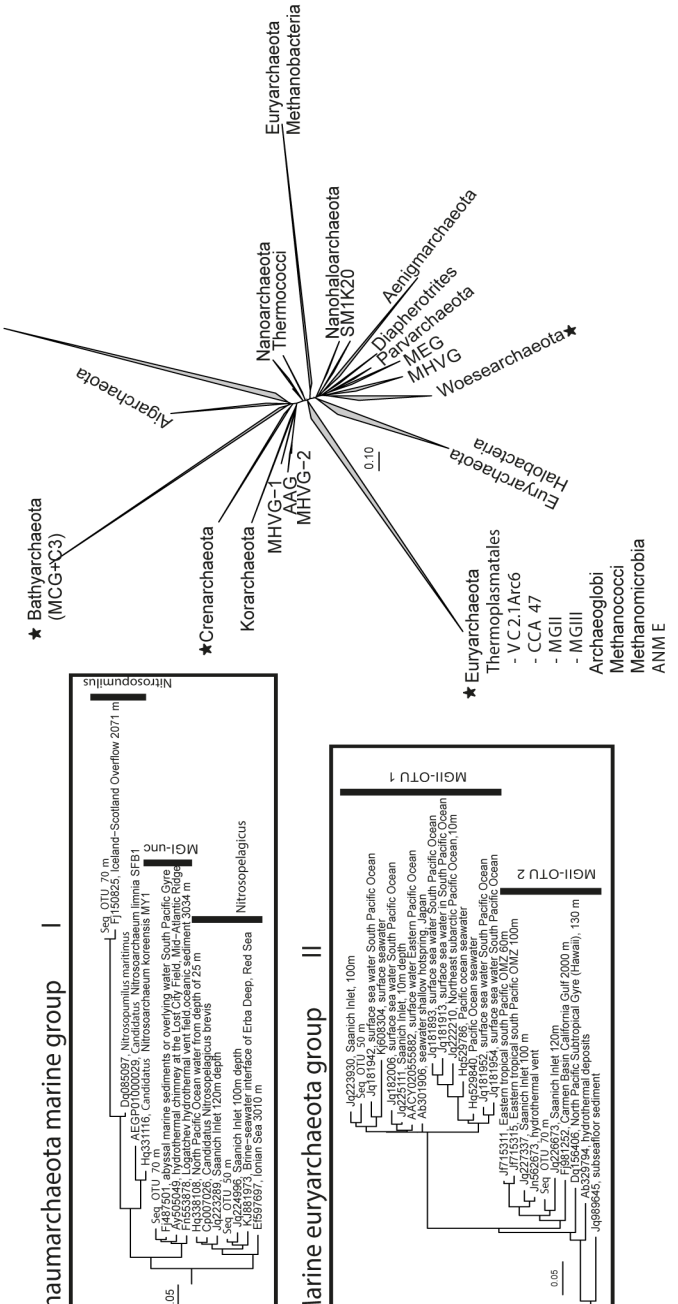

Figure 2. (a General archaeal 16S rRNA gene tree revealing the phylogenetic positions of the archaeal groups (indicated with a star) detected in the Black Sea and discussed in the text. The specific subgroups and their distribution are shown in Fig. 1. (b and c). Sub-trees showing the phylogenetic positions of the three OTUs of Thaumarchaeota, and the two MGII OTUs in relation to other relevant sequences. The trees were obtained using 16S rRNA gene sequences of the Silva release 123 and those obtained in this study

4.4.3. Other archaeal groups in the suboxic zone

Other archaeal classes were also detected in the suboxic waters, such as the MGIII, MCG and the DPANN Woesearchaeota (Table 1; Fig. 1d). The low relative abundance of MGIII and MCG in the suboxic waters (approximately 1% of the total archaeal 16S rRNA gene reads), rule them out as major contributors to the main IPLs (i.e. HPH-GDGT-1, -2 and DH-OH-GDGT-1, -2) in the suboxic water in spite of the positive scores the two archaeal groups had with those IPLs (Fig. 3; Table S5). DPANN Woesearchaeota contributed to an average of 12% of the total archaeal 16S rRNA gene reads in the suboxic waters (Table 1; Fig. 1d), which is relatively minor compared to the percentage of the *Nitrosopumilus*-like sequences. In addition, recent studies suggest that members of the DPANN Woesearchaeota have only small genomes lacking the genes required for the lipid membrane biosynthesis (Castelle et al., 2015; Villanueva et al., 2017). If so, they would be expected to depend on recycling extracellular lipids to build their membranes and therefore do not synthesize their own lipids, but contribute to the total IPL as recently suggested by Lipsewers et al. (2018).

4.4.4. Anaerobic methane oxidizing archaea reside in deep sulfidic waters.

The 16S rRNA gene amplicon sequencing analysis indicated that Euryarchaeota Methanomicrobia ANME of the subgroup 1b were the only ANME representatives in the Black Sea euxinic waters. They were only detectable at 1000 m depth (2.4%) and reached 13% of the total archaeal reads at 2000 m depth (Table 1; Fig. 1d). Considering the quantification of total archaeal 16S rRNA gene, which peaks at 2000 m (Fig. 1c) and the high percentage of 16S rRNA gene sequences attributed to ANME-1b, the group was a significant component of the archaeal community in the deep euxinic waters of the Black Sea at the time of sampling (Fig. 1d). Members of the ANME-1 have previously been detected in Black Sea carbonate chimneys (Blumenberg et al., 2004). Genetic evidence has also indicated the presence of a community dominated by ANME-1 in the deep Black Sea, although the detected copies represented <2% of the total archaeal copies at the deepest water mass (i.e. 1500 m) analyzed (Schubert et al., 2006). Wakeham et al. (2007) employed specifically designed ANME-1 FISH probes but were not able to detect ANME-1. Schubert et al. (2006) also reported the presence of ANME-2 in

the shallower waters of the euxinic zone, but this is not confirmed by our data.

Previous environmental studies have suggested that ANME-1 core lipids include mostly GDGT-0 to -2 and archaeol as core lipids, the latter as a minor membrane component (Blumenberg et al., 2004; Pancost *e*t al., 2001; Wakeham et al., 2003). In the Black Sea waters the ANME-1 distribution was characterized by approximately equal amounts of GDGT-0, -1, and -2 (Wakeham et al., 2003). The stable carbon isotopic composition of the biphytanes comprising these GDGTs revealed that they were depleted in ^{13}C, establishing a direct link with methane in the water column (Wakeham et al., 2003). ANME-2, the other methanotrophic archaeal subgroup, instead predominantly produces primarily *sn*-2-OH-archaeol (Blumenberg et al., 2004; Rossel et al., 2008, 2011; Stadnitskaia et al., 2005; Wakeham et al., 2007;).

The profiles of the 16S rRNA gene ANME-1b reads and of 2PG-GDGT-0, -1 and -2 (Tables 1 and 2) revealed a highly positive correlation ($r > 0.99$), all increasing radically at 1000–2000 m depth (Fig. 3; Tables 2 and S6). This strongly suggests that these IPLs are synthesized by ANME-1b in the deepest part of the euxinic zone. In good agreement with the characteristic CL distribution of ANME-1 in deep Black Sea waters (Wakeham et al., 2003, 2007), these three 2PG IPLs have approximately the same concentration (Table S4). Accordingly, this type of IPLs was previously attributed to communities dominated by ANME-1 associated to sulfate-reducing bacteria of the *Desulfosarcina-Desulfococcus* (DSS) branch in methane-rich sediments and microbial mats of hydrocarbon seeps from multiple locations including the Black Sea floor (Meador et al., 2015; Rossel et al., 2011). The MH-2PG-GDGT-1 and -2, which shared the same depth distribution and also have positive correlation scores with the ANME-1b group ($r = 0.84$ and 0.68) are likely also synthesized as IPLs by this archaeal group (Tables 2 and S5), as also suggested in the same previous study (Rossel et al., 2011). Remarkably, in our study the characteristic 2PG IPLs were already detected at shallower depths in the euxinic zone, albeit at concentrations that are 2–3 orders of magnitude lower. This suggests that ANME-1 also occurs at shallower depths, in agreement with CL GDGT detected earlier (Wakeham et al., 2003, 2007), suggesting that IPL analysis is more sensitive than 16S rRNA gene amplicon sequencing analysis to detect the presence of these methane-oxidizing archaea.

PS-, PG-, and PE-archaeol also displayed depth profiles comparable to the three 2PG-GDGTs in the deep euxinic waters (Table 2) and showed a highly significant correlation ($r > 0.99$) with the depth profile of the ANME-1 reads

(Fig 3; Table S6. PS- and PG-archaeol have previously been tentatively assigned to ANME-2 and -3 (Rossel et al., 2008, 2011, archaeal groups that were not revealed to be present in the Black Sea water column by our genetic approach. PE-archaeol was not detected by these authors, although it has been reported in marine sediments at several locations (Schubotz et al., 2011; Yoshinaga et al., 2011 and in cultures of the hyperthermophylic archaeon *Thermococcus kodakarensis* (Meador et al., 2014). However, Wegener et al. (2016) detected PG-archaeol in their ANME-1 enrichment culture (Wegener et al., 2016). Our results confirm this outcome and strongly suggest that ANME-1 also produces PS-, and PE-archaeol.

Our combined genetic and IPL data together with previous isotopic, core lipid and genetic evidence (Wakeham et al., 2003, 2007 indicate that ANME-1 is a relevant contributor to the archaeal community of the deep Black Sea. This is in contrast with a previous study of IPLs in Black Sea waters by Schubotz et al. (2009 who did not detect any IPLs that could be linked to ANMEs.

4.4.5. Other archaea thriving in the euxinic zone

In addition to ANME-1b, members of the Thermoplasmatales VC2.1Arc6 and CCA47, Crenarchaeota of the Thermoproteales Thermofilum, Bathyarchaeota MCG, and MGIII were predominantly detected in the euxinic zone (Table 1; Fig. 1d, suggesting that all these archaea are anaerobic and can deal with high sulfide concentrations. DPANN Woesearchaeota DHVE-6 also occurred in the suboxic zone, but their relative abundance increased substantially with depth (average 37% from 130 to 2000 m depth, reaching a maximum of almost 50% of archaeal reads at 170 m depth. Bathyarchaeota represented the most prominent group below 170 m. They were barely detectable (i.e. <1% of archaeal reads in the deeper suboxic zone (~105–110 m, then reached >10% at 130 m and reached the highest levels (55% in the deeper part of the euxinic zone (1000 m depth. Other less abundant groups include two subgroups of the Thermoplasmatales (average of 9%, which occurred throughout the euxinic zone with no clear maximum, and Thermoproteales Thermofilum, which only appeared at 130 m at a substantial relative abundance (i.e. 7%; Table 1; Fig. 1d. The 16S rRNA gene sequences affiliated to the Thermoplasmatales and Bathyarchaeota have been mostly detected in sediments (e.g. Lloyd et al., 2013. Thermoplasmatales cluster VC2.1Arc6 was originally described in deep-sea hydrothermal vents on the Mid-Atlantic

Ridge (Reysenbach and Longnecker, 2000), but these archaea have also been detected in deep sea sediments of other locations such as the Marmara Sea (Quaiser et al., 2011). The Thermoplasmatales CCA47 group was originally identified in oxygen-depleted marine environment and anoxic sub-saline sediments (Ferrer et al., 2011; Stoeck and Epstein, 2003), which is compatible with the conditions found in the Black Sea water column.

All members of the complex archaeal community thriving in the euxinic water column detected in our study (Table 1; Fig. 1d) have remained uncultivated. Despite this, we can infer they use some metabolic strategy, either independently or requiring some sort of cooperation with bacterial lineages, to deal with the increasing concentrations of hydrogen sulfide found in the Black Sea water column. Genome analysis of metagenomic reads of these uncultured archaeal classes would shed light on putative sulfur-related metabolisms or strategies to cope with the high sulfide concentrations. The high abundance of MCG in the euxinic water column of the Black Sea is remarkable as it is an archaeal phylum typically associated to marine sub-seafloor sediments (Biddle et al., 2006; Durbin and Teske, 2011; Fry et al., 2008; Inagaki et al., 2003; Kubo et al., 2012). However, MCGs have also been reported to be present in karstic lakes with high sulfide concentrations (i.e. 150 μM; Fillol et al., 2015), which could indicate a role of MCGs in sulfide-rich pelagic systems.

Another remarkable finding of our study is the detection of DPANN Woesearchaeota DHVE-6 which comprised an average of 40% of the total archaeal 16S rRNA gene reads in the euxinic waters and expected to be approximately 1×10^7 cells L^{-1}. This subgroup of the DPANN superphylum is still enigmatic and recent reports based on metagenomic sequencing indicate that they might be involved in carbon and hydrogen metabolism, probably associated with symbiotic and/or fermentation-based lifestyles (Castelle et al., 2015), which is compatible with their presence in anoxic waters. It is plausible that they are also involved in the sulfur cycle considering their high abundance in the euxinic waters of the Black Sea, but future studies would need to address this possibility.

By examining our combined lipidomic and genetic datasets, we may provide clues as to which membrane lipids the uncultivated archaeal groups in the euxinic waters of the Black Sea produces. The high abundance of the DPANN archaea (Table 1) would make them an important IPL source in these waters but their apparent lack of lipid membrane biosynthetic potential

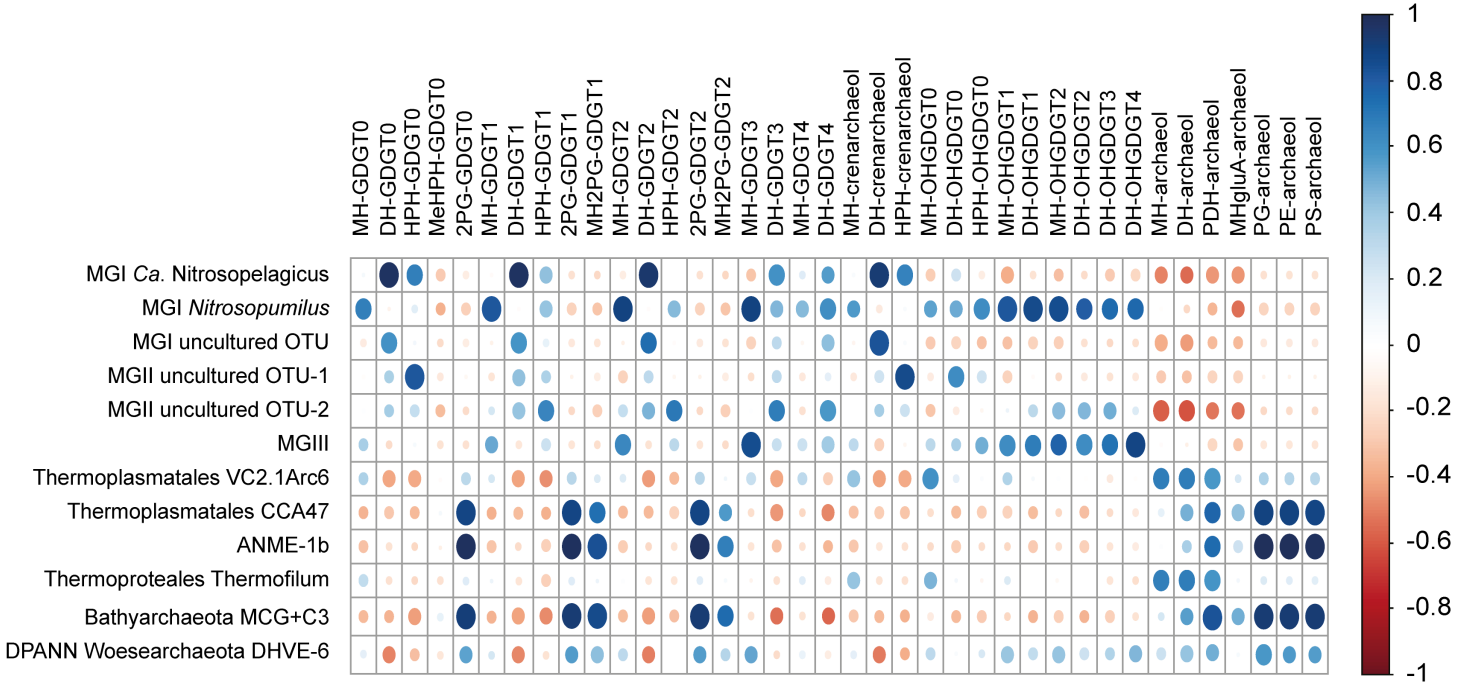

Figure 3. Dot plot of the correlation matrix obtained by applying a Pearson analysis to the total archaeal 16S rRNA gene reads (copies L^{-1}) of the archaeal groups and to the absolute abundances of the archaeal IPLs (response units per Liter; r.u. L^{-1}) detected in the Black Sea water column at station PHOX2. The size of the dot and the intensity of its color relate to the degree of correlation. Dark blue corresponds to r values of +1, indicating a strong positive linear correlation between the concentration of the archaeal IPL and archaeal gene reads; white corresponds to r values of 0, indicating that no correlation exists; dark red corresponds to r values of -1, indicating a strong negative linear correlation.

(Castelle et al., 2015; Lipsewers et al., 2018; Villanueva et al., 2017) makes this implausible. A complication in this approach is that abundance of almost all dominant archaeal groups in the euxinic zone correlate positively to each other (Fig. S5). The correlations between the abundance of ANME-1b, Thermoplasmatales CCA47 and Bathyarchaeota MCG + C3 were high ($r = > 0.91$; Table S6) and the correlations of those groups with Thermoplasmatales VC2.1Arc6, Thermoproteales, and DPANN were moderately positive (Fig. S5; Table S6). In contrast, the abundance of MGIII, whose distribution spanned throughout the suboxic and the upper euxinic zones (Table 1), correlated positively only with that of the DPANN group (Fig. S5; Table S6).

The composition of the IPLs present in the euxinic zone was more diverse compared to the oxic and suboxic zones, including both GDGT- and archaeol-based IPLs. The dominant IPLs are based on common CLs such as GDGT-0 to -2 and archaeol, but attached to a broad variety of polar headgroups. Specifically, we detected 2PG attached to GDGT-0 to -2, MH-2PG-GDGT-1 and -2, MH/DH/PDH/PG/PE/PS-archaeol and the two novel IPLs MeHPH-GDGT-0 and MHgluA-archaeol. Of these IPLs, the abundances of 2PG-GDGT-0, -1 and -2, and archaeol with various head groups (i.e. MH, DH, PDH, MHgluA, PG, and PE) gradually increased with depth (Table 2). The concentration profiles of 2PG-GDGT-0, -1 and -2 and PG-, PE-, and PS-archaeol correlated positively with each other (Fig. S6; Table S7) since, as suggested earlier, they are likely produced by ANME-1b.

Bathyarchaeota represented one of the most abundant groups in the euxinic zone (Table 1; Fig. 1d), which would make this group a potential source for the most abundant IPL classes detected in the euxinic waters (Table 2). A previous study of anoxic estuarine sediments (Meador et al., 2015) proposed BDGT-IPLs as putative biomarkers of Bathyarchaeota MCG. However, BDGTs have recently been associated to methanogens of the Methanomassiliicoccales order, which is closely related to Thermoplasmatales and euryarchaeotal DHVE-2 (Becker et al., 2016). However, BDGT-IPLs were not detected by this study. The depth profiles of the Bathyarchaeota abundance correlated significantly to those of 2PG-GDGT-0, -1 and -2 and PG-, PE-, and PS-archaeol (Fig. 3; $r = 0.92$-0.93, Table S5). However, these correlations were less significant than those with the ANME-1b (see earlier). Furthermore, Bathyarchaeota already appear in the suboxic zone (ca. 90 m) and their relative abundance gradually increased with increasing depth up to the deep euxinic zone (Table 1). The ANME-1b group and the IPLs assigned to them

instead appeared only at the lowermost part of the euxinic zone (1000–2000 m) (Tables 1 and 2).

It is interesting to note that just like the relative abundance of the Bathyarchaeota (Table 1) the IPL MHgluA-archaeol had its maximum abundance in the 250–1000 m depth range (Table 2). At this depth, this IPL was one to two orders of magnitude higher as measured in response units compared to other IPLs (Table S4). Although the response factors for IPLs vary, this strongly suggests that MHgluA-archaeol is one of the dominant IPLs in the upper part of the euxinic zone and should be sourced by one of the dominant groups of archaea residing here (i.e. Bathyarchaeota). Indeed, in the correlation analysis (Fig. 3) Bathyarchaeota MCG was the archaeal group that correlated most positively with MHgluA-archaeol (r = 0.51), although the correlation was less significant than observed for the ANME-1 IPLs. The profile of PDH-archaeol also showed the highest correlation with the Bathyarchaeota profile (r=0.84), suggesting this IPL may also be produced by these archaea.

Two different groups of Thermoplasmatales were detected in the euxinic water column with distinct profiles (Table 1). The CCA47 group had its highest relative abundance in the deep euxinic waters (Table 1). Its abundance profile reveals a high correlation with those of ANME-1b and Bathyarchaeota groups, which, in combination with CCA47 lower relative abundance masks potential relationships with IPLs. The other Thermoplasmatales group, VC2.1Arc6, had a more distinct distribution (Table 1). Its depth profile shows a fairly high correlation with those of MH- and DH-archaeol (r = 0.68; Table S5) and these two IPL profiles are also significantly correlated to each other (r=0.91; Table S6). This suggests that the VC2.1Arc6 group may be producing these two structurally related IPLs. However, the profile of the Thermofilum group, although this group was less prominent (Table 1), shows a similar correlation with the profiles of MH- and DH-archaeol (r = 0.66-0.68; Table S5).

Interestingly, the newly described MeHPH-GDGT-0 IPL displayed a specific depth profile, being only detected in the 250–1000 m interval (Table 2). For this we would have expected to find a clear correspondence of this distinctive IPL profile with a specific archaeal group (Tables 1 and 2). However, there was not such clear match and the correlation analysis confirmed that none of the archaeal lineages detected by this study strongly correlated with the MeHPH-GDGT-0 (Fig. 3; Table S5), suggesting an as yet unidentified source.

4.5. Conclusions

The combination of 16S rRNA gene amplicon sequencing and lipidomic methods applied here for the first time has advanced our understanding of the diversity, distribution and abundance of archaeal groups in the Black Sea water column. The diversity of archaea and archaeal lipids, determined by 16S rRNA gene amplicon sequencing and by high resolution accurate mass/mass spectrometry, respectively, was higher than previously described. We observed dominance of Thaumarchaeota *Ca.* Nitrosopelagicus in the oxic and upper suboxic waters of the Black Sea water column coinciding with a higher dominance of HPH-crenarchaeol, while suboxic waters were dominated by the thaumarchaeon *Nitrosopumilus* and a high relative abundance of DH-OH-GDGT-1/-2, and HPH-GDGT-0/-2. The euxinic waters were characterized by a broader diversity of archaea where members of the Bathyarchaeota (MCG) dominated, but others such as DPANN Woesearchaeota, Thermoplasmatales, MGIII, and ANME-1 were also present. Statistical analyses support a connection between the IPLs MH-2PG-GDGT-1 and -2 and ANME-1b, as well as 2PG-GDGT-0, -1, -2, PG, PE and the newly discovered MHgluA-archaeol and Bathyarchaeota. Although we cannot definitively link these lipid biomarkers with the above mentioned uncultured archaeal groups, these results shed light on the high diversity of IPL biomarkers of the Black Sea water column and provide additional clues on the preferential niches of the uncultured archaeal groups detected which will aid in future cultivation efforts. Finally, our results point to an important role of Bathyarchaeota and DPANN Woesearchaeota groups in the euxinic waters of the Black Sea. Future studies based on full genome metagenomic analyses are likely to unravel their metabolic and membrane lipid potential in this unique ecosystem.

Acknowledgements

We thank Prof C.P. Slomp, the PI of the PHOXY cruise, for the support of this work and the captain, crew, scientists and technicians on board of RV Pelagia. This project was funded by a grant to JSSD from the Darwin Center for Biogeosciences (project nr. 3012). The work was further supported by funding from the Netherlands Earth System Science Center (NESSC) and Soehngen Institute for Anaerobic Microbiology (SIAM) through gravitation grants (NWO 024.002.001 and NWO 024.002.002) from the Dutch Ministry for Education, Culture and Science.

Table S1. Details of SPM sampling during the Phoxy cruise on the Black Sea (station PHOX2), aboard the *R/V Pelagia* (June-July 2013). For each location the table reports the depth of sampling (m) and the corresponding potential density ($\sigma\theta$, kg m^{-3}), the volume of water filtered by each pump deployed (L) as well as physicochemical parameters of the water at those depths, such as temperature (T, °C), salinity (PSU) and dissolved inorganic carbon, (DIC, mmol L^{-1}). [a]The pump was pumping also during the resurgence. This might have caused contamination from the water column. [b]Reading of the flow meter.

Station	Location DMS (lon/lat)	Date dd/mm/yyyy	Depth of SPM sampling (m)	Estimated potential density (kg m^{-3})	[b]Amount of water filtered (L)	Temperature (°C)	Salinity (PSU)	DIC (mmol L^{-1})
PHOX2	42° 53.8' N 30° 40.7' E	09/06/2013	50	14.9	286	7.9	19.4	3.3
		09/06/2013	70	15.7	524	8.4	20.1	3.3
		09/06/2013	80	15.9	400	8.5	20.4	3.3
		09/06/2013	85	16.0	441	8.5	20.5	3.3
		09/06/2013	[a]90	16.0	495	8.5	20.6	3.3
		09/06/2013	95	16.1	290	8.5	20.8	3.3
		09/06/2013	100	16.1	390	8.5	20.9	3.3
		09/06/2013	105	16.2	524	8.6	20.9	3.3
		09/06/2013	110	16.2	535	8.6	20.9	3.4
		10/06/2013	130	16.4	265	8.6	21.1	3.4
		10/06/2013	170	16.6	378	8.7	21.4	3.4
		10/06/2013	250	16.8	456	8.8	21.7	3.5
		10/06/2013	500	17.0	536	8.9	22.1	3.8
		10/06/2013	1000	17.2	796	9.0	22.3	4.1
		10/06/2013	2000	17.2	148	9.1	22.3	4.2

Table S2. Inclusion list of the IPLs targeted by the high-resolution accurate mass/mass spectrometry method used in this study. (n.d.) IPL not detected; (n.c.) spectrum not confirmed.

Core lipid	Headgroup	rt	Spectrum
Glycerol dialkyl glycerol tetraether (GDGT)-0	MH	4.50	confirmed
	DH	19.15	confirmed
	HPH	32.45	confirmed
	PG	-	n.c.
	2PG	28.03	confirmed
	MH-PG	-	n.f.
	DH-PG	-	n.f.
	MH-2PG	-	n.f.
	DH-2PG	-	n.f.
	MeHPH	28.17	confirmed
Glycerol dialkyl glycerol tetraether (GDGT)-1	MH	4.65	confirmed
	DH	19.30	confirmed
	HPH	33.10	confirmed
	PG	-	n.c.
	2PG	28.41	confirmed
	MH-PG	-	n.f.
	DH-PG	-	n.f.
	MH-2PG	42.28	confirmed
	DH-2PG	-	n.f.
	MeHPH	-	n.f.
Glycerol dialkyl glycerol tetraether (GDGT)-2	MH	4.83	confirmed
	DH	19.50	confirmed
	HPH	33.60	confirmed
	PG	-	n.f.
	2PG	28.78	confirmed
	MH-PG	-	n.c.
	DH-PG	-	n.f.
	MH-2PG	42.99	confirmed
	DH-2PG	-	n.f.

Glycerol dialkyl glycerol tetraether (GDGT)-3	MH	5.10	confirmed
	DH	19.70	confirmed
	HPH	-	n.f.
	PG	-	n.c.
	2PG	-	n.c.
	MH-PG	-	n.c.
	DH-PG	-	n.f.
	MH-2PG	-	n.c.
	DH-2PG	-	n.f.
Glycerol dialkyl glycerol tetraether (GDGT)-4	MH	5.20	confirmed
	DH	20.10	confirmed
	HPH	-	n.f.
	PG	-	n.c.
	2PG	-	n.c.
	MH-PG	-	n.c.
	DH-PG	-	n.f.
	MH-2PG	-	n.f.
	DH-2PG	-	n.f.
Crenarchaeol	MH	5.55	confirmed
	DH	20.35	confirmed
	HPH	35.40	confirmed
Monohydroxy glycerol dialkyl glycerol tetraether (OH-GDGT)-0	MH	5.90	confirmed
	DH	20.42	confirmed
	HPH	36.15	confirmed
	PG	-	n.f.
	2PG	-	n.f.
Monohydroxy glycerol dialkyl glycerol tetraether (OH-GDGT)-1	MH	36.32	confirmed
	DH	20.56	confirmed
	HPH	-	n.f.
	PG	-	n.f.
	2PG	-	n.f.
	MH-PG	-	n.f.
	MH-2PG	-	n.f.

Monohydroxy glycerol dialkyl glycerol tetra-ether (OH-GDGT)-2	MH	6.60	confirmed
	DH	20.75	confirmed
	HPH	-	n.f.
	PG	-	n.f.
	2PG	-	n.f.
	MH-PG	-	n.f.
	MH-2PG	-	n.f.
Monohydroxy glycerol dialkyl glycerol tetra-ether (OH-GDGT)-3	MH	-	n.f.
	DH	21.16	confirmed
	HPH	-	n.f.
	PG	-	n.f.
	2PG	-	n.f.
	MH-PG	-	n.f.
Monohydroxy glycerol dialkyl glycerol tetra-ether (OH-GDGT)-4	MH	-	n.f.
	DH	21.50	confirmed
	HPH	-	n.f.
	PG	-	n.f.
	2PG	-	n.f.
	MH-PG	-	n.f.
Monohydroxy (OH)-crenarchaeol	MG	-	n.c.
	DH	-	n.c.
	HPH	-	n.c.
	PG	-	n.f.
	2PG	-	n.f.
	MH-PG	-	n.f.
Glycerol dialkyl glycerol diether (Archaeol)	MH	3.39	confirmed
	DH	14.91	confirmed
	PDH	23.14	confirmed
	MHgluA	26.14	confirmed
	PG	18.43	confirmed
	PE	19.41	confirmed
	PS	23.75	confirmed

Monohydroxy glycerol dialkyl glycerol diether (OH-archaeol)	MH	-	n.f.
	DH	-	n.c.
	PDH	-	n.f.
	PG	-	n.c.
	PE	-	n.f.
	PS	-	n.c.
Dihydroxy glycerol dialkyl glycerol tetraether (2OH-GDGT)-0	MH	-	n.c.
	DH	-	n.c.
	HPH	-	n.f.
	PG	-	n.f.
	2PG	-	n.f.
Dihydroxy glycerol dialkyl glycerol tetraether (2OH-GDGT)-1	MH	-	n.f.
	DH	-	n.c.
	HPH	-	n.f.
	PG	-	n.f.
	2PG	-	n.f.
	MH-PG	-	n.f.
	MH-2PG	-	n.f.
Dihydroxy glycerol dialkyl glycerol tetraether (2OH-GDGT)-2	MH	-	n.f.
	DH	-	n.f.
	HPH	-	n.f.
	PG	-	n.f.
	2PG	-	n.f.
	MH-PG	-	n.f.
	MH-2PG	-	n.f.
Dihydroxy glycerol dialkyl glycerol tetraether (2OH-GDGT)-3	MH	-	n.f.
	DH	-	n.f.
	HPH	-	n.f.
	PG	-	n.f.
	2PG	-	n.f.
	MH-PG	-	n.f.
ihydroxy glycerol dialkyl glycerol tetraether (2OH-GDGT)-4	MH	-	n.f.
	DH	-	n.c.
	HPH	-	n.f.
	PG	-	n.f.
	2PG	-	n.f.
	MH-PG	-	n.f.

Dihydroxy (2OH)-crenarchaeol	MH	-	n.f.
	DH	-	n.f.
	HPH	-	n.c.
	PG	-	n.f.
	2PG	-	n.c.
	MH-PG	-	n.f.
Butane-triol dibiphytanyl glycerol tetraether (BDGT)-0	MH	-	n.f.
	DH	-	n.f.
	HPH	-	n.f.
	PG	-	n.f.
	2PG	-	n.f.
Butane-triol dibiphytanyl glycerol tetraether (BDGT)-1, -2	MH	-	n.f.
	DH	-	n.f.
	HPH	-	n.f.
	PG	-	n.f.
	2PG	-	n.f.
	MH-PG	-	n.f.
	MH-2PG	-	n.f.
Glycerol dialkyl butanetriol tetraether (GDPT)-0, -1, -2, -3, -4	MH	-	n.f.
	DH	-	n.f.
	HPH	-	n.f.
	PG	-	n.f.
	2PG	-	n.f.
	MH-PG	-	n.f.
	MH-2PG	-	n.f.
Glycerol dialkanol diether (GDD)-0, -1, -2, -3, -	MH	-	n.f.
	DH	-	n.f.
	PG	-	n.f.

Table S3. Estimations of the archaeal 16S rRNA gene reads (copies L^{-1}) of specific archaeal groups detected in the Black Sea SPM at station PHOX2 obtained as described in the experimental procedures.

Depth (m)	MGI *Ca.* Nitrosopelagicus	MGI *Nitrosopumilus*	MGI uncultured OTU	MGII uncultured OTU-1	MGII uncultured OTU-2	MGIII	VC2.1Arc6	CCA47	ANME-1b	Thermoprotеales Thermofilum	MCG+C3	DPANN Woesearchaeota DHVE-6	Others
50	5.2E+07	1.4E+07	0.0E+00	7.1E+06	3.2E+05	0.0E+00	0.0E+00	0.0E+00	0.0E+00	0.0E+00	0.0E+00	0.0E+00	0.0E+00
70	7.9E+07	2.7E+07	1.1E+07	7.7E+05	4.7E+06	0.0E+00	0.0E+00	0.0E+00	0.0E+00	0.0E+00	0.0E+00	1.3E+05	6.4E+05
80	4.7E+07	2.6E+07	3.2E+07	2.3E+05	4.1E+06	0.0E+00	0.0E+00	0.0E+00	0.0E+00	0.0E+00	0.0E+00	1.4E+06	1.1E+06
85	1.7E+07	2.2E+07	1.0E+07	8.6E+04	4.6E+06	0.0E+00	0.0E+00	0.0E+00	0.0E+00	6.0E+05	0.0E+00	4.2E+06	7.7E+05
90	5.1E+06	7.2E+07	1.9E+06	1.6E+05	7.8E+06	0.0E+00	0.0E+00	0.0E+00	0.0E+00	2.5E+05	8.2E+04	5.2E+06	4.9E+05
95	3.5E+06	1.3E+08	3.9E+05	0.0E+00	9.0E+06	2.7E+06	0.0E+00	7.8E+05	0.0E+00	0.0E+00	2.0E+06	3.3E+07	0.0E+00
100	1.9E+06	1.2E+08	3.1E+05	0.0E+00	4.6E+05	1.7E+06	4.6E+05	3.1E+05	0.0E+00	0.0E+00	1.5E+06	2.0E+07	0.0E+00
105	5.1E+06	2.0E+08	1.0E+06	0.0E+00	0.0E+00	2.0E+06	3.1E+06	0.0E+00	0.0E+00	0.0E+00	4.1E+06	2.6E+07	0.0E+00
110	3.9E+05	5.4E+07	0.0E+00	0.0E+00	0.0E+00	0.0E+00	1.5E+06	0.0E+00	0.0E+00	0.0E+00	3.5E+06	1.5E+07	3.9E+05
130	0.0E+00	1.8E+07	0.0E+00	0.0E+00	0.0E+00	0.0E+00	3.0E+06	1.5E+06	0.0E+00	3.8E+06	9.0E+06	1.9E+07	0.0E+00
170	0.0E+00	6.4E+05	0.0E+00	0.0E+00	0.0E+00	2.1E+05	1.1E+05	1.1E+05	0.0E+00	0.0E+00	6.4E+05	2.7E+06	1.1E+05
250	2.2E+05	2.2E+06	6.6E+05	0.0E+00	0.0E+00	2.2E+05	2.6E+06	4.0E+06	0.0E+00	0.0E+00	1.5E+07	2.1E+07	3.3E+06
500	0.0E+00	5.2E+05	0.0E+00	0.0E+00	0.0E+00	1.7E+05	8.7E+04	5.2E+05	0.0E+00	0.0E+00	3.0E+06	1.4E+06	2.6E+05
1000	0.0E+00	5.5E+05	0.0E+00	0.0E+00	0.0E+00	0.0E+00	0.0E+00	3.7E+05	5.5E+05	0.0E+00	1.2E+07	7.9E+06	7.4E+05
2000	0.0E+00	0.0E+00	0.0E+00	0.0E+00	0.0E+00	0.0E+00	2.6E+06	9.2E+06	1.6E+07	1.1E+06	4.2E+07	4.1E+07	8.1E+06

Table S4. Absolute abundances of the archaeal IPLs (response units per Liter; r.u. L^{-1}) detected in the Black Sea SPM at station PHOX2.

Depth (m)	GDGT-0					GDGT-1					GDGT-2				
	MH	DH	HPH	MeHPH	2PG	MH	DH	HPH	2PG	MH-2PG	MH	DH	HPH	2PG	MH-2PG
50	2.1E+06	9.7E+06	6.2E+08	0.0E+00	7.3E+06	1.3E+05	1.7E+07	3.2E+07	0.0E+00	0.0E+00	0.0E+00	2.1E+07	9.9E+05	0.0E+00	0.0E+00
70	4.2E+06	2.2E+07	3.2E+08	0.0E+00	1.1E+07	5.2E+05	3.0E+07	2.9E+07	0.0E+00	0.0E+00	1.3E+05	4.6E+07	2.8E+06	0.0E+00	0.0E+00
80	1.0E+06	1.2E+07	1.4E+08	0.0E+00	5.1E+06	1.9E+05	1.7E+07	1.6E+07	0.0E+00	0.0E+00	4.4E+04	3.6E+07	1.1E+06	0.0E+00	0.0E+00
85	1.1E+06	4.9E+06	8.0E+07	0.0E+00	4.5E+05	2.1E+05	8.0E+06	1.0E+07	0.0E+00	0.0E+00	7.0E+04	1.6E+07	1.6E+06	0.0E+00	0.0E+00
90	3.3E+06	3.9E+06	2.6E+08	0.0E+00	4.6E+05	7.5E+05	7.5E+06	4.7E+07	0.0E+00	0.0E+00	2.1E+05	1.4E+07	1.2E+07	0.0E+00	0.0E+00
95	2.3E+06	1.9E+06	1.8E+08	0.0E+00	1.1E+06	4.9E+05	5.4E+06	2.7E+07	0.0E+00	0.0E+00	1.8E+05	7.8E+06	5.6E+06	0.0E+00	0.0E+00
100	4.8E+06	1.2E+06	2.5E+08	0.0E+00	2.0E+06	9.1E+05	3.8E+06	3.3E+07	3.5E+05	0.0E+00	2.8E+05	6.8E+06	6.3E+06	0.0E+00	0.0E+00
105	6.5E+06	1.6E+06	1.0E+08	0.0E+00	1.0E+06	1.0E+06	3.6E+06	1.0E+07	1.2E+05	0.0E+00	3.0E+05	5.6E+06	1.4E+06	0.0E+00	0.0E+00
110	4.3E+06	9.0E+05	7.2E+07	0.0E+00	2.5E+06	6.1E+05	1.9E+06	5.8E+06	5.6E+05	0.0E+00	1.6E+05	2.9E+06	5.8E+05	5.9E+04	0.0E+00
130	5.7E+06	5.9E+05	3.6E+07	0.0E+00	3.9E+06	6.3E+05	2.6E+06	1.7E+06	2.0E+06	0.0E+00	1.4E+05	4.1E+06	7.3E+04	5.2E+05	0.0E+00
170	1.1E+06	3.0E+05	5.9E+06	0.0E+00	7.2E+05	9.0E+04	6.3E+05	1.1E+05	3.8E+05	0.0E+00	1.3E+04	1.2E+06	0.0E+00	3.1E+04	0.0E+00
250	3.0E+05	4.1E+04	1.7E+06	5.0E+05	9.1E+05	2.0E+04	3.0E+05	0.0E+00	6.0E+05	0.0E+00	5.2E+03	4.9E+05	0.0E+00	2.6E+05	0.0E+00
500	1.4E+05	0.0E+00	5.7E+05	7.2E+05	2.3E+06	9.0E+03	4.9E+04	0.0E+00	2.7E+06	0.0E+00	0.0E+00	1.3E+05	0.0E+00	2.5E+06	0.0E+00
1000	4.9E+04	0.0E+00	2.5E+05	4.9E+05	3.6E+07	2.8E+03	0.0E+00	0.0E+00	4.5E+07	7.5E+05	0.0E+00	1.1E+04	0.0E+00	5.0E+07	4.0E+05
2000	4.5E+04	0.0E+00	7.5E+04	0.0E+00	1.8E+08	0.0E+00	0.0E+00	0.0E+00	2.3E+08	1.1E+06	0.0E+00	0.0E+00	0.0E+00	2.5E+08	3.7E+05

Depth (m)	GDGT-3		GDGT-4		Crenarchaeol			OH-GDGT-0			OH-GDGT-1		OH-GDGT-2	
	MH	DH	MH	DH	MH	DH	HPH	MH	DH	HPH	MH	DH	MH	DH
50	0.0E+0	4.3E+06	0.0E+00	2.6E+06	1.1E+06	5.3E+06	3.6E+08	2.3E+05	2.2E+07	4.1E+06	0.0E+00	8.9E+06	0.0E+00	3.7E+06
70	0.0E+0	6.0E+06	6.0E+03	4.5E+06	4.8E+06	1.4E+07	1.7E+08	1.7E+05	7.3E+06	0.0E+00	1.3E+03	5.6E+06	0.0E+00	3.9E+06
80	0.0E+0	3.3E+06	0.0E+00	3.9E+06	1.4E+06	1.3E+07	5.7E+07	1.6E+04	1.4E+06	0.0E+00	0.0E+00	1.6E+06	0.0E+00	1.9E+06
85	0.0E+0	2.7E+06	0.0E+00	2.1E+06	1.3E+06	4.8E+06	4.0E+07	4.4E+04	1.4E+06	0.0E+00	1.6E+03	6.5E+06	2.0E+03	7.6E+06
90	0.0E+0	5.8E+06	0.0E+00	3.6E+06	3.3E+06	1.7E+06	1.7E+08	3.0E+05	4.4E+06	2.3E+06	5.7E+04	2.4E+07	2.0E+04	2.4E+07
95	1.5E+04	4.1E+06	0.0E+00	3.4E+06	2.3E+06	6.7E+05	6.3E+07	2.9E+05	7.6E+06	2.7E+06	4.9E+04	2.1E+07	2.5E+04	1.8E+07
100	1.8E+04	4.3E+06	5.8E+03	4.1E+06	4.4E+06	6.5E+05	7.8E+07	9.2E+05	1.3E+07	8.0E+06	7.0E+04	3.0E+07	2.3E+04	2.3E+07
105	1.9E+04	2.9E+06	4.9E+03	3.5E+06	6.8E+06	4.8E+05	3.6E+07	1.8E+06	1.6E+07	3.2E+06	7.9E+04	2.5E+07	1.7E+04	1.7E+07
110	1.1E+04	1.2E+06	3.6E+03	1.5E+06	4.6E+06	1.6E+05	2.1E+07	1.3E+06	8.6E+06	4.2E+06	4.9E+04	1.2E+07	8.2E+03	8.2E+06
130	4.4E+03	1.3E+06	4.2E+03	1.7E+06	7.4E+06	1.5E+05	1.3E+07	1.9E+06	1.2E+07	1.8E+06	5.6E+04	1.3E+07	6.6E+03	9.2E+06
170	0.0E+00	1.5E+05	0.0E+00	3.3E+05	1.7E+06	0.0E+00	1.4E+06	4.1E+05	3.0E+06	1.9E+05	1.0E+04	3.7E+06	0.0E+00	1.9E+06
250	0.0E+00	1.9E+04	0.0E+00	0.0E+00	5.4E+05	0.0E+00	4.3E+05	4.9E+04	6.9E+05	0.0E+00	1.2E+03	9.6E+05	0.0E+00	6.4E+05
500	0.0E+00	0.0E+00	0.0E+00	0.0E+00	2.6E+05	0.0E+00	1.2E+05	1.2E+04	8.0E+04	0.0E+00	0.0E+00	2.2E+05	0.0E+00	0.0E+00
1000	0.0E+00	0.0E+00	5.1E+02	0.0E+00	6.1E+04	0.0E+00	0.0E+00	1.5E+03	3.1E+04	0.0E+00	0.0E+00	0.0E+00	0.0E+00	0.0E+00
2000	0.0E+00	0.0E+00	0.0E+00	0.0E+00	1.6E+05	0.0E+00	0.0E+00	0.0E+00	0.0E+00	0.0E+00	0.0E+00	0.0E+00	0.0E+00	0.0E+00

Depth (m)	OH-GDGT-3	OH-GDGT-4	Archaeol						
	DH	DH	MH	DH	PDH	MHgluA	PG	PE	PS
50	0.0E+00	0.0E+00	0.0E+00	0.0E+00	0.0E+00	0.0E+00	0.0E+00	0.0E+00	0.0E+00
70	0.0E+00	0.0E+00	0.0E+00	0.0E+00	0.0E+00	0.0E+00	6.3E+05	0.0E+00	0.0E+00
80	0.0E+00	0.0E+00	0.0E+00	0.0E+00	0.0E+00	0.0E+00	1.8E+05	0.0E+00	0.0E+00
85	1.5E+05	0.0E+00	0.0E+00	0.0E+00	0.0E+00	0.0E+00	7.8E+04	0.0E+00	0.0E+00
90	1.7E+06	0.0E+00	0.0E+00	0.0E+00	0.0E+00	5.9E+06	2.2E+05	0.0E+00	0.0E+00
95	1.9E+06	1.0E+06	1.4E+04	3.1E+05	0.0E+00	0.0E+00	5.2E+05	2.1E+05	0.0E+00
100	2.1E+06	1.3E+06	7.4E+04	7.4E+05	2.2E+05	1.6E+05	1.3E+06	4.3E+04	0.0E+00
105	8.4E+05	5.4E+05	2.9E+05	1.4E+06	4.8E+05	6.6E+05	1.6E+06	1.9E+05	0.0E+00
110	4.3E+05	1.9E+05	1.8E+05	9.3E+05	3.1E+05	8.6E+05	1.1E+06	3.7E+04	0.0E+00
130	8.5E+04	0.0E+00	5.4E+05	3.8E+06	1.9E+06	5.6E+06	3.2E+06	2.6E+05	0.0E+00
170	0.0E+00	0.0E+00	3.2E+05	2.4E+06	9.1E+05	7.1E+06	1.8E+06	2.1E+05	0.0E+00
250	0.0E+00	0.0E+00	1.6E+05	1.5E+06	5.6E+05	1.3E+07	1.1E+06	1.1E+05	0.0E+00
500	0.0E+00	0.0E+00	1.5E+05	1.5E+06	1.0E+06	1.6E+07	1.9E+06	1.2E+06	0.0E+00
1000	0.0E+00	0.0E+00	1.3E+05	1.3E+06	9.2E+05	1.3E+07	2.1E+07	2.0E+07	1.1E+06
2000	0.0E+00	0.0E+00	1.5E+05	2.6E+06	2.8E+06	9.3E+06	1.4E+08	1.2E+08	5.2E+06

Table S5. Values of the Pearson correlation coefficients (r values) obtained from the correlation matrix created using the total archaeal 16S rRNA gene reads (copies L^{-1}) of the archaeal groups and the absolute abundances of the archaeal IPLs (response units per Liter; r.u. L^{-1}) detected at station PHOX2 in the Black Sea.

	GDGT-0					GDGT-1					GDGT-2					GDGT-3		GDGT-4	
	MH	DH	HPH	MeHPH	2PG	MH	DH	HPH	2PG	MH-2PG	MH	DH	HPH	2PG	MH-2PG	MH	DH	MH	DH
MGI *Ca.* Nitrosopelagicus	0.08	0.98	0.67	-0.29	-0.13	-0.04	0.98	0.44	-0.19	-0.23	-0.12	0.94	-0.01	-0.19	-0.23	-0.30	0.60	0.19	0.56
MGI *Nitrosopumilus*	0.67	-0.09	0.17	-0.38	-0.27	0.82	-0.03	0.42	-0.26	-0.30	0.89	-0.04	0.47	-0.26	-0.31	0.90	0.47	0.46	0.61
MGI uncultured OTU	-0.13	0.61	0.08	-0.21	-0.12	-0.11	0.59	0.14	-0.15	-0.18	-0.11	0.74	-0.04	-0.15	-0.18	-0.26	0.30	-0.07	0.44
MGII uncultured OTU-1	-0.03	0.36	0.83	-0.16	-0.07	-0.18	0.43	0.36	-0.10	-0.12	-0.26	0.30	-0.07	-0.10	-0.12	-0.20	0.30	-0.15	0.15
MGII uncultured OTU-2	0.02	0.38	0.28	-0.33	-0.21	0.22	0.43	0.65	-0.22	-0.26	0.28	0.48	0.71	-0.22	-0.27	0.02	0.68	-0.20	0.59
MGIII	0.38	-0.22	0.07	-0.19	-0.19	0.53	-0.16	0.27	-0.18	-0.21	0.65	-0.18	0.32	-0.18	-0.21	0.85	0.27	0.26	0.40
VC2.1Arc6	0.35	-0.40	-0.40	-0.03	0.32	0.22	-0.42	-0.47	0.33	0.20	0.19	-0.44	-0.35	0.32	0.11	0.28	-0.41	0.31	-0.27
CCA47	-0.37	-0.29	-0.34	0.08	0.88	-0.37	-0.33	-0.38	0.89	0.74	-0.34	-0.34	-0.25	0.89	0.58	-0.20	-0.45	-0.23	-0.49
ANME-1b	-0.32	-0.18	-0.23	-0.12	0.99	-0.30	-0.22	-0.26	0.99	0.84	-0.28	-0.22	-0.18	0.99	0.68	-0.18	-0.32	-0.19	-0.35
Thermoproteales Thermofilum	0.29	-0.19	-0.23	-0.20	0.18	0.12	-0.18	-0.26	0.19	0.11	0.03	-0.17	-0.17	0.18	0.06	-0.09	-0.19	0.19	-0.14
MCG+C3	-0.34	-0.36	-0.42	0.14	0.92	-0.37	-0.41	-0.48	0.93	0.87	-0.34	-0.42	-0.33	0.93	0.75	-0.18	-0.54	-0.19	-0.56
Woesearchaeota DHVE-6	0.16	-0.49	-0.32	-0.17	0.54	0.22	-0.48	-0.19	0.57	0.45	0.31	-0.50	0.00	0.56	0.33	0.54	-0.22	0.12	-0.13

	Crenarchaeol			OH-GDGT-0			OH-GDGT-1		OH-GDGT-2		OH-GDGT-3	OH-GDGT-4	Archaeol						
	MH	DH	HPH	MH	DH	HPH	MH	DH	MH	DH	DH	DH	MH	DH	PDH	MHgluA	PG	PE	PS
MGI *Ca.* Nitrosopelagicus	0.04	0.93	0.66	-0.28	0.25	-0.13	-0.39	-0.19	-0.33	-0.22	-0.28	-0.24	-0.49	-0.56	-0.45	-0.46	-0.19	-0.19	-0.19
MGI *Nitrosopumilus*	0.58	-0.15	0.05	0.54	0.52	0.62	0.83	0.86	0.85	0.80	0.76	0.76	-0.03	-0.22	-0.36	-0.55	-0.24	-0.25	-0.25
MGI uncultured OTU	-0.09	0.84	0.05	-0.29	-0.25	-0.32	-0.32	-0.26	-0.26	-0.19	-0.22	-0.21	-0.39	-0.44	-0.35	-0.35	-0.15	-0.15	-0.15
MGII uncultured OTU-1	-0.16	0.25	0.87	-0.14	0.62	0.25	-0.25	-0.05	-0.22	-0.15	-0.19	-0.16	-0.28	-0.31	-0.25	-0.25	-0.11	-0.10	-0.10
MGII uncultured OTU-2	0.00	0.38	0.26	-0.31	-0.13	-0.07	0.11	0.31	0.46	0.47	0.51	0.19	-0.58	-0.61	-0.52	-0.53	-0.22	-0.21	-0.22
MGIII	0.30	-0.26	-0.08	0.31	0.37	0.51	0.62	0.69	0.78	0.62	0.73	0.89	-0.03	-0.11	-0.24	-0.30	-0.16	-0.17	-0.17
VC2.1Arc6	0.42	-0.41	-0.39	0.61	0.15	0.04	0.35	0.08	0.02	-0.02	-0.15	-0.03	0.68	0.68	0.58	0.21	0.35	0.33	0.32
CCA47	-0.32	-0.28	-0.30	-0.21	-0.34	-0.28	-0.25	-0.34	-0.23	-0.32	-0.22	-0.15	0.14	0.50	0.77	0.43	0.90	0.89	0.88
ANME-1b	-0.30	-0.17	-0.19	-0.21	-0.28	-0.22	-0.23	-0.28	-0.20	-0.27	-0.18	-0.14	0.03	0.38	0.75	0.25	0.99	0.99	0.99
Thermoproteales Thermofilum	0.43	-0.18	-0.20	0.48	0.09	-0.09	0.20	0.01	-0.06	0.00	-0.18	-0.20	0.67	0.69	0.60	0.08	0.20	0.19	0.18
MCG+C3	-0.30	-0.35	-0.37	-0.14	-0.34	-0.28	-0.23	-0.37	-0.27	-0.36	-0.27	-0.19	0.22	0.56	0.84	0.51	0.93	0.93	0.93
Woesearchaeota DHVE-6	0.16	-0.51	-0.39	0.30	0.05	0.22	0.41	0.29	0.43	0.26	0.35	0.48	0.27	0.43	0.50	0.07	0.58	0.57	0.56

Table S6. Values of the Pearson correlation coefficients (r values) of the correlation matrix created using as variables the total archaeal 16S rRNA gene reads (copies L^{-1}) of the archaeal groups detected at station PHOX2 in the Black Sea.

	MGI *Ca.* Nitrosopelagicus	MGI *Nitrosopumilus*	MGI uncultured OTU	MGII uncultured OTU-1	MGII uncultured OTU-2	MGIII	VC2.1Arc6	CCA47	ANME-1b	Thermoproteales Thermofilum	MCG+C3	Woesearchaeota DHVE-6
MGI *Ca.* Nitrosopelagicus	1.00											
MGI *Nitrosopumilus*	-0.15	1.00										
MGI uncultured OTU	0.59	-0.12	1.00									
MGII uncultured OTU-1	0.52	-0.16	-0.07	1.00								
MGII uncultured OTU-2	0.27	0.28	0.35	-0.11	1.00							
MGIII	-0.25	0.86	-0.22	-0.17	0.27	1.00						
VC2.1Arc6	-0.39	0.18	-0.31	-0.23	-0.50	0.08	1.00					
CCA47	-0.27	-0.29	-0.21	-0.15	-0.25	-0.14	0.55	1.00				
ANME-1b	-0.16	-0.22	-0.13	-0.09	-0.19	-0.15	0.36	0.91	1.00			
Thermoproteales Thermofilum	-0.20	-0.20	-0.13	-0.12	-0.16	-0.22	0.52	0.28	0.20	1.00		
MCG+C3	-0.34	-0.28	-0.26	-0.19	-0.36	-0.17	0.56	0.96	0.91	0.30	1.00	
Woesearchaeota DHVE-6	-0.51	0.42	-0.38	-0.33	-0.07	0.54	0.66	0.67	0.59	0.25	0.67	1.00

Table S7. Values of the Pearson correlation coefficients (r values) obtained from the correlation matrix created using the absolute abundances of the archaeal IPLs (response units per Liter; r.u. L^{-1}) detected at station PHOX2 in the Black Sea.

		GDGT-0					GDGT-1				
		MH	DH	HPH	MeHPH	2PG	MH	DH	HPH	2PG	MH-2PG
GDGT-0	MH	1.00									
	DH	0.15	1.00								
	HPH	0.28	0.61	1.00							
	MeHPH	-0.53	-0.32	-0.41	1.00						
	2PG	-0.35	-0.15	-0.23	-0.06	1.00					
GDGT-1	MH	0.93	0.06	0.24	-0.52	-0.35	1.00				
	DH	0.19	0.99	0.69	-0.38	-0.19	0.11	1.00			
	HPH	0.36	0.49	0.80	-0.46	-0.28	0.52	0.57	1.00		
	2PG	-0.36	-0.21	-0.27	-0.04	1.00	-0.35	-0.26	-0.31	1.00	
	MH-2PG	-0.44	-0.25	-0.32	0.13	0.91	-0.42	-0.30	-0.36	0.92	1.00
GDGT-2	MH	0.86	-0.01	0.18	-0.48	-0.32	0.98	0.04	0.51	-0.32	-0.38
	DH	0.15	0.97	0.59	-0.39	-0.21	0.11	0.98	0.54	-0.26	-0.31
	HPH	0.31	0.11	0.39	-0.32	-0.22	0.57	0.17	0.85	-0.21	-0.25
	2PG	-0.37	-0.21	-0.27	-0.04	1.00	-0.35	-0.25	-0.31	1.00	0.92
	MH-2PG	-0.45	-0.26	-0.33	0.24	0.78	-0.43	-0.31	-0.37	0.79	0.97
GDGT-3	MH	0.67	-0.27	0.04	-0.31	-0.22	0.76	-0.22	0.20	-0.21	-0.24
	DH	0.49	0.67	0.77	-0.56	-0.34	0.59	0.74	0.94	-0.37	-0.44
GDGT-4	MH	0.84	0.26	0.14	-0.32	-0.19	0.74	0.25	0.17	-0.21	-0.24
	DH	0.62	0.63	0.63	-0.62	-0.38	0.71	0.69	0.81	-0.41	-0.49
Crenarchaeol	MH	0.97	0.12	0.12	-0.50	-0.33	0.87	0.15	0.22	-0.35	-0.42
	DH	0.02	0.94	0.46	-0.30	-0.14	-0.04	0.93	0.37	-0.20	-0.23
	HPH	0.18	0.59	0.98	-0.34	-0.19	0.13	0.67	0.75	-0.23	-0.27
OH-GDGT-0	MH	0.87	-0.25	-0.07	-0.36	-0.25	0.74	-0.22	-0.07	-0.24	-0.30
	DH	0.71	0.18	0.70	-0.47	-0.30	0.59	0.27	0.45	-0.32	-0.38
	HPH	0.62	-0.14	0.47	-0.38	-0.25	0.69	-0.06	0.51	-0.25	-0.30
OH-GDGT-1	MH	0.83	-0.31	0.05	-0.41	-0.29	0.92	-0.25	0.34	-0.27	-0.32
	DH	0.76	-0.12	0.34	-0.48	-0.34	0.91	-0.03	0.64	-0.33	-0.39
OH-GDGT-2	MH	0.57	-0.24	0.18	-0.36	-0.26	0.79	-0.16	0.58	-0.24	-0.28
	DH	0.66	-0.12	0.28	-0.46	-0.32	0.86	0.04	0.69	-0.31	-0.37
OH-GDGT-3	DH	0.43	-0.19	0.24	-0.31	-0.23	0.69	-0.11	0.66	-0.21	-0.25
OH-GDGT-4	DH	0.42	-0.20	0.15	-0.25	-0.17	0.59	-0.14	0.38	-0.16	-0.19
Archaeol	MH	0.34	-0.50	-0.51	0.04	0.01	0.14	-0.52	-0.61	0.03	0.01
	DH	0.06	-0.57	-0.61	0.15	0.36	-0.11	-0.61	-0.69	0.39	0.34
	PDH	-0.19	-0.47	-0.54	0.16	0.75	-0.31	-0.52	-0.63	0.77	0.70
	MHgluA	-0.59	-0.50	-0.62	0.85	0.30	-0.65	-0.57	-0.71	0.33	0.44
	PG	-0.34	-0.21	-0.27	-0.07	1.00	-0.33	-0.25	-0.30	1.00	0.89
	PE	-0.36	-0.21	-0.26	-0.05	1.00	-0.34	-0.25	-0.30	1.00	0.91
	PS	-0.37	-0.21	-0.27	-0.04	1.00	-0.35	-0.25	-0.30	1.00	0.92

		GDGT-32					GDGT-3		GDGT-4		Crenarchaeol		
		MH	DH	HPH	2PG	MH-2PG	MH	DH	MH	DH	MH	DH	HPH
GDGT-0	MH												
	DH												
	HPH												
	MeHPH												
	2PG												
GDGT-1	MH												
	DH												
	HPH												
	2PG												
	MH-2PG												
GDGT-2	MH	1.00											
	DH	0.05	1.00										
	HPH	0.60	0.20	1.00									
	2PG	-0.32	-0.26	-0.21	1.00								
	MH-2PG	-0.39	-0.32	-0.26	0.79	1.00							
GDGT-3	MH	0.82	-0.24	0.24	-0.21	-0.25	1.00						
	DH	0.57	0.72	0.73	-0.37	-0.45	0.23	1.00					
GDGT-4	MH	0.68	0.20	0.07	-0.22	-0.23	0.57	0.33	1.00				
	DH	0.69	0.71	0.61	-0.41	-0.50	0.42	0.94	0.49	1.00			
Crenarchaeol	MH	0.79	0.13	0.21	-0.35	-0.43	0.59	0.38	0.83	0.54	1.00		
	DH	-0.09	0.98	0.03	-0.20	-0.24	-0.32	0.56	0.13	0.59	0.02	1.00	
	HPH	0.06	0.56	0.36	-0.23	-0.28	-0.12	0.71	0.02	0.52	0.04	0.44	1.00
OH-GDGT-0	MH	0.67	-0.25	-0.03	-0.25	-0.30	0.65	0.03	0.68	0.22	0.89	-0.32	-0.14
	DH	0.51	0.15	0.14	-0.32	-0.39	0.54	0.48	0.51	0.51	0.59	0.02	0.63
	HPH	0.68	-0.12	0.42	-0.25	-0.30	0.75	0.42	0.51	0.47	0.47	-0.24	0.34
OH-GDGT-1	MH	0.93	-0.25	0.51	-0.27	-0.33	0.83	0.33	0.57	0.46	0.78	-0.38	-0.05
	DH	0.93	-0.05	0.71	-0.33	-0.40	0.79	0.60	0.50	0.65	0.65	-0.22	0.23
OH-GDGT-2	MH	0.86	-0.15	0.75	-0.24	-0.29	0.79	0.51	0.32	0.55	0.48	-0.31	0.06
	DH	0.90	-0.03	0.83	-0.31	-0.38	0.68	0.63	0.38	0.65	0.56	-0.20	0.19
OH-GDGT-3	DH	0.77	-0.11	0.83	-0.21	-0.25	0.69	0.55	0.23	0.55	0.32	-0.25	0.12
OH-GDGT-4	DH	0.68	-0.16	0.41	-0.16	-0.20	0.87	0.34	0.41	0.45	0.31	-0.24	-0.03
Archaeol	MH	0.07	-0.54	-0.44	0.03	0.01	0.15	-0.56	0.28	-0.41	0.48	-0.51	-0.49
	DH	-0.16	-0.63	-0.48	0.38	0.29	-0.02	-0.70	0.10	-0.61	0.20	-0.57	-0.57
	PDH	-0.32	-0.53	-0.45	0.77	0.61	-0.20	-0.67	-0.07	-0.64	-0.08	-0.45	-0.48
	MHgluA	-0.62	-0.59	-0.50	0.33	0.48	-0.41	-0.82	-0.36	-0.88	-0.51	-0.47	-0.53
	PG	-0.30	-0.26	-0.21	1.00	0.75	-0.19	-0.36	-0.20	-0.40	-0.32	-0.20	-0.23
	PE	-0.31	-0.25	-0.21	1.00	0.77	-0.20	-0.36	-0.21	-0.40	-0.34	-0.19	-0.22
	PS	-0.32	-0.26	-0.21	1.00	0.79	-0.20	-0.37	-0.22	-0.41	-0.35	-0.19	-0.22

		OH-GDGT-0			OH-GDGT-1		OH-GDGT-2		OH-GDGT-3	OH-GDGT-4
		MH	DH	HPH	MH	DH	MH	DH	DH	DH
GDGT-0	MH									
	DH									
	HPH									
	MeHPH									
	2PG									
GDGT-1	MH									
	DH									
	HPH									
	2PG									
	MH-2PG									
GDGT-2	MH									
	DH									
	HPH									
	2PG									
	MH-2PG									
GSGT-3	MH									
	DH									
GDGT-4	MH									
	DH									
Creanrchaeol	MH									
	DH									
	HPH									
OH-GDGT-0	MH	1.00								
	DH	0.60	1.00							
	HPH	0.52	0.74	1.00						
OH-GDGT-1	MH	0.80	0.53	0.72	1.00					
	DH	0.58	0.61	0.81	0.92	1.00				
OH-GDGT-2	MH	0.42	0.39	0.69	0.87	0.94	1.00			
	DH	0.45	0.44	0.70	0.87	0.97	0.95	1.00		
OH-GDGT-3	DH	0.22	0.30	0.69	0.75	0.89	0.97	0.93	1.00	
OH-GDGT-4	DH	0.30	0.40	0.75	0.65	0.75	0.82	0.69	0.83	1.00
Archaeol	MH	0.70	0.12	-0.04	0.33	0.00	-0.08	-0.10	-0.25	-0.12
	DH	0.44	-0.11	-0.18	0.11	-0.19	-0.20	-0.26	-0.31	-0.17
	PDH	0.12	-0.27	-0.30	-0.12	-0.35	-0.31	-0.38	-0.37	-0.26
	MHgluA	-0.29	-0.56	-0.51	-0.45	-0.62	-0.50	-0.61	-0.47	-0.37
	PG	-0.22	-0.30	-0.24	-0.25	-0.31	-0.23	-0.29	-0.20	-0.15
	PE	-0.24	-0.31	-0.24	-0.26	-0.32	-0.23	-0.30	-0.20	-0.16
	PS	-0.25	-0.32	-0.25	-0.27	-0.33	-0.24	-0.31	-0.21	-0.16

		Archaeol						
		MH	DH	PDH	MHgluA	PG	PE	PS
GDGT-0	MH							
	DH							
	HPH							
	MeHPH							
	2PG							
GDGT-1	MH							
	DH							
	HPH							
	2PG							
	MH-2PG							
GDGT-2	MH							
	DH							
	HPH							
	2PG							
	MH-2PG							
GDGT-3	MH							
	DH							
GDGT-4	MH							
	DH							
Creanrchaeol	MH							
	DH							
	HPH							
OH-GDGT-0	MH							
	DH							
	HPH							
OH-GDGT-1	MH							
	DH							
OH-GDGT-2	MH							
	DH							
OH-GDGT-3	DH							
OH-GDGT-4	DH							
Archaeol	MH	1.00						
	DH	0.91	1.00					
	PDH	0.61	0.87	1.00				
	MHgluA	0.35	0.56	0.60	1.00			
	PG	0.05	0.40	0.77	0.31	1.00		
	PE	0.03	0.38	0.76	0.31	1.00	1.00	
	PS	0.02	0.38	0.76	0.32	1.00	1.00	1.00

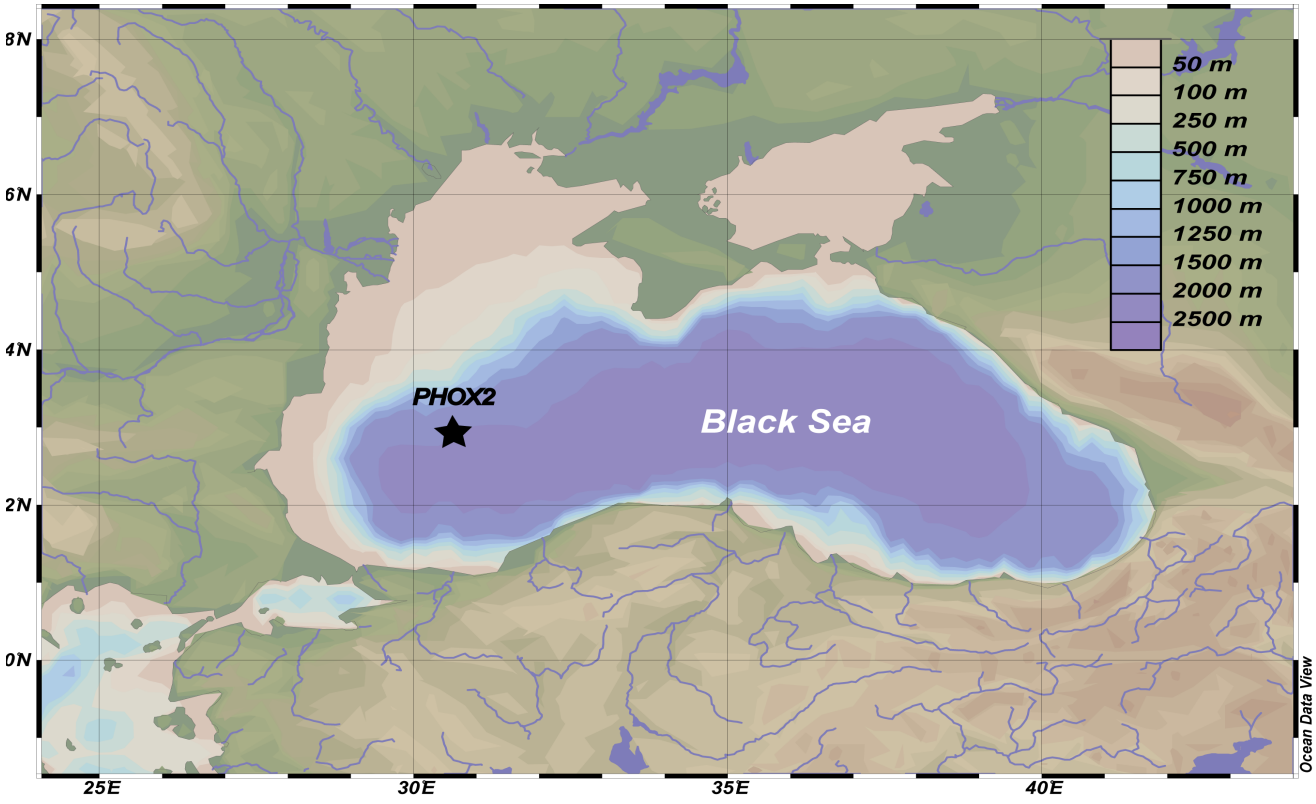

Figure S1. Map of the sampling area in the Black Sea, during the Phoxy cruise (June-July 2013). Station PHOX2, located at 42.9N and 30.7E in the western gyre, was sampled at high depth resolution for suspended particulate matter (SPM) by employing three in situ pump system devices.

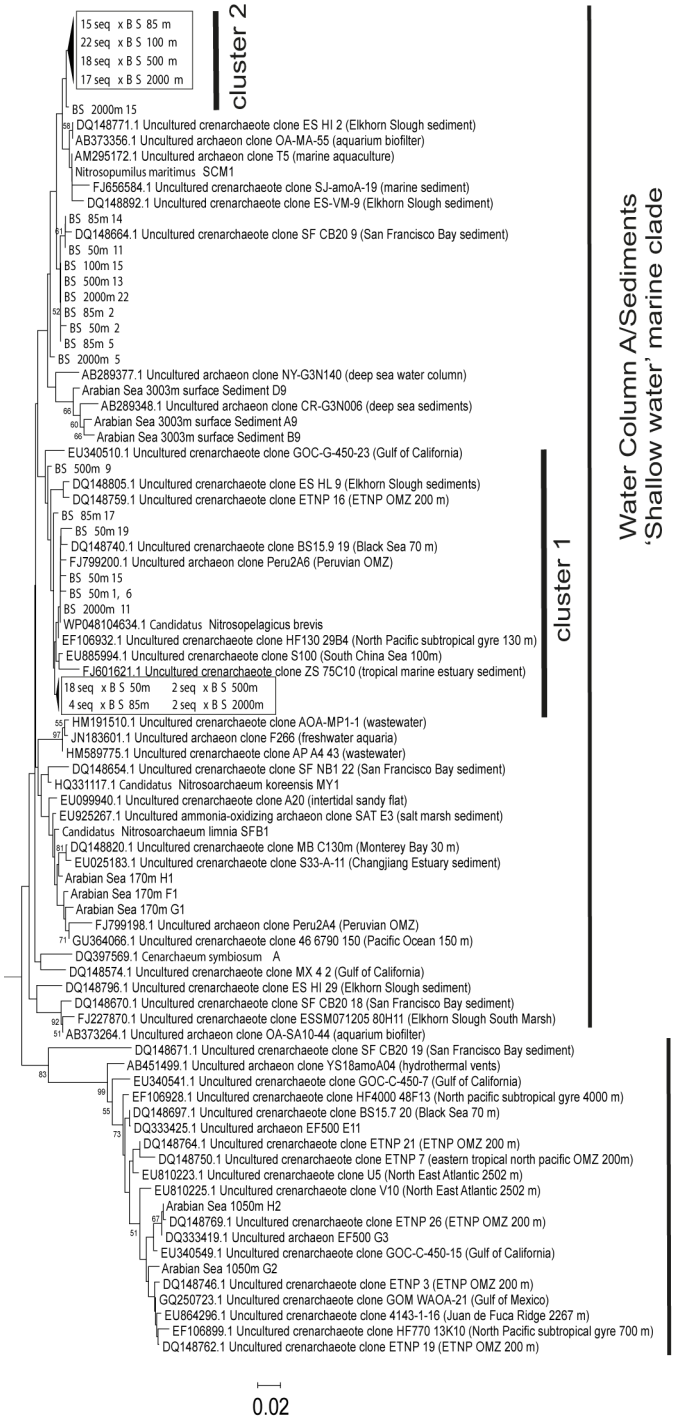

Figure S2. Neighbor-joining tree of *amo*A protein sequences recovered from the Black Sea SPM at 50 m, 85, 100, 500, and 2000 m, constructed with the Neighbor-Joining method (Saitou & Nei, 1987). Scale bar indicates 2% sequence dissimilarity. Clusters of Water column A/Sediments ('shallow water' marine clade) and B ('deep water" marine clade) of the *amo*A gene were defined by Francis et al. (2005). The evolutionary distances were computed using the Poisson correction method with a bootstrap test of 1,000 replicates (values higher than 50% are shown on the branches). The analysis involved 188 amino acid sequences and a total of 211 positions.

(a)

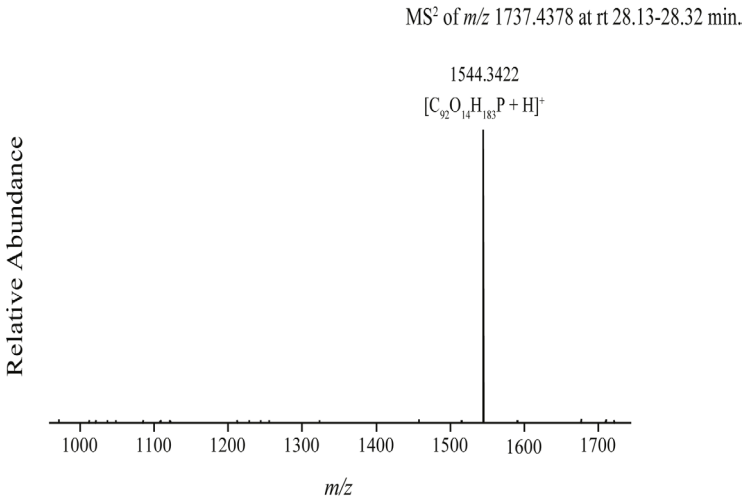

(b)

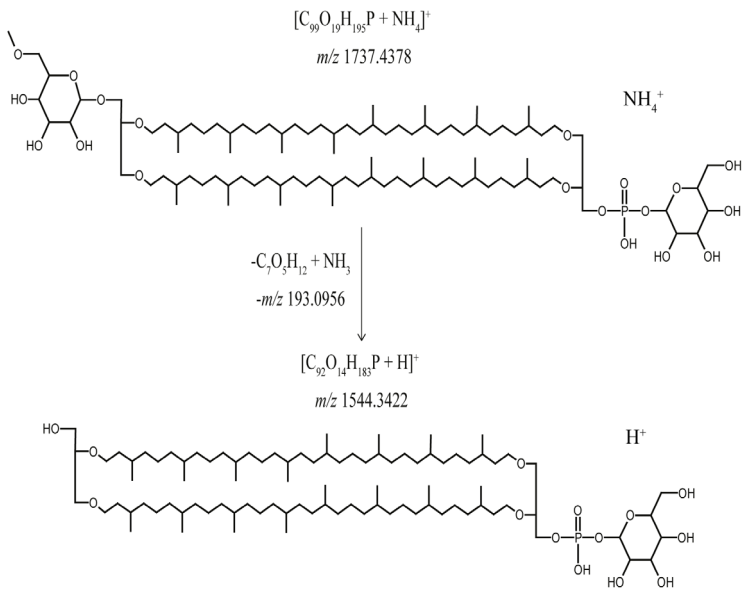

(c)

Compound	Elemental composition	Exact mass (*m/z*)[a]	Accuracy (ppm)[b]
Methoxyhexose phosphohexose-GDGT-0	$C_{99}O_{19}H_{195}P$ $[M + NH_4]^+$	1737.4368	0.6
Loss of methoxyhexose + NH_3	$C_7O_5H_{12}$	193.0950	3.0
Phosphohexose-GDGT-0	$C_{92}O_{14}H_{183}P$ $[M + H]^+$	**1544.3418**	0.2

[a] Diagnostic ions in bold indicate the major base peak observed in MS^2 spectra.

[b] The 3 ppm (parts per million) range was used as a measure of high-confidence molecular formula assignement.

Figure S3. Identification of the IPL methoxyhexose phosphohexose-GDGT-0 (i.e. MeHPH-GDGT-0) detected in the Black Sea SPM (1000 m) by LC/orbitrap-MS. (a) MS^2 fragmentation (stepped normalized collision energies 15, 22.5, 30) of *m/z* 1737.4378. (b) Proposed fragmentation pathway of the MeHPH-GDGT-0. (c) Table of the accurate masses and accuracy for MeHPH-GDGT-0 and diagnostic losses and fragments.

(a)

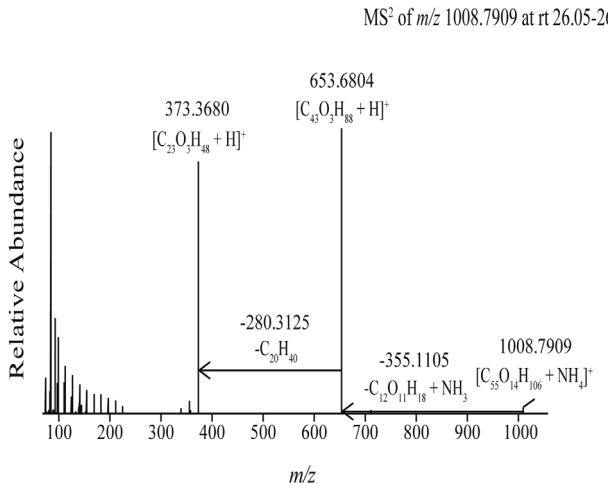

(b)

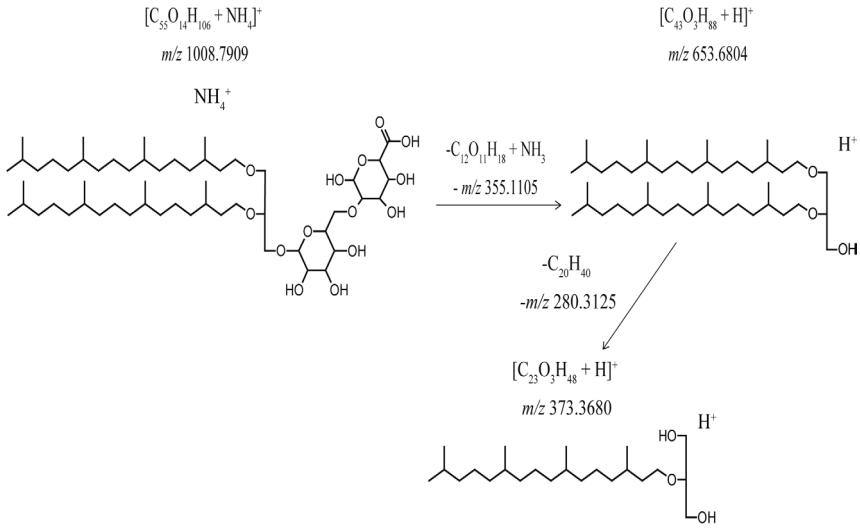

(c)

Compound	Elemental composition	Exact mass (*m/z*)[a]	Accuracy (ppm)[b]
HexoseGluA-archaeol	$C_{55}O_{14}H_{106}$ $[M + NH_4]^+$	1008.7921	-1.2
Loss of hexoseGluA + NH_3	$C_{12}O_{11}H_{18}$	355.1109	-1.2
Loss of phytanyl - 1 H	$C_{20}H_{40}$	280.3125	0.2
Archaeol	$C_{43}O_3H_{88}$ $[M + H]^+$	**653.6806**	-0.3
Phytanyl glycerol	$C_{23}O_3H_{48}$ $[M + H]^+$	**373.3676**	0.9

[a] Diagnostic ions in bold indicate the major base peak observed in MS^2 spectra.

[b] The 3 ppm (parts per million) range was used as a measure of high-confidence molecular formula assignement.

Figure S4. Identification of the IPL monohexose glucuronic acid-archaeol (i.e. MHgluA-archaeol) detected in the Black Sea SPM (1000 m) by LC/orbitrap-MS. (a) MS^2 fragmentation (stepped normalized collision energies 15, 22.5, 30) of *m/z* 1008.7909. (b) Proposed fragmentation pathway of the HgluA-archaeol. (c) Table of the accurate masses and accuracy for HgluA-archaeol and diagnostic losses and fragments.

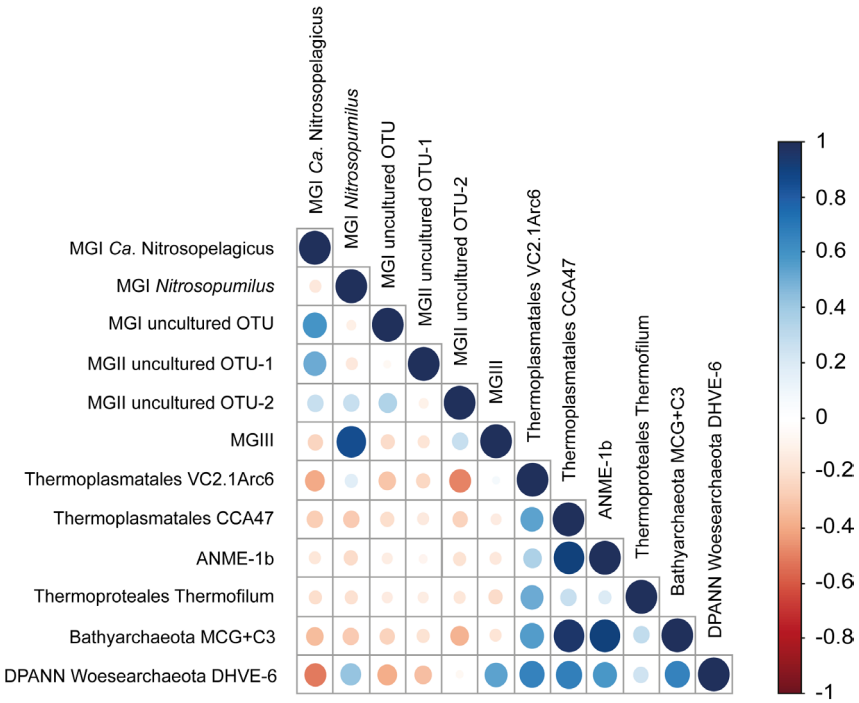

Figure S5. Dot plot of the correlation matrix obtained by applying a Pearson analysis to the total archaeal 16S rRNA gene reads (copies L^{-1}) of the archaeal groups detected across the Black Sea water column at station PHOX2. The size of the dot and the intensity of its color relate to the degree of correlation. Dark blue corresponds to r values of +1, indicating a strong positive linear correlation between archaeal groups; white corresponds to r values of 0, indicating that no correlation exists; dark red corresponds to r values of -1, indicating a strong negative linear correlation.

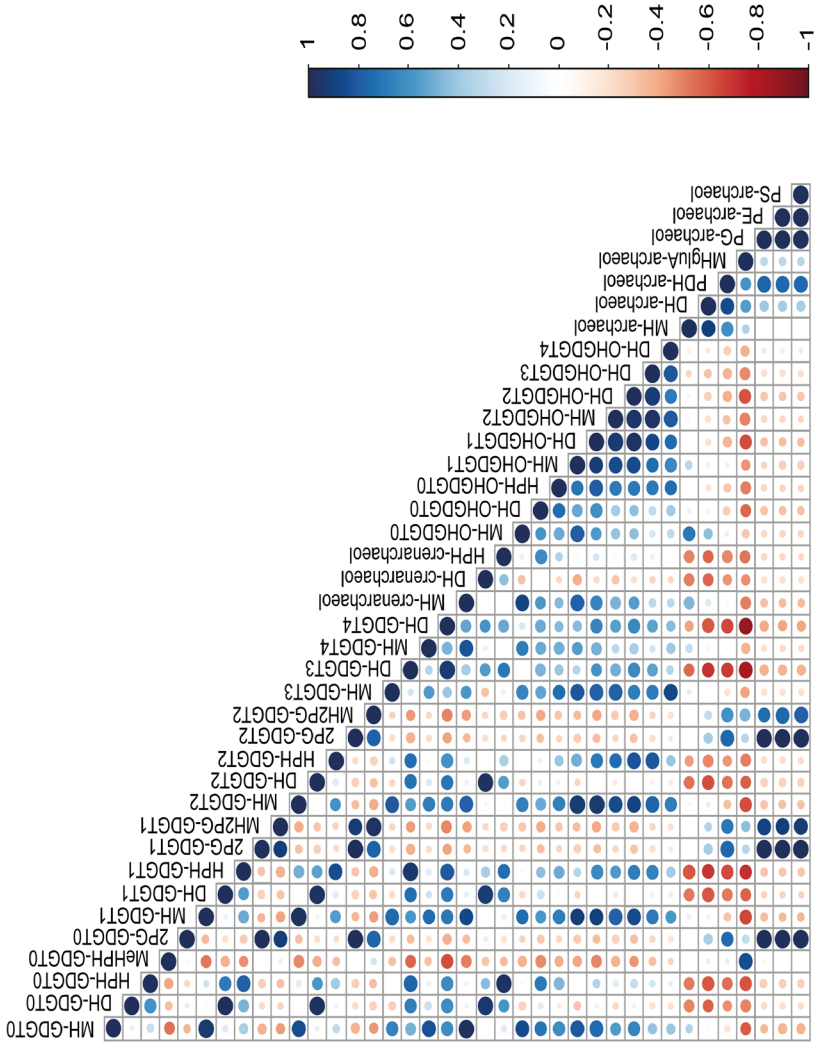

Figure S6. Dot plot of the correlation matrix obtained by applying a Pearson analysis to the absolute abundances of the archaeal IPLs (response units per Liter; r.u. L^{-1}) detected in the Black Sea water column at station PHOX2. The size of the dot and the intensity of its color relate to the degree of correlation. Dark blue corresponds to r values of +1, indicating a strong positive linear correlation between the concentrations of the archaeal IPLs; white corresponds to r values of 0, indicating that no correlation exists; dark red corresponds to r values of -1, indicating a strong negative linear correlation.

Chapter 5

The Holocene sedimentary record of cyanobacterial glycolipids in the Baltic Sea: an evaluation of their application as tracers of past nitrogen fixation

Martina Sollai, Ellen C. Hopmans, Nicole J. Bale, Anchelique Mets, Lisa Warden, Matthias Moros, Jaap S. Sinninghe Damsté

Published in *Biogeosciences*, 14, 5789-5804. 2017

doi: 10.5194/bg-14-5789-2017

Abstract. Heterocyst glycolipids (HGs) are lipids exclusively produced by heterocystous dinitrogen-fixing cyanobacteria. The Baltic Sea is an ideal environment to study the distribution of HGs and test their potential as biomarkers because of its recurring summer phytoplankton blooms, dominated by a few heterocystous cyanobacterial species of the genera *Nodularia* and *Aphanizomenon*. A multi-core and a gravity core from the Gotland Basin were analyzed to determine the abundance and distribution of a suite of selected HGs at a high resolution to investigate the changes in past cyanobacterial communities during the Holocene. The HG distribution of the sediments deposited during the Modern Warm Period (MoWP) was compared with those of cultivated heterocystous cyanobacteria, including those isolated from Baltic Sea waters, revealing high similarity. However, the abundance of HGs dropped substantially with depth, and this may be caused by either a decrease in the occurrence of the cyanobacterial blooms or diagenesis, resulting in partial destruction of the HGs. The record also shows that the HG distribution has remained stable since the Baltic turned into a brackish semi-enclosed basin ~7200 cal. yr BP. This suggests that the heterocystous cyanobacterial species composition remained relatively stable as well. During the earlier freshwater phase of the Baltic (i.e., the Ancylus Lake and Yoldia Sea phases), the distribution of the HGs varied much more than in the subsequent brackish phase, and the absolute abundance of HGs was much lower than during the brackish phase. This suggests that the cyanobacterial community adjusted to the different environmental conditions in the basin. Our results confirm the potential of HGs as a specific biomarker of heterocystous cyanobacteria in paleo-environmental studies.

5.1. Introduction

Cyanobacteria are a broad and diverse group of photoautotrophic bacteria; they are found in many terrestrial and aquatic environments (Whitton and Potts, 2012). They can exist as benthos or plankton and be unicellular or filamentous with or without branches, free-living or endosymbionts (Rippka et al., 1979) and are of biogeochemical significance due to their role in the cycling of carbon and nitrogen through photosynthesis and the fixation of N_2. However, some N_2- fixing cyanobacteria can negatively impact aquatic ecosystems due to their role in harmful algal blooms (HABs): exceptional events of phytoplankton growth causing anomalous feedbacks on food webs, alterations in the geochemical features of the water column (e.g., anoxia) and

sometimes the release of harmful toxins into the environment. Cyanobacterial HABs (cHABs) affect the surface of lacustrine, estuarine and tropical marine environments worldwide; human induced global warming and nutrient overload are blamed for exacerbating the phenomenon (Paerl, 1988; Paerl et al., 2011; Paerl and Huisman, 2009).

The two processes of photosynthesis and N_2 fixation are theoretically incompatible since the nitrogenase enzyme that catalyzes nitrogen fixation is inactivated by O_2. To cope with this, N_2-fixing cyanobacteria have developed several strategies (Stal, 2009). The filamentous diazotrophs of the orders Nostocales and Stigonematales spatially separate the two metabolisms by forming special cells dedicated to the fixation of N_2, called heterocysts (Adams, 2000; Wolk, 1973). Gas exchange is believed to be regulated by the heterocyst cell wall, which consists of two separate polysaccharide and glycolipid layers (Murry and Wolk, 1989; Walsby, 1985), of which the latter acts as the gas diffusion barrier. These layers, known as heterocyst glycolipids (HGs), have been found to date to be unique to heterocyst-forming cyanobacteria (Bryce et al., 1972; Nichols and Wood, 1968), and furthermore their composition has been discovered to be distinct at the level of families and even genera (Bauersachs et al., 2009a, 2014a; Gambacorta et al., 1998; Schouten et al., 2013b). Their structure comprises a sugar moiety glycosidically bound to a long *n*-alkyl chain (Fig. 1) with an even number of carbon atoms (26 to 32) with various functional groups (hydroxyl and keto groups) located at the C-3, ω-1 and ω-3 positions (Gambacorta et al., 1995, 1998; Schouten et al., 2013b). The sugar moiety of HGs found in nonsymbiotic cyanobacteria is typically a hexose (hereafter C_6) (Bryce et al., 1972; Lambein and Wolk, 1973; Nichols and Wood, 1968), while HGs associated with endosymbiotic heterocystous cyanobacteria have a pentose moiety (hereafter C_5) (Bale et al., 2015, 2018; Schouten et al., 2013b). High-performance liquid chromatography coupled to electrospray ionization tandem mass spectrometry (HPLC/ESI-MS^2) has emerged as a rapid method to analyze HGs in cultures (Bauersachs et al., 2009a, 2009b, 2014a) and modern-day ecosystems such as microbial mats, lakes and marine systems (Bale et al., 2015, 2016, 2018; Bauersachs et al., 2009b, 2011, 2013, 2015a; Wörmer et al., 2012).

C_6 HGs have been applied as specific paleo-biomarkers for the presence of N_2-fixing cyanobacteria in marine geological records back to the Pleistocene and in lacustrine deposits back to the Eocene and hence have provided evidence of the high potential for HGs preservation in sedimentary records

(Bauersachs et al., 2010). In addition, temperature induced modifications of the HG composition of heterocystous cyanobacteria were observed both in culture and in the environment and quantified by specific indices, suggesting the possible employment of HGs in reconstructing surface water temperatures (SWTs) (Bauersachs et al., 2009a, 2014b, 2015a). However, in general, the application of HGs as a biomarker in environmental and paleo-environmental studies is still limited.

The Baltic Sea, characterized by the seasonal occurrence of cHABs mainly consisting of the HG-producing family Nostocaceae, presents an interesting location to both apply HGs as biomarkers in the present-day system and to investigate their potential as proxies for the reconstruction of past depositional environments. The modern Baltic, one of the world's largest brackish bodies of water, is a shallow, semi-enclosed basin, characterized by estuarine circulation, having its only connection to the North Sea through the Danish straits (Fig. 2). Irregular winter inflows of marine oxygen-rich water, known as salinity pulses, represent the main mechanism of renewing and mixing the bottom water, which otherwise experiences stagnation and increasing oxygen depletion with permanent stratification and persisting anoxia in its deep waters (Kononen et al., 1996). Since the last deglaciation (ca. 13–9 cal. kyr BP) the Baltic Sea has experienced specific hydrographical phases (Andrén et al., 2011). Following the ice retreat, the Baltic Ice Lake developed, which was followed by the Yoldia Sea phase, a short period when there was a connection with the sea. The subsequent Ancylus Lake phase (ca. 9.5–8.0 cal. kyr BP) was the last extended freshwater phase in the basin before a stable connection to the North Sea was established (Björck, 1995; Jensen et al., 1999). The transition phase began (ca. 7.8–7.3 cal. kyr BP) by a series of weak inflows of saline water, which eventually led to the fully brackish Littorina Sea phase (~7.2–3.5 cal. kyr BP). The less brackish post-Littorina Sea phase (until ~1.3 cal. kyr BP) followed, and the modern Baltic Sea is considered its natural continuation. In the last 1000 years, three consecutive periods occurred: the Medieval Warm Period (MWP), the Little Ice Age (LIA) and the current Modern Warm Period (MoWP, starting at ~1950) (Kabel et al., 2012).

The modern Baltic undergoes summer cHABs primarily composed of a few species of filamentous heterocystous cyanobacteria: *Nodularia spumigena*, *Aphanizomenon flosaquae* and *Anabaena* spp. (Celepli et al., 2017; Hajdu et al., 2007; Hällfors, 2004; Kanoshina et al., 2003; Karjalainen et al., 2007; Ploug, 2008; Sivonen et al., 2007). Deep-water anoxia, high phos-

phorus availability, calm water conditions and high irradiation resulting in a relatively high sea surface temperature (SST) have been identified as the main triggers for these blooms. Anoxic sediments lead to the release of phosphate in the water column, stimulating new cHABs and further enhancing anoxia, resulting in a reinforcing feedback (Finni et al., 2001; Kabel et al., 2012; Paerl, 2008; Paerl et al., 2011; Poutanen and Nikkilä, 2001; Stipa, 2002). The summer cHABs have been documented since the 19th century, with a reported increase in their frequency and intensity in the last 60 years, which has been related to human-induced eutrophication (Bianchi et al., 2000; Finni et al., 2001).

Several studies, based on fossil pigment and other paleoproxy records, suggest that cHABs have been recurring throughout the entire Holocene simultaneously with anoxic events and thus should be considered a natural feature of the basin rather than a consequence of human impact (Bianchi et al., 2000; Borgendahl and Westman, 2007; Funkey et al., 2014; Poutanen and Nikkilä, 2001). SST has been suggested to have played an important role in these events (Kabel et al., 2012; Warden, 2017). Likely, at times of water column stratification and anoxia, high SST would have initiated cHABs in the basin when exceeding a threshold temperature of ~16 °C, which is considered a trigger for the onset of the cHABs in the modern Baltic (Kononen, 1992; Wasmund, 1997). In addition, this would have enhanced the oxygen consumption of the deep water (Kabel et al., 2012).

The intrinsic occurrence of cHABs and their role in intensifying chronic anoxic events is not limited to the Baltic Sea. These same features have been observed in various stratified freshwater lakes in the Northern Hemisphere (Fritz, 1989; McGowan et al., 1999; Schweger and Hickman, 1989; Züllig, 1986). However, there is no full agreement regarding this interpretation, as other authors argue that human perturbation has to be considered to be the main driving force behind the co-occurrence of cHABs with anoxia in the Baltic (Zillén and Conley, 2010). Therefore, more research is required to elucidate the relationship between recurring anoxic events and cHABs in the Baltic Sea.

In this study, we test the potential of HGs as a paleo-proxy to investigate the changes in past communities involved in the summer cHABs in the Baltic Sea over the Holocene and the potential relationship with the anoxic events that occurred in the basin. To this end, a multi-core and a gravity core from the Gotland Basin were analyzed for HGs at a high resolution. The results

of the analysis were compared with the total organic carbon content and the nitrogen isotope record. This may help in further confirming the potential of HGs as specific biomarkers of heterocystous cyanobacteria in environmental studies.

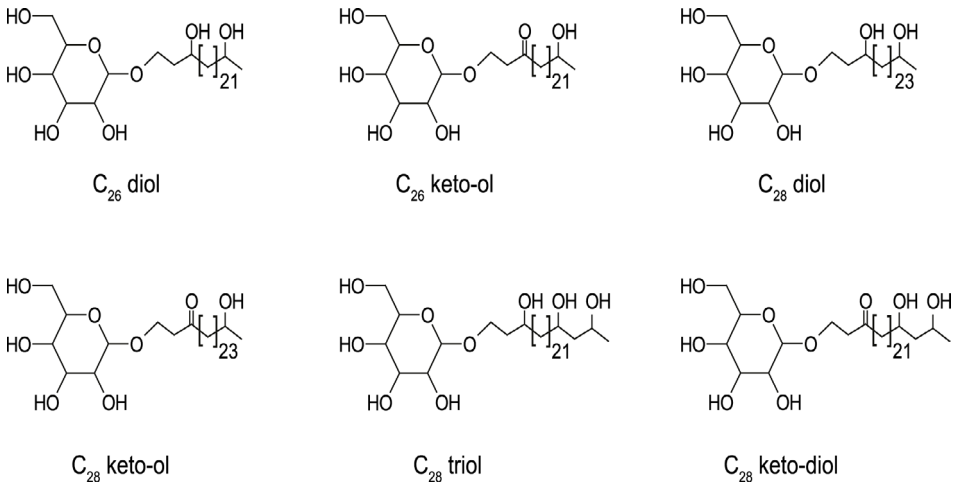

Figure 1. Structures of the C_6 heterocyst glycolipids (HG) targeted by the study. C_{26} diol HG (1-(O-hexose)-3,25-hexacosanediol); C_{26} ketool HG (1-(O-hexose)-3-keto-25-hexacosanol); C_{28} diol HG (1-(O-hexose)-3,27-octacosanediol); C_{28} keto-ol HG (1-(O-hexose)-3-keto-27-octacosanol); C_{28} triol HG (1-(O-hexose)-3,25,27-octacosanetriol); C_{28} keto-diol HG (1-(O-hexose)-27-keto-3,25-octacosanediol).

5.2. Material and Methods

5.2.1. Sample site and sediment cores

Our sampling site is located in the Eastern Gotland Basin, one of the deepest basins (max. 248 m within the Baltic Proper (Fig. 2. The gravity core (GC) 303600 (length 377 cm) was collected in the Gotland Basin (56°55.02' N, 19°19.98' W) at 175 m water depth during a cruise onboard the *R/V Prof. Albrecht Penck* in July 2009. The multi-core (MUC) P435-1-4 (length 51.5 cm) was also collected in the Gotland Basin (56°57.94' N, 19°22.21' E) at 178 m water depth during cruise P435 onboard the *R/V Poseidon* in June 2012. The dating of the MUC and the brackish section of the GC was based on an

age model, obtained by high resolution ^{14}C dating of benthic foraminifera (Warden, 2017; Warden et al., 2017), which allowed us to date the MUC (as calibrated kilo-years before present, cal. kyr BP, and the corresponding AD date) and the GC (as cal. kyr BP) back to 230 cm depth, which corresponds to ca. 7200 cal. yr BP.

The GC was cut into two halves and subsampled at a high resolution with 1 cm slices from 0 to 237 cm and 2 cm slices from 237 to 377 cm. During the procedure, the depths 81–82 cm and 187–188 cm were missed. The MUC was subsampled at 0.5 cm resolution. The sediments obtained were freeze-dried and ground before further analysis.

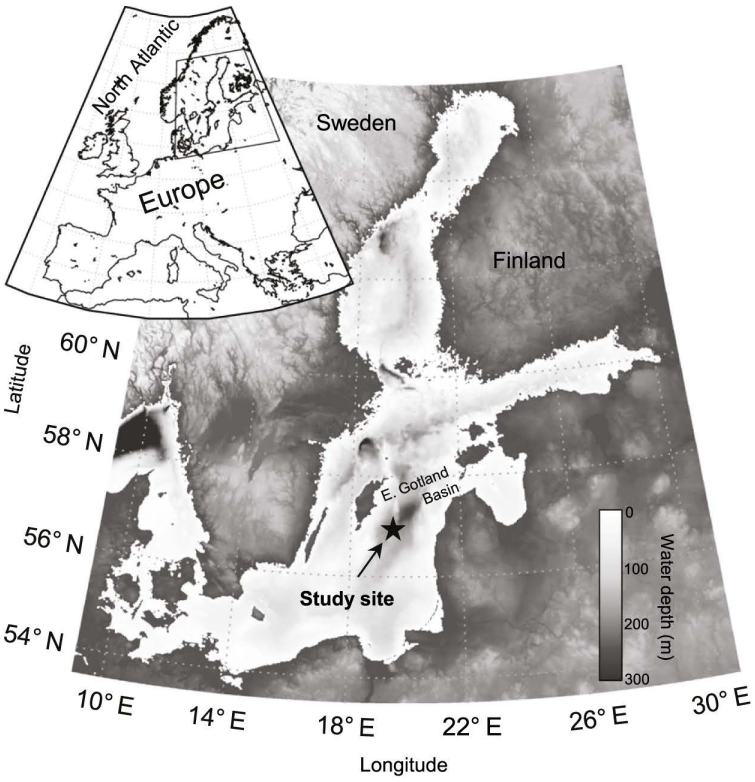

Figure 2. Map of the Baltic Sea. The location of multi-core (MUC) P435-1-4 and gravity core (GC) 303600 in the Eastern Gotland Basin is indicated with a black star (modified from Warden et al., 2017).

5.2.2. Elemental and stable isotope analysis

Subsamples were taken from the GC sediment slices for determination of the total organic carbon (TOC) content at the Leibniz Institute for Baltic Sea Research (IOW) and for the analysis of bulk stable nitrogen isotopes ($\delta^{15}N$) at the Royal Netherlands Institute for Sea Research (NIOZ). The total carbon (TC) content of the sediments of the MUC and GC was measured by using an EA 1110CHN analyzer from CE Instruments, while a Multi EA-2000 Elemental Analyzer (Analytic, Jena, DE) was employed to determine the total inorganic carbon (TIC). The TOC content was calculated as the difference between TC and TIC and expressed in weight percentage (wt %). The $\delta^{15}N$ was analyzed in duplicate on a Thermo Finnigan Delta Plus isotope ratio mass spectrometer (irmMS) connected to a Flash 2000 elemental analyzer (Thermo Fisher Scientific, Milan, Italy). The precision of the isotope analysis was 0.2% for nitrogen measurements.

5.2.3. Lipid extraction and analysis

All slices from the MUC and alternating slices from the GC were extracted and analyzed for their HG content and distribution. The extraction was performed using an accelerated solvent extractor (ASE 200, DIONEX; 100 °C and 7.6×10^6 Pa) with a mixture of dichloromethane (DCM) : methanol (MeOH) (9 : 1, *v*/*v*), to obtain a total lipid extract (TLE), which was dried under a flow of N_2. TLE was redissolved by sonication (10 min) in DCM : MeOH (1 : 1, *v*/*v*), and aliquots were taken and dried under a flow of N_2. These aliquots were dissolved in hexane, isopropanol and water (72 : 27 : 1, *v*/*v*/*v*) and filtered through a 0.45 μm regenerated cellulose syringe filter (4 mm diameter; Grace Alltech). Samples were analyzed by using a HPLC-triple quadrupole mass spectrometry (MS) in multi-reaction monitoring (MRM) mode as described by Bale et al. (2015). For the analysis, an Agilent (Palo-Alto, CA, US) 1100 series HPLC with a thermostat controlled auto-injector was employed coupled to a Thermo TSQ Quantum EM triple quadrupole MS equipped with an Ion Max source with an electrospray ionization (ESI) probe. The MRM method specifically targets C_5 and C_6 HGs with alkyl chains containing 26 and 28 carbon atoms (Bale et al., 2015). HGs were quantified as the integrated peak area per gram of TOC (response units, r.u. $gTOC^{-1}$). The r.u. $gTOC^{-1}$ values were simplified for practical purpose by dividing them by 1×10^{10}. For the MUC, 30% of the samples were reanalyzed as duplicates;

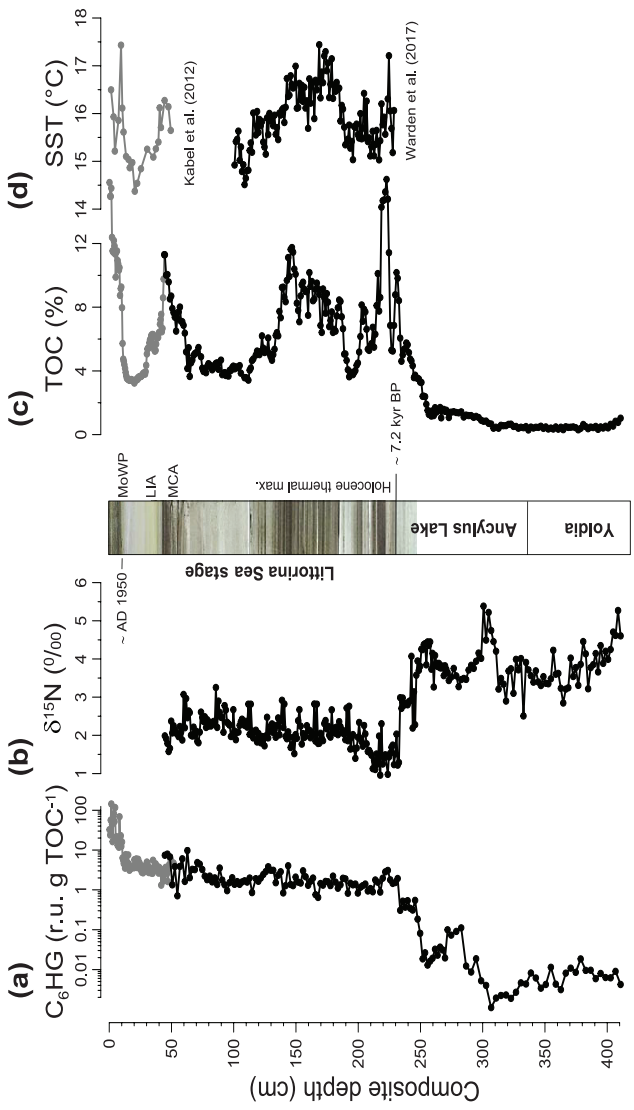

Figure 3. Proxy records of the Baltic Sea cores on a composite depth scale aligned with core photos showing the lamination of the sediments of the post-Ancylus Lake stage. (a) The abundance of the HGs (r.u. g TOC^{-1}) on a log scale; (b) $\delta^{15}N$ (‰); (c) TOC content (%) partly derived from Warden et al. (2017); and (d) TEX_{86}-derived summer sea surface temperatures (SSTs) from Kabel et al. (2012) and Warden et al. (2017). Data points derived from theMUCP435-1-4 core are in gray, and those from the GC 303600 core are in black. The stratigraphy is based on age models published elsewhere (Kabel et al., 2012; Warden et al., 2017), and for the deeper part of the GC 303600 core, it is based on unpublished data on diatom assemblages. The TEX_{86} data of Kabel et al. (2012) were measured on a different core (MUC 303600) obtained from the same site, which was correlated to the MUC P435-1-4 core based on the TOC profiles (Fig. S1 in the Supplement). Note that phases characterized by the deposition of laminated sediments are the periods during the Holocene when the bottom waters of the Baltic Sea were anoxic.

the calculated relative SD was on average 5.3 %. For all GC samples we performed the HPLC/MS^2 analysis twice; in this case the calculated relative SD was on average 12.4 %.

A selected number of samples was analyzed in full scan mode using an ultra high-pressure liquid chromatography high-resolution mass spectrometry (UHPLC-HRMS) method (Moore et al., 2013) as follows: we used an Ultimate 3000 RS UHPLC, equipped with thermostated auto-injector and column oven, coupled to a Q Exactive Orbitrap MS with Ion Max source with heated electrospray ionization (HESI) probe (Thermo Fisher Scientific, Waltham, MA). Separation was achieved on an Acquity UPLC BEH HILIC column (150 × 2.0 mm, 2.1 μm particles, pore size 12 nm; Waters, Milford, MA) maintained at 30 °C. Elution was achieved with hexane-propanol-formic acid 14.8 mol L^{-1} aqueous NH_3 (79 : 20 : 0.12 : 0.04, *v*/*v*/*v*/*v*), hereafter A, and propanol water-formic acid 14.8 mol L^{-1} aqueous NH_3 (88 : 10 : 0.12 : 0.04, *v*/*v*/*v*/*v*), hereafter B, starting at 100% A, followed by a linear increase to 30% B at 20 min, followed by a 15 min hold and a further increase to 60% B at 50 min. The flow rate was 0.2 mL min^{-1}; the total run time was 70 min, followed by a 20 min re-equilibration period. Positive ion ESI settings were as follows: capillary temperature – 275 °C; sheath gas (N_2) pressure – 35 arbitrary units (AU); auxiliary gas (N_2) pressure – 10 AU; spray voltage – 4.0 kV; probe heater temperature – 275 °C; S-lens – 50 V. Target lipids were analyzed with a mass range of *m/z* 350–2000 (resolution 70000 ppm at *m/z* 200), followed by data-dependent tandem MS^2 (resolution 17500 ppm), in which the 10 most abundant masses in the mass spectrum were fragmented successively (normalized collision energy: 35; isolation width: 1.0 *m/z*). The Q Exactive was calibrated within a mass accuracy range of 1 ppm using the Thermo Scientific Pierce LTQ Velos ESI Positive Ion Calibration Solution. During analysis dynamic exclusion was used to temporarily exclude masses (for 6 s) in order to allow the selection of less abundant ions for MS^2.

A number of indices have been suggested to express the correlation between the distribution of HGs and growth temperature (Bauersachs et al., 2009a, 2014b, 2015). We examined our data using two such indices, the HDI_{26} and the HDI_{28} (heterocyst diol index of 26 and 28 carbon atoms, respectively), defined as follows:

$$HDI_{26} = \frac{HG_{26}\,diol}{HG_{26}\,keto\text{-}ol + HG_{26}\,diol}, \quad (1)$$

$$HDI_{26} = 0.0224 \times SWT + 0.4381;\ r^2 = 0.93 \quad (2)$$

$$HDI_{28} = \frac{HG_{28}\,diol}{HG_{28}\,keto\text{-}ol + HG_{28}\,diol}, \quad (3)$$

$$HDI_{28} = 0.0405 \times SWT + 0.0401;\ r^2 = 0.70 \quad (4)$$

These SWT calibrations have been determined in a study of a freshwater lake (Lake Schreventeich, Kiel, Germany; Bauersachs et al., 2015a).

5.2.4. Data analysis

Principal component analysis (PCA) was performed with the R software package for statistical computing (http://cran.r-project.org/), to test the variation observed in the HG distribution.

5.3. Results

5.3.1. Sediment core characteristics

The basin has experienced periodical anoxic bottom waters, which resulted in the alternating deposition of laminated and homogeneous sediments (Fig. 3; see also Andrén et al., 2000). The sediments of the MUC represent almost 1000 years of sedimentation and comprise the MoWP (~0–11 cm depth, corresponding to ~2012–1950 AD or ~0.06 to 0 cal. kyr BP), the LIA (~12–41 cm, corresponding to ~1950–1260 AD or ~0.1–0.7 cal. kyr BP) and almost the entire MWP (~42–52 cm, corresponding to ~0.7–0.9 cal. kyr BP). The upper part of the GC overlaps with the deeper part of the MUC (i.e., ~0 to 17 cm depth in the GC roughly corresponds to ~35 to 52 cm of the MUC). The upper part of the GC covers the initial phases of the LIA (until ca. 6 cm, ~0.6 cal. kyr BP) and the complete Littorina Sea and Ancylus Lake stages, down

to part of the Yoldia Sea stage.

5.3.2. Abundance and distribution of HGs

In total 104 sediment horizons of the MUC and 153 horizons of the GC were analyzed for C_6 and C_5 HGs with alkyl chains with 26 and 28 carbon atoms using HPLC-triple quadrupole MS in MRM mode as described by Bale et al. (2015). Bauersachs et al. (2017) have recently analyzed the HGs of eight representative heterocystous cyanobacterial strains isolated from the Baltic Sea, and the six C_6 HGs targeted in our study form by far the majority (i.e., 97.7–100%) of the HGs of these strains. HGs with longer alkyl chains were not detected, suggesting that, at least for the brackish phase, our analysis method will provide a proper view of changes in the overall HG distribution.

C_5 HGs were not detected at all, but the targeted C_6 HGs were present in all samples of both cores. The C_6 HGs detected in this study were as follows: 1-(O-hexose)-3,25-hexacosanediol (C_{26} diol HG; see Fig. 1 for structures); 1-(O-hexose)-3-keto-25-hexacosanol (C_{26} keto-ol HG); 1-(O-hexose)-3,27-octacosanediol (C_{28} diol HG); 1-(O-hexose)-3-keto-27-octacosanol (C_{28} keto-ol HG); 1-(O-hexose)-3,25,27-octacosanetriol (C_{28} triol HG); 1-(O-hexose)-27-keto-3,25-octacosanediol (C_{28} keto-diol HG). A selected number of samples from the brackish phase was also analyzed in full-scan mode to check for the presence of HGs with longer alkyl side chains, but these were not encountered (Table 2). The HG distribution obtained using this method was comparable to that obtained with the HPLC-triple quadrupole MS method.

The distribution of the six quantified HGs changed substantially with depth (Fig. 4). The C_{26} diol HG was the dominant component, accounting for ~50 to 95% of the HGs, in the sediments recording the brackish phase of the basin. In the sediments deposited during the Ancylus Lake and Yoldia phase (i.e., below 213 cm of the GC), the fractional abundance of the C_{26} diol HG was more variable, reaching only 20–30% at some discrete depths. In the sediments deposited during the brackish phase, the fractional abundance of all keto HGs (i.e., C_{26} keto-ol HG, C_{28} keto-ol HG and C_{28} keto-diol HG) diminished with increasing depth, roughly from 3–15% to < 2% (Fig. 4b). In the sediments deposited during the Ancylus Lake and Yoldia Sea phase, however, their fractional abundance showed more variation, and in general it increased and reached ~10–40% at some specific depths. The fractional abun

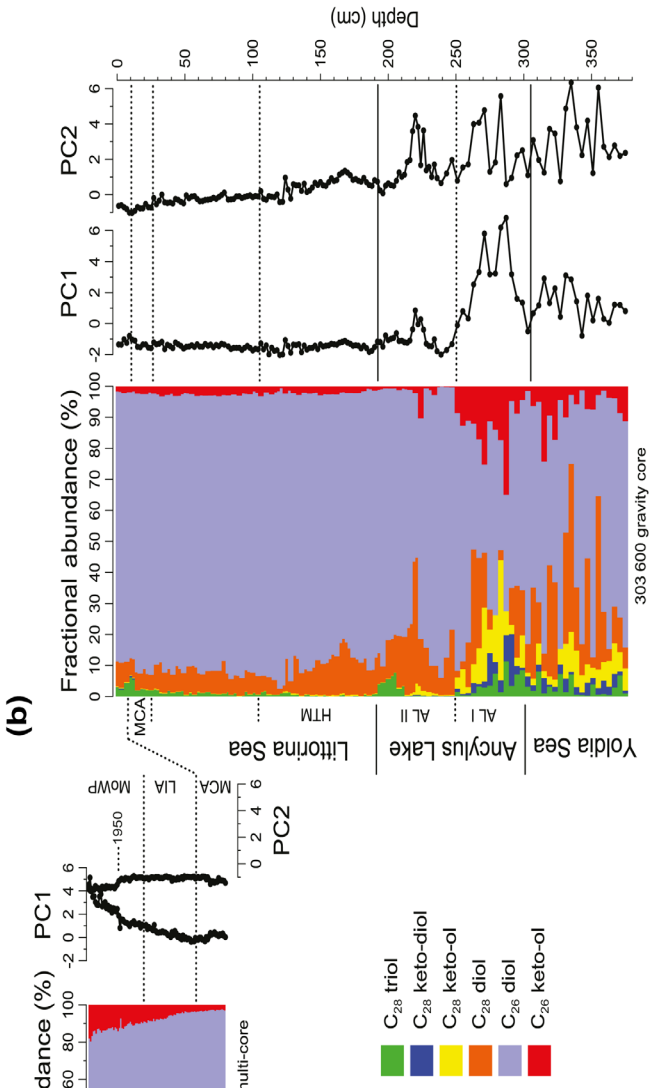

Figure 4. Distribution of HGs, displayed as fractional abundance (%) vs. depth (in cm) for (a) the MUC P435-1-4 core and (b) the GC 303600 core. Color key: light green – C_{28} triol HG; blue – C_{28} keto-diol HG; yellow – C_{28} diol HG; orange – C_{28} keto-ol HG; purple – C_{26} diol HG; red – C_{26} keto-ol HG. Each sample represents a sediment slice of 0.5 cm in the case of the MUC and of 1 or 2 cm in the case of the GC. The stratigraphy of the cores (see Fig. 3) is indicated. The scores on PC1 and PC2 derived from the principal component analysis of the HG distribution are plotted along the fractional abundance plots using the same scale for both cores.

dance of the C_{28} diol HG remained steady for most of the sediments deposited during the brackish phase (~10% on average), although slightly increased values occurred in the oldest part of the brackish section, up to ~15% (Fig. 4b). In the Ancylus Lake and Yoldia Sea section the fractional abundance of the C_{28} diol HG was higher, with values sometimes reaching almost 60%, but it was also more variable. The fractional abundance of the C_{28} triol HG was <2% for most of the sediments deposited during the brackish phase, with the exceptions of the shallower (8–16%) and the deeper part, close to the boundary with the freshwater phase (3–9%). In the Ancylus Lake and Yoldia Sea sections, the relative abundance of the C_{28} triol HG generally remained <2%, although it was between 3–11% in several horizons in the deeper part (Fig. 4b). For the Ancylus Lake and Yoldia Sea section, we did not check the general distribution of the HGs and, therefore, cannot exclude the possibility that HGs with alkyl chains >28 carbon atoms occur during these intervals.

The C_6 HG abundance (sum of the six C_6 HGs; hereafter referred to as HG abundance) profile showed four peaks in the first 8 cm of the MUC of 144, 82, 117 and 69 r.u. $gTOC^{-1}$ (Fig. 3a). After this last peak, the abundance of the HGs decreased substantially by a factor of ~30 in some cases (i.e.,~5 r.u. $gTOC^{-1}$) and remained at this level with increasing depth over the whole of the MUC (Fig. 3a). The HG abundance in the upper part of the GC (up to 3 to 6 times higher (7 to 18 r.u.$gTOC^{-1}$) than that recorded in the corresponding fraction of the MUC (2 to 4 r.u. $gTOC^{-1}$). At ~17 cm of the GC, which is equivalent to ~52 cm or the bottom of the MUC, the abundances were in the same order of magnitude (4 to 5 r.u. $gTOC^{-1}$). Between ~25 and 213 cm depth (~1.3–7.1 cal. kyr BP), the abundance of the HGs decreased substantially further by a factor of ca. 6 to 10, with the exception of several small peaks at discrete depths (~5 r.u. $gTOC^{-1}$ at ~35 cm; ~4 r.u. $gTOC^{-1}$ at
~53 cm, at ~92cm and at ~108 cm; ~3 r.u. $gTOC^{-1}$ at ~188 cm). Deeper in the core (213–375 cm; i.e., the Ancylus Lake and Yoldia phase), the abundance of the HGs was even lower (Fig. 3a).

5.3.3. Principal component analysis of the HG distribution

The variation observed in the HG distribution in the sediments was examined by applying a principal component analysis (PCA) to the fractional abundances of the six HGs (Fig. 5). The first two PCs explained most of the variation observed, accounting for 47 and 29% of the variance (Fig. 5a). The first principal component (PC1) showed a positive loading of all keto HGs

and of the C_{28} triol HG. Specifically, the C_{26} keto-ol HG and the C_{28} keto-diol HG had the most positive loading (Fig. 5a). The C_{26} diol HG was the only component showing a negative loading in PC1; the C_{28} diol HG did not show any loading on PC1. PC2 was primarily determined by the positive loadings of the C_{28} diol and keto-ol HGs, whereas all other HGs had negative loadings on PC2.

Figure 5b shows the scores of all analyzed sediment horizons on PC1 and PC2, which reveals clearly defined different signatures. The brackish phase sediments all scored negatively or just above zero on PC2. However, the score on PC1 was more variable; the MoWP sediments scored most positively on PC1, whereas the pre-MoWP brackish sediment scored less positively on PC1, which is due to the higher fractional abundances of the C_{26} keto-ol and C_{28} keto-diol HGs in the MoWP sediments. The remaining sediments of the Ancylus Lake I and Yoldia Sea phase all scored positively on both PC1 and PC2, and therefore distinctly from the brackish phase sediments, but they also showed much more variability. The sediments of the Ancylus Lake transitional phase II (filled triangles in Fig. 5b) plotted much more closely to those of the brackish phase, with some data points with similar PC1 and PC2 values.

Figure 4 shows the variation in the scores on PC1 and PC2 with depth. The sediments of the MUC exhibited a decreasing trend in PC1 with increasing depth, caused by the reduction in the fractional abundance of the positively scoring keto HGs, in favor of the negatively scoring C_{26} diol (Fig. 4a). For the GC (Fig. 4b), the PC1 scores varied between -2 and -1, from the top up to 213 cm depth (i.e., the brackish phase), consistent with the dominance of the C_{26} diol HG in this section. At greater depth (i.e., the Ancylus Lake and Yoldia Sea phases), large variations in the score of PC1 were observed (Fig. 4b). Scores were mostly positive; negative PC1 scores were only found at three discrete depths, i.e., 239, 303 and 343 cm. The generally positive score in these phases highlights the greater contribution of HGs other than C_{26} diol HG. The PC2 score of the sediments of the MUC was constantly around -1 (Fig. 4a). In the GC, PC2 was close to zero during the brackish water phase (Fig. 4b). In the sediments of the Ancylus Lake and Yoldia Sea phases the PC2 score was generally positive, clearly influenced by the higher fractional abundance of positively scoring C_{28} diol and C_{28} keto-ol HGs, but variable.

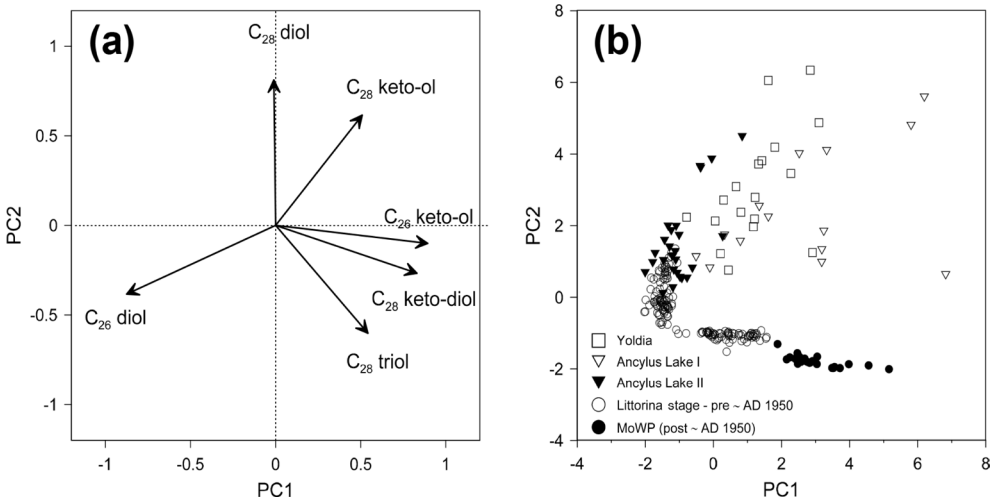

Figure 5. Principal component analysis of the heterocyst glycolipid (HG) distribution in the sediments recovered by the MUC P435-1-4 and the GC 303600 cores from the Gotland Basin, Baltic Sea. (a) The loadings of the six HGs on the first two principal components (PCs), with PC1 accounting for the 47% and PC2 for 29% of the variance. (b) Scores of the sediments from various stages on PC1 and PC2.

5.4. Discussion

This study investigates the presence of HGs in the recent sedimentary record of the Baltic Sea and represents the first attempt to relate them with the recurring anoxic events that took place in the basin during the Holocene as well as the ongoing increase in cHAB over the last 60 years. In our data set we recognized various phases, characterized by different distributions of HGs (cf. Figs. 4 and 5b). Here these records and their implications for the heterocystous cyanobacterial community composition are discussed.

5.4.1. The distribution of HGs

The composition of HGs in cyanobacteria is known to be related to their taxonomy (Bauersachs et al., 2009a, 2014a; Gambacorta et al., 1995, 1998; Schouten et al., 2013b; Wörmer et al., 2012). Hence, we compared the distribution of the HGs observed in our sedimentary record of the Baltic Sea with the HGs produced *in vitro* by different heterocystous cyanobacterial species.

5.4.1.1. Brackish sediments

Firstly, the most recent sediments (MoWP; <11 cm depth of MUC) were compared with species that thrive in the modern Baltic Sea (Table 1). The recurring late summer (July–August) cHABs of the Baltic are dominated by the taxa *Nodularia spumigena*, *Aphanizomenon flos-aquae* and, to a minor extent, by *Anabaena* spp. and other species from the order Nostocales, family Nostocaceae (Celepli et al., 2017; Hajdu et al., 2007; Hällfors, 2004; Kanoshina et al., 2003; Karjalainen et al., 2007; Sivonen et al., 2007). While the *Nodularia* genus is usually prevalent, changes in the composition of the community have been observed from the early to the late stage of the cHAB and from one year to another, resulting in a large variation in its features over time (Finni et al., 2001; Hajdu et al., 2007; Kahru et al., 1994; Wasmund, 1997). A recent extensive meta-omics study revealed that in the Baltic Proper (the predominant area for cHABs), 69% of the heterocystous cyanobacteria belong to *Aphanizomenon*, 23% to *Anabaena* and 8% to *Nodularia* (Celepli et al., 2017).

The HG distribution in the MoWP sediments, with the C_{26} diol as the dominant HG (Fig. 4a, summarized in Table 1), agrees well with the HG distribution in cultures of *Nodularia*, *Aphanizomenon* and *Anabaena* as well as other members of the Nostocaceae family (Table 1), including those that have been isolated from the Baltic (Bauersachs et al., 2009a, 2017). These cultures generally also synthesized minor amounts of the C_{26} keto-ol HG, as was seen in the MoWP sediments. The C_{28} diol, present in trace amounts in the MoWP sediments, was found in varying amounts in the *Nodularia*, *Aphanizomenon* and *Anabaena* cultures. Even between different strains of the same species, the amounts present were highly variable, from a dominant component to not detected (Table 1). The C_{28} keto-ol, C_{28} triol and C_{28} keto-diol HGs were minor components in the MoWP sediments. While not produced consistently across the *Nodularia*, *Aphanizomenon* and *Anabaena* cultures, they were found in certain strains, generally as trace or minor components, in agreement with the distribution in the sediments (Table 1). It is possible, however, that the presence of the C_{28} triol HG in the MoWP sediments may be linked to the presence of the genus *Calothrix* (cf. Table 1), which is commonly found in the rocky seabed of the basin (Sivonen et al., 2007).

Overall, the distribution of the HGs observed in the MoWP sediments was in good agreement with the HG distribution of the family Nostocaceae (Ta-

ble 1), which fits in with the reported dominance of members of this family during the summer cHABs of the Baltic. Furthermore, the HG distribution remained relatively constant throughout the MoWP sediments (Fig. 4a), suggesting that overall the community composition of heterocystous cyanobacteria in the Baltic Sea has remained stable during the last ~60 years. The HG distribution in the sediment from the pre-MoWP brackish phase (i.e., from the Ancylus Lake–Littorina Sea (AL–LS) transition to the start of the MoWP) reconstructed in this study was similar to that of the MoWP, although the C_{26} diol and the C_{28} diol were present in a greater fractional abundance (Table 1; Fig. 4). The other four HGs were either minor or occurred in traces. Although often absent, a number of Nostocaceae strains have been found to contain the C_{28} diol (Table 1), and in one *Anabaena* sp. strain (CCY9402), it was found to be the dominant HG (Bauersachs et al., 2009a). The increased proportion of the C_{28} diol through the pre-MoWP brackish phase suggests there was a somewhat different cyanobacterial community composition than during the MoWP, although most probably still dominated by cyanobacteria belonging to the family Nostocaceae. The HG distribution remained relatively constant from the establishment of the brackish phase to the MoWP (Fig. 4), which suggests that the cyanobacterial community of the Baltic did not undergo major changes from the AL–LS transition to the MoWP and remained dominated by cyanobacteria belonging to the family Nostocaceae.

5.4.1.2. The Ancylus Lake sediments

The Ancylus Lake phase displayed a distinct HG distribution from the brackish phase (Fig. 4b; summarized in Table 1). The C_{28} diol was often dominant and both the C_{26} and C_{28} keto-ol were present in a higher proportion than during the brackish phase. This is most evident for the Ancylus Lake phase I and the middle section (ca. 230–210 cm) of the Ancylus Lake phase II. Yet, at the first (ca. 250–230 cm) and last part (ca. 210–193 cm) of the Ancylus Lake transitional phase II, the HG distribution is more similar to the one observed in the brackish phase (Fig. 4b). This is also evident from the PCA analysis with more negative values for PC1 and PC2 at those depths (Figs. 4b and 5b). The AL–LS transition did not happen instantly (Borgendahl and Westman, 2007; Emeis et al., 1998; Gustafsson and Westman, 2002; Hyvarinen, 1984), and the sediment intervals showing a brackish-like distribution of the HGs probably correspond to weak pulses of marine water that might have occasionally entered the basin already during the Ancylus Lake transitional phase

Table 1. Distribution of the six targeted HGs in sediments from this study and from cultures of selected heterocystous cyanobacteria. Key: ++ – dominant (>25 %); + – minor presence (5–25 %); tr. – traces (<5 %); – – not detected or not reported. Bold strains were isolated from the Baltic Sea.

Baltic Sediment		C_{26} diol	C_{26} keto-ol	C_{28} diol	C_{28} keto-ol	C_{28} triol	C_{28} keto-diol
MoWP		++	+	tr.	tr.	+	+
Pre-MoWP brackish		++	+/tr.	+	tr.	+/tr.	tr.
Ancylus Lake-II		++	+/tr.	++/+	tr./-	tr./-	-
Ancylus Lake-I		++	++/+	++/+	++/tr.	+/tr.	+/tr.
Yoldia Sea		++	+	++/+	+/tr.	+/tr.	tr.
Nostocaceae cultures	Strain ID						
Nodularia sp. [a]	CCY 9414 & 9416	++	+	-	-	-	-
Nodularia sp. [b]	BY1	++	+	-	-	-	-
Nodularia sp. [b]	F81	++	+	-	-	-	-
Nodularia sp. [b]	AV1	++	+	-	-	-	-
Nodularia sp. [b]	HEM	++	+	-	-	-	-
Nodularia chucula [a]	CCY 0103	++	+	-	-	-	-
Aphanizomenon sp. [a]	CCY 0368	++	+	+	-	-	-
Aphanizomenon sp. [a]	CCY 9905	++	+	+	+	tr.	tr.
Aphanizomenon sp. [b]	TR183	++	+	tr.	-	+	tr.
A. aphanizomenoides [c]	UAM 523	+	-	++	+	tr.	-
A. gracile [c]	UAM 521	++	++	tr.	-	tr.	-
A. ovalisporum [c,f]	UAM 290	++	tr.	tr.	tr.	-	-
Anabaena sp. [a]	CCY 0017, 9910	++	+	+	+	-	-
Anabaena sp. [a]	CCY 9402	-	-	++	+	-	-
Anabaena sp. [a]	CCY 9613	+	+	-	-	-	-
Anabaena sp. [a]	CCY 9614, 9922	++	+	-	-	-	-
Anabaena sp. [b]	315	++	++	tr.	tr.	tr.	-
Anabaena sp. [b]	BIR53	++	++	tr.	tr.	tr.	-
Anabaena sp. [b]	BIR169	++	+	tr.	tr.	++	+
Anabaena cylindrica [a]	CCY 9921	++	+	-	-	-	-
Anabaenopsis sp. [a]	CCY 0520	++	+	+	-	-	-
Nostoc sp. [a]	CCY 0012, 9926	++	+	-	-	-	-
Nostoc sp. [c]	MA 4	++	++	tr.	-	tr.	-
Cylindrospermopsis raciborskii [c,f]	UAM 520	++	tr.	+	tr.	+	-
Cyanospira rippkae [e]	ATCC 43194	-	-	++	+	-	-
Rivulariaceae cultures							
Calothrix desertica [d]	PCC 7102	-	-	-	-	++	++
Calothrix sp. [c]	MU 27	-	-	tr.	-	++	++

Calothrix sp. [a]	CCY 0018	-	-	-	-	++	+
Calothrix sp. [a]	CCY 0202	tr.	tr.	-	-	++	+
Calothrix sp. [a]	CCY 0327	-	-	-	-	++	+
Calothrix sp. [a]	CCY 9923	-	-	+	+	++	+
Microchaetaceae cultures							
Microchaete sp. [d,f]	PCC 7126	-	-	+	++	-	-
Tolypothrichaceae cultures							
Tolypothrix tenuis [d,f]	PCC 7101	-	-	++	+	-	-

a = Bauersachs et al. (2009a), b = Bauersachs et al. (2017). c = Wrmer et al. (2012), d = Gambacorta et al. (1998), e = Soriente et al. (1993). f = these species also contain HGs other than the six HGs targeted in this study

II and consequently influenced the overall distribution of the HGs (Fig. 4b). This final stage of this transition is also evident from the lithology and TOC profile (Fig. 3c).

When the Baltic evolved from a freshwater lake into a brackish semi-enclosed basin, it experienced an increase in salinity from fresh to values of 10–15‰ (Gustafsson and Westman, 2002). The observed changes in the HG distribution over the AL–LS transition suggest that this change from freshwater to brackish resulted in a different cyanobacterial species composition and hence a different HG distribution. Indeed, several freshwater species have been found to contain a HG distribution dominated by the C_{28} diol (Table 1), including *Cyanospira rippkae* (Soriente et al., 1993), *Tolypothrix tenuis* (Gambacorta et al., 1998) and *Aphanizomenon aphanizomenoides* (Wrmer et al., 2012), although we emphasize that we did not analyze HGs with C_{28+} alkyl chains for this stage and, therefore, cannot exclude the contributions of cyanobacteria producing such extended HGs. Alternatively, an increased influx of soil organic matter during the Ancylus Lake phase could be responsible for the distributional HG changes. However, since HG lipids contain an attached sugar moiety, we feel it is unlikely that HGs produced in soil will make it to the sediments of the Baltic Sea since they would be exposed extensively to oxygen during transport and only relatively stable components such as lignin, wax lipids, and branched glycerol dialkyl glycerol tetraethers (GDGTs) will likely survive this transport to the middle of the Baltic Sea where our core was taken.

For *Nodularia spumigena*, the most abundant heterocystous cyanobacterium in the present Baltic, its basic physiological features, such as growth, production of the toxin nodularin and differentiation of heterocysts are sub

Table 2. Analysis of HGs in Baltic sediments by Orbitrap MS. Key: (++) Dominant (>25%); (+) Minor presence (5-25%; (tr.) Traces (<5%); (–) Not detected. Relative abundances are based on peak areas.

Sample	$C5_{26}$ diol	Deoxy $C6_{26}$ diol	$C6_{26}$ diol[a]	C_{26} keto-ol	$C6_{28}$ diol	$C6_{28}$ keto-ol	$C6_{28}$ triol	$C6_{28}$ keto-diol	$C6_{30}$ triol	$C6_{30}$ keto-diol	$C6_{32}$ triol	$C6_{32}$ keto-diol
P435-1-4 MUC 4	-	-	++	+	tr.	tr.	++	+	-	-	-	-
P435-1-4 MUC 35	-	-	++	+	tr.	-	+	+	-	-	-	-
P435-1-4 MUC 62	-	-	++	+	tr.	-	++	+	-	-	-	-
P435-1-4 MUC 99	-	-	++	tr.	tr.	-	++	tr.++	-	-	-	-
GC 1-2 cm	-	-	-	++	tr.	tr.	-	+	-	-	-	-
GC 5-6 cm	-	-	-	++	tr.	tr.	-	+	-	-	-	-
GC 17-18 cm	-	-	-	++	tr.	tr.	-	+	-	-	-	-

a = sum of two isomers

stantially affected at extreme salinities (Mazur-Marzec et al., 2005; Moisander et al., 2002). This is thought to be the predominant reason why *Nodularia* blooms only occur within a certain salinity range (i.e., 7–18‰) in nitrogen-deficient waters (Mazur-Marzec et al., 2005). This would imply that during the Ancylus Lake phase, the low salinity was limiting the growth of *Nodularia* sp. Other heterocystous cyanobacteria such as *Anabaena* and *Aphanizomenon* may be better adapted to freshwater conditions.

5.4.1.3. Yoldia Sea sediments

A high variability in the HG distribution is also observed for the Yoldia Sea sediments (Figs. 4b and 5b). The most distinct feature is the relatively high fractional abundance of the C_{28} diol HG, which sometimes reaches 50%, the highest value recorded for all sediments. The Yoldia Sea phase was a relatively short period when a connection with the sea was established and waters may have become brackish. Nevertheless, the HG distribution is not at all similar to that of the brackish phase.

5.4.1.4. Does the distribution of the fossil HGs record a paleotemperature signal?

As a consequence of the retreat of the ice sheet and the entry of sea water through the Danish straits, there was an increase in water temperature during the AL–LS transition (Björck, 1995). It is possible that this increase in water temperature could have been responsible for the changes in the HG distribution, as growth temperature has been reported to affect the distribution of the HGs in cyanobacteria belonging to the order Nostocales (Bauersachs et al., 2009a, 2014b, 2015a). Specifically, increasing temperature positively correlated with increasing relative proportions of HG diols over HG keto-ols. In our record, the ratio of diols to keto-ols increased from the Ancylus Lake towards the brackish phase (Fig. 4b), which would be in agreement with the higher SWTs during the brackish phase. However, when the HG proxies are used to estimate SWT based on the proxy calibrations from a lake (Eqs. 1–4), the predicted temperatures are somewhat unrealistic. For the brackish phase, the HDI_{26} and HDI_{28} values vary between 0.96–1.00 and 0.95–1.00, translating into an average SWT of ca. 24 and 23 °C, respectively. This is too high, even for summer temperatures when the cHABs occur (Kanoshina et al., 2003). TEX_{86}-derived summer temperatures (Kabel et al., 2012; Warden et al., 2017) do not exceed 17.5 °C (Fig. 3d). The application of the HG-based calibrations in this setting assumes that salinity has no impact since they have been established for a freshwater lake (Bauersachs et al., 2015a). For the Ancylus Lake and Yoldia Sea phases, the HDI_{26} and HDI_{28} values are highly variable and range between 0.52–1.00 and 0.00–0.99, translating into average SWTs of ca. 20 and 17 °C, respectively. This is lower than observed for the brackish phase but also seems too high. Apparently, cyanobacterial species composition exerts an important control on the HG distribution in such a way that the HGs are not able to predict accurate temperatures in the brackish–freshwater system of the Baltic. Cultivation experiments with HG-producing strains isolated from the Baltic Sea (see Table 1) at varying temperatures may improve the HG paleo-thermometry of Baltic Sea sediments.

5.4.2. The abundance of HGs

5.4.2.1. Is HG abundance a good measure for cHABs and anoxic events?

In the Baltic the occurrence of summer cHABs has intensified since the

1950s (Kabel et al., 2012; Poutanen and Nikkilä, 2001). Yet, due to the spatial patchiness and interannual variability, it has proven difficult to recognize a clear trend in the cHABs on the scale of the entire Baltic (Finni et al., 2001; Kahru and Elmgren, 2014; Pitarch et al., 2016; Wasmund and Uhlig, 2003). However, the general interest in these events has led to intensified research (see Finni et al., 2001; Kahru and Elmgren, 2014; Kutser et al., 2006 among others) and also led to the establishment of the Baltic Marine Environment Protection Commission (HELCOM) in 1992 to monitor this phenomenon. Disparate indices and parameters have been employed to describe and quantify cHABs over time and were applied in the different areas of the Baltic which are biogeochemically heterogeneous and display distinct seasonal dynamics (Kahru, 1997; Kahru et al., 2007; Kahru and Elmgren, 2014; Kononen, 1992; Kutser et al., 2006; Pitarch et al., 2016; Wasmund and Uhlig, 2003). The methods employed and the frequency of the sampling campaigns have improved in the recent past, reducing the inaccuracy associated with previous sampling methods and measurements (Hansson and Öberg, 2016; Kahru, 1997; Kahru and Elmgren, 2014; Wasmund and Uhlig, 2003). However, intrinsic limitations of the techniques in use may still cause difficulties when comparing measurements from different years, even within the same time series (Finni et al., 2001; Kahru, 1997; Kahru and Elmgren, 2014).

Here, the HG abundance over the past ~30 years (i.e., 2012–1979 of the MoWP), recorded within the first ~7 cm of the MUC, is discussed in comparison with a time series of the cHABs episodes relative to the Eastern Gotland Basin (Fig. 6), whose intensity is expressed as the frequency of cyanobacteria accumulation (FCA) (Kahru and Elmgren, 2014). FCA is determined by ocean color satellite data and expresses the frequency of the occurrence of cHABs in July–August using 1 km^2 pixels (Kahru et al., 2007). Kahru and Elmgren (2014) reported prominent cHABs in the early 1980s, in the period 1990–1996 and again from 1999 until 2008, with the interval 2005–2008 recording the highest FCA percentages with relevant interannual changes of the areal extent (Kahru, 1997; Kahru et al., 1994, 2007; Kahru and Elmgren, 2014). The HG lipid biomarker abundance profile from our sampling site was overall in reasonable agreement with the FCA measurements (Fig. 6).

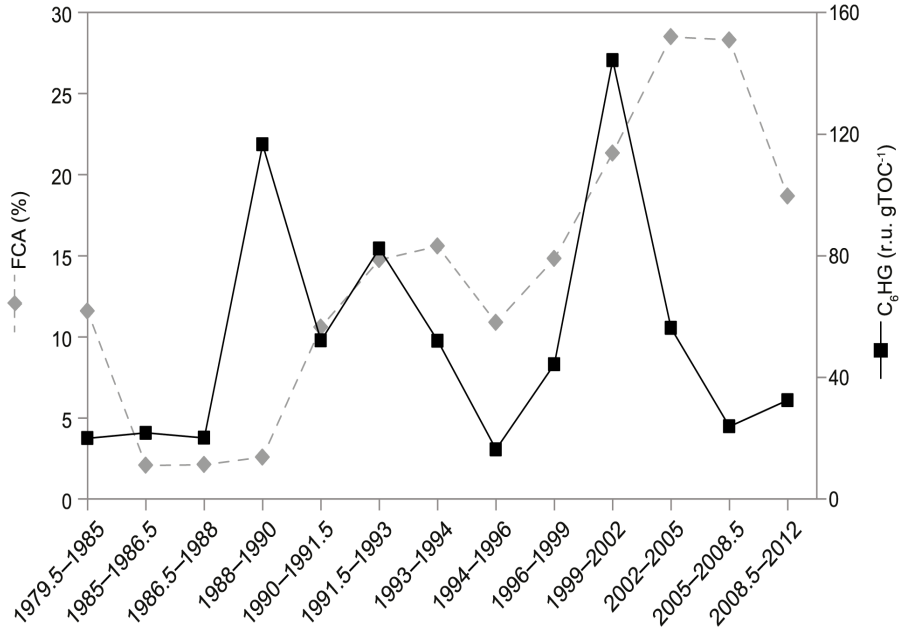

Figure 6. Abundance of heterocyst glycolipids (HGs) in the Baltic Sea over the period 1977–2012 (from MUC) compared with the fractional cyanobacteria accumulation (FCA, %) from the time pe- riod 1979–2012, as reported by Kahru and Elmgren (2014).

However, it failed to record the intense cHABs of the early 1980s, and there is a mismatch of 1 or 2 years in recording the start of the strong cHABs recorded at the end of the same decade (Kahru and Elmgren, 2014). Furthermore, this comparison is complicated by a certain degree of uncertainty in the age model of the sedimentary record. Moreover, the intrinsic temporal and spatial variability in the cHABs in the modern Baltic Sea, together with the difficulties encountered in an attempt of creating a consistent long time series that combines FCA data from multiple satellite sensors, may provide an explanation for the discrepancies observed (Kahru and Elmgren, 2014; Wasmund and Uhlig, 2003).

We observed multiple peaks of the HG abundance in the MoWP section of the MUC core (≤11 cm depth), which reached ~50–150 r.u. $gTOC^{-1}$. Below this in the LIA section, the HG abundance declined sharply to <10 r.u. $gTOC^{-1}$ (Fig. 3a). This decline may be expected given that the MoWP is characterized

by higher summer surface temperature (Fig. 3d), increased organic matter deposition and more frequent anoxic events than the LIA phase (Kabel et al., 2012), all being conditions that lead to increased cHABs. Furthermore, the cooler LIA experienced more oxygenated bottom water, which may have affected HG preservation (see also below). However, a substantially increased HG abundance was not observed below the LIA in the MWP section of the MUC core (Fig. 3a). Similar to the MoWP period, the MWP was characterized by higher summer temperatures (Fig. 3d) and increased stratification of the water column that would favor bottom anoxia and, presumably, the occurrence of cHABs. The top of the GC also records the LIA–MWP transition (Fig. 3). Here, the HG abundance reached ~10–18 r.u. $gTOC^{-1}$ at <30 cm depth, which is up to 4 times higher than the HG abundance observed in the MUC for the same period. This discrepancy between the HGs records in the two related cores is puzzling. After the MWP, HG abundance declined to ≤5 r.u. $gTOC^{-1}$ during the remaining part of the brackish phase, as recorded in the GC (Fig. 3a), with only a minor increase in the HG abundance during the periods when summer temperature was higher and the Baltic Sea was stratified, resulting in bottom water anoxia (Fig. 3; e.g., during the Holocene Thermal Maximum).

Based on these data from the Baltic Sea, it is not possible to confidently couple the HG abundance record directly with cHAB occurrences and anoxic events in the past. Several factors are thought to affect this relationship. Firstly, it is possible that the occurrence of cHABs varied over time. In the shallow part of both sediment cores, HG abundance was generally high, but it started declining with increasing depth, independently of other factors (Fig. 3). This might suggest that cHABs were less common and intense in the past brackish Baltic Sea, even at times of warmer and more stratified conditions. Secondly, the succession of oxic and anoxic bottom water conditions may impact the preservation efficiency of HGs. Such successions took place in the Baltic Sea during the entire Holocene as is evident from the alternation of dark–laminated with light–homogeneous sections in the sedimentary record (Kabel et al., 2012). In the shallow part of both sediment cores, the high abundance of HGs coincided with dark–laminated sediment phases; low HGs, by contrast, co-occurred with light–homogeneous phases. In contrast, in the deeper part of the section this correspondence was lost. Finally, the generally declining trend in the HG absolute abundance in the shallow sediments might also be due to the anaerobic breakdown of the HGs. A decline in lipid biomarkers with depth has been documented before in anoxic Black Sea surface sedi-

ments (Sun and Wakeham, 1994). This process would be seemingly in contrast with previous indications of a high preservation potential of the HGs in ancient marine and lacustrine anoxic sediments (Bauersachs et al., 2010), but it should be realized that even in the older Baltic Sea sediments, HGs are still detected. Apparently, even if diagenesis occurs, it does not result in the complete destruction of HGs.

The HG results seem to partly contrast an earlier study that, based on fossil pigment records, suggested that cHABs have been recurring simultaneously with the mid-Holocene anoxic events (Funkey et al., 2014). However, this study used carotenoids (i.e., zeaxanthin and echinenone) that are not entirely specific to cyanobacteria and are certainly not limited to nitrogen-fixing cyanobacteria, as opposed to the highly specific HGs that were used here. For example, zeaxanthin is also produced by *Synechococcus*, the dominating unicellular cyanobacterial species in the Baltic Sea (Celepli et al., 2017). Furthermore, in this environment of highly variable sediment redox conditions, the effect of diagenesis should be considered. Carotenoids are amongst the most unstable organic biomarkers because of their very labile conjugated system of double bonds. Changes in redox conditions of bottom and sedi-ment pore waters will thus have a major effect on the concentration of carot-enoids, and this may explain the enhanced concentration of carotenoids in the mid-Holocene TOC-enriched sections (Funkey et al., 2014).

5.4.2.2. Changing abundance of the HGs over the AL–LS transition

The general down-core decrease in the HG abundance throughout the brackish phase is continued into the Ancylus Lake and Yoldia Sea phases, where the HG abundance is at least an order of magnitude lower than in the first part of the brackish phase (Fig. 3a). The lower HG abundance in the An-cylus Lake and Yoldia Sea phases, relative to the brackish phase, could indi-cate that N_2-fixing cyanobacteria were much less abundant during this fresh-water phase. Indeed, further evidence for a lower abundance of diazotrophic phytoplankton during the Ancylus Lake and Yoldia Sea phases comes from the record of $\delta^{15}N$ values (Fig. 3b). During these phases the $\delta^{15}N$ values are 4–6‰, indicating that most of the phytoplankton community was relying on ammonium or nitrate as nitrogen sources rather than atmospheric nitrogen (Bauersachs et al., 2009c; Emerson and Hedges, 2008). When other forms of nitrogen are abundant the energetically expensive N_2 fixation becomes dis-advantageous (Arrigo, 2005; Capone et al., 2005; Karl et al., 1997). At the

start of the LS phase, $\delta^{15}N$ values drop to 1–3‰ (Fig. 3b), a range expected when N_2-fixing cyanobacteria contribute substantially to primary production (Bauersachs et al., 2009c; Rejmánková et al., 2004; Zakrisson et al., 2014), and remained in this range.

As discussed above, the salinity change from a freshwater lake to a brackish sea may have had a significant effect on the heterocystous cyanobacterial composition in the Baltic. This environmental change may have also been a cause of the increased abundance of heterocystous cyanobacteria. Another environmental factor change that could have promoted increased blooming of heterocystous cyanobacteria is the increase in water temperature over the AL–LS transition (Björck, 1995). Temperature is a crucial factor influencing the growth rate and other metabolic features of free-living heterocystous cyanobacteria (Bauersachs et al., 2014b; Kabel et al., 2012; Mazur-Marzec et al., 2005; Staal et al., 2003). In the modern Baltic Sea, a minimum temperature of 16 °C is considered essential to initiate cHABs during summer when other crucial factors like a low DIN/DIP ratio, calm winds and high irradiance occur simultaneously (Kanoshina et al., 2003; Kononen, 1992; Kononen et al., 1996; Paerl, 2008; Wasmund, 1997).

It should also be noted, however, that the homogeneous appearance of the sediments and the much reduced TOC content (Fig. 3c) reveal that the water column was generally well mixed and oxygenated during the Ancylus Lake and Yoldia Sea phases, resulting in a higher degradation of organic matter (including HGs) in settling particles and surface sediments. To compensate for this effect, all HG concentrations were normalized to TOC content (Fig. 3a). However, it is known that oxic conditions in the sediment result in a decreased preservation of biomarkers relative to TOC (see Sinninghe Damsté et al., 2002b). This may also explain in part the lower HG abundance in the Ancylus Lake and Yoldia Sea than in the brackish phase. However, it is noteworthy that no substantial change in the concentration of HGs is observed during the brackish phase when bottom water conditions changed from oxic to anoxic (Fig. 3). This suggest that the normalization to TOC content is an effective way to compensate for changing redox conditions of bottom and pore waters. The effect of oxic degradation is probably also not responsible for substantial changes in the distribution of the HGs since they are structurally similar and all contain a relatively labile glycosidic bond, so there is no reason to assume that one HG will degrade faster than another.

5.5. Conclusions

The distribution of the six analyzed C_6 HGs in the Baltic sediments from the brackish phases were closely related to those of cultivated heterocystous cyanobacteria of the family Nostocaceae. The record also shows that the HG distribution has remained stable since the Baltic turned into a brackish semi-enclosed basin ~7200 cal. yr BP. During the freshwater phase of the Baltic (i.e., the Ancylus Lake phase) and an earlier brackish period (the Yoldia Sea phase), the distribution of the HGs was quite distinct but varied much more than in the subsequent brackish phase. This suggests that the cyanobacterial community adjusted to the different environmental conditions in the basin over this transition. We found that the abundance of HGs dropped substantially down-core, possibly either due to a decrease in the cHABs or during oxic degradation during deposition, resulting in the partial destruction of the HGs.

In conclusion, it is likely that both salinity and temperature have influenced the abundance and composition of the heterocystous cyanobacterial community of the Baltic since the last deglaciation. The effects of salinity on the synthesis and distribution of HGs would need to be investigated in controlled conditions to be confirmed, as has been partially done already in the case of temperature. Further studies are also needed to extend the range of heterocystous cyanobacteria species in culture that have been investigated for their HG content.

Acknowledgements

We thank the captain and the crew of the *R/V Prof. Albrecht Penck* (cruise July 2009), and of the *R/V Poseidon* (cruise June 2012) for their support and assistance in the sampling. We thank Mati Kahru for providing FCA data and three anonymous referees and Dan Conley for helpful suggestions on an earlier draft of this paper. This project was funded by a grant to Jaap S. Sinninghe Damsté from the Darwin Center for Biogeosciences (project no. 3012). The work was further supported by funding from the Netherlands Earth System Science Center (NESSC) through a Gravitation grant (NWO 024.002.001) from the Dutch Ministry for Education, Culture and Science to Jaap S. Sinninghe Damsté.

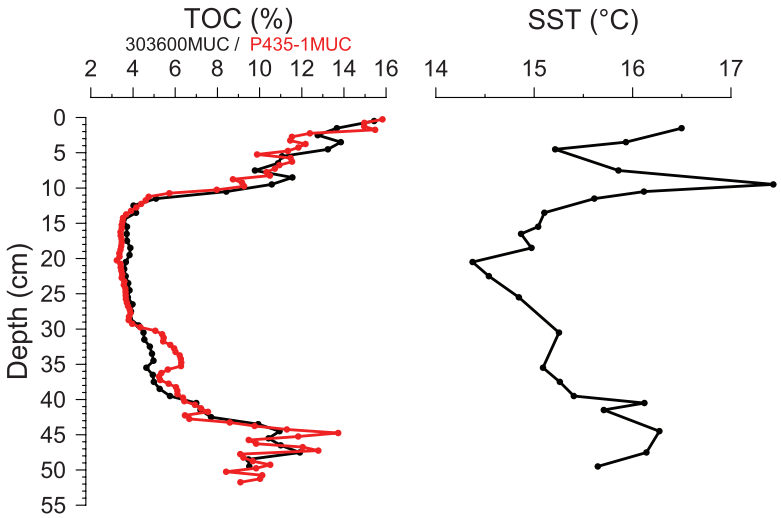

Figure S1. Correlation of the MUC cores 303600 (Kabel et al., 2012) and P435-1 (this work) on the basis of the TOC content. SST data is from MUC 303600 (Kabel et al., 2012).

Synthesis

The understanding of how the marine nitrogen cycle works in oxic, suboxic and anoxic waters and which microorganisms are involved has greatly increased from the late 1990s up to date. Influential discoveries have regarded various aspects of the cycle. For instance, the importance of specific cyanobacteria in the fixation of N_2 into NH_4^+ in the tropical/subtropical oceans (Agawin et al., 2014; Benavides et al., 2011; Falcón et al., 2004; Montoya et al., 2004), the dominant role of Thaumarchaeota (Brochier-Armanet et al., 2008; Spang et al., 2010) in the nitrification process in the marine mesopelagic zone worldwide (Könneke et al., 2005; Venter et al., 2004; Wuchter et al., 2006), including oxygen-depleted waters (Beman et al., 2008; Coolen et al., 2007; Lam et al., 2007; Pitcher et al., 2011b), and the discovery of anammox bacteria (Mulder et al., 1995) and their substantial contribution in the removal of nutrient N from anoxic basins and oceanic oxygen-deficient zones (ODZs) (Hamersley et al., 2007; Kuypers et al., 2003, 2005b; Lam et al., 2009; Pitcher et al., 2011). These discoveries have gone side by side with the development of new methods of investigation, alternative to the isolation and cultivation of environmental microorganisms which are often difficult to achieve (Rappé and Giovannoni, 2003). Different culture-independent approaches combined together offer a powerful way to investigate the marine nitrogen cycle as they allow studying it from multiple points of view and to disentangle different aspects, including the microbial diversity involved. Among the most successful approaches of study is the use of molecular biomarkers specific to a certain microbial group, which include both DNA and lipid molecules.

The importance of Thaumarchaeota in the modern ocean

To strengthen the investigation on the microorganisms involved in the marine nitrogen cycle it is necessary to implement and differentiate the approaches used, for instance by identifying new potential biomarkers. This has been one of the objectives of this thesis. In Chapters 2 to 4 of this thesis I have investigated some key microbial species involved in the nitrogen cycle in two of the most prominent ODZs in the modern ocean – the eastern tropical North Pacific (ETNP; Chapter 2) and the South Pacific (ETPS; Chapter 3) ODZs – and in the Black Sea – the largest permanently stratified anoxic basin in the world (Chapter 4) – by using specific genes (i.e. 16S rRNA gene) and intact polar lipid (IPL) biomarkers. Because of their highly labile structure and taxonomic value, both types of biomarkers are especially suitable to identify and determine the distribution of microorganisms in the present

day ocean (Beman et al., 2008; Coolen et al., 2007; Hamersley et al., 2007; Mincer et al., 2007; Pitcher et al., 2011b; Rossel et al., 2008; Schouten et al., 2012; Schubotz et al., 2009).

The studies comprising chapters 2 to 4 of this thesis support the general prominence of Thaumarchaeota in marine oxic to suboxic waters worldwide (Beman et al., 2008; Coolen et al., 2007; Lam et al., 2007; Pitcher et al., 2011b) but have also highlighted that different thaumarchaeotal groups have a specific niche preference in the water column (Chapters 3 and 4 in particular). In both the ETSP (Chapter 3) and the Black Sea (Chapter 4), the 16S rRNA gene analysis unravels that Thaumarchaeota Marine Group I (MGI) *Candidatus* Nitrosopelagicus brevis (Santoro et al., 2015) is better adapted to shallower and more oxygenated waters as was already suggested by proteomic evidence in an enriched culture from the open ocean (Santoro et al., 2015). *Nitrosopumilus maritimus*-related species on the contrary are especially abundant in deeper suboxic waters, a condition observed also in the other main ODZs (Beman et al., 2008, 2012; Pitcher et al., 2011b). This might depend on a better adaptation of the former species to photoinhibition stress and/or to a more efficient uptake of ammonium (Merbt et al., 2012; Santoro et al., 2015; Smith et al., 2014). *Nitrosopumilus* on the other hand is known for being able to cope with low-oxygen conditions (Coolen et al., 2007; Lam et al., 2007; Park et al., 2010; Pitcher et al., 2011b; Sinninghe Damsté et al., 2002a), as also the study of the ETNP reveals (Chapter 2), and has low substrate requirements (Martens-Habbena et al., 2009). However, in both studies the concentrations of ammonia reported in shallow oxic and deeper suboxic waters are low and constant, which suggests that alternative factors other than ammonia and oxygen levels may play a role in this differentiation.

Other uncultured thaumarchaeotal operational taxonomic units (OTUs) occupy specific niches of the water column in the ETSP and Black Sea. In the ETSP in particular (Chapter 3), the uncultured MGI OTUs detected are especially abundant in the deep oxic water below the ODZ, suggesting that these OTUs form a deep water thaumarchaeotal population which differs from the shallow water one. The existence of a deep water thaumarchaeotal population genetically divergent from the shallow water one has been observed for many locations including the ETSP, the ETNP and the Arabian Sea ODZs among others (Belmar et al., 2011; Beman et al., 2008; Francis et al., 2005; Hallam et al., 2006; Hu et al., 2011; Mincer et al., 2007; Santoro et al., 2010; Villanueva et al., 2015).

The genetic evidence of a depth niche preference of different subgroups of Thaumarchaeota coincides with the specific distribution of the hexose-phosphohexose (HPH)-crenarchaeol, the glycerol dibiphytanyl glycerol tetraether (GDGT) containing four cyclopentane moieties and a cyclohexane moiety, specific of living Thaumarchaeota (Schouten et al., 2008a; Sinninghe Damsté et al., 2002c). Indeed, HPH-crenarchaeol is especially abundant where the percentage of 16S rRNA gene reads of *Nitrosopumilus maritimus* is higher (Chapter 3 and 4). Whilst the lipidome of *Ca.* Nitrosopelagicus has not been determined yet *in vitro*, its close genetic similarity to *Nitrosopumilus* suggests that *Ca.* Nitrosopelagicus IPLs might be similar if not coincide with those of *Nitrosopumilus*. This assumption finds confirmation in the ETSP and in the Black Sea investigations, as HPH-crenarchaeol is also abundant where the percentage of *Ca.* Nitrosopelagicus 16S rRNA gene reads are higher in those two settings. This biogeochemical evidence confirms the high effectiveness of HPH-crenarchaeol as specific biomarker of living and active Thaumarchaeota (Elling et al., 2014; Pitcher et al., 2011b). Another indication of this is evident in Chapter 2, in which HPH-crenarchaeol is used as only biomarker of Thaumarchaeota presence in the ETNP. In fact, Beman and colleagues previously found genetic evidence of the relevant presence of active *Nitrosopumilus*-like Thaumarchaeota at the base of the oxycline, in the water column of the Gulf of California (Beman et al., 2008, 2012). Results found in Chapter 2 of this thesis show the same depth profile for HPH-crenarchaeol.

The IPLs attributed to Thaumarchaeota representatives in Chapters 3 and 4 include also monohexose, dihexose, and HPH-GDGTs containing up to four cyclopentane moieties (i.e. MH/DH/HPH-GDGT-0 to -4). In the Black Sea monohydroxy (OH) GDGTs also occur and are likely made by *Nitrosopumilus*-like Thaumarchaeota (Chapter 4). This suggests that a high variety of IPLs can be associated to Thaumarchaeota and potentially used as biomarkers of this group, albeit they are not as specific as HPH-crenarchaeol. It also hints at a certain degree of variability in the lipidome of the group in different environments.

Relationship between Thaumarchaeota and anammox bacteria

Chapter 2 of this thesis addresses another important aspect of the marine nitrogen cycle that is the distribution of Thaumarchaeota compared to that of anammox bacteria on a local scale and thus the potential for an interaction between the two microbial groups. The setting chosen to investigate this

is the water column of the ETNP ODZ and the IPL biomarkers employed are HPH-crenarchaeol for Thaumarchaeota and phosphatidylcholine (PC) C_{20}-[3]-monoether ladderane (hereafter PC-monoether ladderane) for anammox bacteria, considered the best lipid biomarker available for living anammox bacteria (Pitcher et al., 2011b).

Genetic and geochemical biomarker evidence have shown that the two microbial groups coexist in oxygen-depleted waters and ODZs (Coolen et al., 2007; Francis et al., 2005; Lam et al., 2007; Pitcher et al., 2011b; Woebken et al., 2007), in spite of expected different O_2 tolerances. Cooperation between the two groups has been demonstrated in a laboratory-scale model system, where Thaumarchaeota provided NO_2^- to anammox and concurrently consumed O_2 (Yan et al., 2012). Thaumarchaeota thrive ca. 30 m above anammox bacteria in the coastal ETSP: the former group at the bottom of the oxycline, the latter in the core ODZ. On the contrary, in the open ocean the two groups thrive at the same depth range, coinciding with the upper part of the ODZ. This is the first experimental evidence that the distribution of the two microbial groups can differ on a regional scale and that local environmental parameters, such as O_2 concentration, affect this distribution. This suggests that the potential relationship between the Thaumarchaeota and anammox bacteria is also prone to be modified on a local scale and this should be taken into account when conclusions on regional or larger scale studies are drawn.

Other Archaea in the modern ocean

Archaea play an important role in the biogeochemistry of the oceans as the prominent involvement of Thaumarchaeota in the nitrification process reveals. The role played by other archaeal groups in the marine nitrogen cycle and in other biogeochemical cycles is much less clear. The main reason for this is the scarce knowledge on the physiology of the other archaeal groups due to the substantial lack of pure cultures and enrichments of their representatives. Unfortunately, the biomarkers available are also scarce or not specific enough. In this perspective, Chapters 3 and 4 of this thesis represent an improvement as they investigate the archaeal diversity in two marine regions, the ETSP ODZ and the Black Sea, which are expected to host high archaeal diversity due to the multiple geochemical gradients found in their water column. In addition, in these two studies new potential IPL biomarkers for the archaeal groups found are identified and discussed. To tentatively attribute the IPLs to their archaeal source, I have applied a statistical method (i.e. a

Pearson correlation analysis applied to the archaeal groups and IPLs detected) and considered the physiological features known for each of the archaeal groups detected and their relative abundance. In fact, excluding Thaumarchaeota *Nitrosopumilus* and *Ca*. Nitrosopelagicus whose lipidome is known or inferred from culture experiments (see section 6.1 of this synthesis) there is no culture evidence of the suite of IPLs synthesized by the other archaeal groups reported in Chapters 3 and 4.

Some substantial differences exist between the two locations. The ETSP water column shows the typical features of ODZs, with shallow oxic waters which turn increasingly into suboxic and anoxic within the first ca. 200 m, but return gradually oxygenated below ca. 400 m depth. The Black Sea water column on the other hand turns suboxic/anoxic already within the first ca. 60–70 m and then sulfidic (or euxinic) – meaning that sulfide (HS^-) is present in the water – from ca. 110–130 m down to the sea floor. Such difference clearly affects the archaeal community composition, the relative abundance and the niche occupied by the various archaeal groups. At both locations I have detected higher diversity than previously described (Belmar et al., 2011; Cooleen et al., 2007; Lin et al., 2006; Quiones et al., 2009; Vetriani et al., 2003; Wakeham et al., 2007). In addition to various representatives of the Thaumarchaeota MGI (see section 6.1 of this synthesis), the archaeal community of the ETSP (Chapter 3) comprises representatives of the Marine euryarchaeota Group II (MGII), and III (MGIII), both suggested to be heterotrophic based on available genomes, and the Woesearchaeota DHVE-6 of the DPANN superphylum. Every group occupies a specific niche. In the coastal ETSP, an OTU of the MGII (i.e. OTU-1) was more abundant in the shallow oxic/suboxic waters, and MGII OTU-2 in the deep oxic waters below the ODZ, where instead the group is undetected or extremely low. In the open ocean ETSP the distribution is reversed and a third OTU (MGII OTU-3) is also detected but with a low relative abundance. This implies that MGI (see section 6.1 of this synthesis) and MGII niches overlap to a certain degree in the ETSP. The niches of the MGIII OTUs and of DPANN Woesearchaeota DHVE-6 are restricted to the ODZ. The former group has been suggested to include facultative anaerobes (Martin-Cuadrado et al., 2008); the DPANN Woesearchaeota DHVE-6 group has been reported in the Black Sea (Chapter 4 of this thesis) and in anoxic sediments (Besseling et al., 2018; Lipsewers et al., 2018).

The archaeal IPLs detected in the ETSP comprise MH/DH/HPH-GDGT-0 to -4 and -crenarchaeol which are especially abundant in the shallow oxic and

suboxic waters and again in the deep oxic water below the ODZ. These IPLs are synthesized by the thaumarchaeotal groups detected (see section 6.1 of this synthesis), which have the same distribution as those IPLs in the ETSP. The assignment of specific IPLs to the MGII representatives also occurring in the same depth ranges of the water column is less straightforward because of the lack of pure cultures. In fact, previous attempts to do so remain inconclusive to date (Lincoln et al., 2014a; Schouten et al., 2008b, 2014; Turich et al., 2007). The Pearson correlation applied in Chapter 3 is also not conclusive in this matter, since it only highlights that MGI and MGII occupy the same niche and consequently might be synthesizing similar IPLs. Other IPLs detected – MH/DH/ phosphatidylglycerol (PG) / phosphatidylethanolamine (PE) -diphytanylglycerol diether, known as archaeol – are especially abundant within the ODZ. This suggests that they are made by MGIII and/ or DPANN Woesearchaeota DHVE-6. The latter, however, are expected to be unable to synthesize their own IPLs due to the reported small size of their cells and genomes (Castelle et al., 2015; Rinke et al., 2013). Consequently, the DPANN Woesearchaeota DHVE-6 group would depend greatly on other archaea to acquire a membrane. This hints at the fact that MGIII archaea are synthesizing the IPLs found in the ETSP ODZ. The results of the Pearson correlation analysis also suggest this is highly probable.

The archaeal community found in the Black Sea (Chapter 4) is even more complex than the one of the ETSP. In the Black Sea, Thaumarchaeota *Ca*. Nitrosopelagicus is the most abundant archaeal group in the oxic and shallow suboxic waters (60–70% of the total archaeal 16S rRNA gene reads), whereas the percentage of 16S rRNA gene reads of *Nitrosopumilus* exceeds those of all other archaeal groups in the deeper suboxic and anoxic waters (ca. 20–80% of the total archaeal reads, depending on the depth). This distribution suggests that these two MGI OTUs are mainly responsible for the archaeal IPLs detected in those zones of the Black Sea water column. Specifically, *Ca*. Nitrosopelagicus-like Thaumarchaeota are likely synthesizing MH/DH/ HPH-GDGT-0 to -4 and -crenarchaeol, *Nitrosopumilus*-like Thaumarchaeota instead are most likely responsible for the MH/DH/HPH-OH-GDGTs. This is also suggested by the positive scores in the Pearson correlation analysis between the two thaumarchaeotal groups and the two IPLs groups. Most important, culture experiments have proven that Thaumarchaeota synthesize mainly MH/DH/HPH-GDGT-0 and -crenarchaeol and, in lower abundance, -GDGT-1 to -4, and that the HPH-GDGTs are especially abundant when the Thaumarchaeota are actively growing (Elling et al., 2014; Schouten et al.,

2008a; Sinninghe Damsté et al., 2002c, 2012). In addition, mono- (OH-) and dihydroxy- (2OH-) GDGTs have been recently reported in thaumarchaeotal cultures (Liu et al., 2012).

Some uncultured OTUs related to the MGI, MGII and MGIII groups, sequences related to the Thermoplasmatales VC2.1Arc6 and CCA47 groups, the Bathyarchaeota (MCG+C3) and the DPANN Woesearchaeota DHVE-6 group are also present in the oxic and especially in the suboxic/anoxic water of the Black Sea. The features of these groups are poorly understood and their contribution to the IPLs assemblage detected difficult to establish. This depends on the fact that there are no isolates available to confirm or dismiss the results reported in Chapter 4 of this thesis. All these groups are of secondary relevance in the oxic and suboxic waters of the Black Sea (approximately 1 to 12% of the total archaeal 16S rRNA gene reads), thus their contribution is likely to be also secondary compared to *Ca*. Nitrosopelagicus-like and *Nitrosopumilus*-like Thaumarchaeota respectively. The DPANN Woesearchaeota DHVE-6 group is an exception as it is not expected to synthesize its own IPLs (Castelle et al., 2015; Lipsewers et al., 2018; Rinke et al., 2013; Villanueva et al., 2017).

In the euxinic waters *Nitrosopumilus* gradually disappears, whereas DPANN Woesearchaeota DHVE-6 (ca. 23–60% of the total archaeal reads, depending on the depth) and Bathyarchaeota (ca. 15–55% of the total archaeal reads, depending on the depth) become the two most prominent groups; Thermoplasmatales CCA47 and VC2.1Arc6 also increase but less than the other two groups (up to ca. 8% and up to ca. 6% of the total archaeal reads, respectively). Moreover, the Thermoproteales Thermofilum and the ANME-1b groups are found only at very specific depths: the former group at the upper boundary of the euxinic water (i.e. at 130 m with 7% of the total archaeal reads), the latter between 1000–2000 m, with 2 to 13% of the total archaeal reads. All the archaeal groups present in the euxinic waters of the Black Sea are thus expected to be anaerobic and adapted to cope with high concentrations of HS^-, but with the exception of ANME-1b (Boetius et al., 2000), the strategies they employ to do that are still unknown. ANME-1b depth distribution coincides with that of specific IPLs, which are 2PG-GDGT-0, - 1 and -2, MH-2PG-GDGT-1 and -2 and PS-, PG-, and PE-archaeol. The comparison of the results of the Pearson correlation analysis with previous studies (Meador et al., 2015; Rossel et al., 2011; Schubotz et al., 2011; Yoshinaga et al., 2011) suggests that the ANME-1b group synthesizes those IPLs and that

the group is an important contributor to the archaeal community of the deep Black Sea (Wakeham et al., 2003, 2007). The appointment of specific IPLs to other archaeal groups detected in the euxinic waters is more uncertain. The diversity of the archaeal community and of the IPLs present in the euxinic zone is higher than in the oxic and suboxic zones. All dominant archaeal groups in the euxinic zone correlate positively to each other in the Pearson analysis, because they are co-occurring. The comparison of the genetic and lipidomic datasets and the Pearson correlation analysis suggest that Bathyarchaeota might be synthesizing the phospho-dihexose (PDH)-archaeol and the newly described monohexose-glucuronic acid (MHgluA)-archaeol. The abundance profile of Thermoplasmatales CCA47 reveals a highly positive correlation with the IPLs previously attributed to the ANME-1b and Bathyarchaeota groups. However, the Thermoplasmatales CCA47 lower relative abundance masks potential relationships with specific IPLs. The Thermoplasmatales VC2.1Arc6 group instead has a more distinct distribution and shows a fairly positive correlation with MH- and DH-archaeol. These two IPLs however positively correlate also with the Thermofilum group. Finally, the other newly described methyl-hexose phosphohexose (MeHPH)-GDGT-0 in spite of showing a well-defined depth profile cannot be associated to any specific archaeal group detected in the deep Black Sea, suggesting that this IPL should be derived from an unidentified source.

The role of Cyanobacteria in the past marine nitrogen cycle

Another objective of this thesis was the comparison of the modern marine nitrogen cycle with the one occurring in the geological past. The marine N cycle in fact is believed to have been affected by past ocean anoxic events (OAEs) occurring during the Cretaceous (Kuypers et al., 2005a; Sachs and Repeta, 1999) and to have been similar to the modern Black Sea (Sinninghe Damsté and Köster, 1998) and more generally to the modern ODZs. In addition, processes such as the anammox reaction are believed to have resulted in a loss of fixed nitrogen and consequently the blooming of N_2-fixing cyanobacteria (Kuypers et al., 2005a). In general, IPLs comprise a core lipid moiety (CL) bond to one or two polar headgroups. Upon the depth of the cell the polar headgroup of the IPL is hydrolyzed (Harvey et al., 1986) but the CL portion can potentially persist in the environment thanks to its high chemical stability and be used as biomarker of those organisms in the geological past (Killops and Killops, 2005). Heterocyst glycolipids (HG), the IPLs specific

of heterocystous diazotrophic cyanobacteria (Bryce et al., 1972; Nichols and Wood, 1968), represent an exception as they have shown to preserve intact in the marine geological records back to the Pleistocene and in lacustrine deposits back to the Eocene (Bauersachs et al., 2010). The Baltic Sea is ideal to investigate how the cyanobacterial community has evolved in the geological past. Indeed, after the last deglaciation the basin has undergone specific geochemical phases which include long periods of anoxia (Andrén et al., 2011; Björck, 1995; Jensen et al., 1999; Kabel et al., 2012). Temperature variations are believed to have acted as triggers of these phases and of shifts in the phytoplankton community composition (Kabel et al., 2012). In the modern Baltic bottom water anoxia is a recurring feature during warm summers. In this period of the year high temperature together with other favorable environmental parameters initiate extensive blooms of few heterocystous cyanobacteria species (Celepli et al., 2017). The main effect of these blooms on the water column is to enhance the bottom water anoxia (Kabel et al., 2012).

In Chapter 5 of this thesis a suite of selected of HGs, in a record that comprises the entire Holocene geological history of the Baltic, is used to reconstruct how the community of heterocystous cyanobacteria has changed since the beginning of the Holocene up to date. A comparison between the HGs deposited during the period 1950–2012, known as Modern Warm Period (MoWP), and the HGs synthesized by cultivated heterocystous cyanobacteria, including isolates from Baltic Sea waters (Bauersachs et al., 2009a, 2017; Gambacorta et al., 1998; Soriente et al., 1993; Wörmer et al., 2012), reveals high similarity in the HG distribution and is closely related to heterocystous cyanobacteria of the family Nostocaceae. In addition, the HGs record from ca. 7,200 cal. yr BP – approximately the time when the Baltic from a freshwater lake turned into a semi-enclosed brackish sea – up to date has also maintained constant. These two evidences suggest that since the Baltic has become a brackish sea the resident community of heterocystous cyanobacteria has maintained mostly unchanged, in spite of changes in the temperature, salinity and geochemistry of the water column (Gustafsson, 2002; Warden, 2017). However, the HG record relative to this period of time shows a substantial decrease with increasing depth of the gravity core, independently from other geochemical records (i.e. total organic carbon (TOC) content and temperature record). Potential causes include a decrease in the occurrence of the cyanobacterial blooms or a diagenetic process, resulting in partial degradation of the HGs. This makes the HG abundance record unsuitable to be confidently coupled directly with cyanobacterial blooms and the recurring anoxic events

that happened in the Baltic Sea since it became a brackish sea. Before this, the Baltic was a freshwater lake (i.e. Ancylus Lake phase) and previously and for a short period, a sea named Yoldia. During these two phases the waters column was supposedly well oxygenated as the low TOC signal suggests. The HG abundance continues to decrease in the down core that records these two phases and is at least an order of magnitude lower than in the first part of the brackish phase. This lower abundance might indicate that N_2-fixing cyanobacteria were much less abundant during the freshwater phase than in the subsequent brackish phase. The record of $\delta^{15}N$ values also suggests a lower abundance of diazotrophic phytoplankton during the Ancylus Lake and Yoldia Sea phases (Bauersachs et al., 2009c; Rejmánková et al., 2004; Zakrisson et al., 2014). In addition, the HG distribution was distinct and more diverse than that of the following brackish phase and the modern Baltic Sea, suggesting that the cyanobacterial community adjusted to the different environmental conditions in the basin over this transition. Both salinity and temperature are likely to have influenced the abundance and composition of the heterocystous cyanobacterial community of the Baltic since the last deglaciation (Bauersachs et al., 2014b; Kabel et al., 2012; Mazur-Marzec et al., 2005; Moisander et al., 2002; Staal et al., 2003).

Outlook

In the last few years the methods available to investigate the marine microbial communities and the biogeochemical processes they participate have greatly increased. These improvements are visible in this thesis. The high throughput sequencing techniques now available permit to detect a much broader microbial diversity than in the past. Similarly, the variety of IPL biomarkers we are now able to detect directly from water and sediment samples is much higher than it was when this project started. This has allowed to fill some relevant gaps in the knowledge of the microbial species involved in the modern marine nitrogen cycle and in other elements' cycles and to hypothesize relationships among microbial species. For instance in this thesis we found a broader variety of Archaea living in the ETSP and in the Black Sea water columns than previously known, in a very specific depth partitioning. It would be interesting to continue investigating these communities by dedicated genome analysis to shed light on the energy metabolisms or strategies used by the groups detected to cope with specific environmental features such as the high sulfide concentrations present in the euxinic zone if the Black Sea or

the extremely low oxygen of the ODZs. Similarly, we have identified new potential IPL biomarkers which would need to be further investigated and tested in other settings, until cultures become available. We have confirmed that IPLs can be successfully used as biomarkers of living microorganism such as Thaumarchaeota and anammox bacteria. The relationship between these two groups, however, needs to be further addressed in the future, considering its potential relevance in the ocean. Finally, by applying specific IPLs we have investigated how the cyanobacterial communities have changed in the past ocean in response to changing environmental conditions. Further studies are needed also in this case to extend the range of heterocystous cyanobacteria species investigated in culture for their HG content and to further test the potential of these IPL in paleoclimate studies.

References

Adam, P. S., Borrel, G., Brochier-Armanet, C., and Gribaldo, S. (2017). The growing tree of Archaea: New perspectives on their diversity, evolution and ecology. *ISME J.* 11, 2407–2425. doi:10.1038/ismej.2017.122.

Adams, D. G. (2000). Heterocyst formation in cyanobacteria. *Curr. Opin. Microbiol.* 3, 618–624. doi:10.1016/S1369-5274(00)00150-8.

Agawin, N. S. R., Benavides, M., Busquets, A., Ferriol, P., Stal, L. J., and Arístegui, J. (2014). Dominance of unicellular cyanobacteria in the diazotrophic community in the Atlantic Ocean. *Limnol. Oceanogr.* 59, 623–637. doi:10.4319/lo.2014.59.2.0623.

Altschul, S. F., Gish, W., Miller, W., Myers, E. W., and Lipman, D. J. (1990). Basic local alignment search tool. *J. Mol. Biol.* 215, 403–410. doi:10.1016/S0022-2836(05)80360-2.

Amann, R. I., Ludwig, W., Schleifer, K. H., Amann, R. I., and Ludwig, W. (1995). Phylogenetic identification and in situ detection of individual microbial cells without cultivation. *Microbiol. Rev.* 59, 143–169.

Andrén, E., Andrén, T., and Kunzendorf, H. (2000). Holocene history of the Baltic Sea as a background for assessing records of human impact in the sediments of the Gotland Basin. *The Holocene* 10, 687–702. doi:10.1191/09596830094944.

Andrén, T., Björck, S., Andrén, E., Conley, D. J., Zillén, L., and Anjar, J. (2011). "The Development of the Baltic Sea Basin During the Last 130 ka," in *The Baltic Sea Basin - Central and Eastern European Development Studies (CEEDES)*, eds. J. Harff, S. Björck, and P. Hoth (Springer), 75–97. doi:10.1007/978-3-642-17220-5_4.

Arrigo, K. R. (2005). Marine microorganisms and global nutrient cycles. *Nature* 437, 349–356. doi:10.1038/nature0415.

Babbin, A. R., Keil, R. G., Devol, A. H., and Ward, B. B. (2014). Organic Matter Stoichiometry, Flux, and Oxygen Control Nitrogen Loss in the Ocean. *Science (80-.).*, 1–6. doi:10.1126/science.1248364.

Baker, B. J., Sheik, C. S., Taylor, C. A., Jain, S., Bhasi, A., Cavalcoli, J. D., et al. (2013). Community transcriptomic assembly reveals microbes that contribute to deep-sea carbon and nitrogen cycling. *ISME J.* 7, 1962–1973. doi:10.1038/ismej.2013.85.

Bale, N. J., Hopmans, E. C., Schoon, P. L., de Kluijver, A., Downing, J. A., Middelburg, J. J., et al. (2016). Impact of trophic state on the distribution of intact polar lipids in surface waters of lakes. *Limnol. Oceanogr.* 61, 1065–1077. doi:10.1002/lno.10274.

Bale, N. J., Hopmans, E. C., Zell, C., Lima Sobrinho, R., Kim, J. H., Sinninghe Damsté, J. S., et al. (2015). Long chain glycolipids with pentose head groups as biomarkers for marine endosymbiotic heterocystous cyanobacteria. *Org. Geochem.* 81, 1–7. doi:10.1016/j.orggeochem.2015.01.004.

Bale, N. J., Villanueva, L., Hopmans, E. C., Schouten, S., and Sinninghe Damsté, J. S. (2013). Different seasonality of pelagic and benthic Thaumarchaeota in the North Sea. *Biogeosciences Discuss.* 10, 12593–12624. doi:10.5194/bg-10-7195-2013.

Bale, N. J., Villareal, T. A., Hopmans, E. C., Brussaard, C. P. D., Besseling, M., Dorhout, D., et al. (2018). C_5 glycolipids of heterocystous cyanobacteria track symbiont abundance in the diatom *Hemiaulus hauckii* across the tropical North Atlantic. *Biogeosciences* 15, 1229–1241. doi:10.5194/bg-15-1229-2018.

Bano, N., Ruffin, S., Ransom, B., and Hollibaugh, J. T. (2004). Phylogenetic Composition of Arctic Ocean Archaeal Assemblages and Comparison with Antarctic Assemblages. *Appl. Environ. Microbiol.* 70, 781–789. doi:10.1128/AEM.70.2.781-789.2004.

Bauersachs, T., Compaoré, J., Hopmans, E. C., Stal, L. J., Schouten, S., and Sinninghe Damsté, J. S. (2009a). Distribution of heterocyst glycolipids in cyanobacteria. *Phytochemistry* 70, 2034–2039. doi:10.1016/j.phytochem.2009.08.014.

Bauersachs, T., Compaoré, J., Severin, I., Hopmans, E. C., Schouten, S., Stal, L. J., et al. (2011). Diazotrophic microbial community of coastal microbial mats of the southern North Sea. *Geobiology* 9, 349–359. doi:10.1111/j.1472-4669.2011.00280.x.

Bauersachs, T., Hopmans, E. C., Compaoré, J., Stal, L. J., Schouten, S., and Sinninghe Damsté, J. S. (2009b). Rapid analysis of long-chain glycolipids in heterocystous cyanobacteria using high-performance liquid chromatography coupled to electrospray ionization tandem

mass spectrometry. *Rapid Commun. Mass Spectrom.* 23, 1387–1394. doi:10.1002/rcm.

Bauersachs, T., Miller, S. R., van Der Meer, M. T. J., Hopmans, E. C., Schouten, S., and Sinninghe Damsté, J. S. (2013). Distribution of long chain heterocyst glycolipids in cultures of the thermophilic cyanobacterium *Mastigocladus laminosus* and a hot spring microbial mat. *Org. Geochem.* 56, 19–24. doi:10.1016/j.orggeochem.2012.11.013.

Bauersachs, T., Mudimu, O., Schulz, R., and Schwark, L. (2014a). Distribution of long chain heterocyst glycolipids in N_2-fixing cyanobacteria of the order Stigonematales. *Phytochemistry* 98, 145–150. doi:10.1016/j.phytochem.2013.11.007.

Bauersachs, T., Rochelmeier, J., and Schwark, L. (2015a). Seasonal lake surface water temperature trends reflected by heterocyst glycolipid-based molecular thermometers. *Biogeosciences* 12, 3741–3751. doi:10.5194/bg-12-3741-2015.

Bauersachs, T., Schouten, S., Compaoré, J., Wollenzien, U., Stal, L. J., and Sinninghe Damsté, J. S. (2009c). Nitrogen isotopic fractionation associated with growth on dinitrogen gas and nitrate by cyanobacteria. *Limnol. Oceanogr.* 54, 1403–1411. doi:10.4319/lo.2009.54.4.1403.

Bauersachs, T., Speelman, E. N., Hopmans, E. C., Reichart, G.-J., Schouten, S., and Sinninghe Damsté, J. S. (2010). Fossilized glycolipids reveal past oceanic N_2 fixation by heterocystous cyanobacteria. *Proc. Natl. Acad. Sci.* 107, 19190–19194. doi:10.1073/pnas.1007526107.

Bauersachs, T., Stal, L. J., Grego, M., and Schwark, L. (2014b). Temperature induced changes in the heterocyst glycolipid composition of N_2 fixing heterocystous cyanobacteria. *Org. Geochem.* 69, 98–105. doi:10.1016/j.orggeochem.2014.02.006.

Bauersachs, T., Talbot, H. M., Sidgwick, F., Sivonen, K., and Schwark, L. (2017). Lipid biomarker signatures as tracers for harmful cyanobacterial blooms in the Baltic Sea. *PLoS One*, 1–25. doi:https://doi.org/10.1371/journal.pone.0186360.

Bauersachs, T., Weidenbach, K., Schmitz, R. A., and Schwark, L. (2015b). Distribution of glycerol ether lipids in halophilic, methanogenic

and hyperthermophilic archaea. *Org. Geochem.* 83–84, 101–108. doi:10.1016/j.orggeochem.2015.03.009.

Becker, K. W., Elling, F. J., Yoshinaga, M. Y., Söllinger, A., Urich, T., and Hinrichs, K.-U. (2016). Unusual butane- and pentanetriol-based tetraether lipids in Methanomassiliicoccus Luminyensis, a representative of the seventh order of methanogens. *Appl. Environ. Microbiol.* 82, 4505–4516. doi:10.1128/AEM.00772-16.

Belmar, L., Molina, V., and Ulloa, O. (2011). Abundance and phylogenetic identity of archaeoplankton in the permanent oxygen minimum zone of the eastern tropical South Pacific. *FEMS Microbiol. Ecol.* 78, 314–326. doi:10.1111/j.1574-6941.2011.01159.x.

Beman, J. M., Popp, B. N., and Alford, S. E. (2012). Quantification of ammonia oxidation rates and ammonia-oxidizing archaea and bacteria at high resolution in the Gulf of California and eastern tropical North Pacific Ocean. *Limnol. Oceanogr.* 57, 711–726. doi:10.4319/lo.2012.57.3.0711.

Beman, J. M., Popp, B. N., and Francis, C. A. (2008). Molecular and biogeochemical evidence for ammonia oxidation by marine Crenarchaeota in the Gulf of California. *ISME J.* 2, 429–441. doi:10.1038/ismej.2007.118.

Beman, J. M., Shih, J. L., and Popp, B. N. (2013). Nitrite oxidation in the upper water column and oxygen minimum zone of the eastern tropical North Pacific Ocean. *ISME J.* 7, 2192–2205. doi:10.1038/ismej.2013.96.

Benavides, M., Agawin, N., Arístegui, J., Ferriol, P., and Stal, L. (2011). Nitrogen fixation by *Trichodesmium* and small diazotrophs in the subtropical northeast Atlantic. *Aquat. Microb. Ecol.* 65, 43–53. doi:10.3354/ame01534.

Berg, C., Vandieken, V., Thamdrup, B., and Jurgens, K. (2014). Significance of archaeal nitrification in hypoxic waters of the Baltic Sea. *ISME J.* 9, 1319–1332. doi:10.1038/ismej.2014.218.

Bertagnolli, A. D., and Ulloa, O. (2017). Hydrography shapes *amo*A containing Thaumarcheota in the coastal waters off central Chile. *Environ.*

Microbiol. Rep. 9, 717–728. doi:10.1111/1758-2229.12579.

Besseling, M. A., Hopmans, E. C., Sinninghe Damsté, J. S., and Villanueva, L. (2018). Benthic Archaea as potential sources of tetraether membrane lipids in sediments across an oxygen minimum zone. *Biogeosciences Discuss.*, 1–30. doi:10.5194/bg-2017-289.

Betlach, M. R., and Tiedje, J. M. (1981). Kinetic Explanation for Accumulation of Nitrite, Nitric Oxide, and Nitrous Oxide during Bacterial Denitrification. *Appl. Environ. Microbiol.* 42, 1074–1084. doi:Article.

Bianchi, D., Babbin, A. R., Galbraith, E. D., and Karl, D. M. (2014). Enhancement of anammox by the excretion of diel vertical migrators. *Proc. Natl. Acad. Sci.* 15, 1–6. doi:10.1073/pnas.1410790111.

Bianchi, T. S., Engelhaupt, E., Westman, P., Andrén, T., Rolff, C., and Elmgren, R. (2000). Cyanobacterial blooms in the Baltic Sea: Natural or human-induced? *Limnol. Oceanogr.* 45, 716–726. doi:10.4319/lo.2000.45.3.0716.

Biddle, J. F., Lipp, J. S., Lever, M. A., Lloyd, K. G., Sørensen, K. B., Anderson, R., et al. (2006). Heterotrophic Archaea dominate sedimentary subsurface ecosystems off Peru. *Proc. Natl. Acad. Sci. U. S. A.* 103, 3846–3851. doi:10.1073/pnas.0600035103.

Björck, S. (1995). A review of the history of the Baltic Sea, 13.0-8.0 ka BP. *Quat. Int.* 27, 19–40. doi:10.1016/1040-6182(94)00057-C.

Blumenberg, M., Seifert, R., Reitner, J., Pape, T., and Michaelis, W. (2004). Membrane lipid patterns typify distinct anaerobic methanotrophic consortia. *Proc. Natl. Acad. Sci.* 101, 11111–11116. doi:10.1073/pnas.0401188101.

Boetius, A., Ravenschlag, K., Schubert, C. J., Rickert, D., Widdel, F., Gieseke, A., et al. (2000). A marine microbial consortium apparently mediating anaerobic oxidation of methane. *Nature* 407, 623–626. doi:10.1038/35036572.

Borgendahl, J., and Westman, P. (2007). Cyanobacteria as a trigger for increased primary productivity during sapropel formation in the Baltic Sea—a study of the Ancylus/Littorina transition. *J. Paleolimnol.* 38,

1–12. doi:10.1007/s10933-006-9055-0.

Boschker, H. T. S., and Middelburg, J. J. (2002). Stable isotopes and biomarkers in microbial ecology. *FEMS Microbiol. Ecol.* 40, 85–95. doi:10.1016/S0168-6496(02)00194-0.

Boschker, H. T. S., Nold, S. C., Wellsbury, P., Bos, D., de Graaf, W., Pel, R., et al. (1998). Direct linking of microbial populations to specific biogeochemical processes by ^{13}C-labelling of biomarkers. *Nature* 392, 801–804. doi:10.1038/33900.

Boumann, H. A., Hopmans, E. C., van de Leemput, I., Op den Camp, H. J. M., van de Vossenberg, J., Strous, M., et al. (2006). Ladderane phospholipids in anammox bacteria comprise phosphocholine and phosphoethanolamine headgroups. *FEMS Microbiol. Lett.* 258, 297–304. doi:10.1111/j.1574-6968.2006.00233.x.

De Brabandere, L., Canfield, D. E., Dalsgaard, T., Friederich, G. E., Revsbech, N. P., Ulloa, O., et al. (2014). Vertical partitioning of nitrogen-loss processes across the oxic-anoxic interface of an oceanic oxygen minimum zone. *Environ. Microbiol.* 16, 3041–3054. doi:10.1111/1462-2920.12255.

Braker, G., Fesefeldt, A., and Witzel, K.-P. (1998). Development of PCR Primer Systems for Amplification of Nitrite Reductase Genes (*nir*K and *nir*S) To Detect Denitrifying Bacteria in Environmental Samples. *Appl. Environ. Microbiol.* 64, 3769–3775. Available at: http://aem.asm.org/cgi/content/abstract/64/10/3769.

Bristow, L. A., Dalsgaard, T., Tiano, L., Mills, D. B., Bertagnolli, A. D., Wright, J. J., et al. (2016). Ammonium and nitrite oxidation at nanomolar oxygen concentrations in oxygen minimum zone waters. *Proc. Natl. Acad. Sci.* 113, 10601–6. doi:10.1073/pnas.1600359113.

Brochier-Armanet, C., Boussau, B., Gribaldo, S., and Forterre, P. (2008). Mesophilic Crenarchaeota: proposal for a third archaeal phylum, the Thaumarchaeota. *Nat. Rev. Microbiol.* 6, 245–252. doi:10.1038/nrmicro1852.

Broda, E. (1977). Two kinds of lithotrophs missing in nature. *Zeitschrift für Allg. Mikrobiol.* 493, 491–493.

Bryce, T. A., Welti, D., Walsby, A. E., and Nichols, B. W. (1972). Monohexoside derivatives of long-chain polyhydroxy alcohols; a novel class of glycolipid specific to heterocystous algae. *Phytochemistry* 11, 295–302. doi:10.1016/S0031-9422(00)90006-2.

Buckles, L. K., Villanueva, L., Weijers, J. W. H., Verschuren, D., and Sinninghe Damsté, J. S. (2013). Linking isoprenoidal GDGT membrane lipid distributions with gene abundances of ammonia-oxidizing Thaumarchaeota and uncultured crenarchaeotal groups in the water column of a tropical lake (Lake Challa, East Africa). *Environ. Microbiol.*, 1–34. doi:10.1111/1462-2920.12118.

Bulow, S. E., Rich, J. J., Naik, H. S., Pratihary, A. K., and Ward, B. B. (2010). Denitrification exceeds anammox as a nitrogen loss pathway in the Arabian Sea oxygen minimum zone. *Deep. Res. Part I* 57, 384–393. doi:10.1016/j.dsr.2009.10.014.

Burgin, A. J., and Hamilton, S. K. (2007). Nitrate removal in aquatic ecosystems. *Front. Ecol. Environ.* 5, 89–96.

Cabello, P., Roldán, M. D., and Moreno-Vivián, C. (2004). Nitrate reduction and the nitrogen cycle in archaea. *Microbiology* 150, 3527–3546. doi:10.1099/mic.0.27303-0.

Canfield, D. E., Stewart, F. J., Thamdrup, B., De Brabandere, L., Dalsgaard, T., Delong, E. F., et al. (2010). A cryptic sulfur cycle in oxygen-minimum-zone waters off the Chilean coast. *Science* 330, 1375–1378. doi:10.1126/science.1196889.

Capone, D. G., Burns, J. A., Montoya, J. P., Subramaniam, A., Mahaffey, C., Gunderson, T., et al. (2005). Nitrogen fixation by *Trichodesmium* spp.: An important source of new nitrogen to the tropical and subtropical North Atlantic Ocean. *Global Biogeochem. Cycles* 19, 1–17. doi:10.1029/2004GB002331.

Caporaso, J. G., Kuczynski, J., Stombaugh, J., Bittinger, K., Bushman, F. D., Costello, E. K., et al. (2010). QIIME allows analysis of high-throughput community sequencing data. *Nat. Methods* 7, 335–336. doi:10.1038/nmeth0510-335.

Carpenter, E. J., Montoya, J. P., Burns, J. A., Mulholland, M. R., Subrama-

niam, A., and Capone, D. G. (1999). Extensive bloom of a N_2-fixing symbiotic association in the tropical Atlantic Ocean. *Mar. Ecol. Prog. Ser.* 185, 273–283.

Castañeda, I. S., and Schouten, S. (2011). A review of molecular organic proxies for examining modern and ancient lacustrine environments. *Quat. Sci. Rev.* 30, 2851–2891. doi:10.1016/j.quascirev.2011.07.009.

Castelle, C. J., Wrighton, K. C., Thomas, B. C., Hug, L. A., Brown, C. T., Wilkins, M. J., et al. (2015). Genomic expansion of domain archaea highlights roles for organisms from new phyla in anaerobic carbon cycling. *Curr. Biol.* 25, 690–701. doi:10.1016/j.cub.2015.01.014.

Castro-González, M., Braker, G., Farías, L., and Ulloa, O. (2005). Communities of *nir*S-type denitrifiers in the water column of the oxygen minimum zone in the eastern South Pacific. *Environ. Microbiol.* 7, 1298–1306. doi:10.1111/j.1462-2920.2005.00809.x.

Celepli, N., Sundh, J., Ekman, M., Dupont, C. L., Yooseph, S., Bergman, B., et al. (2017). Meta-omic analyses of Baltic Sea cyanobacteria: diversity, community structure and salt acclimation. *Environ. Microbiol.* 19, 673–686. doi:10.1111/1462-2920.13592.

Chang, B. X., Rich, J. R., Jayakumar, A., Naik, H. S., Pratihary, A. K., Keil, R. G., et al. (2014). The effect of organic carbon on fixed nitrogen loss in the eastern tropical South Pacific and Arabian Sea oxygen deficient zones. *Limnol. Oceanogr.* 59, 1267–1274. doi:10.4319/lo.2014.59.4.1267.

Codispoti, L. A. (1997). The limits to growth. *Nature* 387, 237–238. doi:10.1046/j.1463-1326.1999.00023.x.

Codispoti, L. A., Brandes, J. A., Christensen, J. P., Devol, A. H., Naqvi, S. W. A., Paerl, H. W., et al. (2001). The oceanic fixed nitrogen and nitrous oxide budgets: Moving targets as we enter the anthropocene? *Sci. Mar.* 65, 85–105. doi:10.3989/scimar.2001.65s285.

Coolen, M. J. L., Abbas, B., Van Bleijswijk, J., Hopmans, E. C., Kuypers, M. M. M., Wakeham, S. G., et al. (2007). Putative ammonia-oxidizing Crenarchaeota in suboxic waters of the Black Sea: A basin-wide ecological study using 16S ribosomal and functional genes and mem-

brane lipids. *Environ. Microbiol.* 9, 1001–1016. doi:10.1111/j.1462-2920.2006.01227.x.

Daims, H., Lebedeva, E. V., Pjevac, P., Han, P., Herbold, C., Albertsen, M., et al. (2015). Complete nitrification by *Nitrospira* bacteria. *Nature* 528, 504–509. doi:10.1038/nature16461.

Dalsgaard, T., Canfield, D. E., Petersen, J., Thamdrup, B., and Acuña-González, J. (2003). N_2 production by the anammox reaction in the anoxic water column of Golfo Dulce, Costa Rica. *Nature* 422, 606–608. doi:10.1038/nature01526.

Dalsgaard, T., Thamdrup, B., Farías, L., and Revsbech, N. P. (2012). Anammox and denitrification in the oxygen minimum zone of the eastern South Pacific. *Limnol. Oceanogr.* 57, 1331–1346. doi:10.4319/lo.2012.57.5.1331.

Delong, E. F. (1992). Archaea in coastal marine environments. *Proc. Natl. Acad. Sci.* 89, 5685–5689. doi:10.1073/pnas.89.12.5685.

Deschamps, P., Zivanovic, Y., Moreira, D., Rodriguez-Valera, F., and López-García, P. (2014). Pangenome evidence for extensive interdomain horizontal transfer affecting lineage coreandshell genes inuncultured planktonic thaumarchaeota and euryarchaeota. *Genome Biol. Evol.* 6, 1549–1563. doi:10.1093/gbe/evu127.

Dore, J. E., Brum, J. R., Tupas, L., and Karl, D. M. (2002). Seasonal and interannual variability in sources of nitrogen supporting export in the oligotrophic subtropical North Pacific Ocean . *Limnol. Ocean.* 47, 1595–1607.

Durbin, A. M., and Teske, A. (2011). Microbial diversity and stratification of South Pacific abyssal marine sediments. *Environ. Microbiol.* 13, 3219–3234. doi:10.1111/j.1462-2920.2011.02544.x.

Edgar, R. C. (2004). MUSCLE: Multiple sequence alignment with high accuracy and high throughput. *Nucleic Acids Res.* 32, 1792–1797. doi:10.1093/nar/gkh340.

Eglinton, T. I., and Eglinton, G. (2008). Molecular proxies for paleoclimatology. *Earth Planet. Sci. Lett.* 275, 1–16. doi:10.1016/j.

epsl.2008.07.012.

Ellen, A. F., Albers, S. V., Huibers, W., Pitcher, A., Hobel, C. F. V, Schwarz, H., et al. (2009). Proteomic analysis of secreted membrane vesicles of archaeal *Sulfolobus* species reveals the presence of endosome sorting complex components. *Extremophiles* 13, 67–79. doi:10.1007/s00792-008-0199-x.

Elling, F. J., Könneke, M., Lipp, J. S., Becker, K. W., Gagen, E. J., and Hinrichs, K.-U. (2014). Effects of growth phase on the membrane lipid composition of the thaumarchaeon *Nitrosopumilus maritimus* and their implications for archaeal lipid distributions in the marine environment. *Geochim. Cosmochim. Acta* 141, 579–597. doi:10.1016/j.gca.2014.07.005.

Elling, F. J., Könneke, M., Nicol, G. W., Stieglmeier, M., Bayer, B., Spieck, E., et al. (2017). Chemotaxonomic characterisation of the thaumarchaeal lipidome. *Environ. Microbiol.* 19, 2681–2700. doi:10.1111/1462-2920.13759.

Eloe-Fadrosh, E. A., Ivanova, N. N., Woyke, T., and Kyrpides, N. C. (2016). Metagenomics uncovers gaps in amplicon-based detection of microbial diversity. *Nat. Microbiol.* 1, 15032. doi:10.1038/nmicrobiol.2015.32.

Eme, L., and Ford Doolittle, W. (2015). Microbial diversity: A bonanza of phyla. *Curr. Biol.* 25, R227–R230. doi:10.1016/j.cub.2014.12.044.

Emeis, K.-C., Neumann, T., Endler, R., Struck, U., Kunzendorf, H., and Christiansen, C. (1998). Geochemical records of sediments in the Eastern Gotland Basin--products of sediment dynamics in a not-so-stagnant anoxic basin? *Appl. Geochemistry* 13, 349–358. doi:10.1016/S0883-2927(97)00104-2.

Emerson, S. R., and Hedges, J. (2008). *Chemical oceanography and the marine carbon cycle*. , eds. S. Emerson and J. Hedges Cambridge University Press doi:978-0-521-83313-4.

Erguder, T. H., Boon, N., Wittebolle, L., Marzorati, M., and Verstraete, W. (2009). Environmental factors shaping the ecological niches of ammonia-oxidizing archaea. *FEMS Microbiol. Rev.* 33, 855–869. doi:10.1111/j.1574-6976.2009.00179.x.

Ettwig, K. F., Butler, M. K., Le Paslier, D., Pelletier, E., Mangenot, S., Kuypers, M. M. M., et al. (2010). Nitrite-driven anaerobic methane oxidation by oxygenic bacteria. *Nature* 464, 543–548. doi:10.1038/nature08883.

Evans, P. N., Parks, D. H., Chadwick, G. L., Robbins, S. J., Orphan, V. J., Golding, S. D., et al. (2015). Methane metabolism in the archaeal phylum Bathyarchaeota revealed by genome-centric metagenomics. *Science* 350, 434–438. doi:10.1126/science.aac7745.

Falcón, L. I., Carpenter, E. J., Cipriano, F., Bergman, B., and Capone, D. G. (2004). N_2 Fixation by Unicellular Bacterioplankton from the Atlantic and Pacific Oceans: Phylogeny and In Situ Rates. *Appl. Environ. Microbiol.* 70, 765–770. doi:10.1128/AEM.70.2.765.

Falkowski, P. G. (1997). Evolution of the nitrogen cycle and its influence on the biological sequestration of CO_2 in the ocean. *Nature* 387, 272–275. doi:10.1038/387272a0.

Falkowski, P. G., Scholes, R. J., Boyle, E., Canadell, J., Canfield, D. E., Elser, J., et al. (2000). The Global Carbon Cycle: A Test of Our Knowledge of Earth as a System. *Science (80-.).* 290, 291–296. doi:10.1126/science.290.5490.291.

Feely, R. A., Doney, S. C., and Cooley, S. R. (2009). Ocean acidification: present conditions and future changes in a high-CO_2 world. *Oceanography* 22, 36–47. doi:doi:10.5670/oceanog.2009.95.

Ferrer, M., Guazzaroni, M. E., Richter, M., García-Salamanca, A., Yarza, P., Suárez-Suárez, A., et al. (2011). Taxonomic and Functional Metagenomic Profiling of the Microbial Community in the Anoxic Sediment of a Sub-saline Shallow Lake (Laguna de Carrizo, Central Spain). *Microb. Ecol.* 62, 824–837. doi:10.1007/s00248-011-9903-y.

Fiedler, P. C., and Lavín, M. F. (2006). Introduction: A review of eastern tropical Pacific oceanography. *Prog. Oceanogr.* 69, 94–100. doi:10.1016/j.pocean.2006.03.006.

Fiedler, P. C., and Talley, L. D. (2006). Hydrography of the eastern tropical Pacific: A review. *Prog. Oceanogr.* doi:10.1016/j.pocean.2006.03.008.

Field, C. B., Behrenfield, M. J., Randerson, J. T., and Falkowski, P. G.

(1998). Primary Production of the Biosphere: Integrating Terrestrial and Oceanic Components. *Science (80-.).* 281, 237-. doi:10.1126/science.281.5374.237.

Fillol, M., Alexandre Sànchez-Melsió, F. G., and Borrego, C. M. (2015). Diversity of Miscellaneous Crenarchaeotic Group archaea in freshwater karstic lakes and their segregation between planktonic and sediment habitats. *FEMS Microbiol. Ecol.* 91, 1–9. doi:10.1093/femsec/fiv020.

Finni, T., Kononen, K., Olsonen, R., and Wallström, K. (2001). The history of cyanobacterial blooms in the Baltic Sea. *Ambio A J. Hum. Environ.* 30, 172–178. doi:10.1579/0044-7447-30.4.172.

Francis, C. A., Roberts, K. J., Beman, J. M., Santoro, A. E., and Oakley, B. (2005). Ubiquity and diversity of ammonia-oxidizing archaea in water columns and sediments of the ocean. *Proc. Natl. Acad. Sci.* 102, 14683–14688. doi:10.1073/pnas.0506625102.

Freeland, H., Denman, K. L., Wong, C. S., Whitney, F., and Jacques, R. (1997). Evidence of change in the winter mixed layer in the Northeast Pacific Ocean. *Deep Sea Res. Part I* 44, 2117–2129. doi:10.1016/S0967-0637(97)00083-6.

Frigaard, N.-U. U., Martinez, A., Mincer, T. J., and DeLong, E. F. (2006). Proteorhodopsin lateral gene transfer between marine planktonic Bacteria and Archaea. *Nature* 439, 847–850. doi:Doi 10.1038/Nature04435.

Fritz, A. S. C. (1989). Lake Development and Limnological Response to Prehistoric and Historic Land-Use in Diss , Norfolk , U . K . *J. Ecol.* 77, 182–202.

Fry, J. C., Parkes, R. J., Cragg, B. A., Weightman, A. J., and Webster, G. (2008). Prokaryotic biodiversity and activity in the deep subseafloor biosphere. *FEMS Microbiol. Ecol.* 66, 181–196. doi:10.1111/j.1574-6941.2008.00566.x.

Fuhrman, J. A., McCallum, K., and Davis, A. A. (1992). Novel major archaebacterial group from marine plankton. *Nature* 356, 148–149. doi:-doi:10.1038/356148a0.

Funkey, C. P., Conley, D. J., Reuss, N. S., Humborg, C., Jilbert, T., and Slomp, C. P. (2014). Hypoxia sustains cyanobacteria blooms in the Bal-

tic Sea. *Environ. Sci. Technol.* 48, 2598–2602. doi:10.1021/es404395a.

Galán, A., Molina, V., Thamdrup, B., Woebken, D., Lavik, G., Kuypers, M. M. M., et al. (2009). Anammox bacteria and the anaerobic oxidation of ammonium in the oxygen minimum zone off northern Chile. *Deep Sea Res. II* 56, 1021–1031. doi:10.1016/j.dsr2.2008.09.016.

Galand, P. E., Casamayor, E. O., Kirchman, D. L., Potvin, M., and Lovejoy, C. (2009). Unique archaeal assemblages in the Arctic Ocean unveiled by massively parallel tag sequencing. *ISME J.* 3, 860–869. doi:10.1038/ismej.2009.85.

Galloway, J. N., Dentener, F. J., Capone, D. G., Boyer, E. W., Howarth, R. W., Seitzinger, S. P., et al. (2004). Nitrogen cycles: past, present, and future. *Biogeochemistry* 70, 153–226.

Gambacorta, A., Pagnotta, E., Romano, I., Sodano, G., and Trincone, A. (1998). Heterocyst glycolipids from nitrogen-fixing cyanobacteria other than Nostocaceae. *Phytochemistry* 48, 801–205. doi:https://doi.org/10.1016/S0031-9422(97)00954-0.

Gambacorta, A., Soriente, A., Trincone, A., and Sodano, G. (1995). Biosynthesis of the heterocyst glycolipids in the cyanobacterium *Anabaena cylindrica*. *Phytochemistry* 39, 771–774. doi:10.1016/0031-9422(95)00007-T.

Glaubitz, S., Kießlich, K., Meeske, C., Labrenz, M., and Jürgens, K. (2013). SUP05 Dominates the gammaproteobacterial sulfur oxidizer assemblages in pelagic redoxclines of the central baltic and black seas. *Appl. Environ. Microbiol.* 79, 2767–2776. doi:10.1128/AEM.03777-12.

Golyshina, O. V., Toshchakov, S. V., Makarova, K. S., Gavrilov, S. N., Korzhenkov, A. A., La Cono, V., et al. (2017). "ARMAN" archaea depend on association with euryarchaeal host in culture and in situ. *Nat. Commun.* 8, 1–11. doi:10.1038/s41467-017-00104-7.

van de Graaf, A. A., Mulder, A., de Bruijn, P., Jetten, M. S. M., Robertson, L. A., and Kuenen, J. G. (1995). Anaerobic oxidation of ammoinium is a biologically mediated process. *Appl. Environ. Microbiol.* 61, 1246–1251. doi:PMC167380.

Grote, J., Jost, G., Labrenz, M., Herndl, G. J., and Jürgens, K. (2008). Ep-

silonproteobacteria represent the major portion of chemoautotrophic bacteria in sulfidic waters of pelagic redoxclines of the Baltic and Black seas. *Appl. Environ. Microbiol.* 74, 7546–7551. doi:10.1128/AEM.01186-08.

Gruber, N. (2008). "The Marine Nitrogen Cycle: Overview and Challenges," in *Nitrogen in the marine environment*, eds. D. G. Capone, D. A. Bronk, M. R. Mulholland, and E. J. Carpenter (Elsevier), 1–43.

Gruber, N., and Galloway, J. N. (2008). An Earth-system perspective of the global nitrogen cycle. *Nature* 451, 293–6. doi:10.1038/nature06592.

Gustafsson, B. G., and Westman, P. (2002). On the causes for salinity variations in the Baltic Sea during the last 8500 years. *Paleoceanography* 17, 1–14. doi:10.1029/2000PA000572.

Hajdu, S., Höglander, H., and Larsson, U. (2007). Phytoplankton vertical distributions and composition in Baltic Sea cyanobacterial blooms. *Harmful Algae* 6, 189–205. doi:10.1016/j.hal.2006.07.006.

Hallam, S. J., Mincer, T. J., Schleper, C., Preston, C. M., Roberts, K., Richardson, P. M., et al. (2006). Pathways of carbon assimilation and ammonia oxidation suggested by environmental genomic analyses of marine Crenarchaeota. *PLoS Biol.* 4, 520–536. doi:10.1371/journal.pbio.0040095.

Hällfors, G. (2004). Baltic Sea Environment Proceedings No. 95_Checklist of Baltic Sea Phytoplankton Species.

Hamersley, M. R., Lavik, G., Woebken, D., Rattray, J. E., et al. (2007). Anaerobic ammonium oxidation in the Peruvian oxygen minimum zone. *Limnol. Oceanogr.* 52, 923–933. doi:10.4319/lo.2007.52.3.0923.

Hansson, M., and Öberg, J. (2010). Cyanobacterial blooms in the Baltic Sea in 2010. *HELCOM Balt. Sea Environ. Fact Sheets*.

Harhangi, H. R., Le Roy, M., van Alen, T., Hu, B. lan, Groen, J., Kartal, B., et al. (2012). Hydrazine synthase, a unique phylomarker with which to study the presence and biodiversity of anammox bacteria. *Appl. Environ. Microbiol.* 78, 752–758. doi:10.1128/AEM.07113-11.

Haro-Moreno, J. M., Rodriguez-Valera, F., López-García, P., Moreira, D.,

and Martin-Cuadrado, A.-B. (2017). New insights into marine group III Euryarchaeota, from dark to light. *ISME J.*, 1–16. doi:10.1038/ismej.2016.188.

Härtig, E., and Zumft, W. G. (1999). Kinetics of *nir*S expression (cytochrome *cd*1 nitrite reductase) in *Pseudomonas stutzeri* during the transition from aerobic respiration to denitrification: Evidence for a denitrification-specific nitrate- and nitrite-responsive regulatory system. *J. Bacteriol.* 181, 161–166.

Harvey, H. R., Fallon, R. D., and Patton, J. S. (1986). The effect of organic matter and oxygen on the degradation of bacterial membrane lipids in marine sediments. *Geochim. Cosmochim. Acta* 50, 795–804. doi:10.1016/0016-7037(86)90355-8.

He, Y., Li, M., Perumal, V., Feng, X., Fang, J., Xie, J., et al. (2016). Genomic and enzymatic evidence for acetogenesis among multiple lineages of the archaeal phylum Bathyarchaeota widespread in marine sediments. *Nat. Microbiol.* 1, 16035. doi:10.1038/nmicrobiol.2016.35.

Hebsgaard, M. B., Phillips, M. J., and Willerslev, E. (2005). Geologically ancient DNA: Fact or artefact? *Trends Microbiol.* 13, 212–220. doi:10.1016/j.tim.2005.03.010.

Helm, K. P., Bindoff, N. L., and Church, J. A. (2011). Observed decreases in oxygen content of the global ocean. *Geophys. Res. Lett.* 38, 1–6. doi:10.1029/2011GL049513.

Hernández-Sánchez, M. T., Woodward, E. M. S., Taylor, K. W. R., Henderson, G. M., and Pancost, R. D. (2014). Variations in GDGT distributions through the water column in the South East Atlantic Ocean. *Geochim. Cosmochim. Acta* 132, 337–348. doi:10.1016/j.gca.2014.02.009.

Hernandez, D., and Rowe, J. J. (1987). Oxygen Regulation of Nitrate Uptake in Denitrifying *Pseudomonas aeruginosa*. *Appl. Environ. Microbiol.* 53, 745–750.

Hinrichs, K.-U., Hayes, J. M., Sylva, S. P., Brewer, P. G., and DeLong, E. F. (1999). Methane-consuming archaebacteria in marine sediments. *Nature* 398, 802–805. doi:10.1038/19751.

Hinrichs, K.-U., Summons, R. E., Orphan, V. J., Sylva, S. P., and Hayes, J.

M. (2000). Molecular and isotopic analysis of anaerobic methane- oxidizing communities in marine sediments. *Org. Geochem.* 31, 1685–1701.

Hopmans, E. C., Kienhuis, M. V. M., Rattray, J. E., Jaeschke, A., Schouten, S., and Sinninghe Damsté, J. S. (2006). Improved analysis of ladderane lipids in biomass and sediments using high-performance liquid chromatography/atmospheric pressure chemical ionization tandem mass spectrometry. *Rapid Commun. Mass Spectrom.* 20, 2099–2103. doi:10.1002/rcm.2572.

Hopmans, E. C., Schouten, S., Pancost, R. D., van der Meer, M. T. J., and Sinninghe Damsté, J. S. (2000). Analysis of intact tetraether lipids in archaeal cell material and sediments by high performance liquid chromatography/atmospheric pressure chemical ionization mass spectrometry. *Rapid Commun. Mass Spectrom.* 14, 585–589. doi:10.1002/(SICI)1097-0231(20000415)14:7<585::AID-RCM913>3.0.CO;2-N.

Hu, A., Jiao, N., Zhang, R., and Yang, Z. (2011). Niche partitioning of marine group I Crenarchaeota in the euphotic and upper mesopelagic zones of the East China Sea. *Appl. Environ. Microbiol.* 77, 7469–7478. doi:10.1128/AEM.00294-11.

Hugoni, M., Taib, N., Debroas, D., Domaizon, I., Jouan Dufournel, I., Bronner, G., et al. (2013). Structure of the rare archaeal biosphere and seasonal dynamics of active ecotypes in surface coastal waters. *Proc. Natl. Acad. Sci.* 110, 6004–6009. doi:10.1073/pnas.1216863110.

Hyvärinen, H. (1984). The Mastogloia stage in the Baltic Sea history: diatom evidence from southern Finland. *Bull. Geol. Soc. Finl.*, 99–109.

Inagaki, F., Suzuki, M., Takai, K., Oida, H., Sakamoto, T., Aoki, K., et al. (2003). Microbial Communities Associated with Geological Horizons in Coastal Subseafloor Sediments from the Sea of Okhotsk Microbial Communities Associated with Geological Horizons in Coastal Subseafloor Sediments from the Sea of Okhotsk. *Appl. Environ. Microbiol.* 69, 7224–7235. doi:10.1128/AEM.69.12.7224.

Ingalls, A. E., Huguet, C., and Truxal, L. T. (2012). Distribution of Intact and Core Membrane Lipids of Archaeal Glycerol Dialkyl Glycerol Tetraethers among Size-Fractionated Particulate Organic Matter in

Hood Canal , Puget Sound. *Appl. Environ. Microbiol.* 78, 1480–1490. doi:10.1128/AEM.07016-11.

Iverson, V., Morris, R. M., Frazar, C. D., Berthiaume, C. T., Morales, R. L., and Armbrust, E. V. (2012). Untangling Genomes from Metagenomes: Revealing an Uncultured Class of Marine Euryarchaeota. *Science (80-.).* 335, 587–590. doi:10.1126/science.1212665.

Jaeschke, A., Hopmans, E. C., Wakeham, S. G., Schouten, S., and Sinninghe Damsté, J. S. (2007). The presence of ladderane lipids in the oxygen minimum zone of the Arabian Sea indicates nitrogen loss through anammox. doi:10.4319/lo.2007.52.2.0780.

Jaeschke, A., Rooks, C., Trimmer, M., Nicholls, J. C., Hopmans, E. C., Schouten, S., et al. (2009). Comparison of ladderane phospholipid and core lipids as indicators for anaerobic ammonium oxidation (anammox) in marine sediments. *Geochim. Cosmochim. Acta* 73, 2077–2088. doi:10.1016/j.gca.2009.01.013.

Jahn, U., Summons, R., Sturt, H., Grosjean, E., and Huber, H. (2004). Composition of the lipids of *Nanoarchaeum equitans* and their origin from its host Ignicoccus sp. strain KIN4/I. *Arch. Microbiol.* 182, 404–413. doi:10.1007/s00203-004-0725-x.

Jayakumar, A., O'Mullan, G. D., Naqvi, S. W. A., and Ward, B. B. (2009). Denitrifying bacterial community composition changes associated with stages of denitrification in oxygen minimum zones. *Microb. Ecol.* 58, 350–362. doi:10.1007/s00248-009-9487-y.

Jenkyns, H. C. (1980). Cretaceous anoxic events: from continents to oceans. *J. Geol. Soc. London.* 137, 171–188. doi:10.1144/gsjgs.137.2.0171.

Jensen, J. B., Bennike, O., Witkowski, A., Lemke, W., and Kuijpers, A. (1999). Early Holocene history of the southwestern Baltic Sea: The Ancylus Lake stage. *Boreas* 28, 437–453. doi:10.1111/j.1502-3885.1999.tb00233.x.

Jensen, M. M., Lam, P., Revsbech, N. P., Nagel, B., Gaye, B., Jetten, M. S. M., et al. (2011). Intensive nitrogen loss over the Omani Shelf due to anammox coupled with dissimilatory nitrite reduction to ammonium. *ISME J.* 5, 1660–1670. doi:10.1038/ismej.2011.44.

Jensen, M. M., Petersen, J., Dalsgaard, T., and Thamdrup, B. (2009). Pathways, rates, and regulation of N_2 production in the chemocline of an anoxic basin, Mariager Fjord, Denmark. *Mar. Chem.* 113, 102–113. doi:10.1016/j.marchem.2009.01.002.

Junier, P., Molina, V., Dorador, C., Hadas, O., Kim, O. S., Junier, T., et al. (2010). Phylogenetic and functional marker genes to study ammonia-oxidizing microorganisms (AOM) in the environment. *Appl. Microbiol. Biotechnol.* 85, 425–440. doi:10.1007/s00253-009-2228-9.

Kabel, K., Moros, M., Porsche, C., Neumann, T., Adolphi, F., Andersen, T. J., et al. (2012). Impact of climate change on the Baltic Sea ecosystem over the past 1,000 years. *Nat. Clim. Chang.* 2, 871–874. doi:10.1038/nclimate1595.

Kahru, M. (1997). *Monitoring algal blooms : new techniques for detecting large-scale environmental change*. Berlin ; New York: Springer.

Kahru, M., and Elmgren, R. (2014). Multidecadal time series of satellite-detected accumulations of cyanobacteria in the Baltic Sea. *Biogeosciences* 11, 3619–3633. doi:10.5194/bg-11-3619-2014.

Kahru, M., Horstmann, U., and Rud, O. (1994). Satellite Detection of Increased Cyanobacteria Blooms in the Baltic Sea: Natural Fluctuation or Ecosystem Change? *Ambio A J. Hum. Environ.* 23, 469–472. Available at: http://www.jstor.org/stable/4314262.

Kahru, M., Savchuk, O. P., and Elmgren, R. (2007). Satellite measurements of cyanobacterial bloom frequency in the Baltic Sea: Interannual and spatial variability. *Mar. Ecol. Prog. Ser.* 343, 15–23. doi:10.3354/meps06943.

Kalvelage, T., Lavik, G., Lam, P., Contreras, S., Arteaga, L., Löscher, C. R., et al. (2013). Nitrogen cycling driven by organic matter export in the South Pacific oxygen minimum zone. *Nat. Geosci.* 6, 228–234. doi:10.1038/ngeo1739.

Kanoshina, I., Lips, U., and Leppänen, J. M. (2003). The influence of weather conditions (temperature and wind) on cyanobacterial bloom development in the Gulf of Finland (Baltic Sea). *Harmful Algae* 2, 29–41. doi:10.1016/S1568-9883(02)00085-9.

Karjalainen, M., Engström-Ost, J., Korpinen, S., Peltonen, H., Pääkkönen, J.-P., Rönkkönen, S., et al. (2007). Ecosystem consequences of cyanobacteria in the northern Baltic Sea. *Ambio A J. Hum. Environ.* 36, 195–202. doi:10.1579/0044-7447(2007)36[195:ECOCIT]2.0.CO;2.

Karl, D. M., Letelier, R. M., Tupas, L., Dore, J. E., Christian, J., and Hebel, D. (1997). The role of nitrogen fixation in biogeochemical cycling in the subtropical North Pacific Ocean. *Nature* 388, 533–538.

Karner, M. B., DeLong, E. F., and Karl, D. M. (2001). Archaeal dominance in the mesopelagic zone of the Pacific Ocean. *Nature* 409, 507–510. doi:10.1038/35054051.

Karstensen, J., Stramma, L., and Visbeck, M. (2008). Oxygen minimum zones in the eastern tropical Atlantic and Pacific oceans. *Prog. Oceanogr.* 77, 331–350. doi:10.1016/j.pocean.2007.05.009.

Kartal, B., Kuypers, M. M. M., Lavik, G., Schalk, J., Op den Camp, H. J. M., Jetten, M. S. M., et al. (2007). Anammox bacteria disguised as denitrifiers: Nitrate reduction to dinitrogen gas via nitrite and ammonium. *Environ. Microbiol.* 9, 635–642. doi:10.1111/j.1462-2920.2006.01183.x.

Kartal, B., Maalcke, W. J., De Almeida, N. M., Cirpus, I., Gloerich, J., Geerts, W., et al. (2011). Molecular mechanism of anaerobic ammonium oxidation. *Nature* 479, 127–130. doi:10.1038/nature10453.

Kaur, A. A., Chaudhary, a., Kaur, A. A., Choudhary, R., and Kaushik, R. (2005). Phospholipid fatty acid - A bioindicator of environment monitoring and assessment in soil ecosystem. *Curr. Sci.* 89, 1103–1112.

Keeling, R. E., Körtzinger, A., and Gruber, N. (2010). Ocean deoxygenation in a warming world. *Ann. Rev. Mar. Sci.* 2, 199–229. doi:10.1146/annurev.marine.010908.163855.

van Kessel, M. A. H. J., Speth, D. R., Albertsen, M., Nielsen, P. H., Op Den Camp, H. J. M., Kartal, B., et al. (2015). Complete nitrification by a single microorganism. *Nature* 528, 555–559. doi:10.1038/nature16459.

Kessler, W. S. (2006). The circulation of the eastern tropical Pacific: A review. *Prog. Oceanogr.* 69, 181–217. doi:10.1016/j.pocean.2006.03.009.

Killops, S., and Killops, V. (2005). *Introduction to Organic Geochemistry.* 2nd ed. , eds. S. Killops and V. Killops Blackwell.

Kim, J. H., Schouten, S., Rodrigo-Gámiz, M., Rampen, S., Marino, G., Huguet, C., et al. (2015). Influence of deep-water derived isoprenoid tetraether lipids on the TEX_{86}^{H} paleothermometer in the Mediterranean Sea. *Geochim. Cosmochim. Acta* 150, 125–141. doi:10.1016/j.gca.2014.11.017.

Kim, J. H., Villanueva, L., Zell, C., and Sinninghe Damsté, J. S. (2016). Biological source and provenance of deep-water derived isoprenoid tetraether lipids along the Portuguese continental margin. *Geochim. Cosmochim. Acta* 172, 177–204. doi:10.1016/j.gca.2015.09.010.

Klindworth, A., Pruesse, E., Schweer, T., Peplies, J., Quast, C., Horn, M., et al. (2013). Evaluation of general 16S ribosomal RNA gene PCR primers for classical and next-generation sequencing-based diversity studies. *Nucleic Acids Res.* 41, 1–11. doi:10.1093/nar/gks808.

Koeve, W., and Kähler, P. (2010). Heterotrophic denitrification vs. autotrophic anammox-quantifying collateral effects on the oceanic carbon cycle. *Biogeosciences* 7, 2327–2337. doi:10.5194/bg-7-2327-2010.

Koga, Y., Akagawa-Matsushita, M., Ohga, M., and Nishihara, M. (1993). Taxonomic significance of the distribution of component parts of polar ether lipids in methanogens. *Syst. Appl. Microbiol.* 16, 342–351. Available at: http://cat.inist.fr/?aModele=afficheN&cpsidt=3804808 [Accessed March 30, 2016].

Koga, Y., and Morii, H. (2007). Biosynthesis of Ether-Type Polar Lipids in Archaea and Evolutionary Considerations. *Microbiol. Mol. Biol. Rev.* 71, 97–120. doi:10.1128/MMBR.00033-06.

Könneke, M., Bernhard, A. E., de la Torre, J. R., Walker, C. B., Waterbury, J. B., and Stahl, D. A. (2005). Isolation of an autotrophic ammonia-oxidizing marine archaeon. *Nature* 437, 543–546. doi:10.1038/nature03911.

Könneke, M., Schubert, D. M., Brown, P. C., Hügler, M., Standfest, S., Schwander, T., et al. (2014). Ammonia-oxidizing archaea use the most energy-efficient aerobic pathway for CO_2 fixation. *Proc. Natl. Acad.*

Sci. 111, 8239–8244. doi:10.1073/pnas.1402028111.

Kononen, K. (1992). Dynamics of the toxic cyanobacterial blooms in the Baltic Sea. *Finnish Mar. Reasearch*.

Kononen, K., Kuparinen, J., Kalervo, M., Laanemets, J., Pavelson, J., and Nõmmann, S. (1996). Initiation of cyanobacterial blooms in a frontal region at the entrance to the Gulf of Finland, Baltic Sea. *Limnol. Oceanogr.* 41, 98–112. doi:10.4319/lo.1996.41.1.0098.

Koper, T. E., El-sheikh, A. F., Norton, J. M., and Klotz, M. G. (2004). Urease-Encoding Genes in Ammonia-Oxidizing Bacteria. *Appl. Environ. Microbiol.* 70, 2342–2348. doi:10.1128/AEM.70.4.2342.

Kubo, K., Lloyd, K. G., Biddle, J. F., Amann, R., Teske, A. P., and Knittel, K. (2012). Archaea of the Miscellaneous Crenarchaeotal Group are abundant, diverse and widespread in marine sediments. *ISME J.* 6, 1949–1965. doi:10.1038/ismej.2012.37.

Kutser, T., Metsamaa, L., Strömbeck, N., and Vahtmäe, E. (2006). Monitoring cyanobacterial blooms by satellite remote sensing. *Estuar. Coast. Shelf Sci.* 67, 303–312. doi:10.1016/j.ecss.2005.11.024.

Kuypers, M. M. M. (2015). A division of labour combined. *Nature* 528, 487–8. doi:10.1038/528487a.

Kuypers, M. M. M., Blokker, P., Erbacher, J., Kinkel, H., Pancost, R. D., Schouten, S., et al. (2001). Massive expansion of marine archaea during a mid-Cretaceous oceanic anoxic event. *Science* 293, 92–95. doi:10.1126/science.1058424.

Kuypers, M. M. M., van Breugel, Y., Schouten, S., Erba, E., and Damsté, J. S. S. (2005a). N_2-fixing cyanobacteria supplied nutrient N for Cretaceous oceanic anoxic events. *Geology* 32, 853–856. doi:10.1130/G20458.1.

Kuypers, M. M. M., Lavik, G., Woebken, D., Schmid, M. C., Fuchs, B. M., Amann, R., et al. (2005b). Massive nitrogen loss from the Benguela upwelling system through anaerobic ammonium oxidation. *Proc. Natl. Acad. Sci.* 102, 6478–83. doi:10.1073/pnas.0502088102.

Kuypers, M. M. M., Sliekers, A. O., Lavik, G., and Schmid, M. C. (2003).

Anaerobic ammonium oxidation by anammox bacteria in the Black Sea. *Nature* 422, 2–5. doi:10.1038/nature01526.1.

de la Torre, J. R., Walker, C. B., Ingalls, A. E., Könneke, M., and Stahl, D. A. (2008). Cultivation of a thermophilic ammonia oxidizing archaeon synthesizing crenarchaeol. *Environ. Microbiol.* 10, 810–818. doi:10.1111/j.1462-2920.2007.01506.x.

Labrenz, M., Sintes, E., Toetzke, F., Zumsteg, A., Herndl, G. J., Seidler, M., et al. (2010). Relevance of a crenarchaeotal subcluster related to *Candidatus* Nitrosopumilus maritimus to ammonia oxidation in the suboxic zone of the central Baltic Sea. *ISME J.* 4, 1496–1508. doi:10.1038/ismej.2010.78.

Lam, P., Jensen, M. M., Kock, A., Lettmann, K. A., Plancherel, Y., Lavik, G., et al. (2011). Origin and fate of the secondary nitrite maximum in the Arabian Sea. *Biogeosciences* 8, 1565–1577. doi:10.5194/bg-8-1565-2011.

Lam, P., Jensen, M. M., Lavik, G., McGinnis, D. F., Müller, B., Schubert, C. J., et al. (2007). Linking crenarchaeal and bacterial nitrification to anammox in the Black Sea. *Proc. Natl. Acad. Sci.* 104, 7104–7109. doi:10.1073/pnas.0611081104.

Lam, P., and Kuypers, M. M. M. (2011). Microbial Nitrogen Cycling Processes in Oxygen Minimum Zones. *Ann. Rev. Mar. Sci.* 3, 317–345. doi:10.1146/annurev-marine-120709-142814.

Lam, P., Lavik, G., Jensen, M. M., van de Vossenberg, J., Schmid, M. C., Woebken, D., et al. (2009). Revising the nitrogen cycle in the Peruvian oxygen minimum zone. *Proc. Natl. Acad. Sci.* 106, 4752–7. doi:10.1073/pnas.0812444106.

Lambein, F., and Wolk, C. P. (1973). Structural studies on the glycolipids from the envelope of the heterocyst of *Anabaena cylindrica*. *Biochemistry* 12, 791–798. doi:10.1021/bi00729a002.

Lattuati, A., Guezennec, J., Metzger, P., and Largeau, C. (1998). Lipids of *Thermococcus hydrothermalis*, an archaea isolated from a deep-sea hydrothermal vent. *Lipids* 33, 319–326. doi:10.1007/s11745-998-0211-0.

Lavín, M. F., Fiedler, P. C., Amador, J. A., Ballance, L. T., Färber-Lorda, J.,

and Mestas-Nuñez, A. M. (2006). A review of eastern tropical Pacific oceanography: Summary. *Prog. Oceanogr.* 69, 391–398. doi:10.1016/j.pocean.2006.03.005.

Lazar, C. S., Baker, B. J., Seitz, K. W., and Teske, A. P. (2017). Genomic reconstruction of multiple lineages of uncultured benthic archaea suggests distinct biogeochemical roles and ecological niches. *ISME J.* 11, 1118–1129. doi:10.1038/ismej.2016.189.

Lengger, S. K., Hopmans, E. C., Reichart, G.-J., Nierop, K. G. J., Sinninghe Damsté, J. S., and Schouten, S. (2012). Intact polar and core glycerol dibiphytanyl glycerol tetraether lipids in the Arabian Sea oxygen minimum zone. Part II. Selective preservation and degradation in the water column and consequences for the TEX_{86}. *Geochim. Cosmochim. Acta* 98, 244–258. doi:10.1016/j.gca.2012.05.003.

Lin, X., Wakeham, S. G., Putnam, I. F., Astor, Y. M., Scranton, M. I., Chistoserdov, A. Y., et al. (2006). Comparison of Vertical Distributions of Prokaryotic Assemblages in the Anoxic Cariaco Basin and Black Sea by Use of Fluorescence In Situ Hybridization. *Appl. Environ. Microbiol.* 72, 2679–2690. doi:10.1128/AEM.72.4.2679–2690.2006.

Lincoln, S. A., Wai, B., Eppley, J. M., Church, M. J., Summons, R. E., and DeLong, E. F. (2014a). Planktonic Euryarchaeota are a significant source of archaeal tetraether lipids in the ocean. *Proc. Natl. Acad. Sci.* 111, 9858–9863. doi:10.1073/pnas.1409439111.

Lincoln, S. A., Wai, B., Eppley, J. M., Church, M. J., Summons, R. E., and DeLong, E. F. (2014b). Reply to Schouten: Planktonic Euryarchaeota are a significant source of archaeal tetraether lipids in the ocean. *Proc. Natl. Acad. Sci.* 111, 1409439111-. doi:10.1073/pnas.1409439111.

Lindsay, M. R., Webb, R. I., Strous, M., Jetten, M. S. M., Butler, M. K., Forde, R. J., et al. (2001). Cell compartmentalisation in planctomycetes: Novel types of structural organisation for the bacterial cell. *Arch. Microbiol.* 175, 413–429. doi:10.1007/s002030100280.

Lipp, J. S., and Hinrichs, K.-U. (2009). Structural diversity and fate of intact polar lipids in marine sediments. *Geochim. Cosmochim. Acta* 73, 6816–6833. doi:10.1016/j.gca.2009.08.003.

Lipp, J. S., Morono, Y., Inagaki, F., and Hinrichs, K.-U. (2008). Significant contribution of Archaea to extant biomass in marine subsurface sediments. *Nature* 454, 991–994. doi:10.1038/nature07174.

Lipschultz, F., Wofsy, S. C. C., Ward, B. B., Codispoti, L. A., Friedrich, G., and Elkins, J. W. W. (1990). Bacterial transformations of inorganic nitrogen in the oxygen-deficient waters of the Eastern Tropical South Pacific Ocean. *Deep Sea Res.* 37, 1513–1541. doi:10.1016/0198-0149(90)90060-9.

Lipsewers, Y. A., Bale, N. J., Hopmans, E. C., Schouten, S., Sinninghe Damsté, J. S., Villanueva, L., et al. (2014). Seasonality and depth distribution of the abundance and activity of ammonia oxidizing microorganisms in marine coastal sediments (North Sea). *Front. Ecol. Environ.* 5, 1–12. doi:10.3389/fmicb.2014.00472.

Lipsewers, Y. A., Hopmans, E. C., Sinninghe Damsté, J. S., and Villanueva, L. (2018). Potential recycling of thaumarchaeotal lipids by DPANN Archaea in seasonally hypoxic surface marine sediments. *Org. Geochem.* doi:10.1016/j.orggeochem.2017.12.007.

Liu, X.-L., Lipp, J. S., Simpson, J. H., Lin, Y.-S., Summons, R. E., and Hinrichs, K.-U. (2012). Mono- and dihydroxyl glycerol dibiphytanyl glycerol tetraethers in marine sediments: Identification of both core and intact polar lipid forms. *Geochim. Cosmochim. Acta* 89, 102–115. doi:10.1016/j.gca.2012.04.053.

Liu, X. L., Birgel, D., Elling, F. J., Sutton, P. A., Lipp, J. S., Zhu, R., et al. (2016). From ether to acid: A plausible degradation pathway of glycerol dialkyl glycerol tetraethers. *Geochim. Cosmochim. Acta* 183, 138–152. doi:10.1016/j.gca.2016.04.016.

Lloyd, K. G., Schreiber, L., Petersen, D. G., Kjeldsen, K. U., Lever, M. A., Steen, A. D., et al. (2013). Predominant archaea in marine sediments degrade detrital proteins. *Nature* 496, 215–218. doi:10.1038/nature12033.

López-García, P., Moreira, D., López-López, A., and Rodriguez-Valera, F. (2001). A novel haloarchaeal-related lineage is widely distributed in deep oceanic regions. *Environ. Microbiol.* 3, 72–78. doi:10.1046/j.1462-2920.2001.00162.x.

Ludwig, W., Strunk, O., Westram, R., Richter, L., Meier, H., Yadhukumar, A., et al. (2004). ARB: A software environment for sequence data. *Nucleic Acids Res.* 32, 1363–1371. doi:10.1093/nar/gkh293.

Marine, R., McCarren, C., Vorrasane, V., Nasko, D., Crowgey, E., Polson, S. W., et al. (2014). Caught in the middle with multiple displacement amplification: the myth of pooling for avoiding multiple displacement amplification bias in a metagenome. *Microbiome* 2, 1–8. doi:10.1186/2049-2618-2-3.

Martens-Habbena, W., Berube, P. M., Urakawa, H., de la Torre, J. R., and Stahl, D. A. (2009). Ammonia oxidation kinetics determine niche separation of nitrifying Archaea and Bacteria. *Nature* 461, 976–979. doi:10.1038/nature08465.

Martin-Cuadrado, A.-B., Rodriguez-Valera, F., Moreira, D., Alba, J. C., Ivars-Martínez, E., Henn, M. R., et al. (2008). Hindsight in the relative abundance, metabolic potential and genome dynamics of uncultivated marine archaea from comparative metagenomic analyses of bathypelagic plankton of different oceanic regions. *ISME J.* 2, 865–886. doi:10.1038/ismej.2008.40.

Massana, R., DeLong, E. F., and Pedros-Alio, C. (2000). A Few Cosmopolitan Phylotypes Dominate Planktonic Archaeal Assemblages in Widely Different Oceanic Provinces. *Appl. Environ. Microbiol.* 66, 1777–1787.

Massana, R., Murray, A. E., Preston, C. M., and DeLong, E. F. (1997). Vertical distribution and phylogenetic characterization of marine planktonic Archaea in the Santa Barbara Channel. *Appl. Environ. Microbiol.* 63, 50–56.

Mazur-Marzec, H., Zeglińska, L., and Pliński, M. (2005). The effect of salinity on the growth, toxin production, and morphology of *Nodularia spumigena* isolated from the Gulf of Gdańsk, southern Baltic Sea. *J. Appl. Phycol.* 17, 171–179. doi:10.1007/s10811-005-5767-1.

McCarthy, M. D., Hedges, J. I., and Benner, R. (1998). Major Bacterial Contribution to Marine Dissolved Organic Nitrogen. *Science (80-.).* 281, 231–234. doi:10.1126/science.281.5374.231.

McGowan, S., Britton, G., Haworth, E., and Moss, B. (1999). Ancient

blue-green blooms. *Limnol. Oceanogr.* 44, 436–439. doi:10.4319/lo.1999.44.2.0436.

Meador, T. B., Bowles, M., Lazar, C. S., Zhu, C., Teske, A. P., and Hinrichs, K.-U. (2015). The archaeal lipidome in estuarine sediment dominated by members of the Miscellaneous Crenarchaeotal Group. *Environ. Microbiol.* 17, 2441–2458. doi:10.1111/1462-2920.12716.

Meador, T. B., Gagen, E. J., Loscar, M. E., Goldhammer, T., Yoshinaga, M. Y., Wendt, J., et al. (2014). *Thermococcus kodakarensis* modulates its polar membrane lipids and elemental composition according to growth stage and phosphate availability. *Front. Microbiol.* 5, 10. doi:10.3389/fmicb.2014.00010.

Meng, J., Xu, J., Qin, D., He, Y., Xiao, X., and Wang, F. (2014). Genetic and functional properties of uncultivated MCG archaea assessed by metagenome and gene expression analyses. *ISME J.* 8, 650–659. doi:10.1038/ismej.2013.174.

Merbt, S. N., Stahl, D. A., Casamayor, E. O., Martí, E., Nicol, G. W., and Prosser, J. I. (2012). Differential photoinhibition of bacterial and archaeal ammonia oxidation. *FEMS Microbiol. Lett.* 327, 41–46. doi:10.1111/j.1574-6968.2011.02457.x.

Mincer, T. J., Church, M. J., Taylor, L. T., Preston, C. M., Karl, D. M., and DeLong, E. F. (2007). Quantitative distribution of presumptive archaeal and bacterial nitrifiers in Monterey Bay and the North Pacific Subtropical Gyre. *Environ. Microbiol.* 9, 1162–1175. doi:10.1111/j.1462-2920.2007.01239.x.

Moisander, P. H., McClinton, E., and Paerl, H. W. (2002). Salinity effects on growth, photosynthetic parameters, and nitrogenase activity in estuarine planktonic cyanobacteria. *Microb. Ecol.* 43, 432–442. doi:10.1007/s00248-001-1044-2.

Molina, V., Belmar, L., and Ulloa, O. (2010). High diversity of ammonia-oxidizing archaea in permanent and seasonal oxygen-deficient waters of the eastern South Pacific. *Environ. Microbiol.* 12, 2450–2465. doi:10.1111/j.1462-2920.2010.02218.x.

Montoya, J. P., Holl, C. M., Zehr, J. P., Hansen, A., Villareal, T. A., and Ca-

pone, D. G. (2004). High rates of N_2 fixation by unicellular diazotrophs in the oligotrophic Pacific Ocean. *Nature* 430, 1027–1031. doi:10.1038/nature02744.1.

Moore, E. K., Hopmans, E. C., Rijpstra, W. I. C., Villanueva, L., Dedysh, S. N., Kulichevskaya, I. S., et al. (2013). Novel Mono-, Di-, and trimethylornithine membrane lipids in northern wetland Planctomycetes. *Appl. Environ. Microbiol.* 79, 6874–6884. doi:10.1128/AEM.02169-13.

Moore, E. K., Villanueva, L., Hopmans, E. C., Rijpstra, W. I. C., Mets, A., Dedysh, S. N., et al. (2015). Abundant trimethylornithine lipids and specific gene sequences are indicative of planctomycete importance at the oxic/anoxic interface in sphagnum-dominated northern wetlands. *Appl. Environ. Microbiol.* 81, 6333–6344. doi:10.1128/AEM.00324-15.

Moore, J. K., and Villareal, T. A. (1996). Size-ascent rate relationships in diatoms. *Limnol. Oceanogr.* 41, 1514–1520. doi:10.4319/lo.1996.41.7.1514.

Morel, F. M. M., and Price, N. M. (2003). The Biogeochemical Cycles of Trace Metals in the Oceans. *Science (80-.).* 300, 944–947. doi:10.1126/science.1083545.

Mulder, A., van de Graaf, A. A., Robertson, L. A., and Kuenen, J. G. (1995). Anaerobic ammonium oxidation discovered in a denitrifying fuidized reactor. *FEMS Microbiol. Ecol.* 16, 177–184.

Murry, M. A., and Wolk, C. P. (1989). Evidence that the barrier to the penetration of oxygen into heterocysts depends upon two layers of the cell envelope. *Arch. Microbiol.* 151, 469–474. doi:10.1007/BF00454860.

Nichols, B. W., and Wood, B. J. B. (1968). New Glycolipid specific to Nitrogen-fixing Blue-green Algae. *Nature* 217, 767–768. doi:10.1038/217767a0.

van Niftrik, L. A., Fuerst, J. A., Sinninghe Damsté, J. S., Kuenen, J. G., Jetten, M. S. M., and Strous, M. (2004). The anammoxosome: An intracytoplasmic compartment in anammox bacteria. *FEMS Microbiol. Lett.* 233, 7–13. doi:10.1016/j.femsle.2004.01.044.

Oba, M., Sakata, S., and Tsunogai, U. (2006). Polar and neutral isopranyl glycerol ether lipids as biomarkers of archaea in near-surface sediments

from the Nankai Trough. *Org. Geochem.* 37, 1643–1654. doi:10.1016/j.orggeochem.2006.09.002.

Offre, P., Spang, A., and Schleper, C. (2013). Archaea in Biogeochemical Cycles. *Annu. Rev. Microbiol.* 67, 437–57. doi:10.1146/annurev-micro-092412-155614.

Orphan, V. J., Hinrichs, K.-U., Ussler, W. I., Paull, C. K., Taylor, L. T., Sylva, S. P., et al. (2001a). Comparative Analysis of Methane-Oxidizing Archaea and Sulfate-Reducing Bacteria in Anoxic Marine Sediments. *Appl. Environ. Microbiol.* 67, 1922–1934. doi:10.1128/AEM.67.4.1922.

Orphan, V. J., House, C. H., and Hinrichs, K.-U. (2001b). Methane-Consuming Archaea Revealed by Directly Coupled Isotopic and Phylogenetic Analysis. *Science (80-.).* 293, 484–488. doi:10.1126/science.1061338.

Orsi, W. D., Smith, J. M., Wilcox, H. M., Swalwell, J. E., Carini, P., Worden, A. Z., et al. (2015). Ecophysiology of uncultivated marine euryarchaea is linked to particulate organic matter. *ISME J.* 9, 1747–1763. doi:10.1038/ismej.2014.260.

Ortiz-Alvarez, R., and Casamayor, E. O. (2016). High occurrence of Pacearchaeota and Woesearchaeota (Archaea superphylum DPANN) in the surface waters of oligotrophic high-altitude lakes. *Environ. Microbiol. Rep.* 8, 210–217. doi:10.1111/1758-2229.12370.

Pachiadaki, M. G., Kallionaki, A., Dählmann, A., De Lange, G. J., and Kormas, K. A. (2011). Diversity and Spatial Distribution of Prokaryotic Communities Along A Sediment Vertical Profile of A Deep-Sea Mud Volcano. *Microb. Ecol.* 62, 655–668. doi:10.1007/s00248-011-9855-2.

Padilla, C. C., Bristow, L. A., Sarode, N., Garcia-Robledo, E., Gómez Ramírez, E., Benson, C. R., et al. (2016). NC10 bacteria in marine oxygen minimum zones. *ISME J.* 10, 2067–2071. doi:10.1038/ismej.2015.262.

Paerl, H. (2008). Nutrient and other environmental controls of harmful cyanobacterial blooms along the freshwater–marine continuum. *SpringerLink*, 217–237. doi:10.1007/978-0-387-75865-7_10.

Paerl, H. W. (1988). Nuisance phytoplankton blooms in coastal, estuarine,

and inland waters. *Limnol. Oceanogr.* 33, 823–847. doi:10.4319/lo.1988.33.4_part_2.0823.

Paerl, H. W., Hall, N. S., and Calandrino, E. S. (2011). Controlling harmful cyanobacterial blooms in a world experiencing anthropogenic and climatic-induced change. *Sci. Total Environ.* 409, 1739–1745. doi:10.1016/j.scitotenv.2011.02.001.

Paerl, H. W., and Huisman, J. (2009). Climate change: A catalyst for global expansion of harmful cyanobacterial blooms. *Environ. Microbiol. Rep.* 1, 27–37. doi:10.1111/j.1758-2229.2008.00004.x.

Palenik, B., and Morel, F. M. M. (1990a). Amino acid utilization by marine phytoplankton: A novel mechanism. *Limnol. Oceanogr.* 35, 260–269. doi:10.4319/lo.1990.35.2.0260.

Palenik, B., and Morel, F. M. M. (1990b). Comparison of cell-surface L-amino acid oxidases from several marine phytoplankton. *Mar. Ecol. Prog. Ser.* 59, 95–201. doi:10.3354/meps059195.

Pancost, R. D., Hopmans, E. C., and Sinninghe Damsté, J. S. (2001). Archaeal lipids in mediterranean cold seeps: Molecular proxies for anaerobic methane oxidation. *Geochim. Cosmochim. Acta* 65, 1611–1627. doi:10.1016/S0016-7037(00)00562-7.

Pancost, R. D., Sinninghe Damsté, J. S., De Lint, S., van deer Maarel, M. J. E. C., Gottschal, J. C., and Party, T. M. S. S. (2000). Biomarker Evidence for Widespread Anaerobic Methane Oxidation in Mediterranean Sediments by a Consortium of Methaogenic Archaea and Bacteria. *Appl. Environ. Microbiol.* 66, 1126–1132. doi:10.1128/AEM.66.3.1126-1132.2000.Updated.

Park, B. J., Park, S. J., Yoon, D. N., Schouten, S., Sinninghe Damsté, J. S., and Rhee, S.-K. (2010). Cultivation of autotrophic ammonia-oxidizing archaea from marine sediments in coculture with sulfur-oxidizing bacteria. *Appl. Environ. Microbiol.* 76, 7575–7587. doi:10.1128/AEM.01478-10.

Park, S. J., Ghai, R., Martín-Cuadrado, A.-B., Rodriguez-Valera, F., Chung, W. H., Kwon, K. K., et al. (2014). Genomes of two new ammonia-oxidizing archaea enriched from deep marine sediments. *PLoS One* 9,

1–10. doi:10.1371/journal.pone.0096449.

Paulmier, A., and Ruiz-Pino, D. (2009). Oxygen minimum zones (OMZs) in the modern ocean. *Prog. Oceanogr.* 80, 113–128. doi:10.1016/j.pocean.2008.08.001.

Peng, X., Jayakumar, A., and Ward, B. B. (2013). Community composition of ammonia-oxidizing archaea from surface and anoxic depths of oceanic oxygen minimum zones. *Front. Microbiol.* 4, 177. doi:10.3389/fmicb.2013.00177.

Pester, M., Schleper, C., and Wagner, M. (2011). The Thaumarchaeota: an emerging view of their phylogeny and ecophysiology. *Curr. Opin. Microbiol.* 14, 300–306. doi:10.1016/j.mib.2011.04.007.

Pinto, A. J., Marcus, D. N., Ijaz, Z., Bautista-de los Santos, Q. M., Dick, G. J., and Raskin, L. (2016). Metagenomic Evidence for the Presence of Comammox *Nitrospira*-Like Bacteria in a Drinking Water System. *Msph. Appl. Environ. Sci.* 1, e00054-15. doi:10.1128/mSphere.00054-15.

Pinto, A. J., and Raskin, L. (2012). PCR biases distort bacterial and archaeal community structure in pyrosequencing datasets. *PLoS One* 7, 1–16. doi:10.1371/journal.pone.0043093.

Pitarch, J., Volpe, G., Colella, S., Krasemann, H., and Santoleri, R. (2016). Remote sensing of chlorophyll in the Baltic Sea at basin scale from 1997 to 2012 using merged multi-sensor data. *Ocean Sci.* 12, 379–389. doi:10.5194/os-12-379-2016.

Pitcher, A., Hopmans, E. C., Mosier, A. C., Park, S. J., Rhee, S. K., Francis, C. A., et al. (2011a). Core and intact polar glycerol dibiphytanyl glycerol tetraether lipids of ammonia-oxidizing Archaea enriched from marine and estuarine sediments. *Appl. Environ. Microbiol.* 77, 3468–3477. doi:10.1128/AEM.02758-10.

Pitcher, A., Hopmans, E. C., Schouten, S., and Sinninghe Damsté, J. S. (2009). Separation of core and intact polar archaeal tetraether lipids using silica columns: Insights into living and fossil biomass contributions. *Org. Geochem.* 40, 12–19. doi:10.1016/j.orggeochem.2008.09.008.

Pitcher, A., Rychlik, N., Hopmans, E. C., Spieck, E., Rijpstra, W. I. C., Ossebaar, J., et al. (2010). Crenarchaeol dominates the membrane lipids of *Candidatus* Nitrososphaera gargensis, a thermophilic group I.1b Archaeon. *ISME J.* 4, 542–552. doi:10.1038/ismej.2009.138.

Pitcher, A., Villanueva, L., Hopmans, E. C., Schouten, S., Reichart, G.-J., and Sinninghe Damsté, J. S. (2011b). Niche segregation of ammonia-oxidizing archaea and anammox bacteria in the Arabian Sea oxygen minimum zone. *ISME J.* 5, 1896–1904. doi:10.1038/ismej.2011.60.

Pitcher, A., Wuchter, C., Siedenberg, K., Schouten, S., and Sinninghe Damsté, J. S. (2011c). Crenarchaeol tracks winter blooms of ammonia-oxidizing Thaumarchaeota in the coastal North Sea. *Limnol. Oceanogr.* 56, 2308–2318. doi:10.4319/lo.2011.56.6.2308.

Ploug, H. (2008). Cyanobacterial surface blooms formed by *Aphanizomenon* sp. and *Nodularia spumigena* in the Baltic Sea: Small-scale fluxes, pH, and oxygen microenvironments. *Limnol. Oceanogr.* 53, 914–921. doi:10.4319/lo.2008.53.3.0914.

Podlaska, A., Wakeham, S. G., Fanning, K. A., and Taylor, G. T. (2012). Microbial community structure and productivity in the oxygen minimum zone of the eastern tropical North Pacific. *Deep. Res. Part I Oceanogr. Res. Pap.* 66, 77–89. doi:http://dx.doi.org/10.1016/j.dsr.2012.04.002.

Poutanen, E.-L. L., and Nikkilä, K. (2001). Carotenoid Pigments as Tracers of Cyanobacterial Blooms in Recent and Post-glacial Sediments of the Baltic Sea. *Ambio A J. Hum. Environ.* 30, 179–183. doi:10.1579/0044-7447-30.4.179.

Qin, W., Amin, S. A., Martens-Habbena, W., Walker, C. B., Urakawa, H., Devol, A. H., et al. (2014). Marine ammonia-oxidizing archaeal isolates display obligate mixotrophy and wide ecotypic variation. *Proc. Natl. Acad. Sci.* 111, 12504–12509. doi:10.1073/pnas.1324115111.

Quaiser, A., Zivanovic, Y., Moreira, D., and López-García, P. (2011). Comparative metagenomics of bathypelagic plankton and bottom sediment from the Sea of Marmara. *ISME J.* 5, 285–304. doi:10.1038/ismej.2010.113.

Quast, C., Pruesse, E., Yilmaz, P., Gerken, J., Schweer, T., Yarza, P., et al.

(2013). The SILVA ribosomal RNA gene database project: improved data processing and web-based tools. *Nucleic Acids Res.* 41, 590–596. doi:10.1093/nar/gks1219.

Quiñones, R. A., Levipan, H. A., and Urrutia, H. (2009). Spatial and temporal variability of planktonic archaeal abundance in the Humboldt Current System off Chile. *Deep. Res. Part II Top. Stud. Oceanogr.* 56, 1073–1082. doi:10.1016/j.dsr2.2008.09.012.

Ranjard, L., Poly, F., and Nazaret, S. (2000). Monitoring complex bacterial communities using culture-independent molecular techniques: Application to soil environment. *Res. Microbiol.* 151, 167–177. doi:10.1016/S0923-2508(00)00136-4.

Rappé, M. S., and Giovannoni, S. J. (2003). The Uncultured Microbial Majority. *Annu. Rev. Microbiol.* 57, 369–394. doi:10.1146/annurev.micro.57.030502.090759.

Rattray, J. E., van de Vossenberg, J., Hopmans, E. C., Kartal, B., van Niftrik, L. A., Rijpstra, W. I. C., et al. (2008). Ladderane lipid distribution in four genera of anammox bacteria. *Arch. Microbiol.* 190, 51–66. doi:10.1007/s00203-008-0364-8.

Reichart, G.-J., Sancar, U., Radan, S., Jilbert, T., Sulu-Gambari, F., Dijkstra, N., et al. (2013). Cruise report 64PE371 PHOXY.

Rejmánková, E., Komárková, J., and Rejmánek, M. (2004). $\delta^{15}N$ as an indicator of N_2-fixation by cyanobacterial mats in tropical marshes. *Biogeochemistry* 67, 353–368. doi:10.1023/B:BIOG.0000015790.28584.ed.

Revsbech, N. P., Larsen, L. H., Gundersen, J., Dalsgaard, T., Ulloa, O., and Thamdrup, B. (2009). Determination of ultra-low oxygen concentrations in oxygen minimum zones by the STOX sensor. *Limnol. Oceanogr. Methods* 7, 371–381. doi:10.4319/lom.2009.7.371.

Reysenbach, A., and Longnecker, K. (2000). Novel Bacterial and Archaeal Lineages from an In Situ Growth Chamber Deployed at a Mid-Atlantic Ridge Hydrothermal Vent Novel Bacterial and Archaeal Lineages from an In Situ Growth Chamber Deployed at a Mid-Atlantic Ridge Hydrothermal Vent. *Appl. Environ. Microbiol.* 66, 3768–3806. doi:10.1128/AEM.66.9.3798-3806.2000.Updated.

Rinke, C., Schwientek, P., Sczyrba, A., Ivanova, N. N., Anderson, I. J., Cheng, J.-F., et al. (2013). Insights into the phylogeny and coding potential of microbial dark matter. *Nature* 499, 431–437. doi:10.1038/nature12352.

Rippka, R., Deruelles, J., Waterbury, J. B., Herdman, M., and Stanier, R. Y. (1979). Generic Assignments, Strain Histories and Properties of Pure Cultures of Cyanobacteria. *J. Gen. Microbiol.* 111, 1–61. doi:10.1099/00221287-111-1-1.

Risgaard-Petersen, N., Langezaal, A. M., Ingvardsen, S., Schmid, M. C., Jetten, M. S. M., Op Den Camp, H. J. M., et al. (2006). Evidence for complete denitrification in a benthic foraminifer. *Nature* 443, 93–96. doi:10.1038/nature05070.

Robertson, C. E., Spear, J. R., Harris, J. K., and Pace, N. R. (2009). Diversity and stratification of archaea in a hypersaline microbial mat. *Appl. Environ. Microbiol.* 75, 1801–1810. doi:10.1128/AEM.01811-08.

Rossel, P. E., Elvert, M., Ramette, A., Boetius, A., and Hinrichs, K.-U. (2011). Factors controlling the distribution of anaerobic methanotrophic communities in marine environments: Evidence from intact polar membrane lipids. *Geochim. Cosmochim. Acta* 75, 164–184. doi:10.1016/j.gca.2010.09.031.

Rossel, P. E., Lipp, J. S., Fredricks, H. F., Arnds, J., Boetius, A., Elvert, M., et al. (2008). Intact polar lipids of anaerobic methanotrophic archaea and associated bacteria. *Org. Geochem.* 39, 992–999. doi:10.1016/j.orggeochem.2008.02.021.

Rotthauwe, J., and Witzel, K. (1997). The ammonia monooxygenase structural gene *amo*A as a functional marker Molecular fine-scale analysis of natural ammonia-oxidizing populations. *Appl. Environ. Microbiol.* 63, 4704–4712. doi:10.1128/AEM.NA.

Rush, D., Wakeham, S. G., Hopmans, E. C., Schouten, S., and Sinninghe Damsté, J. S. (2012). Biomarker evidence for anammox in the oxygen minimum zone of the Eastern Tropical North Pacific. *Org. Geochem.* 53, 80–87. doi:10.1016/j.orggeochem.2012.02.005.

Rütters, H., Sass, H., Cypionka, H., and Rullkötter, J. (2002). Microbial

communities in a Wadden Sea sediment core - Clues from analyses of intact glyceride lipids, and released fatty acids. *Org. Geochem.* 33, 803–816. doi:10.1016/S0146-6380(02)00028-1.

Sachs, J. P., and Repeta, D. J. (1999). Oligotrophy and nitrogen fixation during eastern Mediterranean sapropel events. *Science* 286, 2485–2488.

Saitou, N., and Nei, M. (1987). The Neighbor-joining Method: A New Method for Reconstructing Phylogenetic Trees. *Mol. Biol. Evol.* 4, 406–425. doi:citeulike-article-id:93683.

Santoro, A. E., Casciotti, K. L., and Francis, C. A. (2010). Activity, abundance and diversity of nitrifying archaea and bacteria in the central California Current. *Environ. Microbiol.* 12, 1989–2006. doi:10.1111/j.1462-2920.2010.02205.x.

Santoro, A. E., Dupont, C. L., Richter, R. A., Craig, M. T., Carini, P., Mcilvin, M. R., et al. (2015). Genomic and proteomic characterization of "*Candidatus* Nitrosopelagicus brevis": An ammonia-oxidizing archaeon from the open ocean. *Proc. Natl. Acad. Sci.* 112, 1173–1178. doi:10.1073/pnas.1416223112.

Schalnger, S. O., and Jenkyns, H. C. (1976). Cretaceous oceanic anoxic events: causes and consequences. *Netherlands J. Geosci.* 55, 179–184.

Schmidt, I., and Bock, E. (1997). Anaerobic ammonia oxidation with nitrogen dioxide by *Nitrosomonas eutropha*. *Arch. Microbiol.* 167, 106–111. doi:10.1007/s002030050422.

Schouten, S., Hopmans, E. C., Baas, M., Boumann, H. A., Standfest, S., Könneke, M., et al. (2008a). Intact membrane lipids of "*Candidatus* Nitrosopumilus maritimus," a cultivated representative of the cosmopolitan mesophilic group I Crenarchaeota. *Appl. Environ. Microbiol.* 74, 2433–2440. doi:10.1128/AEM.01709-07.

Schouten, S., Hopmans, E. C., Pancost, R. D., and Sinninghe Damsté, J. S. (2000). Widespread occurrence of structurally diverse tetraether membrane lipids: evidence for the ubiquitous presence of low-temperature relatives of hyperthermophiles. *Proc. Natl. Acad. Sci.* 97, 14421–14426. doi:10.1073/pnas.97.26.14421.

Schouten, S., Hopmans, E. C., and Sinninghe Damsté, J. S. (2013a). The organic geochemistry of glycerol dialkyl glycerol tetraether lipids: A review. *Org. Geochem.* 54, 19–61. doi:10.1016/j.orggeochem.2012.09.006.

Schouten, S., Huguet, C., Hopmans, E. C., Kienhuis, M. V. M., and Sinninghe Damsté, J. S. (2007a). Analytical Methodology for TEX_{86} Paleothermometry by High-Performance Liquid Chromatography/Atmospheric Pressure Chemical Ionization-Mass Spectrometry. *Anal. Chem.* 79, 2940–2944. doi:10.1021/ac062339v.

Schouten, S., van der Meer, M. T. J., Hopmans, E. C., Rijpstra, W. I. C., Reysenbach, A. L., Ward, D. M., et al. (2007b). Archaeal and bacterial glycerol dialkyl glycerol tetraether lipids in hot springs of Yellowstone National Park. *Appl. Environ. Microbiol.* 73, 6181–6191. doi:10.1128/AEM.00630-07.

Schouten, S., van der Meer, M. T. J., Hopmans, E. C., and Sinninghe Damsté, J. S. (2008b). Comment on "Lipids of marine Archaea: Patterns and provenance in the water column and sediments" by Turich et al. (2007). *Geochim. Cosmochim. Acta* 72, 5342–5346. doi:10.1016/j.gca.2008.03.028.

Schouten, S., Middelburg, J. J., Hopmans, E. C., and Sinninghe Damsté, J. S. (2010). Fossilization and degradation of intact polar lipids in deep subsurface sediments: A theoretical approach. *Geochim. Cosmochim. Acta* 74, 3806–3814. doi:10.1016/j.gca.2010.03.029.

Schouten, S., Pitcher, A., Hopmans, E. C., Villanueva, L., van Bleijswijk, J., and Sinninghe Damsté, J. S. (2012). Intact polar and core glycerol dibiphytanyl glycerol tetraether lipids in the Arabian Sea oxygen minimum zone: I. Selective preservation and degradation in the water column and consequences for the TEX_{86}. *Geochim. Cosmochim. Acta* 98, 228–243. doi:10.1016/j.gca.2012.05.002.

Schouten, S., Strous, M., Kuypers, M. M. M., Rijpstra, W. I. C., Baas, M., Schubert, C. J., et al. (2004). Stable carbon isotopic fractionations associated with inorganic carbon fixation by anaerobic ammonium-oxidizing bacteria. *Appl. Environ. Microbiol.* 70, 3785–3788. doi:10.1128/AEM.70.6.3785-3788.2004.

Schouten, S., Villanueva, L., Hopmans, E. C., van der Meer, M. T. J., and Sinninghe Damsté, J. S. (2014). Are Marine Group II Euryarchaeota significant contributors to tetraether lipids in the ocean? *Proc. Natl. Acad. Sci.* 111, E4285. doi:10.1073/pnas.1416176111.

Schouten, S., Villareal, T. A., Hopmans, E. C., Mets, A., Swanson, K. M., and Sinninghe Damsté, J. S. (2013b). Endosymbiotic heterocystous cyanobacteria synthesize different heterocyst glycolipids than free-living heterocystous cyanobacteria. *Phytochemistry* 85, 115–21. doi:10.1016/j.phytochem.2012.09.002.

Schouten, S., Wakeham, S. G., and Sinninghe Damsté, J. S. (2001). Evidence for anaerobic methane oxidation by archaea in euxinic waters of the Black Sea. *Org. Geochem.* 32, 1277–1281. doi:10.1016/S0146-6380(01)00110-3.

Schubert, C. J., Coolen, M. J. L., Neretin, L. N., Schippers, A., Abbas, B., Durisch-Kaiser, E., et al. (2006). Aerobic and anaerobic methanotrophs in the Black Sea water column. *Environ. Microbiol.* 8, 1844–1856. doi:10.1111/j.1462-2920.2006.01079.x.

Schubotz, F., Lipp, J. S., Elvert, M., and Hinrichs, K. U. (2011). Stable carbon isotopic compositions of intact polar lipids reveal complex carbon flow patterns among hydrocarbon degrading microbial communities at the Chapopote asphalt volcano. *Geochim. Cosmochim. Acta* 75, 4399–4415. doi:10.1016/j.gca.2011.05.018.

Schubotz, F., Wakeham, S. G., Lipp, J. S., Fredricks, H. F., and Hinrichs, K.-U. (2009). Detection of microbial biomass by intact polar membrane lipid analysis in the water column and surface sediments of the Black Sea. *Environ. Microbiol.* 11, 2720–2734. doi:10.1111/j.1462-2920.2009.01999.x.

Schweger, C. E., and Hickman, C. (1989). The Holocene Paleohydrology of Central Alberta - Testing the General-Circulation-Model Climate Simulations. *Can. J. Earth Sci.* 26, 1826–1833. doi:10.1139/e89-155.

Shoun, H., Kim, D. H., Uchiyama, H., and Sugiyama, J. (1992). Denitrification by fungi. *FEMS Microbiol. Lett.* 94, 277–281. doi:10.1016/0378-1097(92)90643-3.

Sinninghe Damsté, J. S., and Köster, J. (1998). A euxinic southern North Atlantic Ocean during the Cenomanian/Turonian oceanic anoxic event. *Earth Planet. Sci. Lett.* 158, 165–173. doi:10.1016/S0012-821X(98)00052-1.

Sinninghe Damsté, J. S., Rijpstra, W. I. C., Hopmans, E. C., Jung, M.-Y., Kim, J.-G., Rhee, S.-K., et al. (2012). Intact polar and core glycerol dibiphytanyl glycerol tetraether lipids of group I.1a and I.1b Thaumarchaeota in soil. *Appl. Environ. Microbiol.* 78, 6866–6874. doi:10.1128/AEM.01681-12.

Sinninghe Damsté, J. S., Rijpstra, W. I. C., Hopmans, E. C., Prahl, F. G., Wakeham, S. G., and Schouten, S. (2002a). Distribution of Membrane Lipids of Planktonic Crenarchaeota in the Arabian Sea. *Appl. Environ. Microbiol.* 68, 2997–3002. doi:10.1128/AEM.68.6.2997.

Sinninghe Damsté, J. S., Rijpstra, W. I. C., and Reichart, G.-J. (2002b). The influence of oxic degradation on the sedimentary biomarker record II. Evidence from Arabian Sea sediments. *Geochim. Cosmochim. Acta* 66, 2737–2754. doi:10.1016/S0016-7037(02)00865-7.

Sinninghe Damsté, J. S., Schouten, S., Hopmans, E. C., van Duin, A. C. T., and Geenevasen, J. A. J. (2002c). Crenarchaeol: the characteristic core glycerol dibiphytanyl glycerol tetraether membrane lipid of cosmopolitan pelagic crenarchaeota. *J. Lipid Res.* 43, 1641–1651. doi:10.1194/jlr.M200148-JLR200.

Sinninghe Damsté, J. S., Strous, M., Rijpstra, W. I. C., Hopmans, E. C., Geenevasen, J. A. J., van Duin, A. C. T., et al. (2002d). Linearly concatenated cyclobutane lipids form a dense bacterial membrane. *Nature* 419, 8–12. doi:10.1038/nature01067.1.

Sintes, E., De Corte, D., Haberleitner, E., and Herndl, G. J. (2016). Geographic distribution of archaeal ammonia oxidizing ecotypes in the Atlantic Ocean. *Front. Microbiol.* 7, 1–14. doi:10.3389/fmicb.2016.00077.

Sivonen, K., Halinen, K., Sihvonen, L. M., Koskenniemi, K., Sinkko, H., Rantasärkkä, K., et al. (2007). Bacterial diversity and function in the Baltic Sea with an emphasis on cyanobacteria. *Ambio A J. Hum. Environ.* 36, 180–185. doi:10.1579/0044-7447(2007)36[180:bdafit]2.0.co;2.

Smith, J. M., Chavez, F. P., and Francis, C. A. (2014). Ammonium uptake by phytoplankton regulates nitrification in the sunlit ocean. *PLoS One* 9. doi:10.1371/journal.pone.0108173.

Sollai, M., Villanueva, L., Hopmans, E. C., Reichart, G.-J., and Sinninghe Damsté, J. S. (2018). A combined lipidomic and 16S rRNA gene amplicon sequencing approach reveals archaeal sources of intact polar lipids in the stratified Black Sea water column. *Submitt. to Geobiol.*, 1–30.

Soriente, A., Gambacorta, A., Trincone, A., Sili, C., Vincenzini, M., and Sodano, G. (1993). Heterocyst glycolipids of the cyanobacterium *Cyanospira rippkae*. *Phytochemistry* 33, 393–395.

Spang, A., Hatzenpichler, R., Brochier-Armanet, C., Rattei, T., Tischler, P., Spieck, E., et al. (2010). Distinct gene set in two different lineages of ammonia-oxidizing archaea supports the phylum Thaumarchaeota. *Trends Microbiol.* 18, 331–340. doi:10.1016/j.tim.2010.06.003.

Spang, A., Saw, J. H., Jørgensen, S. L., Zaremba-Niedzwiedzka, K., Martijn, J., Lind, A. E., et al. (2015). Complex archaea that bridge the gap between prokaryotes and eukaryotes. *Nature* 521, 173–179. doi:10.1038/nature14447.

Staal, M., Meysman, F. J. R., and Stal, L. J. (2003). Temperature excludes N_2-fixing heterocystous cyanobacteria in the tropical oceans. *Nature* 425, 504–507. doi:10.1038/nature01999.

Stadnitskaia, A., Muyzer, G., Abbas, B., Coolen, M. J. L., Hopmans, E. C., Baas, M., et al. (2005). Biomarker and 16S rDNA evidence for anaerobic oxidation of methane and related carbonate precipitation in deep-sea mud volcanoes of the Sorokin Trough, Black Sea. *Mar. Geol.* 217, 67–96. doi:10.1016/j.margeo.2005.02.023.

Stahl, D. A., and de la Torre, J. R. (2012). Physiology and Diversity of Ammonia-Oxidizing Archaea. *Annu. Rev. Microbiol.* 66, 83–101. doi:10.1146/annurev-micro-092611-150128.

Stal, L. J. (2009). Is the distribution of nitrogen-fixing cyanobacteria in the oceans related to temperature? *Environ. Microbiol.* 11, 1632–1645. doi:10.1111/j.1758-2229.2009.00016.x.

Stewart, E. J. (2012). Growing unculturable bacteria. *J. Bacteriol.* 194,

4151–4160. doi:10.1128/JB.00345-12.

Stewart, F. J., Ulloa, O., and DeLong, E. F. (2011). Microbial metatranscriptomics in a permanent marine oxygen minimum zone. *Environ. Microbiol.* 14, 23–40. doi:10.1111/j.1462-2920.2010.02400.x.

Stipa, T. (2002). The dynamics of the N/P ratio and stratification in a large nitrogen-limited estuary as a result of upwelling: A tendency for offshore Nodularia blooms. *Hydrobiologia* 487, 219–227. doi:10.1023/A:1022990116669.

Stoeck, T., and Epstein, S. (2003). Novel eukaryotic lineages inferred from small-subunit rRNA analyses of oxygen-depleted marine environments. *Appl. Environ. Microbiol.* 69, 2657–2663. doi:10.1128/AEM.69.5.2657-2663.2003.

Stolper, D. A., Peter Revsbech, N., Canfield, D. E., and Revsbech, N. P. (2010). Aerobic growth at nanomolar oxygen concentrations. *Proc. Natl. Acad. Sci.* 107, 18755–18760. doi:10.1073/pnas.1013435107.

Stramma, L., Johnson, G. C., Sprintall, J., and Mohrholz, V. (2008). Expanding Oxygen-Minimum Zones in the Tropical Oceans. *Science* 320, 655–658. doi:10.1126/science.1153847.

Stramma, L., Prince, E. D., Schmidtko, S., Luo, J., Hoolihan, J. P., Visbeck, M., et al. (2011). Expansion of oxygen minimum zones may reduce available habitat for tropical pelagic fishes. *Nat. Clim. Chang.* 2, 33–37. doi:10.1038/nclimate1304.

Strauss, H. (2006). "Anoxia through time," in *Past and Present Water Column Anoxia*, ed. L. N. Neretin (Springer), 3–21.

Strous, M., Fuerst, J. A., Kramer, E. H. M., Logemann, S., Muyzer, G., Van De Pas-Schoonen, K. T., et al. (1999). Missing lithotroph identified as new planctomycete. *Nature* 400, 446–449.

Strous, M., Pelletier, E., Mangenot, S., Rattei, T., Lehner, A., Taylor, M. W., et al. (2006). Deciphering the evolution and metabolism of an anammox bacterium from a community genome. *Nature* 440, 790–794. doi:10.1038/nature04647.

Sturt, H. F., Summons, R. E., Smith, K., Elvert, M., and Hinrichs, K.-U.

(2004). Intact polar membrane lipids in prokaryotes and sediments deciphered by high-performance liquid chromatography/electrospray ionization multistage mass spectrometry—new biomarkers for biogeochemistry and microbial ecology. *Rapid Commun. Mass Spectrom.* 18, 617–628. doi:10.1002/rcm.1378.

Sun, M., and Wakeham, S. G. (1994). Molecular evidence for degradation and preservation of organic matter in the anoxic Black Sea Basin. *Geochim. Cosmochim. Acta* 58, 3395–3406. doi:10.1016/0016-7037(94)90094-9.

Suzumura, M. (2005). Phospholipids in marine environments: A review. *Talanta* 66, 422–434. doi:10.1016/j.talanta.2004.12.008.

Taylor, K. W. R., Huber, M., Hollis, C. J., Hernandez-Sanchez, M. T., and Pancost, R. D. (2013). Re-evaluating modern and Palaeogene GDGT distributions: Implications for SST reconstructions. *Glob. Planet. Change* 108, 158–174. doi:10.1016/j.gloplacha.2013.06.011.

Teske, A. P., and Sørensen, K. B. (2008). Uncultured archaea in deep marine subsurface sediments: have we caught them all? *ISME J.* 2, 3–18. doi:10.1038/ismej.2007.90.

Thamdrup, B., and Dalsgaard, T. (2002). Production of N_2 through anaerobic ammonium oxidation coupled to nitrate reduction in marine sediments. *Appl. Environ. Microbiol.* 68, 1312–1318. doi:10.1128/AEM.68.3.1312-1318.2002.

Thamdrup, B., Dalsgaard, T., Jensen, M. M., Ulloa, O., Farías, L., and Escribano, R. (2006). Anaerobic ammonium oxidation in the oxygen-deficient waters off northern Chile. *Limnol. Oceanogr.* 51, 2145–2156.

Thamdrup, B., Dalsgaard, T., and Revsbech, N. P. (2012). Widespread functional anoxia in the oxygen minimum zone of the Eastern South Pacific. *Deep Sea Res. Part I* 65, 36–45. doi:10.1016/j.dsr.2012.03.001.

Tiano, L., Garcia-Robledo, E., Dalsgaard, T., Devol, A. H., Ward, B. B., Ulloa, O., et al. (2014). Oxygen distribution and aerobic respiration in the north and south eastern tropical Pacific oxygen minimum zones. *Deep. Res. Part I* 94, 173–183. doi:10.1016/j.dsr.2014.10.001.

Tiedje, J. M. (1988). "Ecology of denitrification and dissimilatory nitrate

reduction to ammonium," in *Environmental Microbiology of Anaerobes* (John Wiley and Sons, N.Y.), 179–244.

Turich, C., Freeman, K. H., Bruns, M. A., Conte, M. H., Jones, A. D., and Wakeham, S. G. (2007). Lipids of marine Archaea: Patterns and provenance in the water-column and sediments. *Geochim. Cosmochim. Acta* 71, 3272–3291. doi:10.1016/j.gca.2007.04.013.

Ulloa, O., Canfield, D. E., DeLong, E. F., Letelier, R. M., and Stewart, F. J. (2012). Microbial oceanography of anoxic oxygen minimum zones. *Proc. Natl. Acad. Sci.* 109, 15996–6003. doi:10.1073/pnas.1205009109.

Venter, J. C., Remington, K., Heidelberg, J. F., Halpern, A. L., Rusch, D., Eisen, J. A., et al. (2004). Environmental genome shotgun sequencing of the Sargasso Sea. *Science* 304, 66–74. doi:10.1126/science.1093857.

Vestal, J. R., and White, D. C. (1989). Lipid Analysis in Microbial Ecology. *Bioscience* 39, 535–541.

Vetriani, C., and Jannasch, H. W. (1999). Population structure and phylogenetic characterization of marine benthic archaea in deep-sea sediments. *Appl. Environ. Microbiol.* 65, 4375–4384. Available at: http://aem.asm.org/content/65/10/4375.short.

Vetriani, C., Tran, H. V, and Kerkhof, L. J. (2003). Fingerprinting Microbial Assemblages from the Oxic/Anoxic Chemocline of the Black Sea. *Appl. Environ. Microbiol.* 69, 6481–6488. doi:10.1128/AEM.69.11.6481–6488.2003.

Villanueva, L., Schouten, S., and Sinninghe Damsté, J. S. (2015). Depth-related distribution of a key gene of the tetraether lipid biosynthetic pathway in marine Thaumarchaeota. *Environ. Microbiol.* 17, 3527–3539. doi:10.1111/1462-2920.12508.

Villanueva, L., Schouten, S., and Sinninghe Damsté, J. S. (2017). Phylogenomic analysis of lipid biosynthetic genes of Archaea shed light on the "lipid divide". *Environ. Microbiol.* 19, 54–69. doi:10.1111/1462-2920.13361.

Villareal, T. A., Pilskaln, C., Brzezinski, M., Lipschultz, F., Dennett, M., and Gardner, G. B. (1999). Upward transport of oceanic nitrate by migrat-

ing diatom mats. *Nature* 397, 423–425. doi:10.1038/17103.

Volkov, I. I., and Neretin, L. N. (2007). "Hydrogen Sulfide in the Black Sea," in *The Black Sea Environment. The handbook of environmental chemistry*, eds. A. G. Kostianoy and A. N. Kosarev (Springer), 309–331. doi:10.1016/0143-1471(82)90111-8.

Voss, M., Bange, H. W., Dippner, J. W., Middelburg, J. J., Montoya, J. P., and Ward, B. B. (2013). The marine nitrogen cycle: recent discoveries, uncertainties and the potential relevance of climate change. *Philos. Trans. R. Soc.* 368, 1–11. doi:10.1098/rstb.2013.0121.

Wakeham, S. G., Amann, R., Freeman, K. H., Hopmans, E. C., Jørgensen, B. B., Putnam, I. F., et al. (2007). Microbial ecology of the stratified water column of the Black Sea as revealed by a comprehensive biomarker study. *Org. Geochem.* 38, 2070–2097. doi:10.1016/j.orggeochem.2007.08.003.

Wakeham, S. G., Hopmans, E. C., Schouten, S., and Sinninghe Damsté, J. S. (2004). Archaeal lipids and anaerobic oxidation of methane in euxinic water columns: A comparative study of the Black Sea and Cariaco Basin. *Chem. Geol.* 205, 427–442. doi:10.1016/j.chemgeo.2003.12.024.

Wakeham, S. G., Lewis, C. M., Hopmans, E. C., Schouten, S., and Sinninghe Damsté, J. S. (2003). Archaea mediate anaerobic oxidation of methane in deep euxinic waters of the Black Sea. *Geochim. Cosmochim. Acta* 67, 1359–1374. doi:10.1016/S0016-7037(02)01220-6.

Wakeham, S. G., Turich, C., Schubotz, F., Podlaska, A., Li, X. N., Varela, R., et al. (2012). Biomarkers, chemistry and microbiology show chemoautotrophy in a multilayer chemocline in the Cariaco Basin. *Deep. Res. Part I* 63, 133–156. doi:10.1016/j.dsr.2012.01.005.

Walsby, A. E. (1985). The Permeability of Heterocysts to the Gases Nitrogen and Oxygen. *Proc. R. Soc. B Biol. Sci.* 226, 345–366. doi:10.1098/rspb.1985.0099.

Wang, J. X., Wei, Y., Wang, P., Hong, Y., and Zhang, C. L. (2015). Unusually low TEX_{86} values in the transitional zone between Pearl River estuary and coastal South China Sea: Impact of changing archaeal community composition. *Chem. Geol.* 402, 18–29. doi:10.1016/j.chem-

geo.2015.03.002.

Ward, B. B. (2013). How Nitrogen Is Lost. *Science (80-.).* 341, 352–353. doi:10.1126/science.1240314.

Ward, B. B., Devol, A. H., Rich, J. J., Chang, B. X., Bulow, S. E., Naik, H. S., et al. (2009). Denitrification as the dominant nitrogen loss process in the Arabian Sea. *Nature* 461, 78–81. doi:10.1038/nature08276.

Ward, B. B., Tuit, C. B., Jayakumar, A., Rich, J. J., Moffett, J. W., and Naqvi, S. W. A. (2008). Organic carbon, and not copper, controls denitrification in oxygen minimum zones of the ocean. *Deep. Res. Part I* 55, 1672–1683. doi:10.1016/j.dsr.2008.07.005.

Warden, L. A. (2017). Paleoenvironmental reconstructions in the Baltic Sea and Iberian Margin Assessment of GDGTs and long-chain alkenones in Holocene sedimentary records.

Warden, L., Moros, M., Neumann, T., Shennan, S., Timpson, A., Manning, K., et al. (2017). Climate induced human demographic and cultural change in northern Europe during the mid-Holocene. *Sci. Rep.* 7, 1–11. doi:10.1038/s41598-017-14353-5.

Wasmund, N. (1997). Occurrence of Cyanobacterial Blooms in the Baltic Sea in Relation to Environmental Conditions. *Int. Rev. Hydrobiol.* 82, 169–184.

Wasmund, N., and Uhlig, S. (2003). Phytoplankton trends in the Baltic Sea. *ICES J. Mar. Sci.* 60, 177–186. doi:10.1016/S1054–3139(02)00280-1.

Wegener, G., Krukenberg, V., Ruff, S. E., Kellermann, M. Y., and Knittel, K. (2016). Metabolic capabilities of microorganisms involved in and associated with the anaerobic oxidation of methane. *Front. Microbiol.* 7, 1–16. doi:10.3389/fmicb.2016.00046.

White, D. C., Davis, W. M., Nickels, J. S., King, J. D., and Bobbie, R. J. (1979). Determination of the sedimentary microbial biomass by extractible lipid phosphate. *Oecologia* 40, 51–62. doi:10.1007/BF00388810.

Whitney, F. A., Freeland, H. J., and Robert, M. (2007). Persistently declining oxygen levels in the interior waters of the eastern subarctic Pacific.

Prog. Oceanogr. 75, 179–199. doi:10.1016/j.pocean.2007.08.007.

Whitton, B. A., and Potts, M. (2012). "Introduction to Cyanobacteria," in *Ecology of Cyanobacteria II. Their Diversity in Space and Time*, ed. B. A. Whitton (Springer), 1–15. doi:10.1007/978-94-007-3855-3.

Willerslev, E., Hansen, A. J., Rønn, R., Brand, T. B., Barnes, I., Wiuf, C., et al. (2004). Long-term persistence of bacterial DNA. *Curr. Biol.* 14, 13–14. doi:10.1016/j.cub.2003.12.012.

Woebken, D., Fuchs, B. M., Kuypers, M. M. M., and Amann, R. (2007). Potential interactions of particle-associated anammox bacteria with bacterial and archaeal partners in the Namibian upwelling system. *Appl. Environ. Microbiol.* 73, 4648–4657. doi:10.1128/AEM.02774-06.

Wolk, C. P. (1973). Physiology and cytological chemistry blue-green algae. *Bacteriol. Rev.* 37, 32–101.

Wörmer, L., Cirés, S., Velázquez, D., Quesada, A., and Hinrichs, K.-U. (2012). Cyanobacterial heterocyst glycolipids in cultures and environmental samples: Diversity and biomarker potential. *Limnol. Oceanogr.* 57, 1775–1788. doi:10.4319/lo.2012.57.6.1775.

Wörmer, L., Lipp, J. S., Schröder, J. M., and Hinrichs, K.-U. (2013). Application of two new LC-ESI-MS methods for improved detection of intact polar lipids (IPLs) in environmental samples. *Org. Geochem.* 59, 10–21. doi:10.1016/j.orggeochem.2013.03.004.

Wright, J. J., Konwar, K. M., and Hallam, S. J. (2012). Microbial ecology of expanding oxygen minimum zones. *Nat. Rev. Microbiol.* 10, 381–394. doi:10.1038/nrmicro2778.

Wuchter, C., Abbas, B., Coolen, M. J. L., Herfort, L., van Bleijswijk, J., Timmers, P., et al. (2006). Archaeal nitrification in the ocean. *Proc. Natl. Acad. Sci.* 103, 12317–12322. doi:10.1073/pnas.0600756103.

Xie, S., Liu, X.-L., Schubotz, F., Wakeham, S. G., and Hinrichs, K.-U. (2014). Distribution of glycerol ether lipids in the oxygen minimum zone of the Eastern Tropical North Pacific Ocean. *Org. Geochem.* 71, 60–71. doi:10.1016/j.orggeochem.2014.04.006.

Yakimov, M. M., Cono, V. La, and Denaro, R. (2009). A first insight into

the occurrence and expression of functional *amo*A and *acc*A genes of autotrophic and ammonia-oxidizing bathypelagic Crenarchaeota of Tyrrhenian Sea. *Deep. Res. Part II* 56, 748–754. doi:10.1016/j.dsr2.2008.07.024.

Yakimov, M. M., Cono, V. La, Smedile, F., DeLuca, T. H., Juárez, S., Ciordia, S., et al. (2011). Contribution of crenarchaeal autotrophic ammonia oxidizers to the dark primary production in Tyrrhenian deep waters (Central Mediterranean Sea). *ISME J.* 5, 945–961. doi:10.1038/ismej.2010.197.

Yan, J., Haaijer, S. C. M., Op den Camp, H. J. M., van Niftrik, L., Stahl, D. A., Könneke, M., et al. (2012). Mimicking the oxygen minimum zones: stimulating interaction of aerobic archaeal and anaerobic bacterial ammonia oxidizers in a laboratory-scale model system. *Environ. Microbiol.* 14, 3146–3158. doi:10.1111/j.1462-2920.2012.02894.x.

Yan, J., Op den Camp, H. J. M., Jetten, M. S. M., Hu, Y. Y., and Haaijer, S. C. M. (2010). Induced cooperation between marine nitrifiers and anaerobic ammonium-oxidizing bacteria by incremental exposure to oxygen. *Syst. Appl. Microbiol.* 33, 407–415. doi:10.1016/j.syapm.2010.08.003.

Yoshinaga, M. Y., Kellermann, M. Y., Rossel, P. E., Schubotz, F., Lipp, J. S., and Hinrichs, K.-U. (2011). Systematic fragmentation patterns of archaeal intact polar lipids by high-performance liquid chromatography/electrospray ionization ion-trap mass spectrometry. *Rapid Commun. Mass Spectrom.* 25, 3563–3574. doi:10.1002/rcm.5251.

Zakrisson, A., Larsson, U., and Hoglander, H. (2014). Do Baltic Sea diazotrophic cyanobacteria take up combined nitrogen *in situ*? *J. Plankton Res.* 36, 1368–1380. doi:10.1093/plankt/fbu053.

Zehr, J. P., and Ward, B. B. (2002). Nitrogen Cycling in the Ocean: New Perspectives on Processes and Paradigms. *Appl. Environ. Microbiol.* 68, 1015–1024. doi:10.1128/AEM.68.3.1015.

Zhang, C. L., Xie, W., Martin-Cuadrado, A.-B., and Rodriguez-Valera, F. (2015). Marine Group II Archaea, potentially important players in the global ocean carbon cycle. *Front. Microbiol.* 6, 1–9. doi:10.3389/fmicb.2015.01108.

Zhang, Y. G., Zhang, C. L., Liu, X. L., Li, L., Hinrichs, K.-U., and Noakes, J. E. (2011). Methane Index: A tetraether archaeal lipid biomarker indicator for detecting the instability of marine gas hydrates. *Earth Planet. Sci. Lett.* 307, 525–534. doi:10.1016/j.epsl.2011.05.031.

Zhu, C., Meador, T. B., Dummann, W., and Hinrichs, K.-U. (2013). Identification of unusual butanetriol dialkyl glycerol tetraether and pentanetriol dialkyl glycerol tetraether lipids in marine sediments. *Rapid Commun. Mass Spectrom.* 28, 332–338. doi:10.1002/rcm.6792.

Zhu, C., Wakeham, S. G., Elling, F. J., Basse, A., Mollenhauer, G., Versteegh, G. J. M., et al. (2016). Stratification of archaeal membrane lipids in the ocean and implications for adaptation and chemotaxonomy of planktonic archaea. *Environ. Microbiol.* 18, 4324–4336. doi:10.1111/joms.12099.

Zillén, L., and Conley, D. J. (2010). Hypoxia and cyanobacteria blooms - are they really natural features of the late Holocene history of the Baltic Sea? *Biogeosciences* 7, 2567–2580. doi:10.5194/bg-7-2567-2010.

Zink, K. G., Wilkes, H., Disko, U., Elvert, M., and Horsfield, B. (2003). Intact phospholipids - Microbial “life markers” in marine deep subsurface sediments. *Org. Geochem.* 34, 755–769. doi:10.1016/S0146-6380(03)00041-X.

Züllig, H. (1986). Carotenoids from plankton and photosynthetic bacteria in sediments as indicators of trophic changes in Lake Lobsigen during the last 14000 years. *Hydrobiologia* 143, 315–319. doi:10.1007/BF00026676.

Zumft, W. G. (1997). Cell biology and molecular basis of denitrification. *Microbiol. Mol. Biol. Rev.* 61, 533–616. Available at: http://mmbr.asm.org/cgi/reprint/61/4/533?view=long&pmid=9409151.

It is with a bittersweet feeling that I write the acknowledgments on my PhD thesis. In fact, if on the one hand I am very happy to have safely made it to this point, on the other this means the official end of this great adventure.

I want to thank you Jaap for hire me and made me part of your amazing research group. Thank you for being such an inspiring person and scientist. Thank you for have been a patient and motivating mentor over these years, for always come up with brilliant comments and questions, and for giving me autonomy on many aspects of this project and great opportunities. Thank you for your work ethic and for your humor. It has been a real pleasure to collaborate and learn from you. I could have not wished for a better supervisor and boss. Laura you became my second supervisor and I am very happy of that! Thank you for always have an encouraging attitude. We share two chapters of this thesis, but most important we share "the journey" that took to get them ready which meant a lot of multi-tasking from your side and I admire you very much for this. Thank you Stefan for guide me through joys and pains of the writing of my first paper. The pain surely exceeded the joy at that time and I am super grateful for your patience and the ideas you brought to improve that paper. Thank you for being a great teacher, for your advices before conferences and your knowledge of lab procedures which you always shared willingly when I was doubtful. Talking of advices before conferences: thank you Marcel for your insightful comments and encouraging attitude every time I was rehearsing my talks. Ellen, it is truly challenging and inspiring to get to work with you! I admire very much the dedication, the efficiency, the preciseness and the passion you put in your work. And everything is well mixed with Dutch humor and funny stories at coffee breaks. All I know about chromatography, mass spectrometry, IPLs analysis and data interpretation I have learnt it from you. And also – and not less important – how to be more efficient and organized in the lab and outside when trying to get something nice out of my data. I owe you a lot, thank you so much! Talking of IPLs analysis and everything it involves I owe special thanks to you Nicole, because together with Ellen you really taught me a lot about lipids and how to analyze them and interpret the data and be organized in general. In addition you and Yvo are great party hosts, which is something I appreciate a lot! But I will come back to this later.

The lipid lab is the heart of the BGC department (sorry, MMB) and I thank all the people who worked there during my time in the department. Anchelique and Denise have been my lab bench neighbors and always nice and fun to

chat with and helpful in any possible way. Thanks a lot Anchelique for your invaluable contribution to the Baltic Sea project! Marianne, thank you for teach me how to program the *in situ* pumps and how to keep them happy, before I went to the sea, and thank you for being always helpful in the lab. Irene thanks for sharing your lab knowledge and teach me acid hydrolysis. Thank you Kevin and Jort for introducing me to the tedious world of the decalcification and elemental/isotope analysis, and for being very helpful on this subject. Jort, I also owe you special thanks for being the kindest person every time I needed extra help with the HPLC-MS and for keeping my pc alive – with the precious help of Marcel and Ronald at some point – because without that help this thesis would have not been done, and I mean it! Thank you Monique for being always nice and helpful. Thanks also to Sharyn for your help with the nutrient data of the Black Sea and to Elda for helping in the genetic lab with my Black Sea and ETSP samples, thank you Judith for the nice time we shared in New Orleans at the OSM, and thanks to all the other technicians of the department for keeping a friendly and helpful environment.

Thank you Jolanda for being always helpful, cheerful and kind.

Thanks to my coauthors from outside the department: Mathias, Gert-Jan and Rick. Rick, thank you also for been my mentor during the ETNP cruise and a very nice person and a great scientist. I was very happy to meet you again in Liege. Thanks to Stuart Wakeham, Bess Ward and Al Devol who made possible my participation in the ETNP cruise. And thanks to the brilliant people I have met at sea: Jaqui, Allison, Andrew & Laura T. (i miei amicissimi a bordo!), Nick, Bonnie, Carly, Brittany, Randie, Hantten among many others.

Thank you to the members of the assessment and reading committee of this thesis.

And now to my colleagues and friends who helped me to overcome the very long Texel winters. To my paranimfen Yvonne, Anna and Marta: your friendship is one of the most precious gifts from Texel and I gladly take it with me in my next adventure! I had the fortune to be welcomed at BGC by two great officemates, Darci and Sebastian. Thank you guys for always find the weirdest YouTube videos to share and comment. Extra thanks to Darci from who I have inherited the coolest lab bench. I think it came back to you when you returned at NIOZ, right? Well, may the Meatloaf pie chart always put a smile on your face! And then I shared the office with you Sabine: thank you for show me the Bligh Dyer extraction and how to optimize it timewise and

for all the fun in the lab! Lisa you have been the first friend I made on Texel and from that moment on we shared so much beyond science. Thank you for your friendship over these years. Thank you Yvonne, Marta, Claudia and Santi, Raquel, Cornelia, Cindy and Rob, Petra, Sandra, Elisabeth and family, Nicole and Yvo, Laura and Douwe, Dorien, Daniela, Dave, Luke, Lisa and Eli, Seabastian, Marc, Sebastiaan, Kim, Alina, Cecile and Rik, Els, Rodrigo and family, Evgenia, Sergio, Julie, Saara, Gabriella, Sophie, Laura S., Sigrid, Marijke, Caitlyn, Kasia, Mireia, Loes, Frederike, Argiro, Eva, Luciane, Sujin, Yuki, Marlen, Anuar, Laura M., Nikki, Libby, Jenny W., Jenny U., Borja, Stefani, Natalia, Simona, Leandro, Marta Ribo, Paolo and Elisa, Fatimah, Mathilde, Dorina, Catia, John and Catarina L., Arno and Catarina D., Santi, Kristina, Lise, Anouk, Irene and Andres, Ginny, Susanne, Sarina, Jorge, Tristan and Maram, Alex L., Tobi, Miri, Johann, Juliane, Meinard, Sofia and family, Elisa B. and everybody I have met during my time at NIOZ for the great time together, either if it was in the lab, in the canteen, for ferry beers on Friday afternoon, running to catch the ferry, building my new wardrobe and bed, moving from De Potvis to Den Burg to Oudeschild, making homemade pizza, at wonderfully bizarre dancing parties, at bachelorette parties or weddings, at De 12 Balcken, at dinners, lunches or barbeques at someone's house, biking to or from work, lost in the forest, making goofy videos for someone's defense, at the gym in Oudeschild, at conferences or summer schools, during day trips around the island and in the mainland, or sharing long distance trips.

Thank you Yvonne for all the chats and the laughs at lunch breaks and now on Skype. And thank you for your priceless support in the last part of my PhD.

Anna, Andrea, Paolo, Elisa, Moka, Sara e Carlo grazie per l'amicizia e il grande divertimento in giro per l'Olanda e non solo.

Riccardo e Cristina, Matteo, Antonello e famiglia, Francesca, Monica, Teresa, Luisa, Vittorio grazie per l'amicizia e il sostegno.

Grazie alla mia bella famiglia: Siro e Greca ce l'abbiamo fatta, complimenti e grazie! Nicola e Giuliana, Ilaria, Alessandro e Aurora, grazie!

Luca grazie per il buon umore e i molti modi in cui ti prendi cura di me.

And now for something completely different

Ad maiora!


Picture by Laura Tiano

About the Author

Martina Sollai was born on the 30th of October 1980 in Cagliari, Italy. After considering a career as designer she decided she liked biology enough to spend the next ten years of her life studying it, which she did at the Università degli Studi di Cagliari and at the Universiteit van Amsterdam. In September 2011 she started a PhD project at the Department of Marine Organic Biogeochemistry (now Department of Marine Microbiology and Biogeochemistry) at the Royal Netherlands Institute for Sea Research, under the supervision of Prof. Jaap S. Sinninghe Damsté, which resulted in this thesis.